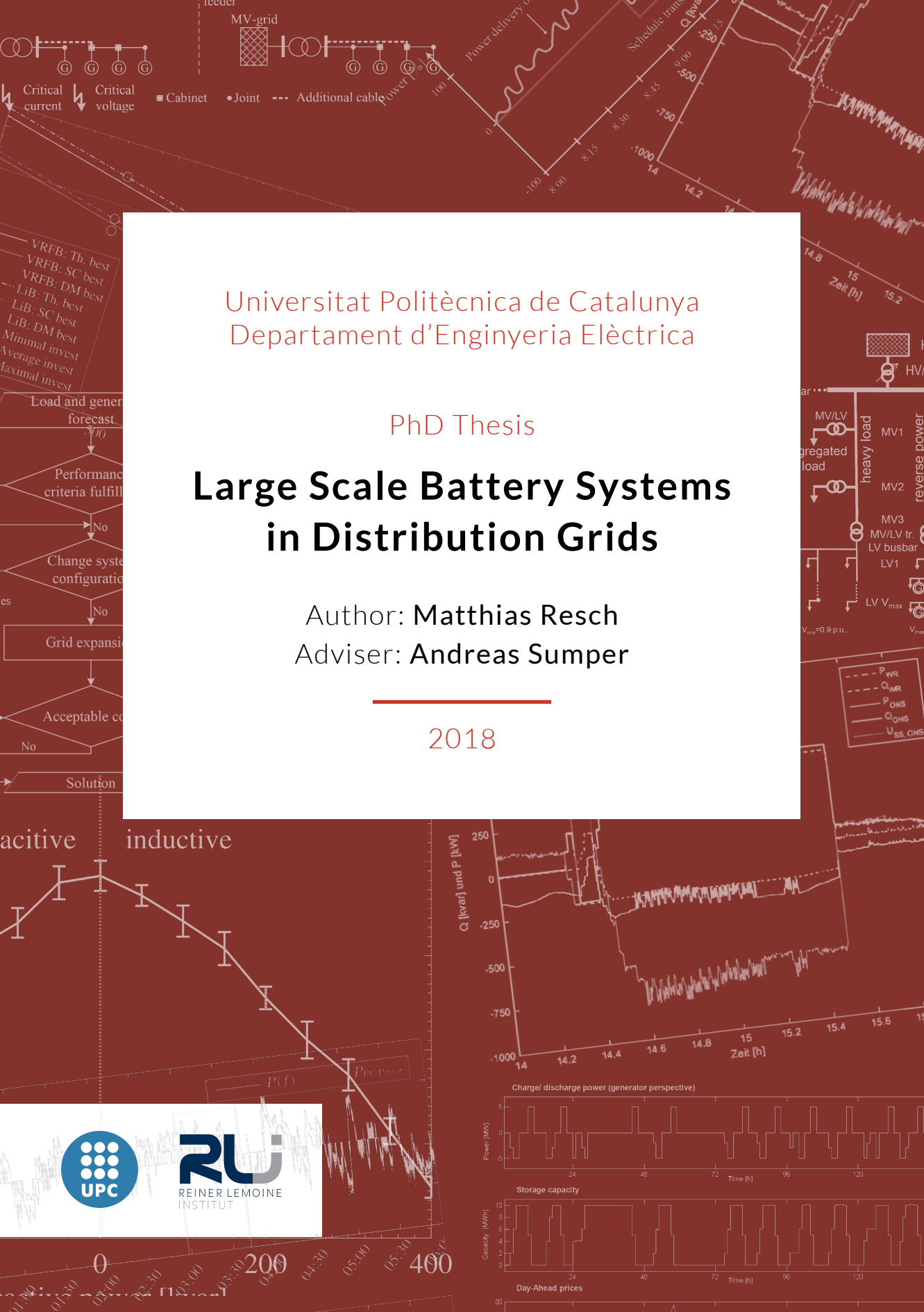

Universitat Politècnica de Catalunya
Departament d'Enginyeria Elèctrica

PhD Thesis

Large Scale Battery Systems in Distribution Grids

Author: **Matthias Resch**
Adviser: **Andreas Sumper**

2018

Universitat Politècnica de Catalunya

Electrical Engineering Department

PhD Thesis

Large Scale Battery Systems in Distribution Grids

Author: **Matthias Resch**

Adviser: **Andreas Sumper**

Trondheim, July 2018

Universitat Politècnica de Catalunya
Departament d'Enginyeria Elèctrica
Centre d'Innovació Tecnològica en Convertidors Estàtics i Accionaments
Av. Diagonal, 647. Pl. 2
08028 Barcelona

Primera impressió, 09/2018

To Tom

Acknowledgements

Doing a thesis can be compared to climbing a very hard route: First you see the beauty of the line and get motivated. Then you try it and think it might be possible and start working on it. After going through all phases of despair, happiness and just pure work, it comes together one day and you send the route. But this is only possible when you follow the whole process, there are no short cuts and this is why enjoying the process is its essence. I enjoyed it a lot.

I would like to thank my adviser Andreas Sumper for his support. He encouraged and followed the whole process, giving me the opportunity to do a PhD with all it means: learning, writing papers and above all his scientific support was very valuable. Moreover, somewhere on the way he became a friend and I hope to work with him in future research projects. I would also like to thank my second adviser Holger Hesser for the wonderful stay in Munich and the nice collaboration when we wrote the openBEA application together.

I would like to also acknowledge the support from my colleagues from the Reinier Lemoine institute, especially Jochen Bühler and Birgit Schachler, and all colleagues from the "SmartPowerFlow" project.

The author like to thank Hannah Krauth and especially Andreas Shackleford for the proofreading and the research group Solar Storage Systems of the HTW Berlin for their contributions.

Last but not least: Gracias familia por todo.

This work was supported by the German Federal Ministry of Economics and Technology (BMWi) and the Projektträger Jülich GmbH (PTJ) within the framework of the project "SmartPowerFlow" (FKZ0325523A).

Abstract

The increasing integration of renewable energy installations at the distribution grid level has led to a strong increase in grid reinforcement measures in recent years. Since the costs are being passed on to the general public via the grid user charges, it is necessary to investigate and evaluate alternatives.

As part of the project, that is investigated in this thesis, a large-scale vanadium redox flow battery storage system was integrated into the power grid of a German distribution grid operator for the first time. The battery system is a prototype and its inverter and battery have been developed specifically for the analysed project. The main objective of the project was to quantify the extent to which grid expansion measures can be avoided by the use of batteries and to what extent the balancing act between an economic and grid supportive operation is possible. Finally, the battery application was compared technically and economically with other flexibility options for a pilot region.

A preliminary analysis of possible business cases for large battery systems shows that the application of batteries in the primary control power market is by far the most lucrative application in the current German framework. It is followed by an application for cost reduction where self consumption of PV power is favoured over grid power. Both business cases are analysed in further detail.

The thesis is mainly focused on the grid supportive primary control application. The grid supportive behaviour of the analysed battery has been ensured by regulating the voltage in the low voltage grid via a reactive power control and thus increasing the grid capacity. The developed battery system was tested in the field during a one-year field test. The battery prototype and the grid of the pilot region was modelled based on measurement data. Furthermore, a method to derive an optimal operating strategy for electricity storage was developed and implemented. The strategy was developed with the aim to identify a self-sufficient operation mode which ensured the highest possible profit and validated in a field test. Albeit being the most lucrative battery application in Germany today, economic calculations have shown that the average cost of vanadium redox batteries would have to fall by about 60 % to achieve profitable operation. Nonetheless, since this is a new technology, both the expectations and potential for cost reduction are high.

The second most promising application, the maximisation of self-consumption, is also analysed through the means of a simulation for the pilot region, but without a implementation in the field. For this purpose a battery model for a vanadium redox flow battery based on measurement data is applied. To ensure grid supportive behaviour, an autonomous reactive power control based on a Q(V)-characteristic and peak shaving is implemented. The technical and economic assessment of this operation strategy is compared with a lithium-ion battery providing the same service. It is shown that this business case could already be profitable, with a more favourable legal framework in place. However, at present the investment costs of the vanadium redox flow battery has to fall by at least 77 % to break even for this operation strategy. Nonetheless, it could be demonstrated that it has almost no negative economic impacts if the battery storage system is operated in a grid supportive way in addition to its primary purpose.

Finally, a technical and economic assessment of the impact of the two large scale battery applications on distribution grid planning is conducted. Additional flexibility options such as a $\cos\varphi$(P) and Q(V)-control of PV systems and the use of residential storages are considered as well. For this purpose, a future PV expansion pathway was developed for the pilot region, as well as an automatic (traditional) grid expansion without flexibility option as a reference scenario. The PV expansion pathway is based on the identification of suitable roof areas for PV systems using aerial photographs. It has been shown that the hosting capacity for renewable energy installations increases in all cases compared to the scenario without flexibility options, sometimes by up to 45 %. In addition, it was found that from the perspective of grid operators it is more profitable to apply the presented flexibility option instead of a traditional grid expansion.

Contents

List of Figures

List of Tables

Nomenclature

Acronyms

AbLaV	Verordnung über Vereinbarungen zu abschaltbaren Lasten (English: Ordinance on Agreements Concerning Interruptible Loads)
AC	Air Conditioning Profile
APF	Adaptive Persistence Forecast (Control Strategy)
BGH	Bundesgerichtshof (English: Federal Court of Justice)
BGM	Balancing Group Management
BM	Biomas/Biogas Power Plant(s)
BMWi	Bundesministeriums für Wirtschaft und Energie (English: Federal Ministry of Economics and Technology)
BSS	Battery Storage System(s)
CAPEX	Capital Expenditures
CES	Community Electricity Storage(s)
CLR	Curtailment Loss Ratio
DA	Day-ahead (Market)
DG	Distributed Generator(s)
DOF	Degree(s) of Freedom
DSO	Distribution System Operator(s)
E2P-ratio	Nominal Energy to Nominal Power Ratio of Battery Storage Systems

ECM	Energy Cost Management
EEG	Erneuerbare Energien Gesetz (English: Renewable Energy Act)
EHV	Extra-high Voltage
EnWG	Energiewirtschaftgesetz (English: Energy Industry Act)
ENTSOE	European Network of Transmission System Operators for Electricity
FIT	Feed-in Tariff(s)
HLF	Heavy Load Flow
HP	Heat Pump Profile
RPF	Reverse Power Flow
HT	High Time
HV	High Voltage
ID	Intra-day (Market)
KWKG	Kraft-Wärme-Kopplungsgesetz (English: Combined Heat and Power Act)
LCOE	Levelised Cost of Electricity
LiB	Lithium-ion Battery Storage System(s)
LT	Low Time
LV	Low Voltage
LVN	Lechwerke Verteilnetz GmbH
MV	Medium Voltage
NA	Night Active Profile
NEG	Negative Control Reserve
OL	Over-loading
OLTC	On-load Tap Changer
OPEX	Operational Expenditures
OV	Over-voltage
PCC	Point of Common Coupling
PCR	Primary Control Reserve
POS	Positive Control Reserve
PV	Photovoltaic

reBAP	Regelzonenübergreifender einheitlicher Bilanzausgleichsenergiepreis(Englisch: Balancing Energy Price)
RES	Residential Photovoltaic Storage System(s)
RESC	Renewable Energy Self-Consumption
ASC	Self-Consumption (Control Strategy)
SCR	Secondary Control Reserve
SCR	Self-consumption Ratio
SLP	Standard Load Profile
SMCCP	Schedule Mode with Constant Charging Power (Control Strategy)
SOC	State of Charge
SPF	SmartPowerFlow
SSR	Self-supply Ratio
StromNEV	Stromnetzentgeltverordnung (English: Electricity Grid Charges Ordinance)
StromStG	Stromsteuergesetz (English: Electricity Tax Act)
TCR	Tertiary Control Reserve
TSO	Transmission System Operator(s)
UPS	Uninterrupted Power Supply
VRFB	Vanadium Redox Flow Battery Storage System(s)

List of Units and Symbols — Unit

c_C	specific cost of the components needed for the capacity	EUR
C_{per}	costs for the system periphery	EUR
x	coincidence factor	–
C	nominal storage capacity	Wh
$E_{\mathrm{PV\_c}}$	consumed PV production	Wh
$cos\varphi$	power factor	–
E_{cur}	total curtailment loss	Wh
E_{corr}	energy purchased in the scheduled transactions	Wh
ep	electricity price	EUR

η_{AC}	AC-power dependent round trip efficiency	–
η_{bat}	round trip efficiency of the battery system	–
ft	feed-in tariff	EUR
I	current	A
I_0	investment costs	EUR
LC	annual load consumption	Wh
E_{Load}	load demand	Wh
c_P	specific cost of the power electronics	EUR
P	active power	W
$p.u.$	per unit	–
P_{pq}	pre-qualified power	W
P_{STC}	module power under standard test conditions STC [1]	W
P_{AC}	total active power of a BSS	W
P_{PCP}	required PCR power	W
P_{import}	imported power from the electrical grid	W
E_{PV}	total energy generated by the PV system	W
P_{PV}	PV power	W
Q	reactive power	var
R	resistance	Ω
S	apparent power	VA
SOC_{av}	availability limit	%
ΔSLR	change of SLP versus SC strategy	–
SOC_{corr}	correction limit	%
ΔSSR	change of SSR versus SC strategy	–
t	time step	s
E_{use}	usable capacity (of a BSS)	Wh
V	voltage	V
X	reactance	Ω

[1] STC: cell temperature of 25°C, irradiance of 1000 W/m2, air mass 1.5

Z	impedance	Ω

Indices

agg	aggregated
C	charging of the BSS with constant power
cos	costumer
D	discharging of the BSS with constant power
f	final value
i	initial value
$loss$	loss
max	minimal value, minimal limit
min	maximal value, maximal limit
n	nominal value
opt	set (optimal) target value
p	active
PL	peak load
q	reactive
r	rated value
res	residual value, e.g. residual power of load and generation
s	apparent
t	transformer
$thres$	threshold value

Chapter 1

Introduction

1.1 Motivation

The energy system in Germany is currently changing. In the past, electrical energy was injected by large power plants into the transmission system (220 kV and 380 kV) to cover long distances. It was then delivered to costumers via distribution grids (1 kV to 110 kV). Since the German Federal Government decided to withdraw from the nuclear energy programme and to reduce the greenhouse gas emissions in order to mitigate climate change, the expansion of renewable energy sources was subsidised by introducing the German Renewable Energy Act (EEG) in 2000. This led to a huge increase of the renewable energy share in the German electricity mix from 7 % in the year 2000 to 32 % in the year 2016 [1]. Furthermore, as a consequence of the sinking levelised cost of electricity (LCOE) of renewable energy sources, grid parity was reached in 2012 for photovoltaic (PV) power plants in Germany [2]. Grid parity means, that renewable energy sources are able to produce electricity below the purchase power price from an electricity provider.

This trend will probably continue as the German Federal Government committed itself to a renewable energy ratio of 80 % of the gross electricity production in the year 2050 [3]. In contrast to conventional power plants, renewable energy sources are mainly realised as distributed generators (DG), as defined by [4,5]. Due to their relatively small installed nominal power they are mainly connected to the distribution grid at medium voltage (MV) and low voltage (LV) levels [6,7]. For example, 80 % of photovoltaic power plants in Germany are connected to the LV grid [8]. Due to this, the nominal

DG power installed in the distribution grid surpassed the power installed in the transmission grid in 2010 [9]. Furthermore, the DG are distributed very inhomogeneous in Germany with wind power plants in the north and photovoltaic systems in the south [10]. This, and the fact that the power feed-in of DG is not necessarily simultaneous to the local load demand, results in a transformation process of the distribution grids. Formerly these grids were characterised by the consumption whereas now the reverse power flow becomes increasingly common. This means that in some moments of the year there is a power flow from the distribution grid to the transmission grid [11].

As German electricity grids are planned to work uni-directional with a power flow from high to low voltage levels, this could lead to several problems. For example, the protection concept is designed such as to work for a uni-directional power flow and may not work in a bi-directional way [12]. Furthermore, power quality issues can arise. In some grids the maximum possible PV penetration rate is reached as DG are often installed in (weak) rural grids [13]. Therefore, an additional installation of DG is often followed by grid reinforcement in order to solve over-voltage (OV) and equipment over-loading (OL) issues caused by the DG.

The drawback of this traditional grid planning procedure is large investment in infrastructure with a low utilisation rate. Historically, grid expansion planning has been based on maximum load scenarios, but in the case of a high penetration with DG the grid is dimensioned to deal with maximum generation [14]. But unlike for large thermal power plants, the power output of wind and PV systems is dependant on the weather. This can be illustrated with an example: The number of hours in which PV-systems (in south Germany) feed more than 90 % of their rated power into the grid is below 100 hours a year [15]. Nonetheless, the grid has been sized for 100% of the rated power [16]. Due to this, traditional grid planning may cause inefficient grid operation and higher grid utilisation fees that have to be borne by the general public (cost increase of 9,2 % from 2008 to 2014) [17]. As in [18] predicted, this will lead to a linear cost increase for DG induced grid reinforcement due to OV and over-loading issues of 331 EUR/ kW until 2030. The cost can be attributed to different voltage levels (400V: 13 % / 1 kV-36 kV: 29 % /60 kV-380 kV: 58 %). Therefore, the German Government initialised and funded, amongst others, the project SmartPowerFlow (SPF), to analyse and evaluate alternatives to traditional grid expansion. The scientific evaluation of the SPF project is an essential part of this work.

Within this project a large scale vanadium redox flow battery prototype has been integrated in the grid of a distribution system operator for the first time in Germany. The battery storage system (BSS) is composed by the

following main components: the battery (named CellCube FB200-400 DC) of the company Gildemeister energy solutions GmbH and the inverter (SCS 630) and inverter control software which were developed for this project.

The BSS prototype was installed in the market town Tussenhausen in the administrative district Unterallgäu. The BSS has been implemented in the LV-grid of the Lechwerke Verteilnetz GmbH (LVN), as this distribution system operator experienced a huge expansion of installed DG in the last years (Figure 1.1).

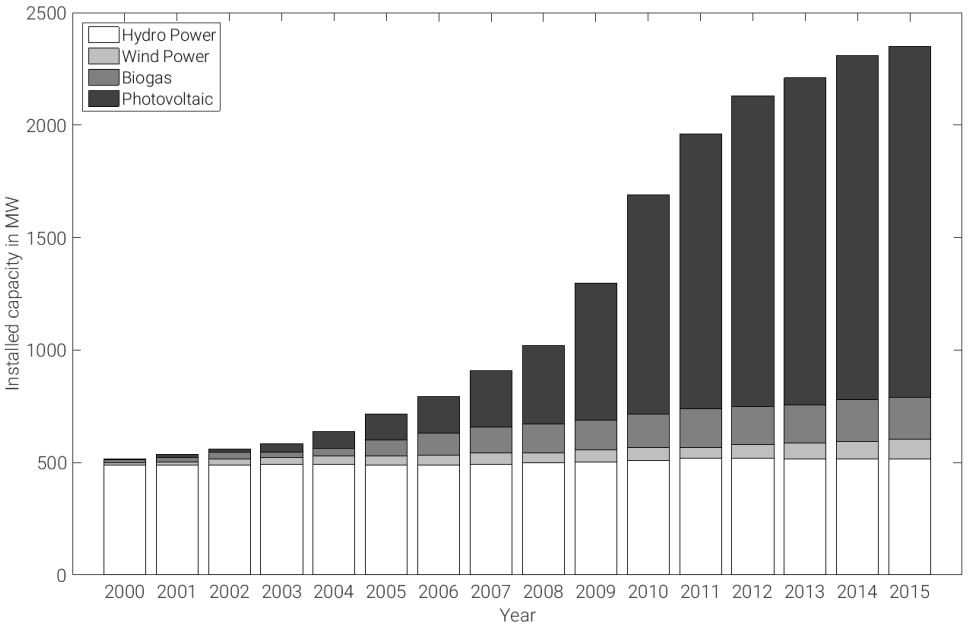

Figure 1.1: Installed cumulated power of DG in the grid of LVN.

The objectives of the project are interlinked with the objectives of the thesis and described in the following section.

1.2 Objectives

The integration of large scale BSS as grid equipment implemented by the DSO with the only purpose to reduce grid expansion costs tends to be non-profitable [19,20]. This is particularly true for distribution grids, due to the relatively low costs of grid equipment compared to other voltage levels. The costs for grid equipment in LV is usually considerably lower than the costs for the implementation of large scale BSS [21]. For instance, the costs of

one MV/ LV transformer can be assumed to be around 35,000 EUR (630 kVA, including switchgear and station) [21], whereas the nett price of one CellCube FB200-400 DC (200 kW; 400 kWh) was listed for 849,000 EUR in 2015. Therefore, the implementation of such a BSS would have to replace more than 20 MV/ LV transformers. This seems very unrealistic even with the falling battery prices that can be observed at present. Furthermore, within the legal framework in place in Germany, the reimbursement of the battery owner for the avoided grid expansion costs is controversial and unclear [22, 23]. Thus, the implementation of a large scale BSS with the only purpose to reduce grid expansion costs does not seem profitable (in most cases) and feasible at present.

The combination of a grid supportive behaviour with a profit orientated operation strategy might be a feasible solution. Thus, the main objective of the thesis is to evaluate, whether grid expansion measures to increase the hosting capacity for DG can be reduced in distribution grids by integrating a grid supportive and profit orientated large scale BSS.

Therefore, if a profitable and feasible combination is found, the number of large scale BSS in distribution grids might increase. Nevertheless, other alternatives to traditional grid expansion and large scale BSS need to be considered as well, in order to evaluate the benefit of the different options. The main objectives of the thesis are:

- **Identification** of the two most profitable business cases for large scale BSS in distribution grids under the current legal framework in Germany: The aim is to find the most profitable market based business case and the most profitable cost reduction business case.
- **Field test** of the most profitable combination of a market based profit orientated operation strategy with a grid supportive behaviour: The aim is to show that it is possible to reduce the main driver for grid expansion (OV issues) and at the same time react with the active power to market signals, even if the power flow of the active power is unfavourable from the point of view of the DSO.
- **Evaluation**, if for the two identified business cases the given BSS prototype can be operated profitably and reduce grid expansion costs at the same time: The aim is to achieve this by applying a reactive power control strategy, additionally to the active power control strategy which is used to earn revenues. An additional aim is to quantify the

additional cost burden of the reactive power control strategy for each of the two business cases.

- **Techno-economic comparison** of profitable grid supportive business opportunities for large scale BSS with other flexibility options, with the focus on the impact on distribution grid planning: The aim is to quantify for a given DG expansion pathway of a pilot region the future grid expansion costs of traditional distribution grid planning and compare them with the costs caused by the implementation of large scale BSS (applying the two identified grid supportive business cases). Several more common alternatives to traditional grid expansion are also assessed, in order to evaluate the relevance of the large scale BSS options.

1.3 SmartPowerFlow: Project Overview

As stated before, it is a great challenge for distribution grid operators to integrate fluctuating DG into their grid. To ensure a safe and stable energy supply with increasing DG, investment decisions have to be made. It is still unclear if and how the implementation of large scale BSS into distribution grids may be used as a tool to increase the expansion of renewable energy systems. Within the SmartPowerFlow project [24] a vanadium redox flow battery (VRFB) prototype has been developed for this purpose and integrated into the grid operation. It was installed into a suitable distribution grid in Swabia in Bavaria, to demonstrate the cost optimised integration of DG. The VRFB has a rated power of 200 kW and a capacity of 400 kWh.

As stated before, the main goal of the project is a comparison of traditional grid expansion versus battery implementation, as well as a techno-economic assessment of the storage application at the distribution grid level. This three year project was divided into three major phases:

- Phase 1: Optimal allocation of a large scale VFRB within the grid of the DSO LEW Verteilnetz GmbH (LVN), based on load flow simulations under consideration of technico-economic criteria. Development of an inverter for this battery (first year).

- Phase 2: Integration of the BSS into the grid of LVN and validation of simulation models based on measured data (second year).

- Phase 3: Development of a holistic concept to integrate large scale BSS into distribution grids, as well as a techno-economic comparison of grid

Figure 1.2: The vanadium redox flow battery installed in the SmartPower-Flow project.

expansion versus battery integration (second and third year).

The four project partners had different tasks. These were:

- LEW Verteilnetz GmbH: Provision of detailed generator and load data of distribution girds, as well as defining criteria for the allocation of optimal BSS locations and operation strategies.
- Younicos AG: Development and realisation of a energy and battery management system as well as the integration of the battery to the control system of the distribution grid operator.
- SMA Solar Technology AG: Development and evaluation of a battery inverter for redox flow batteries.
- Reiner Lemoine Institut gGmbH: Project coordination, systematic analysis of the grid optimisation and economic analysis of different battery applications.

This project was granted by the German Federal Ministry of Economics and Technology (BMWi) and the Projektträger Jülich GmbH and was one of the few lighthouse projects (grant number: FKZ0325523A).

1.4 Structure of the Thesis

Chapter 2 is a review chapter. At the beginning, the legal framework for the operation of distribution grids in Germany and the challenges that arise with the integration of high shares of DG, are described briefly. Furthermore, traditional distribution grid planning and new grid reinforcement planning methods are presented. Finally, the gap in research is derived and the contributions of this thesis to fill this gap are linked to the respective chapters.

In chapter 3 the applied VRFB prototype and its implementation is described. Furthermore, the pilot region along with an assumed PV expansion pathway is presented.

A brief overview based on a literature review of different BSS applications and their possible profit margins for the German energy market is presented in chapter 4. In the same chapter possible revenue streams for several market based applications with single and combined revenue streams are calculated for the BSS prototype and discussed. As a result of this comparison, the most profitable market based application is derived. The application with the highest cost saving potential is assessed, too. Finally, for these two applications, the regulatory frameworks and technical restrictions are described and the consequences on their respective operating strategy is discussed.

The two most profitable applications primary control reserve and self-consumption maximisation are combined with a grid supportive behaviour and are assessed in detail in chapter 5 and chapter 6, respectively. The primary control reserve application (chapter 5) has been implemented and tested in the field. Furthermore, the results gained of simulating the operation strategy are validated with measured data. The self-consumption application is discussed in detail in chapter 6. As in 2018 self-consumption is mostly implemented in residential storage devices, these applications are used as a starting point. As for this application the control strategy is not strictly determined by the regulatory framework a review is conducted to select the most profitable one. This strategy is then adapted to a grid supportive operation strategy large scale BSS and used for a techno-economic assessment.

The implementation of large scale battery systems in distributions grids is discussed in chapter 7. The focus lies on BSS that apply self-consumption maximisation and primary control reserve, due to their economical relevance. Traditional as well as alternative approaches of grid planning are applied and compared. These two BSS applications are compared with traditional grid expansion measures, as well as with other alternatives.

The conclusion and a outlook for future work is given in chapter 8.

Chapter 2

Review of the Impact of Large Scale Battery Systems in Distribution Grid Planning

In this chapter the literature concerning grid planning and the integration of large scale BSS in the distribution grid in Germany is reviewed. Essential definitions for the understanding of this chapter and the thesis are introduced in section 2.1. The definitions are followed by section 2.2, in which the operation of distribution grids under the current legal framework in Germany and the challenges that arise with an increasing penetration of DG are presented. Furthermore, the methodology for traditional distribution grid planning along with an extensive review of grid reinforcement measures for LV and MV is given in section 2.3. New planning methods for integrating DG and BSS in distribution grids are presented and discussed in section 2.4. Finally, the gap in research is derived from the literature review in section 2.5 and the contributions of this thesis to fill this gap are linked to the respective chapters.

2.1 Definitions

2.1.1 Voltages

In this work, voltages and voltage changes are stated as absolute values in Volt (V), as relative values in % or per unit (p.u.), according to DIN 5485. The reference value is always the nominal voltage V_n of the grid. Phasor

diagrams and time-dependant values are expressed according to DIN 5483-3:1994-09.

2.1.2 Distribution Grid

The focus of this work is on distribution grids. All grids in this work are electrical grids and can be categorised according to their nominal voltage. V_n is defined in DIN VDE 0175 for German grids. In urban areas with a high load density, the 60 kV and 110 kV levels may be included in distribution grids [25]. As the grids analysed in this work are all rural or semi-rural grids, these voltage levels are not considered. Thus, distribution grids are defined according to Table 2.1.

Table 2.1: Categorisation of the common voltage levels in Germany

Grid category	V_n [kV]	Voltage level
Transmission grid	380	Extra-high voltage level EHV
	220	
High voltage grid	110	High voltage level HV
	60	
Distribution grid	20	Medium voltage MV
	10	
	0.23/ 0.4	Low voltage LV

In conclusion, in this work the term distribution grid refers to all MV and LV grids that are connected physically to the MV busbar of one particular HV/MV substation.

2.1.3 Decentralised Generation

Within this work decentralised generation is defined as [5]:

"Distributed generation is an electric power source connected directly to the distribution network or on the customer side of the meter."

Although, in general, this definition includes various technologies, in this work DG specifically refers to renewable energy sources. The customer side of the meter means that the DG can be installed "behind the meter", as it may be the case for PV especially, if it is used for self-consumption.

2.1.4 Autonomous Control in the Context of Distribution System Operation

Autonomous control in the context of distribution system operation is based on the extensive definition of [26]. In the context of this work autonomous control strategies are defined as operating strategies that rely entirely on locally measured values and need no communication infrastructure. Furthermore, there is no communication between the single grid participants applying an autonomous operating strategy. Thus, it is a local control approach (in contrast to a centralised control approach) according to IEC IEV 60050-351-26.

2.1.5 Hosting Capacity

The technical restrictions for OV and OL are commonly used to determine the hosting capacity, as defined in [27], to integrate DG into existing grids. An exhaustive international overview of the main technical issues limiting the hosting capacity for DG of distribution feeders is given in [28].

2.1.6 Flexibility Option in the Context of Distribution Grid Planing

The term flexibility option is based on [29], who uses it to describe *"control strategies to provide greater flexibility and use of existing network assets."*

Another more extensive definition of flexibility in the context of distribution grid planing is provided by [30]:

"Flexibility is a generic term for a bundle of different topics such as demand-side, infeed and storage management for system, market and grid condition purposes. Flexibility can be provided by all grid-connected technical units, which are able to temporary modulate their power consumption or production. This ability is usually the result of a certain energy storage capacity, which may be a physical storage (e.g. gas storage) or an inherent storage capacity of a process (e.g. thermal inertia). Furthermore, flexibility can be provided by curtailment of RES or processes with alternative energy supplies (e.g. combined electrical and gas heating)."

[29] proposes a centralised control strategy which applies a AC optimal power flow (OPF) based technique to increase the hosting capacity for DG in a distribution grid with an Active Network Management. In contrast to the centralised Active Network Management, the focus of this work is set on the local control approach of autonomously operating strategies that avoid OL

and OV. Nonetheless, their aim is the same: to increase the hosting capacity for DG in distribution grids.

In conclusion, if a control strategy is applied by a grid participant for the goal of increasing the hosting capacity, it is defined in this work as flexibility option.

2.1.7 Large Scale Battery Storage Systems

Generally large scale BSS may be defined through various aspects, which may lead to conflicting or unclear definitions. They may be defined by their type of operation, as in [31, 32]. In [31] large scale BSS are delimited from small scale BSS, if they supply peak levelling services and are grid connected or if power-quality control applications are applied. Another definition of the application of large scale BSS is given in [32], where the distinction is made between energy related or power related applications. In energy related applications the storage is charged and discharged during several hours, reaching one cycle a day. In contrast to this, for power applications the BSS is cycled several times a day and discharged and charged in shorter periods (typically seconds and minutes). The type of application directly affects the range in which the rated power range of the BSS tends to be and might be used as an indication, as listed in Table 2.2 according to [33].

Table 2.2: Energy and power related applications for BSS [33]

Application	Nominal power P
Energy related:	
Peak shaving	0.1 MW to 10 MW
Load levelling	1 MW to 100 MW
Energy arbitrage	50 MW to 500 MW
Power related:	
Frequency control	1 MW to 30 MW
Voltage regulation	1 MW to 30 MW
Power quality regulation	1 MW to 30 MW
Bridging power	1 MW to 30 MW

2.1.8 Definitions of Behaviours of Battery Storage Systems

BSS may provide active and reactive power. The application dependent power flow may either lead to less or to additional grid reinforcement cost [18]. In this section different system behaviours of the BSS are defined, in order to quantify their impact on the distribution grid planning. In this study the term system refers to electrical systems only. Every BSS may be categorised in one or several of the four categories [34, 35]:

(a) Grid compatible
If the minimal technical requirements in regard to quality, reliability and safety imposed by the DSO are fulfilled by the BSS, it can be considered as grid compatible. In the near future operators of DG will need to prove this behaviour via certificates to the DSO. Based on the technical specifications of to PV systems, possible future capabilities which have to be proven by the BSS, are [36]:

(i) Short-circuit current capability, (continuous) current carrying capacity ampacity and switching capacity of the main components

(ii) Active power feed-in

(iii) Active power concept

(iv) Network disturbances like rapid voltage drops, long-term flicker, harmonics and interharmonics

(v) Fault ride through

(vi) Contribution to the short circuit current

(vii) Static provision of reactive power

(viii) Conditions for connecting and protection concept for disconnecting the system

(b) Grid supportive
This characteristics describes the behaviour of the BSS to be able to actively stabilise the grid to a level that goes beyond the minimal prerequisites described before. It has a local component to it, since some issues like OV and OL have to be solved locally. OL may be solved with active or/and reactive power control [35]. The market incentive programme from the German Federal Government and the state-owned KfW banking group is coupled to several technical requirements. The most important measure to receive this incentive is the limitation of maximum feed-in power of the PV storage system to 50 % of its nominal power at the point of common coupling [37].

(c) System compatible
Analogue to a grid compatible behaviour, a system compatibility is given with the fulfilment of the minimal requirements of the BSS to ensure a safe operation of the whole electrical system. In this case the contribution to the spinning reserve, as well as the provision of ancillary services as for instance black start capability and frequency control play an important role. Some of these services, like the provision of primary frequency control, are remunerated, whereas some, such as the provision of spinning reserve or active power reduction in case of over-frequency, are not [35].

(d) System supportive
A BSS can be considered system supportive, if it leads to greater flexibility of the electrical system. The operation of the BSS is then optimised to minimise local issues as described for the grid supportive behaviour and at the same time to provide services for the whole electrical system. An example may be the provision of reactive power to reduce local OV issues and the provision of active power to provide frequency control and/or spinning reserve.

2.2 Legal Framework, Arising Challenges and Possible Solutions for DG and BSS Connected to Distribution Grids in Germany

2.2.1 Legal Framework for the Operation of Distribution Grids

According to the German Energy Act (EnWG) section 14(1) [38] the grid operators are legally bound to ensure a safe and stable energy supply. Especially the power quality issues of OL of cables and transformers as well as OV are of major interest. The requirements that should be fulfilled regarding OL of transformers and LV-cables are defined in DIN EN 60076-2:2011 [39] and DIN VDE 0276-603 [40], respectively.

Table 2.3 shows the load factors of the rated apparent power S_r for different components according to [18] under normal operation conditions that are defined in [41]. For the heavy load flow (HLF) and reverse power flow (RPF) different maximum load factors apply. This is due to the different shape of the profiles in both cases. Furthermore, the (n-1)-criterion as defined in [16] and further specified in [18] applies for MV-cables and HV/ MV transformers for the load case. In the case of a HLF for MV-cables and HV/ MV transformers [18] sets the maximum loading to 120 %. For all other components and scenarios it is set to 100 %. Nevertheless, the maximum loading of MV/ LV transformers depends not only on the profile but is also not consistent in the literature: it ranges from 150 % for oil immersed transformers only [42, 43] to 120 % [44, 45] and 100 % [18] for all kind of transformers in the case of a RPF caused by PV systems.

Table 2.3: Equipment load factors [18]

Equipment	Load factor of S_r Heavy load flow	Load factor of S_r Reverse power flow
LV-cable	max. 100 %	max. 100 %
MV/LV tran.	max. 100 %	max. 100 %
MV-cable	max. 60 %	max. 100 %
HV/MV tran.	max. 60 %	max. 100 %

Voltage characteristics in distribution grids are defined in [41]. The most important restrictions are that the frequency has to be kept at 50 Hz $\pm$1 Hz and the 10−minute RMS average of the voltage at the point of common coupling (PCC) has to be kept with in an interval $\pm$10 % of the nominal

voltage. To ensure this, two technical specifications for DG quantify the permitted voltage rise of 2 % in the MV [46] and of 3 % in the LV [47], respectively . These technical specifications apply if the MV or the LV are calculated separately, otherwise these thresholds don't have to be considered. Furthermore, all generators connected to the electrical grid have to comply with the specifications in [48], [49] and [50], respectively. Furthermore, the technical note [51] has to be considered for BSS connected to the LV.

The technical restrictions for OV and OL are commonly used to determine the hosting capacity, as defined in [27], to integrate DG into existing grids. An exhaustive international overview of the main technical issues limiting the hosting capacity for DG of distribution feeders is given in [28].

2.2.2 Challenges and Solutions for Electrical Grids with Fluctuating Feed-in of Renewable Energies

Several challenges may arise from the integration of high shares of RES into the electrical grid [26,28,52]:

For distribution grids:

- Thermal OL of network equipment
- Voltage rise
- Increased fault levels, especially for MV grids
- Power quality issues
- Impact on grid protection due to RPF
- Effect on the operation of voltage regulators and tap changers because of RPF
- Impact on grid losses

For the whole electrical system:

- Increased demand of control power
- Increase of transmission line bottlenecks
- Decreasing spinning reserve

The most important challenge in distributions grids on an international level is due to OV issues [28]: In Germany for example, 80 % of the grid reinforcement is due to OV issues in distribution grids [53]. Besides grid reinforcement, ancillary services have to be provided by generators and loads to cope with these issues. These services are defined in [54] and are classified for normal operation conditions by their purpose:

- Frequency control
- Voltage control
- Remote automatic generation control
- Grid loss compensation

All these ancillary services can be provided by DG and in particular by BSS [55]. Therefore, the technical and economic applications of BSS are analysed with the requirement to supply ancillary services and as an alternative to traditional grid reinforcement.

2.3 Traditional Distribution Grid Planning

The distribution grid planning process is determined by three main aspects: economics, reliability and environmental issues. Concerning the economics, the high investment cost and the long lifetime of the technical equipment are the most important criteria. Reliability is quantified through the "System Average Interruption Duration Index" (SAIDI) which is the average outage duration for each customer served in minutes. For the German LV and the MV combined this value ranges from 12 to 21 min/a (reliability of 99.996 % to 99.998 %) between 2006 and 2014 [56].

Further parameters for the planning process can be found in [57] and [58]. These restrictions lead to a planning process as described in [58–60] which may have different tasks and may be divided in a structural and a temporal category. The structural differences are, whether a greenfield or a reinforcement planning of existing grid equipment is considered [59]. In the temporal category three different time horizons can be distinguished: long term (up to 30 years), medium-term (6-10 years) and short-term (3-5 years) [61–63].

Although, there are various guidelines for distribution grid planning on a national [58] and an international level [64], as well as additional recommendations [65], every DSO has a different planning process because of the different characteristics of each distribution grid and DSO [57]. To standardise the different planning approaches a study was conducted that summarises the methodology of 17 DSO, covering more than 50 % of all distribution grids in Germany [18]. It can be regarded as the state-of-the-art approach. Figure 2.1 describes the conventional distribution grid planning schematically:

One problem of this approach lies in the input data, since the LV load is usually not measured and has to be estimated. The estimated LV load may be gained from the (measured) annual maximum load of the secondary

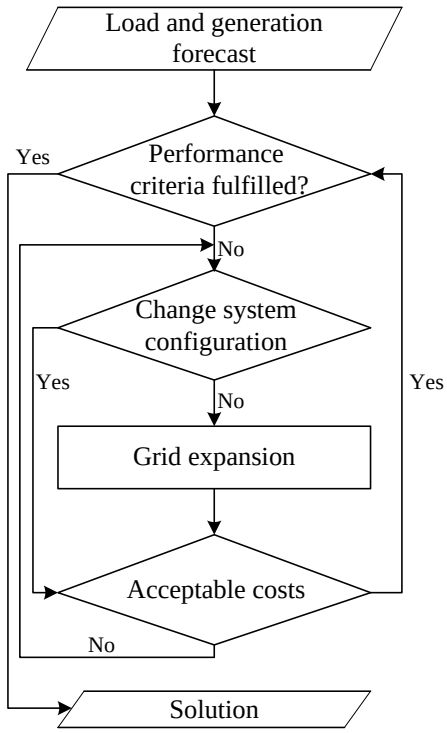

Figure 2.1: Distribution grid planning schematic [18,60] (adapted)

transformers [66], the rated power of these transformers [59] or from structural data as the degree of electrification or population density [58,66]. Approaches employing combinations of these datasets are possible [18]. On the generation side, the rated power of the generators is usually known and published [67].

To evaluate whether a certain threshold is reached (as described in section 2.2) a power flow calculation is conducted in which the powers of the loads and the generator are adjusted to certain worst case scenarios, specified in subsection 2.3.1. If a threshold is passed, the grid is reinforced according to the methodology described in subsection 2.3.2.

2.3.1 Assumed Scenarios - Worst Case Parameters

Distribution grids are traditionally planned in a deterministic manner [64]. The traditional scenario used to perform a power flow only considers max-

imum demand, whereas the generation is assumed to be constant. Higher penetration rate of DG leads to two worst case considerations: the heavy load flow and the reverse power flow scenario. Generally, the considered the worst cases are [64]:

1) Heavy load flow: Max load; no generation.
2) Reverse power flow: Min load; max generation.

For each of these extreme scenarios a pair of factors (diversity and coincidence factor) is determined to adjust the power of the loads and generators of a grid to one of these worst cases. For loads, this factor is called coincidence factor and is defined in [64] as the average power absorbed related to the installed power. For generators, this factor is referred to as diversity factor by [68], and is defined as the quotient of the actual and the installed capacity. These factors do not consider the time variability of demand and generation. Thus, a simple probabilistic determination of these factors that covers all possible grid states for Germany sets the scenarios closer to reality. To quantify the coincidence and the diversity factor, taking into account the simultaneity of generation and consumption, several studies have been conducted [7, 18, 69, 70]. The diversity factors of [7] apply for ten generators of the same type. The same study shows that diversity factors differs, if the correlation between the generators is taken into account. The results are listed in Table 2.4 and Table 2.5.

Table 2.4: Diversity factors for generators connected in MV/ LV [7,18,69,70]

	Wind	PV	Biomass	Hydro
HLF	0 [18]	0 [7, 18, 69, 70]	0 [18] 0.6 [7]	1 [18]
RLF	0.95 [7] 1 [18]	0.85 [18, 69, 70] 0.89 [7]	0.98 [7] 1 [18]	1 [18]

Table 2.5: Coincidence factors for loads connected in LV/ MV [18, 71]

	Load (LV)	Load (MV)	C. load (MV)
HLF	1 [18]	1 [18]	1 [71]
RPF	0.1 [18]	0.15 [18]	0.5 [71]

Both, the coincidence and diversity factors, apply to the maximum/rated power of the generators and loads. In case of PV the diversity factor refers to the installed module power P_{STC} [69, 70]. In the reverse power flow case the factor for the load of the MV is higher, as a higher blending of the stochastic behaviour of the loads is taken into account. Some bigger costumers/loads (called Costumer load by the DSO LVN; hereinafter referred as C. load) have their own secondary transformer and are connected directly to MV. The maximum power of these loads can be assumed as 40 % of the rated apparent power $S_{r,t}$ of the secondary transformer [71].

Based on experience, these simple worst case factors cover all possible grid states and are commonly used [18, 72, 73], as they provide a high level of reliability without measurements in the LV [58]. However, the likelihood of occurrence of these extreme states is not considered with this practice, and may never occur in reality [74]. Furthermore, no time interdependencies of the assets are considered. As a consequence, the distribution grids tend to be over-dimensioned. Thus, new planning approaches should be taken into account [64, 75], as they may use infrastructure more efficiently [65], as well as avoid redundant investments and minimise O&M costs [76].

There are plenty of different approaches to come to a more realistic assessment of the scenario factors, as for example [68, 71, 77]. To estimate the minimum and maximum load that are aggregated for an entire LV grid and connected to the LV side of the secondary substations, the top down approach of [71] is based on the measured time series in the substation. Another publication concentrates on the correlation of the different DG from measured time series for individual grids and estimates their coincidence factors [68]. It is also possible to synthesise time series instead of using measured data, as for example [77], where coincidence factors are derived for BSS by using an agent-based simulation. In general, there is a wide field of different new planning approaches for different BSS applications. The approaches are analysed in detail in subsection 2.4.

2.3.2 Grid Reinforcement Methodology

In this section the methodology of grid reinforcement for distribution grids, especially for low and medium voltage grids, is described. The methodology depicted in Figure 2.2 to Figure 2.6 applies for radial grid structures in LV and for open ring structures in MV. Nevertheless, these methodologies are transferable to other grid topologies and can be considered as state-of-the-art in Germany [18]. Grid reinforcements are triggered due to are either local OV or OL of a cable or a transformer. First, a load-flow is conducted and mea-

sures against OL are implemented, then an additional load-flow is calculated. If there are still OV problems in the grid, measures to solve these are applied.

Methodology for low voltage grids:

As depicted in Figure 2.2, an OV is solved by installing a parallel cable (type see Table 2.4) from the distribution substation to the next distribution cabinet over 2/3 of the line length. A critical OL of a line is solved by installing a parallel line till the next distribution cabinet, starting to search from half of the line onwards.

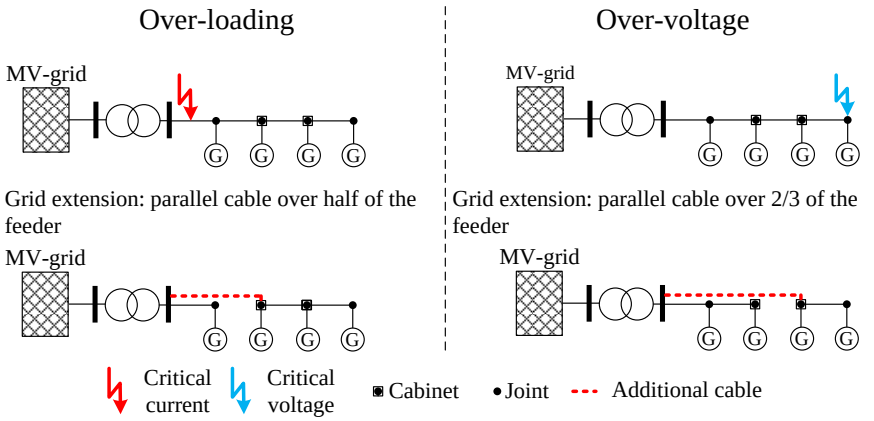

Figure 2.2: LV grid reinforcement via a parallel line

If more than one line is affected, as shown in Figure 2.3, all affected lines are divided at the distribution cabinet that lies closest behind one half of the line. The lines in the second half are connected to a new secondary substation. The rated apparent power $S_{r,t}$ of the additional MV/LV transformer is the same as the one that was formerly feeding the entire LV-grid. If there is an OL in a transformer and its apparent power $S_{r,t} \leq 400\,kVA$, it is replaced by the next bigger standard transformer (630 kVA). If the OL is not solved through this measure, a parallel 630 kVA transformer is installed.

Methodology for medium voltage grids:

Similar to LV a parallel line is installed in the case of OL or OV. In case of OV the length of the new line is 2/3rd of the length of the affected feeder, whereas for OL the parallel line is installed between the primary substation and the DG that causes the issue (see Figure 2.4). In both cases no secondary substations are installed on the parallel MV line which is connected to the

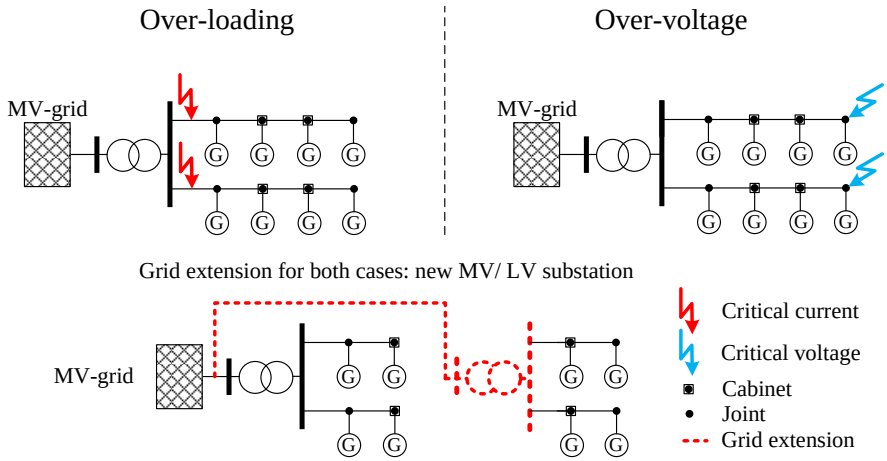

Figure 2.3: LV grid reinforcement via an additional secondary substation

bus bar of the primary substation. At the connection points an additional breaker is installed in the affected feeder.

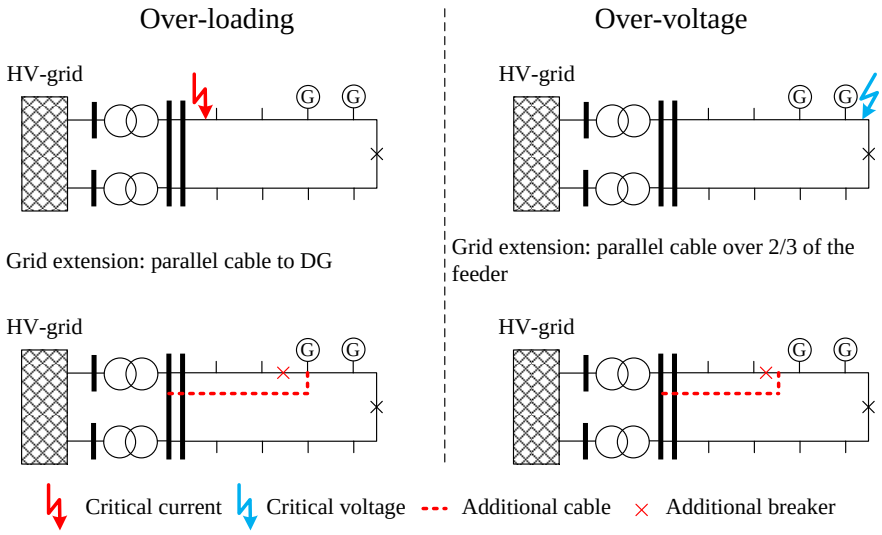

Figure 2.4: MV grid reinforcement via a parallel line

If the parallel cable does not solve the issue, a new MV ring is installed according to Figure 2.5. Through measure the critical part of the affected

open MV ring is circumvented by splitting the ring into two uncritical open MV rings by separating the DG that causes the problems with a parallel MV line. The costs for the earthworks apply only once, as it is assumed that both lines share the same trench.

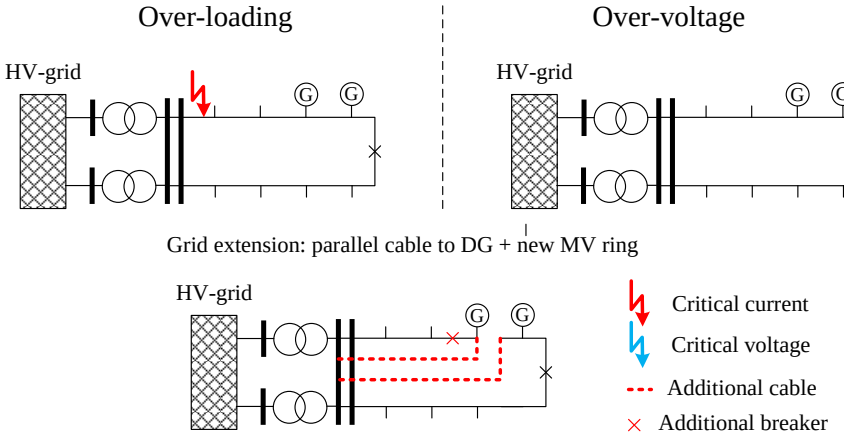

Figure 2.5: MV grid reinforcement via an additional MV ring

If the HV/MV transformer is over-loaded it is replaced with a 40 MVA transformer. If the OL still remains, a parallel 40 MVA transformer for the same feeder is installed. In case all the aforementioned measures do not solve the problems, a new primary substation is installed as depicted in Figure 2.6. In this case, the placements of the new substation and new breakers are done manually, in order to solve all occurring issues in the MV-grid manually.

Other studies [44, 45, 78–80] suggest slightly different approaches and are described briefly hereafter to complete the review of different methodologies. Nonetheless, the methodology of [18] is chosen for this thesis as it has been agreed upon by the largest DSO (covering more than 50 % of the distribution grids in Germany) and can be regarded as state-of-the-art.

[78] considers only the reverse power case as the critical scenario and take into account LV exclusively. Therefore, only OV of $U > 1.09$ p.u. and OL of $> 100\,\%$ are taken into account. If this OV threshold or OL threshold is exceeded, a parallel line ($4x150mm^2$ NAYY) is installed between the secondary substation and the distribution cabinet closest to the critical node within the feeder. If this alone is not sufficient to solve the problems, the existing line is replaced with a $4x240mm^2$ NAYY cable from the distribution cabinet to the critical node. In case of transformer over-loadings or if the replacement of the transformer solves voltage issues in several feeders simultaneously, the

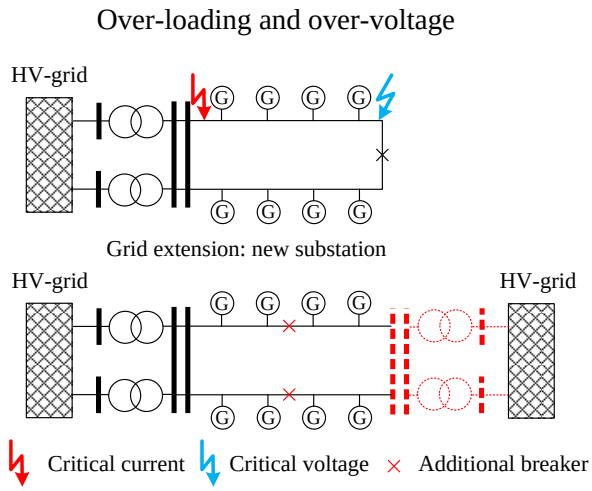

Figure 2.6: MV grid reinforcement via an additional primary substation

transformer is replaced.

In another study only the MV is considered [79]. In this case all threshold violations are solved by installing parallel lines. The same authors also conducted a study only considering the LV [80]. In [80] a three step deterministic algorithm is employed. In the first step it is checked whether the transformer is over-loaded, and if necessary it is replaced by a transformer with the next higher standard nominal power. In the second step, in the case of an over-loaded line, a parallel line from the MV/LV transformer to the closest cabinet of the over-loaded line is installed. The aim of the third step is to prevent critical voltages by installing a parallel line to the cabinet which is closest to the critical node, similar to step two.

[44] analyses MV and LV separately but is very close to the methodology of [18]. The difference in the case of MV is, that the topology is adapted by changing the switching status so that feeders with a high penetration of DG are shortened. It is claimed that as a rule of thumb, MV lines that are longer than 20 km should be avoided. If the switching of lines does not solve the issues, all lines with over-voltages are exchanged with $3x1x240mm^2$ cables. This measure is performed until all critical current and voltage values are within the allowed range. For the LV [44] adopted the measures of [18].

[45] focusses on LV grids. In this study, the allowed node voltage ranges between 0.91 p.u and 1.09 p.u. for scenarios with OLTC transformers (0.01 p.u. is considered as measurement inaccuracy). These threshold values can

be transferred to BSS placed at the LV-busbar of the secondary transformer, since they behave similar, if a reactive power control is integrated in the BSS. In case of line OL of $> 100\,\%$, a $4x300mm^2$ NYY cable is placed parallel to the existing one. In the case of OV a parallel $4x300mm^2$ NYY cable is installed from the secondary transformer to the distribution cabinet closest to the critical node within the feeder, similar to [78].

According to [18, 45, 78] all new lines are supposed to be underground cables, instead of overhead lines due to the higher acceptance of the general public. For an easier automation the reinforcement equipment is standardised but differs from case to case as shown in Table 2.6.

Table 2.6: Standard equipment for grid expansion

Equipment	dena [18]	Stetz et al. [78]	Idlbi et al. [80]	Ackermann et al. [44]
LV-cable (NAYY)	4x150 mm^2	(3x150; 3x240) mm^2	4x150 mm^2	4x150 mm^2
MV/LV tran. ($S_{r,t}$)	630 kVA	(400; 600; 800) kVA	(400; 600; 800; 1000) kVA	630 kVA
MV-cable (NA2XS2Y)	3x1x185 mm^2	-	-	3x1x240 mm^2
HV/MV tran. ($S_{r,t}$)	40 MVA	-	-	-

According to [13], where a statistical analysis of distributions grids in southern Germany is conducted, the NAYY $4x240mm^2$ is the most commonly used cable type in LV (36 % in rural grids, 84 % in villages and 38 % suburban grids) and is used twice as often as any other cable type.

2.4 New Planning Methods for Integrating DG and BSS in Distribution Grids

The aim of the reviewed studies in this section is to determine, besides other network parameters, the optimal number, location and size of DG and BSS units. This is achieved by optimising the total capital expenditures (CAPEX) and operational expenditures (OPEX) including DG and BSS. Several objectives have been pursued via this optimisation of DG integration in distribution grids. Some of the most common objectives are: minimisation of energy losses, maximisation of DG capacity or energy via sizing and allocation of DG, minimising curtailment losses, minimising costs, as well as the minimisation of the grid reinforcement cost associated with DG [81]. The planning process can be described as a non-linear mixed integer optimisation problem. There are several comprehensive reviews for new distribution grid planning approaches. While [82–84] describe and classify the planning approaches from a global perspective, [81, 85, 86] concentrate on DG integration. Hereafter, the criteria and definitions as well as the three-level tree-structure according to [82], which are used to classify the planning methods used in a selection of reviewed studies that are listed in Table 2.7.

According to the first level of the tree-structure, all methods can be divided into models with or without reliability considerations. In planning models without reliability features the grid is operated under operational constraints. The aims of planning optimisations are minimising the CAPEX of substations, feeders or feeder branches (assets), minimising the costs of capacity upgrades of the existing facilities, as well as minimising the OPEX and the energy losses.

In the second level, the models may or may not include uncertainty considerations. In contrast to deterministic planning, uncertainty models consider the unpredictability of future load demand and generation at the design stage. The reliability considerations may be considered in the planning and can be incorporated either under normal conditions or under contingency conditions. To include the maximum network reliability under normal conditions, a reliability objective function minimising the expected outage cost or expected annual non-delivered energy is added to the other objective functions. In order to include predefined fault/ contingency conditions an objective function similar to the aforementioned reliability objective function is employed.

The third level categorises all types of optimisation models depending on the type of (decision) variables and objectives. There are (a) mixed-integer

(b) discrete and (c) continuous models [82]. Commonly, integer variables in distribution system planning problems are used for decisions on whether or not new assets are installed or existing equipment is replaced or extended. Discrete variables are usually used for the dimensioning of the equipment, whereas continuous variables are generally used for voltages and power flows. In mixed-integer models, all three types of variables can be optimised. Discrete and continuous models on the other hand are restricted to discrete and continuous decision variables, respectively. All reviewed studies are categorised within these three models and listed in Table 2.7 including their type of solution strategy. The different solution strategies are discussed in [82] with more detail. For reasons of conciseness the various methods have been denoted with indices, which are used in Table 2.7.

(a) **Mixed-integer models**
Mixed-integer models are the most common ones. They combine binary decision variables (1(Yes), 0(No)) with a set of continuous and discrete variables.

- Mixed-integer linear programming (MILP)[a]
  MILP is a two-step approach. In the first step, an initial solution is determined by solving a linear problem, where all variables are treated as continuous variables, usually using the simplex algorithm. In the second step, successive searches are performed to obtain better solutions for the integer variables.
  For example in [87] MILP is used to determine the achievable gross margin in the different electricity markets for BSS and its resulting operation, as well as for the determination of the storage redispatch and DG curtailment measures and their respective power flows. Whereas, [88] uses MILP to calculate the optimal size and location of feeders and substations over the planning horizon of 10 years.
- Mixed-integer non-linear programming (MINLP)[b]
  MINLP refers to optimisation problems with continuous and discrete variables and a non-linear objective function and/or non-linear constraints.
  In [89] a MINLP is used to decide whether to invest in DG and/or purchase power from the main grid and invest in feeders and substations in case of future load growth. Another approach is used by [90], where the MINLP is formulated as a TRIBE particle swarm optimisation and ordinal optimisation with the aim of minimising

total costs by optimal allocation of DG. Furthermore, the reactive capabilities of different DG and uncertainty in load demand and generation have been analysed. However, BSS have not been considered.

- Bender's decomposition (BD)[c]
  In this algorithm the mixed-integer model is separated into two discrete models: the discrete 'relaxed master problem' and a quadratic 'sub-problem'. First, the master problem is solved to decide on investments in new equipment. Secondly, the quadratic sub-problem is solved to optimise the power flow in order to minimise the operational costs.
  A long-term multi-stage model has been presented by [91] and [92]. This model uses new-path and fencing constraints to reduce the complexity of the solution space. This grid expansion planning method minimises investment costs for growing load demand including DG, similar to [89].

- Genetic algorithm (GA)[d]
  Inspired by natural evolution processes in genetic algorithms generations of individuals exist. Simulating the evolutions of individuals by emulating the process of selection, mutation and recombination of genes, the reproduction is based on fitness functions preferring the best individuals. GA can be used for different purposes in distribution grid planning: In [93] it is used to find the optimal grid topology. In [87]the GA is used for BSS allocation and calculation of grid reinforcement measures. The optimal trade-off between traditional grid expansion and implementation and/or the energy purchase of DG is explored in [94–97].

- Particle swarm optimisation (PSO)[e]
  PSO is another evolutionary algorithm that simulates individuals (particles) in a swarm and their social behaviour. A vector is used to locate every particle and its velocity in the swarm. The population of particles searches for the optimal solutions using the individual experience of the particles and sharing it with the others. The swarm can also return to promising regions found before. It has been employed to allocate DG [90, 98, 99] and/or BSS [100], or on-load tap-changer [79]. PSO might also be used to calculate the minimal reactive power output of DGs to solve OV problems [79].

- Expert system (ES)[f]

Expert systems are knowledge-based systems, that try to emulate the decisions a human would make. Besides heuristic rules a broad data basis like GIS-Data, economic data from asset-management databases, as well as the grid topology and measured data are combined for this purpose to create a semi-automatic grid planning process [101].

Qualitative evaluation
Mixed-integer linear models allow a high degree of generalisation. Nevertheless, in order to optimise real grids, non-linear characteristics like cost functions and grid characteristics have to be linearised. Consequently, the optimal solution is not necessarily the best for the real system, due to the simplifications [102, 103].

(b) **Discrete models**
In these models, discrete and binary variables (yes/ no) are used in the objective function formulation to deal with the decision of finding locations for and sizing of grid facilities.

Qualitative evaluation
Discrete models allow the determination of the timing of reinforcement measures for long term planning, but only discrete variables are allowed. Generally, the same restrictions for large scale systems apply as for mixed integer models due to high number of possibilities [82]. To the authors knowledge discrete models are not applied for DG integration in distribution grids, as no work has been published on this topic in the public domain.

(c) **Continuous models**
In continuous models the considered variables have to be continuous and thus the need for discrete decision variables is eliminated.

- Dynamic programming (DP)[g]
  Dynamic programming allows to represent the ever-changing nature of the planning process. This is realised by modelling the states of the network in nodes with certain states. These states can change in time with every investment in grid reinforcement and are based on the former state. In [104] this method is used to realise a long-term planning (10 years) for the optimal sizing, allocation and most important the timing of investment in DG based on measured parameters (current and voltage).

- Non-linear programming (NLP)[h]
  NLP is a numerical method, which only accepts continuous variables. The most common application for NLP in the context of distribution grid planning is AC optimal power flow (AC-OPF), as used in [87] to minimise active power redispatch for all DG and BSS. NLP is applied by [88] to determine the optimal capacities and production of DG.

Qualitative evaluation
The biggest advantage of these models are, that no linearisation is required making it a good choice for expansion planning purposes of large scale distribution grids. The drawbacks are, besides the large computational effort [76], that these models are badly suited for greenfield considerations [105].

All methods might be either deterministic or consider uncertainty in the model. The uncertainty can be considered by using a possibilistic[y] approach, as it is used in models that apply a fuzzy total installation and operational cost, or a fuzzy non-delivered energy as objective function [82]. A multi-objective optimisation based on fuzzy logic has been presented in [106], where a Bellman-Zadeh algorithm is used to analyse a wide range of technical, economic and environmental criteria to find optimal allocation of DG in distribution grids.

Another approach to handle uncertainty is called probabilistic[z] approach. In this model the uncertainty is calculated by applying a probability distribution function. The power generation or the size of the DG is a common example for a probabilistic approach.

Table 2.7: New distribution grid planning approaches with DG integration

	without reliability		with reliability under normal conditions		with reliability under contingency conditions	
	deterministic	uncertain	deterministic	uncertain	deterministic	uncertain
mixed integer	[89][b], [92][c], [91][c], [88][a,b] [93][d], [101][f], [79][e], [87][a,d]	[107][b,z], [106][y] [108][y]	[100][e], [98][e] [99][e]	[97][d,z] [90][e,z] [94][d,z]	-	[95][d,z]
continuous	[88][h], [87][h]	[104][g,z]	-	-	[96][d]	-

[a]MILP, [b]MINLP, [c]BD, [d]GA, [e]PSO, [f]ES, [g]DP, [h]NLP, [y]possibilistic, [z]probabilistic

As presented in Table 2.7, deterministic approaches without reliability considerations show the highest variety of numerical and evolutionary methods, and are the most commonly used ones. In studies that implement reliability

considerations, evolutionary algorithms seem to be the predominant method, because of their advantage to optimise several criteria at the same time.
In most of the cited studies the DSO is at the same time the owner of the DG, BSS or OLTC-transformer and can decide on the allocation and/or the operating strategy of the equipment [89–100, 104, 106, 107]. Only few works consider that the equipment might be privately owned and operated, as is the case in Germany [79,87,88,101,108]. In Germany, due to unbundling the DSO is normally not the owner of the DG or BSS and therefore has only very little or no influence on the location. Furthermore, the volatile character of the DG, as well as the stochastic behaviour of loads and the possible participation of DG, BSS and loads at the energy market, lead to extreme scenario parameters. Consequently, the grid is over-dimensioned, if the conventional planning based on worst case scenarios is applied. The over-sizing problem remains with the presented new grid distribution planning methods as long as extreme scenarios are used, even if the systematic approach of the new methods eliminate the uncertainty of manual planning. The problem can be solved by applying possibilistic or probabilistic methods. Probabilistic algorithms use probability density functions for loads and generation to quantify the likelihood of grid states, as for example very rare loading situations and can derive the reliability of the electrical power supply. The main drawback is that high quality time-series of the grid participants are needed to generate the probability density functions, which are often not available in LV grids. This applies especially for the active power flow of BSS, since their operation strategy depends on the business case, which itself might depend on the energy market, for instance. Furthermore, the reactive power flow of the BSS, depends on other network participants and on the current grid state. Consequently, to generate realistic time-series, existing interdependencies in the distribution grid as well as business case related issues have to be considered. These time series can be used as an input for any planning optimisation method mentioned above and should be an improvement to traditional worst case considerations.

Several studies combine grid planning with DG and take the active power control of large scale batteries for peak shaving into account [14,98,100,109]. Nevertheless, from the studies mentioned above only [100] and [109] consider reactive power control, even though [110] highly recommends further studies on this issue. This is due to the fact that reactive power control from BSS is a very easy and cost-effective way of voltage control, which is independent from the state of charge of the battery.

2.5 Chapter Summary, Research Gap and Thesis Contribution

In this chapter, traditional approaches and recent advances in distribution grid planning, alongside with alternative possibilities to traditional grid expansion with large scale battery storage systems, are described. A clear methodology for grid expansion measures in distribution grids is presented. Notably, there is a great variety of these models with their respective pros and cons that have to be considered for the given planning task. Nevertheless, the over-sizing problem of traditional grid planning remains, even for advanced grid planning methods, if worst case scenarios are applied. The main issue with most of the reviewed studies is that the DSO is at the same time the owner of the DG and the BSS. Due to unbundling of the energy sector, this ownership structure is not possible in Europe (and thus in Germany neither). Only few works consider that the equipment might be privately owned and operated and don't contribute towards easing OV or OL issues, but might even increase the grid expansion, if they are not operated in a grid supportive way. In this thesis, an expert system is chosen as planning methodology due to its high relevance in an unbundled energy sector, in which the DSO can not generate profits with it and thus has (almost) no influence on the location, the size or the operation of the BSS. The modelled expert system uses heuristic rules for an automatic grid planning process.

Due to the unbundling, it is mandatory to analyse the goals of the two stakeholders of large scale BSS separately. In this thesis the assumed goal of the BSS owner is to maximise profit, and the goal of the DSO is to reduce grid expansion costs. The innovative idea of this thesis is to combine both goals. This is only possible if the BSS is operated in a grid supportive way additionally to its main purpose of earning revenues. This combination (and conflict of interests) is rarely addressed in the reviewed literature, although [110] highly recommends it. Out of all reviewed studies, only [109] considers active and reactive power control of large scale BSS. The limitation of this study is that the application is only analysed for a special island grid of an island of the German North Sea, which does not represent the typical (rural) grid structure in Germany. Furthermore in [109], the reactive power control is implemented with a central approach, which requires additional ICT and an active participation of the DSO. This active role of the DSO is not always pursued, as experiences with the DSO in the SmartPowerFlow project show.

Research Gap

In none of the reviewed studies a combination of a profit orientated market based application and an autonomous voltage control is analysed from a techno-economic perspective. In none, a large scale BSS operation strategy is optimised to maximise profits (for a third party operator) and the potential to reduce grid expansion costs with an autonomous voltage control is quantified (for the DSO). This is especially true for a primary control reserve business cases applied to a large scale VRFB with an additional autonomous voltage control. This research gap is addressed in this thesis with three contributions:

Thesis Contribution 1

It is shown in this chapter that there is a great need for detailed and verified simulation models to generate combined active and reactive power flows of BSS that are profit-driven and grid/ system supportive at the same time. This gap is addressed, by creating two simulation models based on measured values for the most profitable market based business case and the business case with the highest cost reduction potential. Both applications are combined with an autonomous reactive power control. As a result, high quality time-series are created by detailed simulation models, which are applied to distribution grid planning.

Thesis Contribution 2

A techno-economic assessment of both grid supportive business cases applied to a VRFB prototype and a pilot region is conducted. As a result, the possible profits and the additional cost burdens of the grid supportive behaviour for the two business cases are quantified.

Thesis Contribution 3

The high quality time-series for both grid supportive business cases are applied to an alternative distribution grid methodology (expert system). As a result, future grid expansion costs are quantified for a given DG expansion pathway for a pilot region. Finally, the costs are compared with the costs caused by the implementation of large scale BSS (applying the two identified grid supportive business cases) and other more common alternatives to traditional grid expansion.

Chapter 3

Implementation of the BSS Prototype and Modelling of the Pilot Region

In this chapter the implementation of the BSS prototype and the grid model of the pilot region, for a status quo and a future PV expansion is presented.

As described in section 1.3, this work is based on the SmartPowerFlow project of the partners SMA Solar Technology AG, Younicos AG, Lechwerke Verteilnetze GmbH (LVN) and Reiner Lemoine Institut gGmbH. The aim is to evaluate the application of a large scale BSS, developed particularly for this project, as an alternative to traditional grid expansion, including a proof of concept with a field test.

In section section 3.1 the components of the BSS prototype are presented. In the following section 3.2 an overview of the grid area of the distribution grid operator LVN is given, followed by a presentation of the methodology, which has been applied to identify a suitable pilot region within the grid region of LVN. The field test setting and the grid implementation of the BSS prototype in the pilot region is shown section 3.3. The model of the pilot region is presented in section 3.4. A comparison of the time series of a load flow simulation, for a one year period with measured values at the HV/ MV substation, is used to validate the grid model. A PV expansion pathway for this pilot region based on the expansion goals of the Bavarian Government is given in section 3.5. The chapter is concluded in section 3.6.

3.1 Description of the Vanadium Redox Flow Prototype Developed for the Project SmartPowerFlow

The battery system consists of a redox flow battery and a newly developed battery inverter from SMA Solar Technology.

3.1.1 Vanadium Redox Flow Battery (VRFB)

The battery applied in the project is a vanadium redox flow battery with the type designation FB 200-400 delivered by Cellstrom GmbH with a nominal power of 200 kW and a nominal capacity of 400 kWh (further specifications see data sheet appendix B.1). The word *redox* is a conjunct word combing a chemical reduction and oxidation. These kinds of batteries are also called flow batteries as the active material is a liquid electrolyte in which the vanadium is dissolved. The low energy density compared to other electrochemical storages is due to the solubility limit of the salt, making it suitable for stationary applications. The electrolyte of VRFB consists of vanadium ions in different valency states. Charging or discharging changes the valency state. A detailed description of the chemical and physical background is given in [111]. There are plenty of publications discussing the pros and cons of VRFB compared to other battery technologies, as well as their possible applications [112–116]. The unique feature of this technology compared to other batteries is the independence between power and capacity, which provides an additional degree of freedom concerning dimensioning and operation.

3.1.2 Inverter

For the BSS prototype an inverter based on the inverter type CP 630 XT of SMA AG has been developed especially for this project (see Sunny Central Storage 630 data sheet, appendix B.2). The inverter provides a nominal apparent power of 630 kVA (up to 50 °C). As the nominal power of the battery is 200 kW the active power is limited to 200 kW. Unlike common PV inverter, with a operate range of the power factor of $\cos\varphi$ 0.9_{ind} and 0.9_{cap}, this prototype it is able to operate in all four quadrants. Therefore, it is perfectly suited to provide inductive or capacitive reactive power to control the voltage at the point of common coupling.

3.2 Identifying the Pilot Grid for the BSS Implementation

The methodology for an optimal allocation of large scale BSS is described in detail in [71] and is resumed hereafter.

3.2.1 Overview of the Distribution Grid of Lechwerke Verteilnetze GmbH

The examined grid area is more or less identical with the political border of the administrative region of Swabia in Bavaria with a total of 6 895 km^2. The DSO Lechwerke Verteilnetze GmbH (LVN) operates with 860 employees the electrical grid of different grid owners (LEW AG, Überlandwerk Krumbach GmbH and Stadtwerke Augsburg). Furthermore, some parts of Upper Bavaria are supplied with electricity from LVN. At the end of 2013 the grid consisted of 1 785 km HV lines, 7 210 km MV lines and 24 996 km LV lines and cables and around 10 500 local grid transformer stations. According to [67] a cumulated power of 1 544 MW from RES has been connected to the LV until February 2014. This power is distributed to 204 MW from biogas power plants, 21 MW from wind turbines, 69 MW from hydro power plants and 1 249 MW from PV power plants. In vast parts of the region the PV exceeds the average in Germany of 54.3 kW/km^2 by the factor of 3 [117]. Unlike northern Germany with its high shares of wind power, 98 % of the RES are connected to the MV and LV grid. This led to a massive reinforcement of the grid, to solve OV and OL issues. Based on the higher irradiation in southern Germany it is expected that the PV penetration will further increase [117]. The combination of these circumstances makes this grid the perfect test grid to analyse, whether the implementation of BSS may mitigate grid reinforcement measures in the LV and MV level, and to test different applications for large scale battery systems.

3.2.2 Basics of Identifying Critical Voltage Levels

MV and LV grids are coupled in a direct way, hence the last possibility to regulate the voltage directly is via the tap changer of the HV/ MV transformer in a substation. The voltages of every node in the electrical grid depend on the power flows in a given moment. The electrical grid has to be planned to ensure that the voltage stays within the given limits according to [41]. To ensure this, the DSO apply load flow simulations using worst case scenarios, as described in section 2.2. In grids with DG it is possible that

some feeder have a heavy load demand (power flows from substation to the end of the feeder), while at the same time on another feeder there is a reverse power flow (power flows towards the substation). In Figure 3.1 a simplified distribution grid and a worst case scenario is shown to depict the situation. In feeder 1 there is a simultaneous reverse power flow, while whereas in feeder 2 there is a heavy load demand. This leads to a voltage increase towards the end of feeder 1 and to a decrease in feeder 2 (see Figure 3.2). Furthermore the maximum and minimum allowed voltage limits, i.e. Vmin = 0.9 p.u. and Vmax = 1.1 p.u., of the most critical PCC are plotted in red in Figure 3.1. This resulting voltage difference between Vmin and Vmax of 0.20 p.u. can not be compensated by the tap changer of the transformer in the substation.

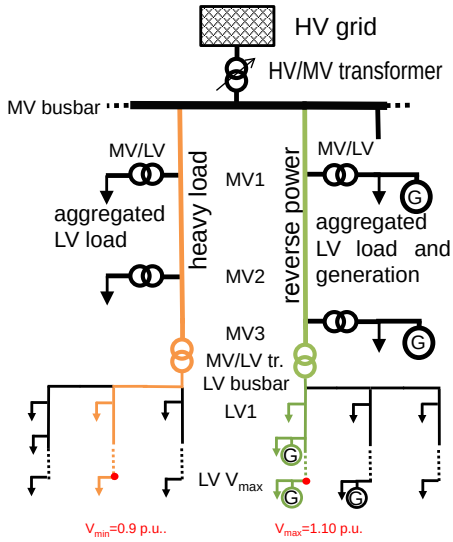

Figure 3.1: Grid schematic with the MV and LV of a simplified distribution grid in the worst case scenario

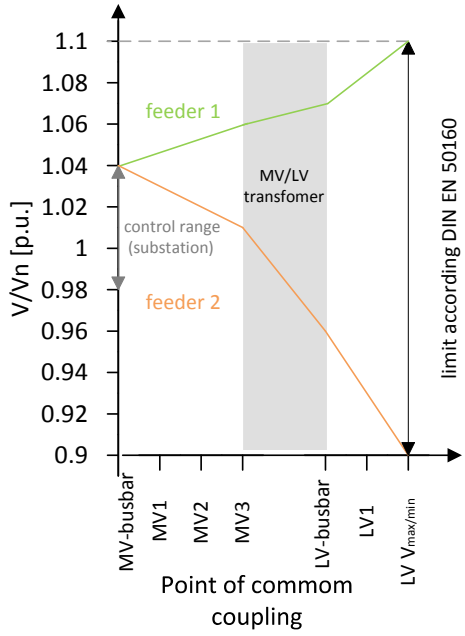

Figure 3.2: Voltage drop/ increase on two feeders from the substation to the PCC with the maximum/minimum voltage

3.2.3 Global Parametrisation of Generators and Loads

As described in section 2.3 and subsection 3.2.2, traditional distribution grid planning is based on power flow calculations with worst case scenarios (heavy load and reverse power flow). To adapt a grid to these assumptions every load and every generator of this grid has to be adapted to these two cases. To achieve this, the grid state adaptation procedure of LVN has been automatised and extended for distribution grids with detailed LV grid information. In a first step, the power of the loads of households, industry and agriculture connected to a PCC on a LV level are parametrised globally whereas the power of the DG are adapted according to the technology. In a second step, for every MV feeder the power of the aggregated LV loads are adjusted via an iterative top down approach to obtain a more realistic worst case scenario (described in the following subsection 3.2.4).

In this section the parameters to adjust the loads and the generator for step one, as mentioned before, are discussed. The installed apparent power of the loads and the generator are adjusted by a coincidence factor and a diversity factor, respectively (see also section 2.3). These factors are empirical, best practise planning assumption or based on literature values and are applied by LVN. They are also used for this BSS allocation methodology.

In the heavy load case peak loads are assumed for industry and agriculture. In the reverse flow case only stand-by losses are considered to calculate the loads. According to [118] these losses are approximately 10 % of the apparent peak load S_{PL} of private households, leading in the case of reverse power flow to a diversity factor of 0.1. This assumption is only valid if more than 150 households are considered. As there is no homogeneous data on standby losses for industry and agriculture the same coincidence factor is assumed for these loads. Some bigger costumers/loads (referred as Costumer load or C. load) have their own secondary transformer and are connected directly to MV. The maximum apparent power S_{cos} of these loads can be assumed to be 40 % of the rated apparent power $S_{r,t}$ of the secondary transformer. The variable coincidence factors for aggregated LV loads for the heavy load flow case x_{HLF} and for the reverse power flow case x_{RPF} are used to calculate the maximal aggregated apparent load S_{agg}.

For the reverse power flow case all DG are assumed to feed in with 90 % of their apparent power. For PV systems a maximal output of 85 % of the power at the maximum power point P_{STC} can be assumed [69, 119]. As the maximal power of PV systems in the grid data from LVN refers to the nominal inverter power, and the inverter is usually under-dimensioned, a diversity factor for PV systems of 0.9 is assumed. For the heavy load case

the feed-in power of the PV system is set to 0 %, for a biomas/biogas power plant (BM) to 80 % and for wind (wind) and hydro power plants to 50 %.

The assumed factors, listed in listed in Table 3.1 and Table 3.2, are not as extreme as the diversity and coincidence factors of the German Energy Agency [18] (see also Table 2.1), resulting in a more realistic extreme scenario.

Table 3.1: Diversity factors for generators connected in MV or LV

	Wind	PV	BG/BM	Hydro
HLF	0.5	0.9	0.8	0.5
RPF	0.9	0	0.9	0.9

Table 3.2: Coincidence factors for loads connected in LV and MV

	Load (LV)	Load (MV)	Costumer load (MV)
HLF	1	x_{HLF}	1
RPF	0.1	x_{RPF}	0.4

3.2.4 Automatic Adaptation of Aggregated Low Voltage Loads to Worst Case Assumptions

In this section, a method to automatically adapt aggregated LV loads to worst case assumptions, based on the planning approach of the LVN, is presented. In the previous paragraph the parametrisation of the loads of private households, industrial and agricultural costumers, as well as the costumers with own transformers and a PCC in the MV, has been discussed. Nevertheless, the biggest unknown factor in the distribution grid planning remains the coincidence factor of the aggregated LV loads. To calculate it for these loads for each MV feeder of the distribution grid the cetris paribus assumption is applied. In the heavy load case, all factors of Table 3.1 and Table 3.2 are hold constant, whereas x_{HLF} is varied till the set power at the node, where the MV feeder is connected to the MV busbar of the HV/ MV substation, is reached. This set point is appraised via measurement data at the substation and the threshold is set according to the investigated scenario. This is repeated for every MV feeder of the substation until x_{HLF} for every feeder is determined. For the substations of LVN there is a constant measurement of active power P, reactive power Q, current I and the voltage V of the MV busbar in 15 min steps. The method is depicted in Figure 3.3.

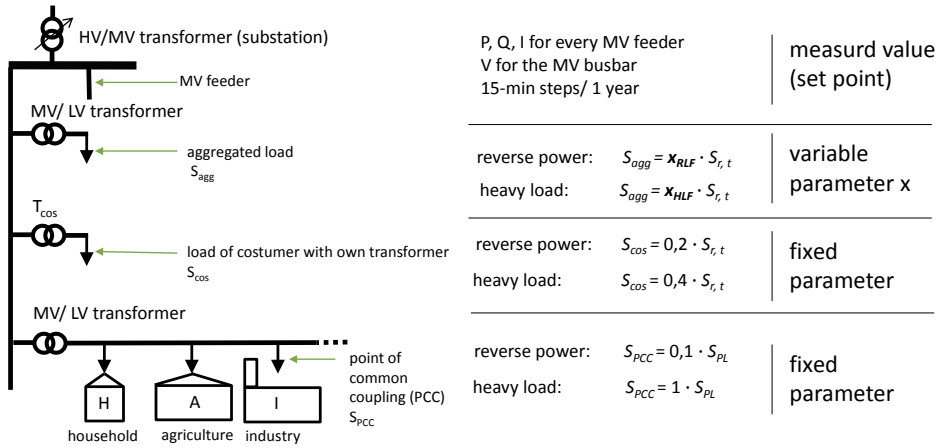

Figure 3.3: Schematic representation for the calculation of the coincidence factor x_{HLF} and x_{RPF} for the aggregated LV loads

3.2.5 Allocation Algorithm

According to the current legal framework the DSO is obliged to implement grid expansion measures whenever permitted tolerance limits are exceeded. The economic aspect of these grid reinforcement measures is coupled to questions when it will take place and how high the CAPEX will be. The presented heuristic allocation algorithm searches for locations where potential grid reinforcement costs are high and have to be realized in a short term. The fundamental question therefore is:

At which location and distribution grid, out of several possible distribution grids, does a BSS minimise grid expansion costs?

To answer this question the factors that lead to maximum grid expansion expenditures have to be identified. There is a location and time dependant component to the answer. The location is evaluated by the quantity of components that can be relieved by the BSS and by their CAPEX as well. The time dependant component analyses if the investment has to be realised in short or long term and if the investment can be mitigated or even prevented. There is a increased inconvenience of discounting short term investment compared to mid or long term investment if the CAPEX are the same. At the same time large scale BSS should relief a whole grid area and not only one critical node. Nevertheless, OV problems have to be solved close to where

they occur, which means in the LV part of the grid. For this reason, locations on the LV busbar of an MV/ LV transformer are analysed, in order to control the voltage with the reactive power from the power electronics of the BSS

As the OV issues in the analysed distribution grid of LVN are mainly induced by PV systems, the BSS is installed in a LV grid where the voltage is close to the upper limit of the nominal voltage V_n of 1.1 p.u. (according to DIN EN 50160). The voltage control of the BSS can be used to decouple the LV grid from the MV grid and use the bandwidth of $V_n \pm 10\,\%$ (0.2 p.u.) to increase the hosting capacity for PV systems without a grid reinforcement in this grid area. Furthermore, LV grids in the same MV feed are also relieved and the voltage can be manipulated with the BSS, but in a far smaller extend as the LV grid to which the BSS is connected. Another reason to install the BSS on the busbar and not closer to the end of a LV feeder is that, depending on the application of the battery, OL of the LV cable may occur when installed at the end of the line.

Since short term grid reinforcements measures should be prevented, the grids with most critical OV issues have a high priority. The OV on a PCC is to be considered critical if it can not be regulated by the tap changer of the HV/ MV transformer of the substation(see also Figure 3.2). This is the case if the voltage difference between two nodes in LV of two different MV feeders is higher than 0.2 p.u..

If a homogeneous installation of additional PV system is postulated, grid reinforcement measures have to be executed to reduce the voltage on this critical PCC. Considering the worst case scenario the feeder pair with the highest voltage difference has to be found. If all maximal voltage spreads ΔV_{max} are summed to one value for a local LV grid this value is referred hereafter as $\sum \Delta V_{max}$. The threshold value $\sum \Delta V_{thres}$ is introduced to avoid that local grids with a high amount of LV feeder but a LV spread achieves a high $\sum \Delta V_{max}$ value. The more LV feeders exceed the given threshold value ΔV_{thres} the higher the short term CAPEX for grid expansion measures. ΔV_{thres} has been set in accordance with the experts of the DSO LVN to 0.15 p.u.. Therefore, ΔV_{max} can be considered as an indicator for grid expansion costs. Figure 3.4 depicts an exemplary distribution grid, with a heavy load case on feeder A and a reverse power flow on feeder B.

In the whole distribution grid the LV loads and LV generators are connected as an aggregated generator or load directly to the LV busbar of the distribution transformer. If the topology of the LV grid is available, LV loads and LV generators are connected individually to a PCC . The described PCC are marked in red in the figure. In feeder A a heavy load case is assumed.

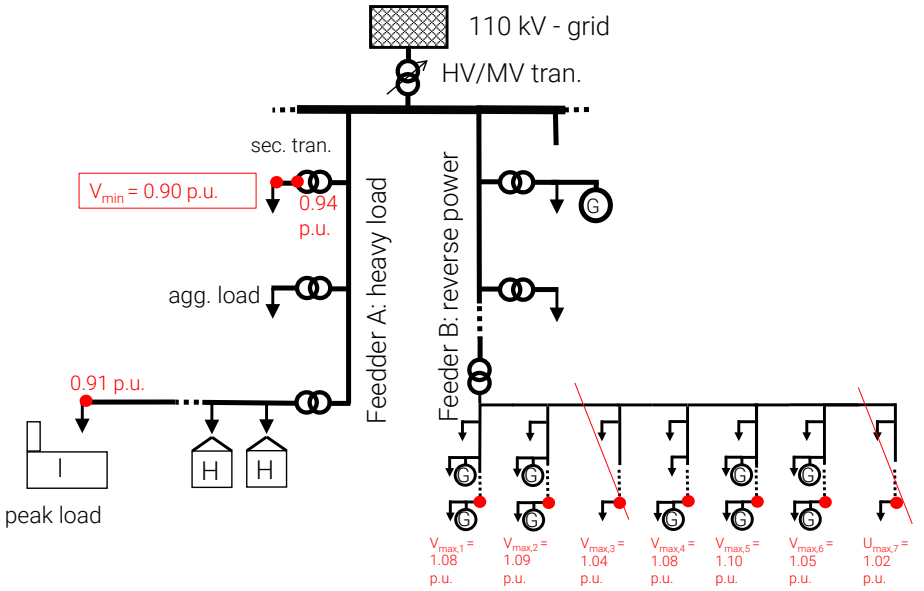

Figure 3.4: Schematic representation of the calculation of the parameter $\sum \Delta V_{max}$

As a result, one of the nodes in a LV grid shows a minimal voltage of 0.91 p.u.. Furthermore, on another distribution transformer an aggregated load is connected which reduces the voltage of this node to 0.94 p.u.. To calculate the voltage drop in the LV feeder a voltage drop of 0.04 p.u., as in [18], is assumed. The minimal voltage of this local grid is therefore 0.9 p.u.. In this example it is the lowest voltage in the feeder V_{min} and marked with a red frame in Figure 3.4.

On feeder B there is a reverse power flow. For every LV feeder n the maximum voltage $V_{max,n}$ is taken into account. In the case the voltage spread of $V_{max,n}$ and V_{min} is equal or higher than ΔV_{thres} the spread is summed to $\sum \Delta V_{max}$ for this local LV grid, with the following equation:

$$\sum \Delta V_{max} = \sum_{i=1}^{n} (V_{max,i} - V_{min}) \tag{3.1}$$

where i is the number of the LV feeder, in which the ΔV_{max} value is equal or higher than ΔV_{thres}. For the given example, the LV grid under consideration has a $\sum \Delta V_{max}$ value of 0.9 p.u.. The advantage of this method is that an indicator is defined, which allows a comparison of low voltage grids of different distribution grids and therefore allows the optimal allocation of

large scale BSS within a whole grid area with different distribution grids.

3.2.6 Implementation, Results and General Conclusions

The allocation search algorithm can be described as an optimization problem. To solve it a brute force method is applied, in which all possible combinations are calculated and the maximum of the sum of voltage spreads $\sum \Delta V_{max}$ for a number of given local grids is found.

To determine the techno-economic optimal allocation for large scale batteries the method presented in this chapter has been implemented in MATLAB. Before applying the search algorithm, the parametrisation of the distribution grids for the worst case scenarios as described in subsection 3.2.3 and subsection 3.2.4 has to be conducted in advance. As output an Excel-list is created that prioritizes the given LV grids according to the $\sum \Delta V_{max}$ in descending order. With a standard off-the-shelf desktop PC (i5-2520M CPU @ 2.50GHz) the calculation time takes less than 10 min.

The search algorithm has been tested with different distribution grids of the distribution system operator LVN of Swabia in southern Germany. The DSO preselected 80 local LV grids spread over eleven different distribution grids with a high share of PV systems installed in the LV. The search algorithm has been applied to these potential LV grids. In total 15.461 nodes of eleven real distribution grids of the grid area of LVN have been analysed.

The calculated values for $\sum \Delta V_{max}$ lie within 0 and 1.60 p.u. with one to eight LV feeder that show critical voltages for every local LV grid. An excerpt of the resulting Excel list is depicted in appendix B.3. This list has been used to allocate the large scale battery prototype as described in section 3.3. By analysing the grid parameters of the five most promising potential battery locations three general selection criteria were deduced. Besides voltage criteria several other criteria, like installed PV power and data of the grid topology, have been taken into account. The following three selection criteria can be used by distribution system operators to easily preselect local LV grids as potential battery locations in their electrical grid.

- The LV grid is located in the second half of a MV feeder with a high share of PV systems.
- Within the LV grid the installed nominal PV power exceeds the 50 % of the rated apparent power of the MV/ LV transformer. Furthermore their point of common coupling is spread over half of the LV feeders.
- In another MV feeder there is at least one node with an under-voltage in a local LV grid.

Besides these techno-economic planning criteria other practical issues like noise emission of the BSS, the load of the MV/ LV transformer and the accessibility of the locations have to be considered. Because of these issues, the location with the highest priority has not been selected for the field test of the BSS, but rather number 14 out of 80 (see appendix B.3).

3.3 System Description and Grid Implementation

The vanadium redox flow BSS prototype developed for the project SmartPowerFlow has been integrated end of may 2015 in the pilot grid selected by the allocation algorithm presented in the previous section. As stated before, the pilot grid has been selected from 80 possible locations, inter alia because of the high PV density in this area, as can be seen in Figure 3.5, in which the BSS is depicted along with its surroundings.

Figure 3.5: Aerial photo of the SmartPowerFlow BSS prototype.

In Figure 3.6 a simplified connection schematic of the BSS is depicted. As can be seen, the system is connected to the power grid on the power side and to the control room of LVN on the communication side. A SCADA connection to the DSO's control room (realised with the communication protocol IEC60870-5-104) is not usual and thus represents a special feature of the project SmartPowerFlow. It serves both the monitoring of the system and the possibility of remote control.

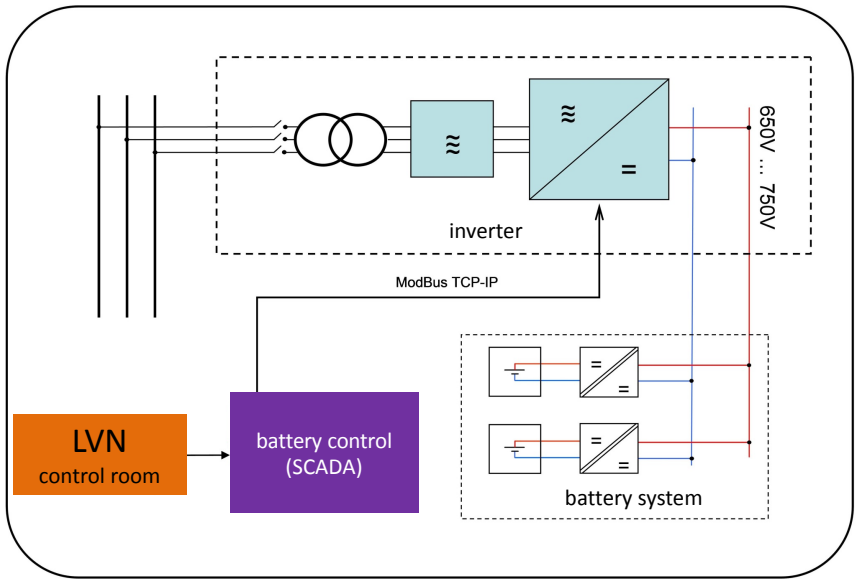

Figure 3.6: Electrical and communication schematics of the SmartPowerFlow battery storage system.

The inverter and vanadium redox flow battery described in section 3.1 were combined with a SCADA system. The SCADA system, consisting of energy and battery management system, was especially developed by Younicos AG for the project. It was implemented on a Bachmann MPC 240 industrial computer and represents the heart of the communication between the grid control room, battery and inverter.

The battery system was connected to a LV busbar, as depicted in Figure 3.7. The single line circuit diagram of the battery system is depicted together with other implementation details in appendix B.5.

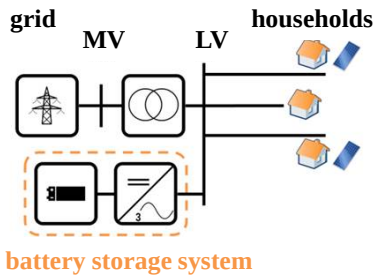

Figure 3.7: Simple grid connection schematic of the BSS

The reason for the connection of the BSS to the MV/LV transformer station, and not to a LV feeder, is the grid supportive focus of the SmartPowerFlow project, since the thesis core objective is to maximise the hosting capacity for renewable energy systems. Accordingly, the position of the battery was selected, such as not to stress the electrical grid additionally, but on the contrary relieving the largest possible grid area (if possible).

However, as explained in chapter 1, the application of market driven business models is suitable for an economic operation of large batteries at the distribution grid level and therefore the battery should respond to the current market situation in its active power output (for example reserve power market) and not on the current grid situation. Thus, it is necessary to install the battery in a location where the market-driven active power delivery does not cause any additional grid expansion measures. At the distribution grid level, these measures are triggered mainly by voltage problems, as mentioned in chapter 1. As the active power output at the LV busbar of the MV/LV-transformer has only a minimal effect on the voltage in the local LV grid due to the more favorable R/X ratio compared to LV lines, the decision was made to search specifically for such locations in subsection 3.2.5. Another reason for busbar a connection was not to increase the thermal load of the LV lines additionally by using the battery. Furthermore, the reactive power applied by the BSS on the LV busbar, can regulate the voltage in the entire LV grid and thus increase its hosting capacity in a similar way a MV/LV transformer with on-load tap changer (OLTC) would do.

It has been shown in the field test that the BSS prototype can be grid supportive in spite of an unfavourable active power output. A proof of concept which has been conducted in the LV grid during a high irradiance day in summer 2015, is depicted in Figure 3.8.

As shown in the graph, the BSS is discharging with its maximal (active) power of 200 kW and thus has a behaviour like a generator. Additionally, there is a reverse power flow from the LV-grid to the MV-grid of 300 kW due to the high PV-system power installed in this LV grid. Nevertheless, the grid voltage at the LV-busbar could be decreased due to a reactive power output of 500 kvar (inductive) from the battery system. This voltage reduction affects all LV-feeder of this LV grid and relives this grid from OV issues caused by the PV systems for instance. Thus, the BSS increases the hosting capacity for this LV grid in spite of a maximal active power grid feed-in.

For flexible storage use, three operating modes have been defined in which the BSS can operate. These operating modes can be switched on-site and remotely:

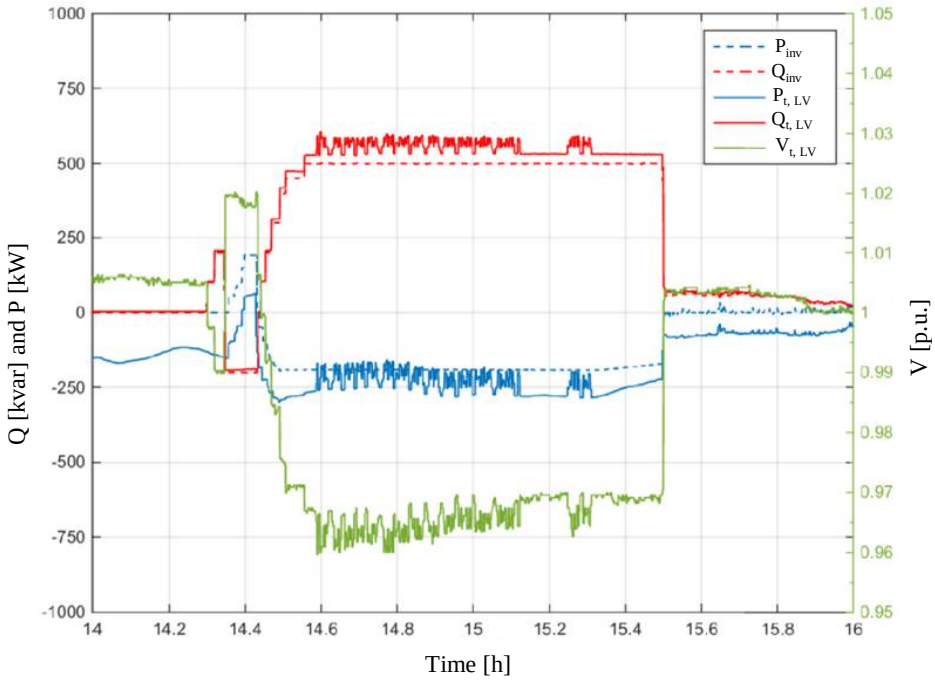

Figure 3.8: Demonstration of the grid supportive behaviour of the BSS prototype in spite of maximal grid feed-in (load perspective); measured values on day 19/8/2015 P_{inv} is the active power and Q_{inv} the reactive power measured at the inverter output, $P_{t,LV}$ is the active power, $Q_{t,LV}$ the reactive power and $V_{t,LV}$ the voltage measured at the LV busbar of the MV/ LV transformer.

- Active and reactive power are set by the DSO.
- P(f) and Q(V)-charcteristics can be set separately with up to four set-points each (e.g. for primary control reserve).
- Schedule operation mode for active and reactive power (24 set points for one day) (e.g. for self-consumption maximisation or trading at the energy market).

A special feature of the battery system is that it was designed with two separate P(f) and Q(V)-characteristics according to different needs. This enables the BSS operator to optimise this operation strategy. Furthermore the BSS is able to work autonomously, which is one of the main requisites of

the BSS control (see also chapter 2), since neither the BSS operator nor the DSO plan to remote-control the BSS continuously.

Both the P(f) and Q(V) characteristics can be defined by setting four pairs of values between which linear interpolation is performed. These set points can be 175 kW and 49.8 Hz for the P(f)-control or 400 kvar and 420 V for the Q(V)-control for instance. Examples for the P(f) and Q(V) characteristics are depicted in Figure 4.1 and Figure 5.10. In case of an activated P(f)-opertion mode, the degrees of freedom defined by the transmission system operators and explained in chapter 4 may be used additionally.

To monitor and control the battery system, three SENTRON PAC3200 measuring systems from Siemens AG were installed. They were installed at the LV busbar of the MV/ LV transformer, the auxiliary power feeder and at the PCC of the battery system (see communication scheme Figure B.7 and auxiliary power diagram Figure B.8 in the appendix). The PAC3200 provide, together with the internal measuring instruments of the Cellcube and the inverter, the measuring data needed by the MPC 240 for a real time monitoring and control. The MPC 240 sends the data to a server at the Reiner Lemoine Institut in Berlin and to the control room of the DSO. Furthermore, the MPC 240 uses the measurements to autonomously control the battery system (via a P(f) or Q(V) characteristic for example (see above)).

The installed measuring devices transmit current, voltage as well as active and reactive power (per phase) from the respective measuring points to the industrial computer. In addition, they transmit the measured grid frequency. The internal measuring instruments of the Cellcube supply the MPC 240 with the state of charge, the electrolyte temperature as well as the DC active input and output power of the battery. In addition, the inverter transmits the active and reactive power values (three-phase) to the MPC 240 at its AC connection point. The measurement resolution is at 10 seconds for all values. An exception is grid frequency and the measured active power at the AC connection point of the inverter. These have a second-by-second measurement resolution. The reason for this is that the battery system should be tested for application in the primary control power market, which requires resolution of these values in one second steps (see chapter 5).

This chapter shows that the battery system has been designed in such a way that it can be used in a variety of applications and can operate autonomously. The aim is to show that a autonomous grid supportive and at the same time profitable operation of the battery system is possible. Thus, the selected system design is suitable to show and proof the thesis goals described in chapter 2 and the more specific requisites of chapter 3.

3.4 Grid Model of the Pilot Region

The model of the electrical grid in which the BSS is integrated is presented and validated in this section.

3.4.1 Grid Model

The grid model consists of one MV feeder of the distribution grid in which the VRFB is implemented. The MV feeder is connected to the HV via a 20 kV/ 110 kV transformer. The slack is located on the HV side of the transformer and its tap ratio is set to reach the voltage of 1.03 p.u. at the MV busbar at the substation. The total length of the MV feeder is 20.2 km and 44 LV grids are connected to it. Twelve of these LV grids form a village which is simulated in detail, whereas the other 32 LV grids are simulated in an aggregated way. The configuration of the grid consists of different elements: loads, generators, lines and transformers. These elements are distributed along the grid on 1208 nodes.

Loads

A total of 470 loads are connected to the grid. 441 individual loads are located inside the village and 29 accumulated loads in the surrounding area. To model the consumption behaviour, three different German standard load profiles [120] in one-minute time steps are employed, along with heat pump profiles [121] for four houses. The distribution of the different profiles is as follows: 264 loads with a H0 household profile, 38 commercial loads with a G0 profile and 35 agricultural loads with a L0 load profile [120]. Additionally, a real heat pump profile from [121] is used in four houses. For the 29 accumulated loads a residential load profile (H0) is used. To dimension the accumulated load a coincidence factor was deduced by analysing 17 different MV feeders of eleven distribution grids within the grid area of the DSO. The mean coincidence factor is quantified to be 17 % of the rated power of the MV/ LV transformer apparent power, which agrees well with the coincidence factor of 15 % assumed in [18].

To adjust the normalised load profiles the measured historical yearly load consumption from 2013 is used in the village. The maximum total yearly consumption of the village is 3.73 GWh. A fixed power factor of 0.97 (inductive) is assumed for all loads.

Generators

The generated power in this LV grid consists of a group of different types of generators. Along the MV feeder there are 30 aggregated PV systems and 119 residential PV systems with a total power of 7.7 MVA, four (small) hydro power plants with an aggregated power of 0.51 MVA and one biogas plant of 0.35 MVA. The PV power profile is based on measured data in one-minute time steps from 2013-2014, and from a south oriented PV system with a nominal power of 107kWp, which is connected to a nearby village (10km). These values were measured on a south oriented system with a nominal power of 107 kWp. The normalised PV profile is adjusted by multiplying it with each PV system's nominal power. In order to take into account different orientations, cloud impact etc. the diversity factor for the PV systems', as defined in [68], is set to 0.85 [69]. If several PV systems are connected to the same PCC they were treated as one PV system with the sum of the nominal powers of the single system.

For the hydro generator a normalised load profile was calculated with the aid of generation profiles of several hydro plants located in the South of Germany and published at the EEX Transparency Platform [122]. The biogas plant was assumed to operate at full power for every time step, according to measured data from a biogas plant in upper Bavaria at the period between 2012 and 2014.

Transformers

Within the village there are 12 MV/LV transformers (20kV/0.4kV), as depicted in Fig. 3.14 and listed in Table 3.3. In the surrounding area the remaining 32 MV/LV transformers are connected to the same MV feeder.

Table 3.3: Transformer types within the village.

Rated apparent power of transformer $S_{r,\,t}$ [kVA]											
T1	T2	T3	T4	T5	T6	T7	T8	T9	T10	T11	T12
1000	160	160	250	160	400	250	160	400	400	400	250

Lines

The loads, generators and transformers are connected via 1210 lines. For the twelve LV grids of the village (named after their MV/LV transformers T1 to

T12), the R/X ratio varies between 2.3 (T9) and 5.9 (T7) with a mean value of 3.5.

Table 3.4: R/X ratios of the LV grids in the village.

T1	T2	T3	T4	T5	T6	T7	T8	T9	T10	T11	T12
2.6	2.8	3.2	3.0	3.5	4.2	5.9	3.0	2.3	4.8	2.6	3.8

An overview of the three most common line types and lengths for this distribution grid is listed in Table 3.5.

Table 3.5: Common lines types for LV and MV.

	LV (only in village)			MV		
Type	NAYY	NYY	NAYY	NA2X2Y		
Diameter $[mm^2]$	70	95	150	150	185	300
Length $[km]$	5.6	3.7	5.7	10.1	2.1	4.7

3.4.2 Validation of the Grid Model

To validate the simulated grid model the difference between the measured and the simulated active power at the slack is depicted in Figure 3.9. The histogram shows the results of a yearly simulation in 1-min steps of the baseline scenario. It can be seen that the simulated active powers P are higher than the measured ones, thus showing a more extreme grid state in the simulation. Although, the data for the simulation is based on the years 2012-2014 and the data of the substation is from 2015, the graph shows a statistical correlation, nonetheless.

3.5 Modelling a Expansion Pathway for Photovoltaic Systems

In order to assess a hosting capacity for the pilot grid, a spatially resolved forecast must be made for the DG (see also chapter 7). Since PV systems in the grid area of LVN represent by far the largest share of installed DG capacity in recent years (see Figure 1.1) and bigger DG tend to be connected to the MV level, the expansion pathway is limited to PV rooftop systems. The aim of the presented methodology is to predict the size and location of

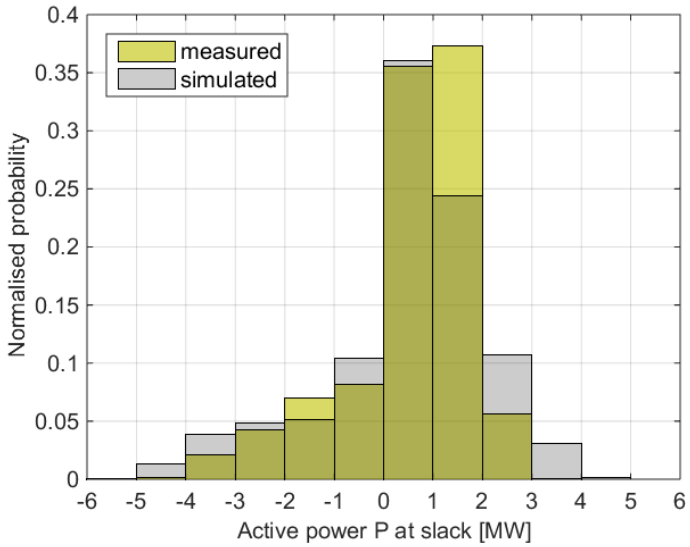

Figure 3.9: Histogram of the active power P of the MV busbar (slack) of the HV/MV transformer at the substation of the pilot grid.

future PV systems on rooftops, based on data that is generally accessible and easily reproducible on a building scale for other rural villages. As input data high-resolution aerial imagery, GIS building footprints from the Land-register map and the Bavarian database of PV systems are used. In addition, the method is tested applying two types of images: a) official orthophotos from the Bavarian Land-survey Office and b) Google Earth^{TM} orthophotos, to assess the accuracy of freely available data to the project. The results are compared with each other on the discussion section. The methodology is based on [123] and depicted in Figure 3.10. For this work the methodology was applied to the pilot grid and the village Tussenhausen. Furthermore, only open data and open source software are used, so that the methodology can be reproduced easily.

Identification of Suitable Building Rooftops

To accurately quantify the available rooftop area for PV installation, high-resolution orthophotos from the Bavarian Land-survey Office and Google Earth^{TM} images (both recorded RGB bands with 0.2 m and 0.4 m spatial resolution respectably) are processed to identify suitable rooftop areas, roof obstructions and shadows. First, the current status quo is analysed, cross-

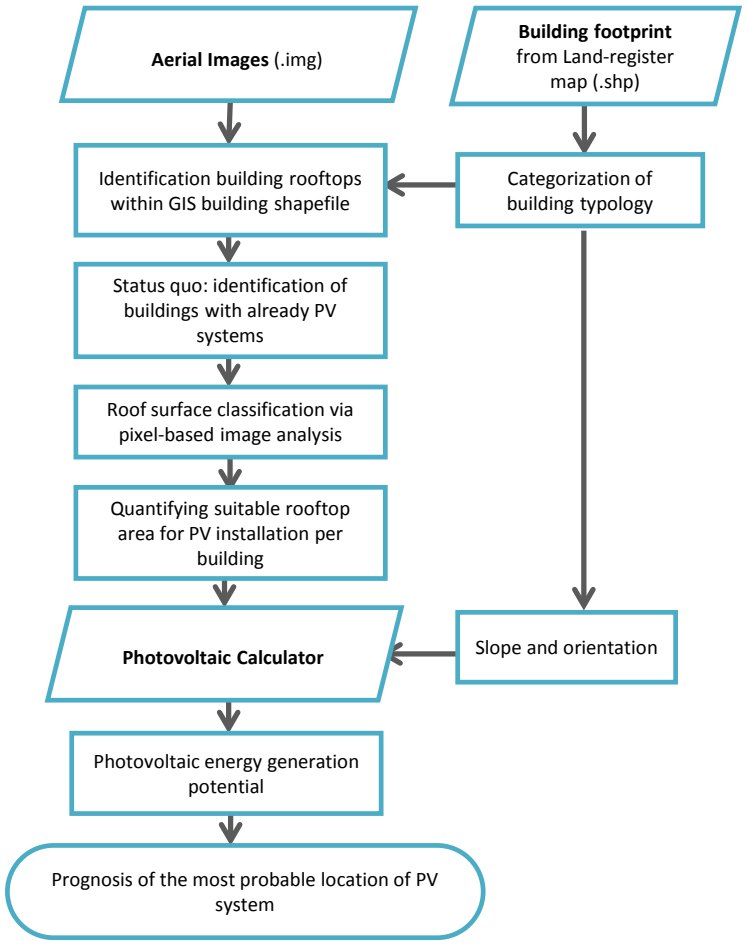

Figure 3.10: Applied methodology to estimate spatial distributed PV potential in rural communities [123].

referencing the files from the Bavarian register of PV systems [124] and the Land-register map. The Bavarian Register of PV systems offers free access throughout its web page. These buildings were then excluded from the dataset in order to avoid assigning them as potential buildings in the future. Building rooftops were isolated cropping the images with building footprints from the Land-register map. Directly integrating the building footprint shape file limits the subsequent pixel-based image analysis within the rooftop surface and thus excludes data from outside the building rooftop. An example

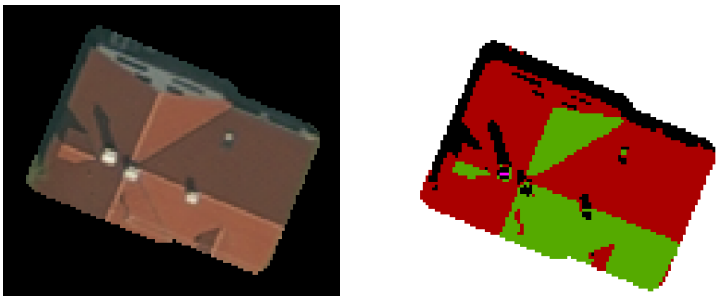

(a) (b)

Figure 3.11: Original orthophoto clipped by the building footprint (a) and (b) classified output after supervised image classification [black=shadow, red=non suitable, green=suitable, pink=obstruction].

of an original orthophoto clipped by the building footprint cross-referenced is depicted in Figure 3.11(a).

Calculation of Suitable Rooftop Area

To identify the suitable areas per rooftop, a supervised image classification is conducted on the subset image of the building rooftops. The purpose is to identify four zones: (1) shadows, (2) obstructions, (3) suitable areas, (4) non-suitable areas. The expansion of semi-automatic image classification from QGIS was used to perform this step, seeking to build a methodology based on accessible data and open-source software. The output of the image classification analysis, shown in Figure 3.11(b), is converted to vector data and the potential suitable area is assigned to each building. The rooftop orientation and average slope are spatially joined to each rooftop.

PV Energy Calculation and Prognosis Expansion Pathway

The yearly yield of every PV system is calculated with the open source python tool pvlib-python [125] using size, orientation, tilt and type of every PV system as well as weather data. The weather data used are extracted from the CoastDat2 dataset of the Helmholtz-Zentrum Geesthacht [126]. Every PV system is ranked according to its specific annual yield (ratio of annual energy production to installed power in kWh/kW_p). The PV system with the highest yield is ranked best and will be installed first and so on. In the

next step, based on the aims of the Bavarian Government every PV system is assigned a year of grid connection. The aim of the government is to increase the share of electricity from PV systems from 9.1 % in 2012 to 22-25 % in 2025 [127]. Thus, the installed PV capacity has to be increased by the factor of 2.5. This means that for Tussenhausen the installed PV capacity has to be increased from 2134 kW_p to 4579 kW_p. A linear expansion is assumed until all additional systems are installed until 2040.

Results

In 2012 2.1 MW_p were installed (status quo marked in blue in Figure 3.12(a)). The classification of the orthophotos of the Bavarian Surveying Administration and Google Earth^{TM} showed that about 80 % of the remaining buildings are suitable for the installation of a PV system with roof areas with more than 6 m^2 respectively. Of the roof areas of suitable buildings, about 40 % are suitable for PV systems. These surfaces are shown in Figure 3.12(a). The total technical PV potential of the village is calculated to 7.6 MW_p, with system sizes between 1 kW_p and 130 kW_p. In Figure 3.12(b) the specific yield potentials of the buildings which determine the expansion ranking are shown. According to the ranking between 2012 and 2025 PV systems will be installed on 203 buildings (see Figure 3.13). In 2025 a total of 4.6 MW_p of PV systems will be integrated. A linear expansion is assumed until all additional systems are installed on the remaining 208 buildings until 2040, reaching the full PV potential of Tussenhausen of 7.6 MW_p (marked in orange Figure 3.14).

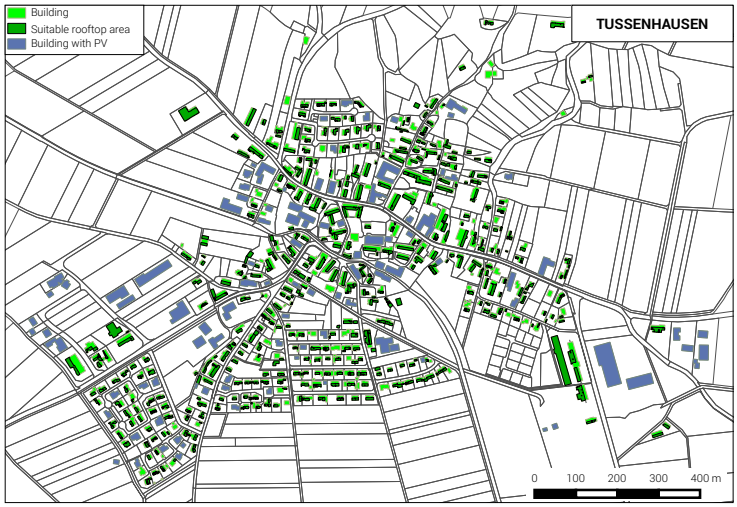

(a)

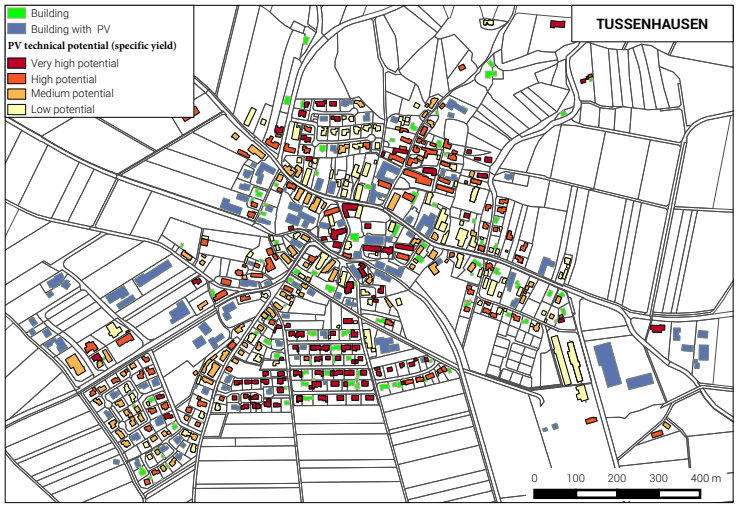

(b)

Figure 3.12: Suitable rooftop areas for PV systems (a) and specific yield of these PV systems (b).

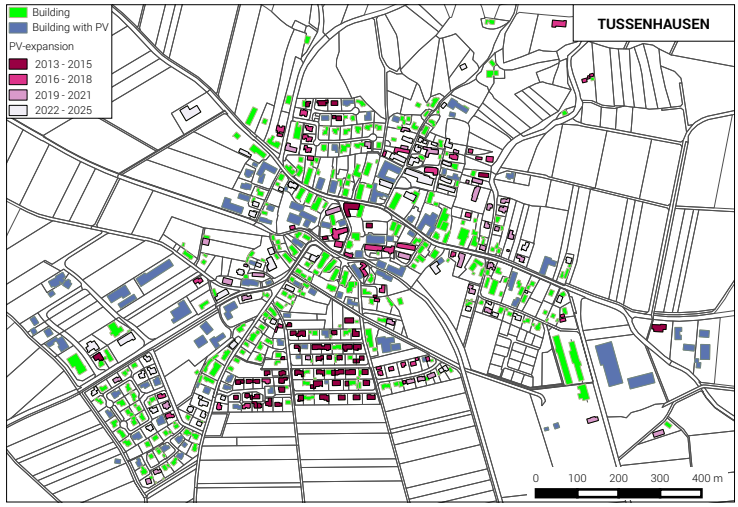

Figure 3.13: PV-expansion pathway from 2013 till 2025.

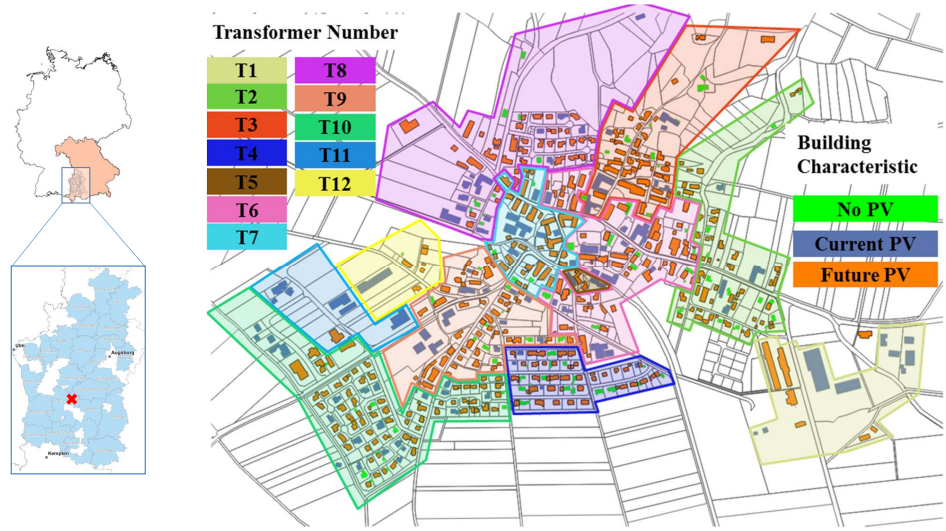

Figure 3.14: Buildings in the village highlighted according to the MV/ LV transformers (LV-grids) and expansion pathway of PV systems until 2040.

3.6 Chapter Summary

In this chapter the foundations are laid for a comprehensive and coherent approach to investigate the research objectives of this thesis.

First, the components of the BSS prototype are presented. Furthermore, an allocation search algorithm to find a BSS allocation within the DSO grid area is developed and applied. The aim is to find a search criteria, which allows to find a location on which the BSS prevents the highest grid expansion costs for a given grid area. Besides fulfilling this aim, the presented criteria allows also a comparison of locations of different distribution grids and is applied to create a ranking list of given possible allocations. This list is used to find the pilot grid in which the BSS prototype is installed. Furthermore, three selection criteria are identified to preselect potential BSS locations.

The implementation of the BSS in the pilot region is followed by a proof of concept. The latter reveals that the BSS is able to operate autonomously and is able to reduce the voltage at the PCC in spite of an unfavourable active power flow. This is due to the location of the BSS and its ability to operate with separate active and reactive power control strategies. Thus, the active power can be used to generate profit and the reactive power to exhibit a grid supportive behaviour and increase the hosting capacity of the LV grid to which the BSS is connected.

In order to conduct steady-state load flow calculations of the pilot region, the pilot grid is modelled. A load flow simulation of the grid model for one year is conducted and compared with measured values of the same grid. Through this, the status quo of pilot grid model could also be validated successfully.

Finally, a PV expansion pathway, in accordance with the expansion goals of the Bavarian Government is modelled and presented. This expansion is used, inter alia, to asses the grid supportive behaviour by calculating the additional hosting capacity and future grid expansion costs that can be reached with the implementation of large scale BSS and other flexibility options.

Chapter 4

Economic Analysis of Large Scale Battery Applications in Germany

Possible single and combined BSS applications are analysed in this chapter. The aim is to identify and select the two most profitable applications. Thus, in depth technical and economical assessments of both business opportunities are performed in chapter 5 and chapter 6 by applying them to the SPF prototype. The impact on the distribution grid planning by the two applications is analysed in chapter 7.

In section 4.1 large scale BSS applications along the electricity value chain in Germany are analysed. After a short description of each application, the section is concluded with a benefit estimation. The two most promising applications for large scale BSS are identified and analysed further in section 4.2 and section 4.3.

The application with the highest revenue potential (PCR) for market based applications is assessed in section 4.2, since. The legal framework and the technical restrictions for the PCR applications are presented and discussed in detail. They determine the operation strategy, as well as the size of the BSS. Finally, the PCR application is compared with other single and combined BSS applications in order to select the most profitable one.

The application with the highest cost reduction potential (maximisation of self-consumption) is assessed primarily in section 4.3. The actual legal framework of applying large scale BSS to this business case is discussed in detail. Further, the different charges, levies and taxes that occur for different scenarios are presented.

Finally, the chapter is concluded in section 4.4.

4.1 Analysis of Potential Revenue Streams for Large Scale BSS Applications

In broad terms, there are two ways to gain monetary benefits along the electricity value chain with existing BSS applications in the German electricity market: first, revenues received by the storage owner or operator and second, cost reduction or avoidance by the storage owner or operator [128]. Generally, revenues can be achieved through existing markets and bilateral contracts. Cost reduction or avoidance on the other hand is highly based on individual use cases. Some important application analyses have been summarised for the German electricity market in [129–132] and are shortly presented in the next sections together with their potential benefit estimations:

(a) Market revenues

(i) Power exchange markets:

As electricity is a homogeneous commodity and the majority of the power supply must be consumed at the time of production, electricity prices show a high volatility. In addition, the short-term demand is not very price elastic [133]. These circumstances allow inter-temporal arbitrage transactions at the EPEX-Spot (day-ahead and intraday market). Arbitrage contains purchases of electricity in times of low energy prices (off-peak prices) and sales of electricity when prices are comparatively high (peak prices) [134]. The attractiveness of the application depends on price spreads and the frequency of price spreads in these markets. On the day-ahead market, 24 hour single contracts and diverse block contracts are traded for the next day via a daily static auction. The intraday market starts shortly after the day-ahead market (trades for the following day start at 3 pm and end 30 minutes before the actual physical delivery of the respective contract) and is organised by continuous trading.

(ii) Control reserve markets:

A stable operation of the power supply system at a system frequency of 50 Hz requires that the system balance of feed-in, off-take and losses are balanced at any time or that it will be balanced in case of any deviations in a short period of time [135]. An increase or decrease in net output of BSS can ensure a real-time system balance [136]. Since 2001, the German TSOs procure their needs for different control reserves (primary, secondary and tertiary control reserve) on an open, transparent and non-discriminatory market. The main differences between the three control reserve forms are the tender time and period, the product time-

slice, the award criteria and the remuneration. In addition, positive and negative SCR and TCR are separately marketed, whereas in the case of PCR the power increase and decrease must be ensured by a single offer, but the forms of control reserve can be provided by various technical units (also known as pooling).

(b) Revenues based on bilateral contracts
(i) Voltage support:
In order to maintain stable network operation, the voltage level must be kept in certain ranges. The static voltage support can, among others be achieved by a local offset of reactive power [137]. BSS with an inverter and a corresponding power electronic can principally provide reactive power [138]. A compensation of reactive power is exclusively paid on the high and extra high voltage level by the respective TSO. On the distribution level the requirements are part of the FNN-guidelines but there is no monetary compensation [34].
(ii) System restoration:
BSS can be used to energise transmission and distribution lines and have the ability to synchronise sub-systems as well as back-up other black start units [131]. In Germany, each of the four TSOs in cooperation with the DSOs are obliged to have a sufficient capacity of black start units plus a concept for the restoration of supply in their control area. The black start capability is not explicitly defined in the Transmission Code. The requirements for the type, scope and remuneration are negotiated bilaterally.
(iii) Redispatch:
In many areas in Germany, transmission capacities are not keeping pace with the changing feed-in and off-take infrastructure. In order to ensure security of supply, TSOs with the help of DSOs take redispatch measures, adjusting feed-in from particular generating and storage facilities [139]. A transparent market for redispatch does not exist. The selection of generators for redispatching is based on their location in the network, their generation form and their size, which determines either the cost-based (where the adequacy of costs is regulated) or market-based (based on individual bids submitted by the generators) redispatch [140].

(c) Cost reduction or avoidance
(i) Uninterrupted power supply (UPS):
Large and long power interruptions (>3 minutes) arise relatively arbitrarily in Germany. However, voltage dips (<1 minute) as well as short

interruptions (< 3 minutes) occur 10 to 100 times per year [140]. Therefore, depending on the specific outage times and individual power quality needs (e.g. voltage, frequency, harmonics), a UPS system can consist of a BSS in combination with a generation unit like a diesel or gas generator or of a battery only [132].

(ii) Balancing group management (BGM):

With the liberalisation of electricity markets in Europe and Germany, the balancing group system was established. Accordingly, each producer or consumer must belong to a balance group and all balance groups must be levelled at a quarter-hourly basis. The German TSOs are liable for determining and settling the amounts of balancing energy in their control area, using a common symmetric imbalance price for each 15-minute time period (German: regelzonenübergreifender einheitlicher Bilanzausgleichsenergiepreis, reBAP) [141]. Consequently, a BSS can optimise the individual energy balancing costs.

(iii) Energy cost management (ECM):

The benefit area is similar to arbitrage at power exchange markets. In this case not wholesale prices but individual end-user tariffs are relevant. The BSS can avoid high price energy purchases during peak demand hours for residential and commercial/industrial users [142]. Since 2010, according to section 40(5) EnWG energy suppliers are obliged to offer load-variable and daytime dependent tariffs. The tariff-structure and -spreads depend mainly on the respective supplier and individual electrical demand amounts (e.g. industrial, residential).

(iv) Reactive power management (RPM):

Producers and network operators need to transfer the apparent power according to the active and reactive power demand of the end user. Common supply contracts in the industry allow that 50 % of the active energy can be obtained free of charge as reactive energy, which corresponds to a $cos\varphi$ of 0.89 [143]. In case of a higher demand for reactive power an additional fee must be paid, which is subject to individual negotiations. This inductive reactive power demand can be covered amongst others by a BSS.

(v) Demand management:

As standard load profiles are applied in the customer segment and only annual energy consumptions are measured, no tariffs with power limits or incentives are available at the moment. This can potentially change with the roll out of smart meters. However, industrial consumers typically have two price components: expenses of the peak power demand and expenses for the consumed energy [129]. Usually, demand management

is done by the retraction of running processes. Therefore, a load-shift via BSS may have (alongside with economic aspects) production-related benefits.

(vi) Renewable energy self-consumption (RESC):

End-consumers with generation capacity (e.g. photovoltaics) can increase the amount of self-consumed energy by adding BSS. With the increasing difference between cost of generation and purchase price BSS become more and more attractive to end-consumers. For instance, PV-generation costs and feed-in tariffs have dropped well below purchase prices from the grid, whereas purchase prices have increased continuously [129]. It is noteworthy that due to the EEG amendment from 2014, newly installed systems over 10 kW or 10.000 kWh/a are surcharged for own consumption. Overall, the attractiveness of RE self-supply depend highly on electricity fee regulations.

(vi) Grid expansion relief:

Due to the growing energy demand, decoupled supply and demand regions, as well the fluctuating nature of most renewable energy generation, further investment in new lines, transformers and substations may become necessary [144]. According to the usual load characteristics, the available transmission capacity limits only the maximum transmittable power, but not the energy [145]. BSS can help defer or avoid grid expansions by storing energy. Nevertheless, BSS in general are more cost intensive and the current incentive regulation (ARgeV) does not consider alternative and perhaps more expansive infrastructure investments.

According to a German market analysis based on data from 2013 the benefits can be grouped in accordance to their market potential (see Table 4.1). The market potential consists of three core aspects: conceivable revenue, applicability for BSS and a favourable legal framework. Only a low potential for BSS benefits lies in grid expansion relief, voltage support and system restoration; redispatch, demand management and reactive power management hold a medium benefit potential. A high market potential is given by energy trading at the day-ahead and intra-day market, frequency support, un-interruptible power supply, balancing group management, energy cost management and renewable energy self-consumption. The highest revenue potential for the market based applications lies in the primary control reserve market whereas the highest cost reduction potential can be seen in maximising the self-consumption using renewable energies, especially for households. The same market analysis was updated showing very similar results for the year 2015 [146]. Therefore, many BSS projects, especially in

Germany, but also world-wide focus on these two applications [147]. An up-to-date world-wide database on energy storage systems and their applications is maintained by the US Department of Energy [148], which confirms that these two applications are the most common. Ergo, the focus of this work lies on BSS applications primary frequency control (chapter 5) and the maximisation of self-consumption (chapter 6). Both applications are also assessed in this chapter preliminarily: PCR at subsection 4.2.1 and self-consumption at section 4.3. Furthermore, the market based PCR application is compared with other marked based applications with combined complementary business models in subsection 4.2.3.

Table 4.1: Potential benefit estimations for the German electricity market in 2013

	Application	Benefit potential	Notes
Market based revenues	day ahead market	0.00-51.29 EUR/MWh [149]	based on mean hourly rates
	intra-day market	0.00-69.10 EUR/MWh [149]	
	PCR	17.60-20.01 EUR/MWh [150]	min.= average power price; max.= average marginal power price; potential for SCR and TCR higher because energy price not included
	SCR(pos.)	7.87-11.91 EUR/MWh [150]	
	SCR (neg.)	11.83-53.17 EUR/MWh [150]	
	TCR (pos.)	0.95-1.58 EUR/MWh [150]	
	TCR (neg.)	5.72-8.63 EUR/MWh [150]	
Bilateral contracts	voltage support	0.60 -8.70 EUR/Mvarh [151–153]	based on available TSOs-price sheets
	system restoration	6.85 EUR/MWh [154]	high uncertainty, based on US-data
	redispatch	9.72-47.54 EUR/MWh [155]	based on marginal cost of conventional power plants (= cost-based redispatch) min.= marginal costs nuclear; max.= marginal costs natural gas
Cost reduction	UPS	12.72 -27.72 EUR/MW/h [156]	high uncertainty, based on US-data
	BGM: reBAP (pos.)	0.01-43.05 EUR/MWh [17]	max.= average volume-weighted reBAP prices; potential ascending
	BGM: reBAP (neg.)	0.01-9.39 EUR/MWh [17]	
	ECM (households)	9.00-98.00 EUR/MWh [157–160]	exemplary cost analysis of the "big four" (E.on, RWE, Vattenfall and EnBW); difference between high and low tariffs
	ECM (industry)	10.7 EUR/MWh [149]	based on day-ahead market data: average price block-contracts, peakload (hours: 09-20) and offpeak (hours: 21-08)
	RPM	13.00 EUR/Mvarh [143]	based on capacitor bank prices by [143]
	demand management	15.00 EUR/MWh [152,161–163]	based on TSOs power prices on the high voltage level <2,500 h/a
	RE SC (hh)	85.00-191.00 EUR/MWh [164,165]	residential PV-system costs [164] and av. electricity costs for households [165]
	RE SC (ind.)	0.00-50.00 EUR/MWh [164,166]	Based on LCOE of large scale PV [164] and el. price for large consumers [166]
	grid expansion relief	0.10-0.20 EUR/MWh [18,167,168]	grid expansion costs: costs based on the "Bundesländerszenario" [18]; grid asset lifespan 40 years; consumption in the distribution network 300 TWh

4.2 Review and Assessment of Market Opportunities for Large Scale BSS

4.2.1 Primary Control Reserve with Large Scale BSS

Due to the fact that there is only very limited possibility of storing electric energy in the electrical system at present, a constant equilibrium between active power generation and consumption must be maintained. An indicator for the deviation from this balance is the system frequency, since it is a measure for the rotational speed of the synchronised generators. An increase in the total load will decrease the speed of the generators and hence lower the system frequency. A decrease in the demand on the other hand leads to an increase of the system frequency. [169]

Since frequency deviations can not only damage electronic devices connected to the grid, but also endanger the stability of the whole electrical network, the German transmission system operators (TSO) are legally obliged to maintain the system frequency within the strict limits of $50\,\mathrm{Hz} \pm 1\,\%$ (see also chapter 2) [38,41]. In order to achieve this goal, a certain level of active power reserve is required to re-establish the equilibrium between demand and generation in case of unbalances (this can be unbalances between instantaneous power consumption and generation, but also major power disturbances in the grid) [169].

The "Operational Handbook" of the European Network of Transmission System Operators for Electricity (ENTSOE), which sets general rules and technical recommendations regarding reserve power levels and their associated control performance, defines three different reserve levels: primary, secondary and tertiary control reserve [170,171]. According to the Grid Code of the German TSOs these reserve levels are also valid in Germany [170]. The primary control reserve is automatically activated within a few seconds after detecting a frequency deviation according to the curve depicted in (Figure 4.1). It has the aim to balance the consumed and generated power in the system so that the system frequency stabilises.

The main goals of the secondary control reserve are to restore the rated frequency of the system, to release primary reserves and to restore active power interchanges between control areas to their set points. The tertiary control reserve aims to replace the secondary reserve, manage eventual congestions and bring back the frequency to its rated value if secondary reserves are not sufficient. [16]

In Figure 4.2 the interaction as well as the starting and deployment times for the three reserve levels according to the guidelines of the German Grid

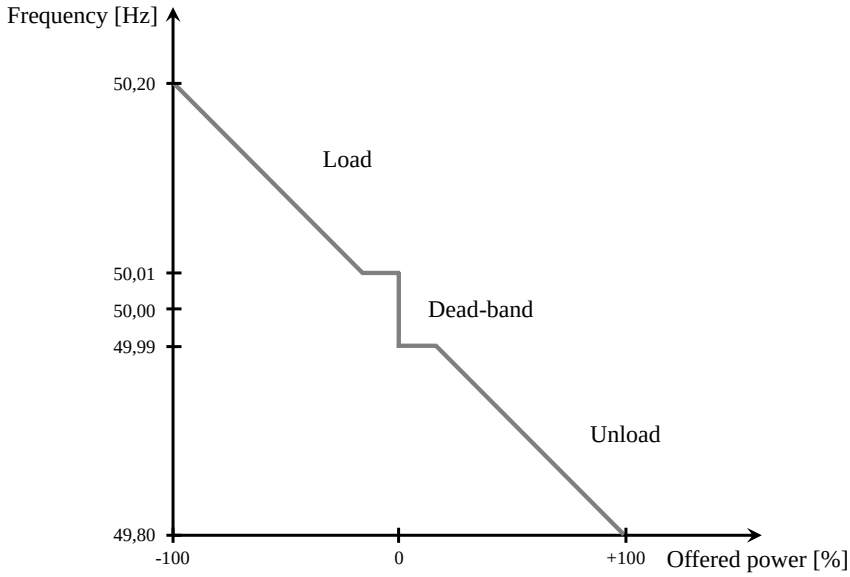

Figure 4.1: Relation between frequency deviation and provided primary control reserve

Code is shown [16].

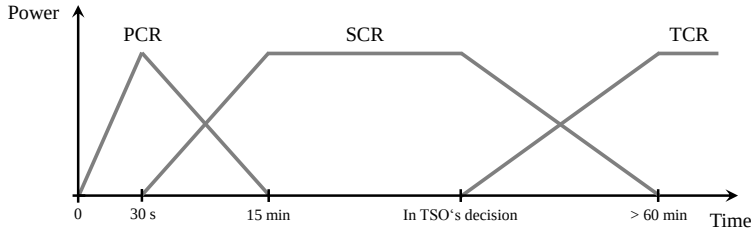

Figure 4.2: Starting and deployment times of primary (PCR), secondary (SCR) and tertiary control reserve (TCR)

In Germany, large scale BSS are almost exclusively used to provide PCR. There are several technical as well as economical reasons for this. From a technical point of view batteries perfectly suit the operational requirements

for providing PCR since they are able to deliver the requested power very accurately within a time frame of less than one second with a very high reliability [172, 173]. Although large scale batteries usually have a very limited storage capacity compared to other storage technologies such as pump storage systems [137], this storage capacity is fully sufficient (when made sure that the state of charge of the battery is kept at an optimal level during operation (see below)) to bypass the time until primary control reserve is relieved by secondary control reserve (see Figure 4.2) [174]. The need for a relatively low storage capacity of course also has the benefit of reducing investment costs and hence has a positive effect on the profitability of the BSS.

From a financial point of view, however, there are further points that make the provision of PCR the most attractive business case for large scale batteries at present [52]. As shown in section 4.1, the main reason for this is, that under the actual economical and legal framework, the weekly income is the highest when compared to other business cases. Because of this, it is foreseen that already existing PCR battery projects will turn out as being profitable in the near future [52, 174]. Another argument making the provision of PCR with large scale BSS very attractive from an investor's point of view is the already existing PCR market with its clear rules. This on the one hand reduces the risk for future income uncertainties and on the other hand lowers marketing expenses.

The mentioned technical as well as economic reasons for providing PCR with large scale batteries have led to an increase of existing as well as planned primary frequency control battery projects in Germany over the last years. A chronological overview of recent large scale BSS projects for primary frequency control in Germany are listed in Table 4.2. The probably first battery providing PCR within the European grid was a NAS battery. This battery was integrated into the German network in the year 2012 by the Younicos AG. As can be noticed, since then the installed power of the battery systems has been steadily increasing. Furthermore, it can be derived from Table 4.2 that almost all projects apply Li-Ion technology. One of the main reasons for this are the rapidly falling costs for Li-Ion batteries over the last years [174, 175]. Besides this, Li-Ion batteries have also one of the highest round-trip efficiencies in comparison to other battery technologies, a very high energy density, high lifetime expectancy as well as a very favourable power to energy ratio for providing PCR [176, 177]. This means that a high installed power does not lead to an unnecessarily high storage capacity. Nonetheless, flow batteries in primary reserve applications have also been discussed in literature [178]. It is also claimed that short response times as

well as the ability of some systems of being overloaded give BSS an advantage over conventional facilities [178]. As more and more private companies plan PFC projects without federal funding one can deduce that this business case seems promising from their point of view and is technically mature. Still, the pre-qualification that allows the facility to operate at the PFC market is the bottle neck at the moment, as most of the commissioned projects did not pass the pre-qualification yet. Another trend is the increase of the system size of large scale BSS as it can be seen for the most recent systems under construction in 2016 and 2017 (see Table 4.2).

Table 4.2: Overview of recent large scale BSS projects for primary frequency control in Germany, based on [148] and contact with the BSS owners

Project name	BSS type	Rated power P_r [kW]	Duration at P_r [HH:MM]	Commissioning date	Funding source	Pre-qualified	Lifetime [a]
WEMAG Younicos Battery Park [a]	LIB	5,000	1:00	16/09/2014	federal/ private	yes	20
Younicos and Vattenfall Project: Sodium Sulfur / Lithium Ion	NaSB/LIB	1,000/ 200	6:00/ 1:00	01/12/2012	federal/ private	yes	20
M5BAT (Modular Multi-Megawatt Multi-Technology Medium-Voltage Battery Storage)	PbB/LIB	5,000	1:00	mid 2016	federal/ private	no	2
Feldheim Regional Regulating Power Station (RRKW)	LIB	10,000	1:00	21/09/2015	federal/ private	no	10+x
Bosch Braderup ES Facility	LIB/ VRFB	2,000/ 325	1:00/ 3:50	11/07/2014 // 15/09/2014	private	no	15
1.3 MW Battery in Alt Daber	advanced PbB	1,300	0:40	10/2014	federal/ private	yes	15
Bosch Second Life Batteries	LIB	2,000	1:00	Q3 2016	private	no	10
REDMONDIS Electrorecycling Plant	LIB	13,000	1:00	mid 2016	private	no	10+x
3 MW Battery Storage - Dörverden, Germany - Statkraft	LIB	3,000	N/A	15/12/2015	N/A	N/A	N/A
LESSY	LIB	1,000	0:42	01/02/2014	federal	yes	N/A
90 MW Energy Storage - STEAG GmbH	LIB	6 x 15,000	1:30	mid 2016 to early 2017	private	no	N/A
SmartPowerFlow	VRFB	200	2:00	02/09/2015	federal	no	1

[a] First stand alone battery in Europe, according to [179]

Whether the number of grid connected large scale battery systems will continue to rise in the future depends to a great extent on the price decline for BSS and the future development of the remuneration for primary control reserve. Since the demand for batteries has steadily been increasing over the past years, battery costs are generally expected to fall in the future [173, 180–182]. The future development of the remuneration for PCR, however, is relatively unclear since it depends on many factors that are barely predictable. These are for example the number of players in the PCR market and the future demand for primary reserves. In [183] and [184] it is estimated that the future demand for primary reserves will rise due to an expected increase of the share of fluctuating renewable energy sources along with their low predictability of electricity production. In [52] and [185] on the other hand it is estimated that the demand for primary reserves will stay more or less constant in the future. This is explained by the fact that the demand for PCR in Europe is actually determined on the basis of the simultaneous loss of the two largest power plants within the European grid, which is not expected to change significantly in the future. A comprehensive work studies the rise of variable renewable energies and the reserve market interacted in Germany in the past years [141]. Possible reasons for the reduction of the balancing reserves and costs and the simultaneous increase of installed wind and solar power are given in [141]. One of the major findings is that the wind and solar power forecast errors might not be the most prominent driver for the balancing reserve requirement, but that other factors like the design of the control market might be more important. Due to all these uncertainties, the prediction of the price development for PCR is hardly possible and expert opinions strongly differ in this point [141, 173, 185].

Another important factor that can have a big influence on the development of the number of large scale batteries in the German grid are future adjustments of the participation conditions for the PCR market. On their basis it is not only decided who is able to enter the market and who is not, but they also set the operational framework for PCR providers. On the other hand, this can have a big influence on the economics of PCR projects. For example, if the required storage capacity of PCR batteries has to be increased, as it is currently discussed [173, 186], it would have a negative impact on the economics of those projects.

The guidelines for entering the PCR market are defined by the TSOs, since they are legally obliged to ensure that all technical standards for operating the electrical network are safely fulfilled [38]. The actual key parameters for the provision of PCR are summarised in Table 4.3. Furthermore, according to the German Grid Code all prospective providers of PCR have to com-

plete a pre-qualification procedure to demonstrate their ability to meet the requirements in this respect [16].

Table 4.3: Key parameters for the provision of primary control reserve [16, 187, 188]

Max. frequency response insensitivity	±10	mHz
Full activation frequency deviation	±200	mHz
Full activation time	30	s
Tendering period	1	week
Min. bid size	±1	MW
Time availability	100	%

As can be seen in Table 4.3, the primary control reserve has to be provided for a tendering period of one week with an availability of 100 %. For battery storages this would mean that they would have to be dimensioned for the case that the full offered power is requested continuously during a whole week. The dimensioning for this unrealistic worst case scenario, however, would make all battery projects uneconomical. Because of this, the German TSOs have defined degrees of freedom, which give battery operators the chance to readjust the SOC of the storage system during operation [189]. As a consequence, the required storage capacity is reduced, since the SOC can be kept at a level, where it is ensured that the battery is able to provide the requested balancing power until primary control reserve is relieved by the secondary control reserve (see Figure 4.2). For this case a power to energy ratio of one (e.g. 1 MWh / MW) is fully sufficient [174, 175].

According to [172] and [175] the optimal SOC for batteries providing primary control reserve lies around 50 %. The reason for this is that the network frequency generally fluctuates approximately normally distributed around the nominal value of 50 Hz [129]. Therefore, approximately the same amount of balancing power has to be provided in positive (unload) as well as negative (load) direction. Due to the losses of the storage system, however, the SOC tends to fall in the long run. Hence, it is advisable to keep the SOC slightly above fifty percent [172]. The TSOs in total defined six degrees of freedom for SOC adjustments. They can be found in [189]. The main difference between them is that some generate extra costs for the battery operator and some do not. Those degrees of freedom that do not generate costs can be applied as often as required. Those that do generate costs on the other hand should be applied as seldom as possible. In this case the decision whether to use the degree of freedom or not becomes more complex and should be determined on the basis of a cost benefit calculation. All six degrees of free-

dom listed in [189] are briefly described hereafter (italic letters): As can be seen in Figure 4.3 the *optional overfulfillment* gives the battery operator the chance to provide 20 % more balancing power than required, if it is useful for an adjustment of the SOC.

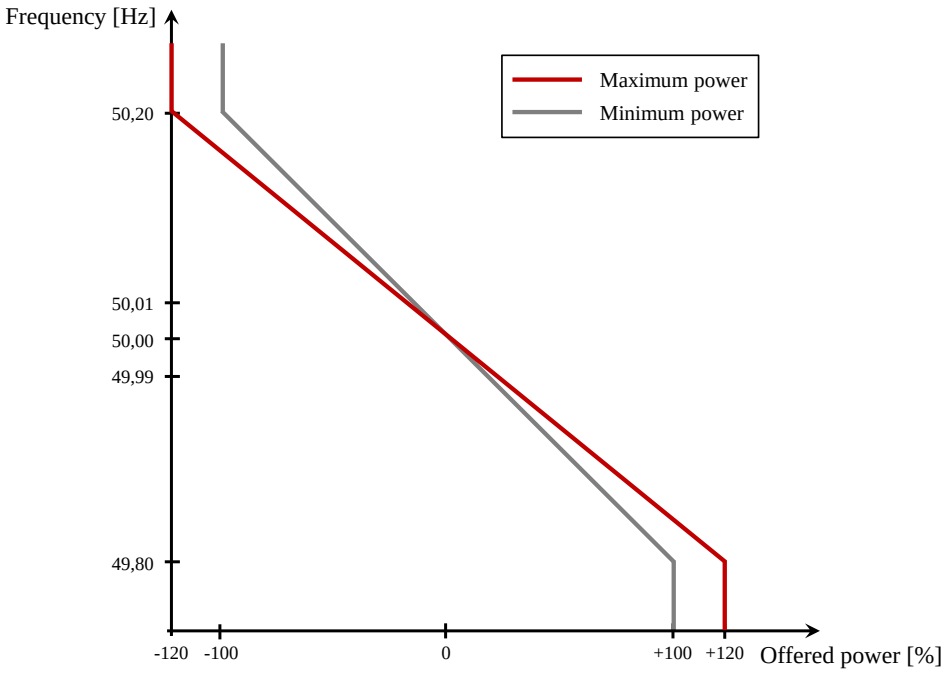

Figure 4.3: Degree of freedom "optional overfulfillment"

The degree of freedom *dead-band* makes it possible to readjust the battery SOC by using the dead-band (Figure 4.4). One condition for the application of this degree of freedom is that the behaviour of the battery must always support the stability of the electrical network, meaning that, for example the battery is not allowed to charge when positive primary control reserve (unload) is required.

One degree of freedom that has to be remunerated when applied is the option to charge or discharge the battery with *schedule transactions*. In this case the SOC can be optimised by purchasing or selling energy at the energy market (stock market or over the counter transactions). Of course, when using this degree of freedom the battery operator has to make sure that the sum of battery output and purchased / sold energy corresponds exactly

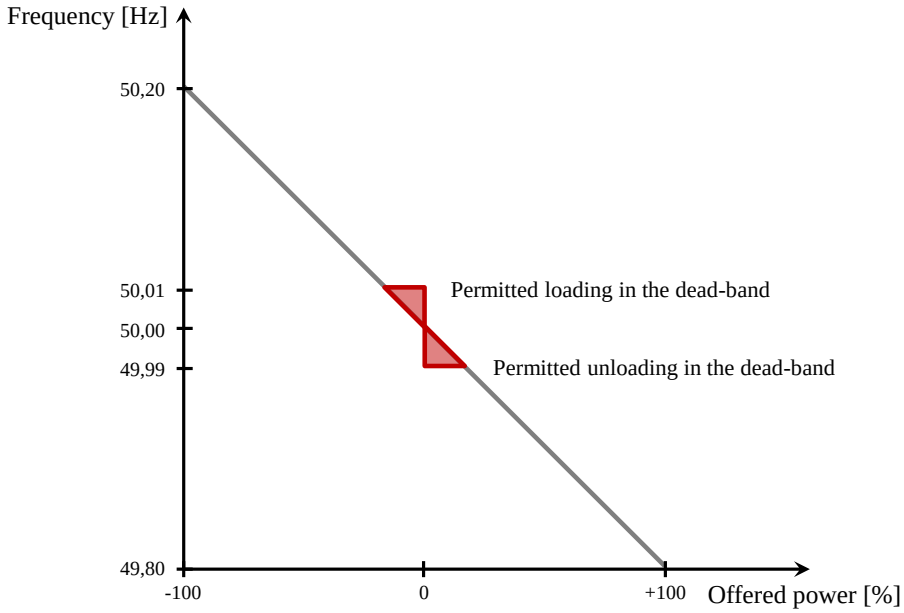

Figure 4.4: Degree of freedom dead-band

to the requested value by the TSO at any point in time. An exemplary behaviour of the battery during a schedule transaction is shown in Figure 4.5 and Figure 4.6. In this case the SOC of the battery is in its lower half at 8:00 o'clock. Since the battery has to keep continuously unloading due to low grid frequencies, a schedule transaction is carried out between 9:00 and 9:15 o'clock. As can be noticed, this prevents the SOC from reaching a critical value, since the battery is loaded instead of unloaded in this time window (see Fig. 4.6).

Similarly to the just described degree of freedom it is possible to *load or unload the battery with another technical unit.* One condition for doing this is that all entities involved in the re- or discharging process must belong to the same balancing group. Furthermore, an optimal interaction of the involved units has to be demonstrated in advance.

Another degree of freedom for batteries consists in the *relocation of the dead-band when grid-time corrections are planned.* When required the PCR provider is informed one day in advanced about the target frequency for the upcoming day by the TSO. In this way the PCR provider is able to prepare the dead-band shifting for the time period of the grid-time correction.

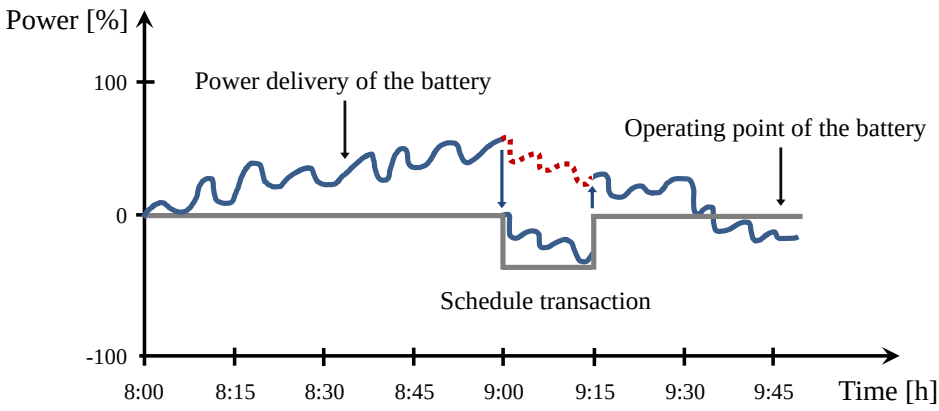

Figure 4.5: Degree of freedom schedule transactions

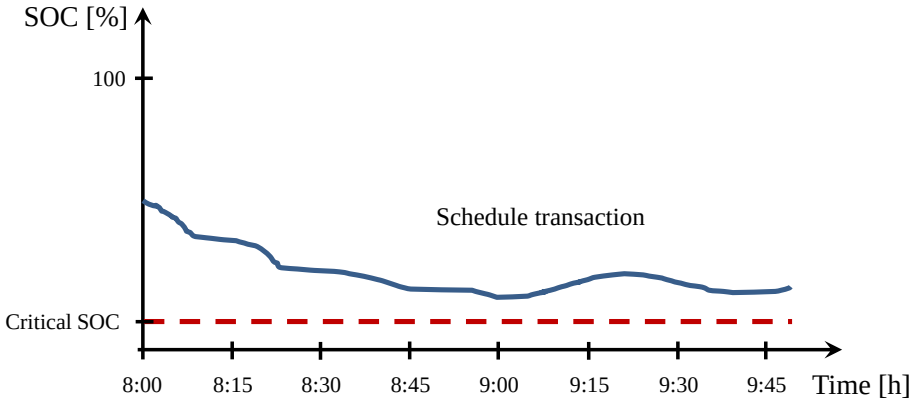

Figure 4.6: Schematic SOC profile for schedule transactions.

According to [169], the maximum deployment time for PCR increases linearly with the requested primary control power. Starting from a value of zero the maximum offered power by a PCR provider must be fully activated after 30 seconds at the latest. However, BSS that are able to provide the requested power much faster are allowed to use this characteristic as a degree of freedom. This means that battery operators are allowed to use the whole *permissible operating range* depicted in Figure 4.7 to readjust the SOC of their storages.

Additionally to the above-discussed document "Eckpunkte und Freiheitsgrade bei Erbringung von Primärregelleistung" (eng. key features and de-

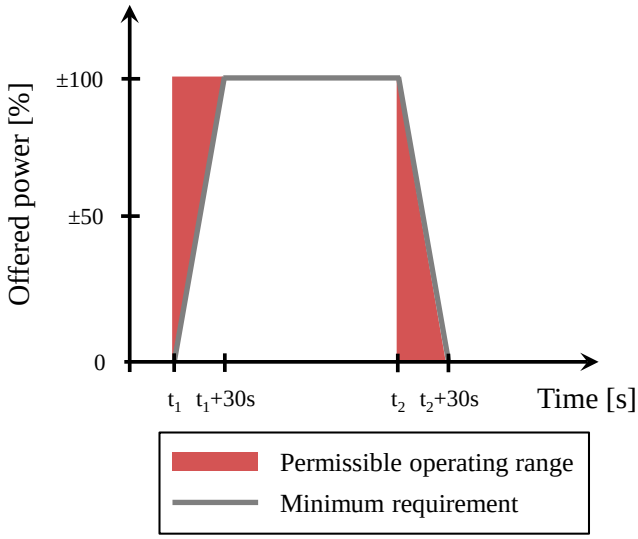

Figure 4.7: Degree of freedom permissible operating range

grees of freedom for the provision of primary control reserve) [189], which was published by the TSOs on 03.04.2014, the document "Anforderungen an die Speicherkapazität bei Batterien für die Primärregelleistung " (eng. storage capacity requirements for batteries for primary control power) has been published on 29.09.2015 [190]. [190] includes the requirement for stand-alone batteries to consistently maintain capacity for 30 minutes of full pre-qualified/ offered power. From this, depending on the ratio of the usable capacity of the storage to the pre-qualified power, a symmetrical charge level range is mathematically derived as permissible (see operating range Figure 4.8).

Since a constant SOC of 50 % is unrealistic during operation, the ratio of usable capacity to pre-qualified power is necessarily greater than one. Thus, with increasing capacity, the permissible operation range area increases, but so does the investment cost, without increasing the marketable/ pre-qualified power (see Figure 4.8). The usable capacity is determined by the TSOs as part of the pre-qualification procedure by discharging the battery from the highest possible charge level until the pre-qualified power can no longer be provided (for the SPF prototype in section 5.4.1).

However, it is currently argued that the same conditions of entry into the PRL market must apply to all participants and therefore, as therefore the less strict 15 minute criteria, as defined in [191] and depicted in Figure 4.8, might

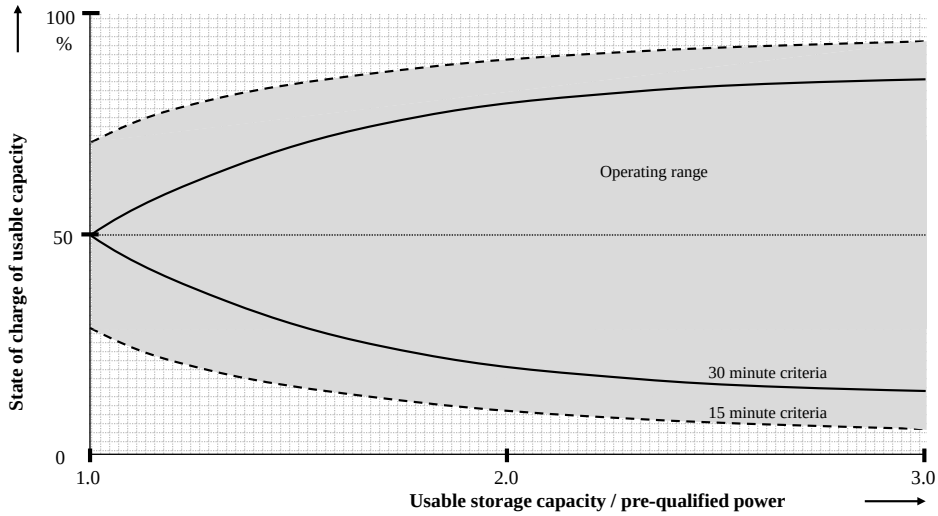

Figure 4.8: Requirements on usable capacity

apply for stand alone BSS, too. This would ease the system requirements for the BSS. In addition, the EU Guideline on Electricity System Operation (SO GL) is currently in the comitology procedure [192], which causes the TSOs of the Continental Europe Synchronous Area to review the capacity requirements on the basis of a cost-benefit analysis (SO GL art.156(9). According to [190] there might be other options accepted to exclude critical SOC, not listed in the SO GL. From an investor's point of view, this represents considerable uncertainty. Regarding the battery technologies that can be used in the PCR market, the flexibility of the energy-to-power ratio of the vanadium redox flow batteries could be advantageous in the future, given that for a given battery power the required capacity can be adjusted as needed.

On the other hand, in 80 % of the time the BSS has to provide less than ± 10 % of its nominal (pre-qualified) power, as shown in Figure 4.9.

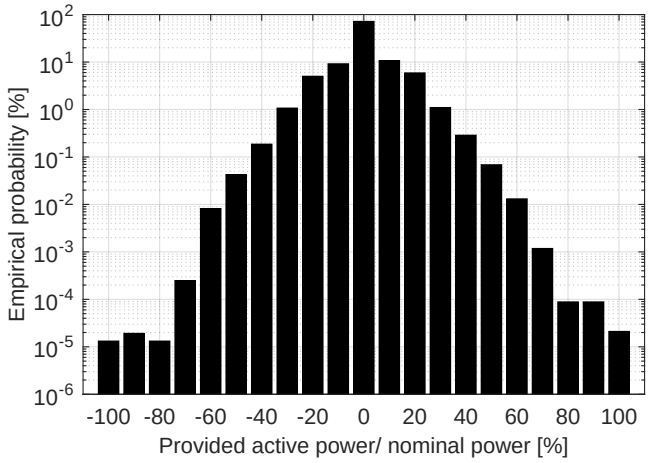

Figure 4.9: Statistical requests of PCR power in the UCTE grid, based on [129]

In conclusion, it can be stated that a final technical guideline of storage capacity requirements and a clear definition of the corresponding prequalification tests remain unclear. From an investor‘s point of view it would be more profitable to install as little capacity as possible, since this capacity can be regarded as stranded investment.

4.2.2 SCR in Combination with Day-ahead and Intra-day Trading for Large Scale BSS

Another approach is to combine complementary business models, this may increase the profit compared to a single revenue stream [193]. As described in section 4.1 combined business cases of intra-day, day-ahead and secondary control reserve might be profitable business cases and they are analysed in this section. In order to quantify total revenue potentials for a BSS, the maximum achievable proceeds for a single and combined storage operation mode are simulated. Two operation modes are considered: Firstly, the BSS operates based on a load-levelling principle, only at the day-ahead market (DA), and secondly the BSS is additionally marketed in the secondary reserve control market (DA+SCR). This combination is selected, because both BSS application areas operate on existing markets with uniform and standardised product requirements (see Table 4.4).

Optionally, possible intra-day (ID) revenues were estimated if the downtime hours can be used in which the storage is used primarily for the day-

Table 4.4: Main product characteristics DA and SCR [16].

	Secondary Control Reserve (SCR)	Day-Ahead (DA)
Tender period	weekly	daily
Product	peak (HT): Mo-Fri	Mo-Sun hourly
Time-slice	8 am to 8 pm	
Product	off-peak (LT):	Mo-Sun hourly
Time-slice	residual period	
Award criteria	power price (pay-as-bid)	unifrom price auction auction
Remuneration	power price and energy price	energy only (marginal cost)
Minimum power	±5 MW; 5 MWh (incl. pooling)	0.1 MW
Capacity	≥12 h x offered power	1 h x offered power

ahead trading. In order to quantify total revenue potentials for a BSS, the maximum achievable proceeds for a single and combined storage operation mode are simulated using a linear optimisation model. The mathematical description of the two models (DA and DA+SCR) is presented along with the objective function and the constraints in [193].

The simulation model has several simplifications. The arbitrage model for the day-ahead market does not distinguish between charging and discharging efficiency losses. The total efficiency losses of a storage cycle are attributed to charge the BSS. In addition, self-discharge losses of the BSS due to internal processes are neglected. It is assumed that there are no durable downtimes and that VRFB habe no cyclic ageing. Besides, the times for charging and discharging are supposed to be identical, which is not the case for some storage technologies. The reaction time or ramp rate is also neglected in the model, because it is anticipated that for a time horizon of one hour this is of minor relevance. Moreover, the death of discharge is not explicitly addressed in the model and needs to be adjusted for technology specific considerations. Due to the perfect foresight assumption price uncertainties are neglected and the maximal theoretical profit is calculated. This applies to the arbitrage model of the DA and for the SCR bidding strategy. Another restriction is that the energy price of the BSS providing SCR is selected high enough, such that no energy has to be provided by the BSS.

In order to participate in the secondary control reserve market, the SPF prototype used in in the SPF project is scaled up from 200 kW to 5 MW for the simulation. The energy-to-power ratio is kept the same. The storage parameters for the model simulation are listed in Table 4.5.

Table 4.5: BSS model simulation parameters.

Parameter	Value	Description
P_{max}	5 MW	maximum charge/discharge power
$P_{pq,min}$	0.75 MW	minimal pre-qualified power
$P_{pq,max}$	5 MW	maximal pre-qualified power
c_{max}	10 MWh	maximum storage capacity
η	0.8	round-trip efficiency

For both operation modes (DA and DA+SCR), it is assumed that the hourly rates at the day-ahead market and secondary control reserve power prices are known. Therefore, the simulation is carried out based on ex post data from 2013 of the EPEX-SPOT [149] and the German secondary control reserve market, published on regelleistung.net [194].

There are four ways to market secondary control reserve. Two of which are different product time-slices: Low Time (LT) with work days from 8 pm to 8 am and High Time (HT) with work days from 8 am to 8 pm. Furthermore, negative (NEG) and positive (POS) control reserve are bided separately. Positive control reserve in the context of BSS means charging and vice versa. The four possibilities to participate at the SCR market are therefore: HT_POS, LT_POS, HT_NEG, LT_NEG. These four options are combined with the DA market and modelled in yearly simulations in 1-h steps additionally to the pure DA trading. The resulting modelled options are: DA, DA+HT_POS, DA+LT_POS, DA+HT_NEG, DA+LT_NEG. To speed up computation time a year is divided into twelve periods (months) which are calculated in parallel. The SOC is set to 1 % for the first time step of the twelve periods. Assuming that the battery system has to provide its full power during the twelve hours of the tender period, only 0.75 MW (SCR_MIN) can be offered and remunerated, if the BSS is at its full capacity of 10 MWh at the beginning of the marketed period. This offered power can be considered as the lower limit of the revenue model. If the supply periods are shortened or recharging transactions are possible like for the provision of PCR, the maximum marketable power would be 5 MW (SCR_MAX).

The principle function of the two operation modes (DA und DA+SCR) are described and illustrated by a sample week (September 2-9, 2013) for arbitrage (DA) in Figure 4.10 and arbitrage in combination with secondary control power provision (DA+SCR), in this case HT_POS in Figure 4.11.

Principally, in the arbitrage operation mode (DA) the BSS stores electricity in hours of comparatively low market clearing prices and discharges the energy again in times of comparatively high market clearing prices in

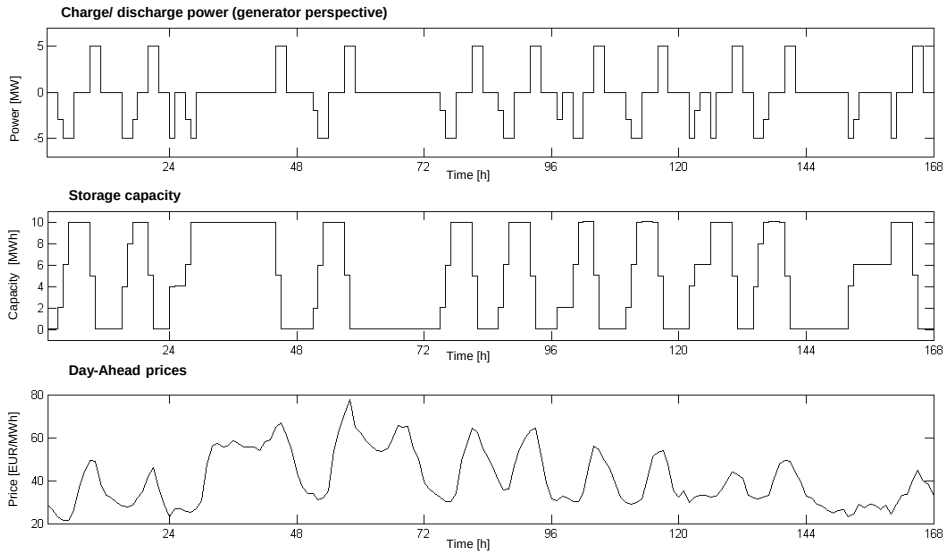

Figure 4.10: Sample week DA optimisation results, September 2-9, 2013.

EUR/MWh. A positive income can only be generated if the discharge revenues exceed the charge spendings plus the included efficiency losses. Consequently, the storage capacity behaves inverse to the price development at the day-ahead market (low price leads to charging and a high storage capacity). Besides, the battery discharges at full power and for these seven days at a rate of approximately 1.5 charge/discharge cycles per day. In 67% of the 168 h there is no activity at all (standstill hours).

The combination of DA+HT_POS is shown in Figure 4.11. In the grey periods, the battery system is applied on the DA market, while in the white-marked periods (weekdays 8 am - 8 pm), it participates in the SCR market by offering positive control power. One of the constraints is that the BSS is fully charged when a SRC period starts, in order to be able to provide its offered power during the whole period (if negative SRL is offered, the SOC is minimal). To fulfil this constraint, the BSS is charged at the DA periods, for example at the first DA period 0 bis 8 am when the price is minimal. Furthermore, regardless of the demand for secondary control energy, which is set to zero, the BSS completes roughly eight cycles a week. Even during arbitrage periods (for one week HT_POS), only 40 % of the time is used for load-levelling via day-ahead market price signals.

Assuming that the storage operator has perfect foresight of the day-ahead

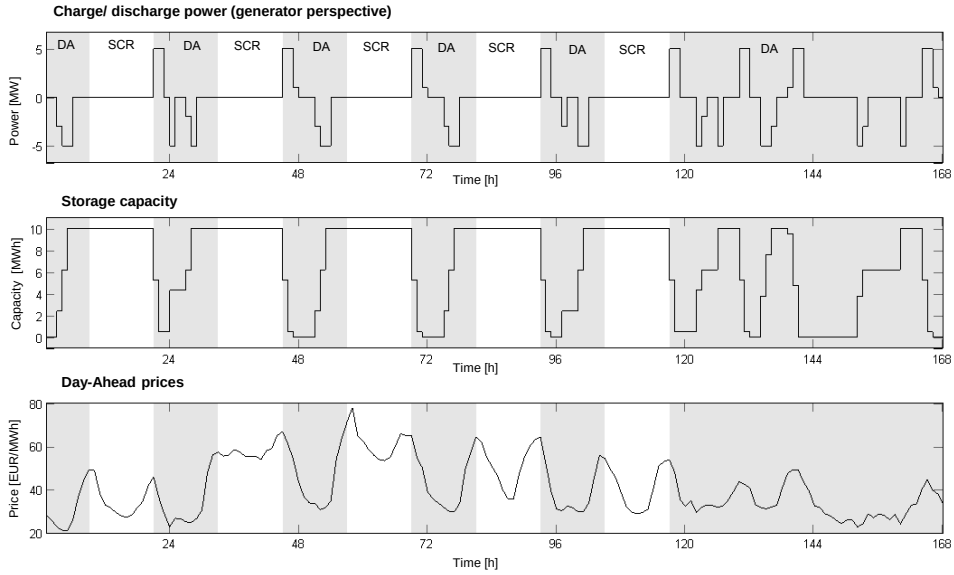

Figure 4.11: Combined DA and SCR trading (DA+HT_POS), exemplary week, September 2-9, 2013 with a offered power of 0.75 MW

market and behaves as a price taker (quantities are too marginal to be price or/and quantity-dominant on the market), the maximum arbitrage revenues for 2013 are 120 kEUR (see Figure 4.13), with total standstill hours of 5,946 h corresponding to a load factor of 32 % per year, as depicted in Figure 4.12.

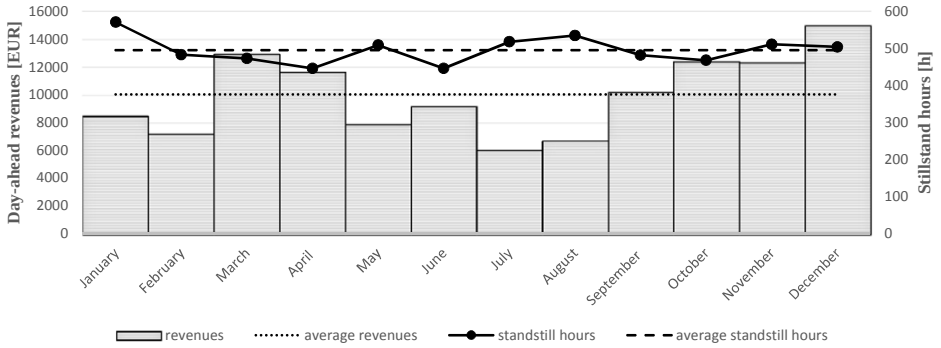

Figure 4.12: Revenues for arbitrage at the DA market and downtime in 2013.

Since the focus of the model is to estimate the revenues for a combined business model for arbitrage at the day-ahead market and provision of sec-

ondary control reserve, the third combination option is the participation at the intra-day market (ID), which is roughly estimated. The basis for the estimation are the standstill hours in each combination case. The estimations for the intra-day market are based on the investigations in [195], where a sodium sulphur battery and a vanadium redox flow battery are used for an arbitrage business case in the day-ahead and intra-day market. As stated before, the primary focus of the simulation is on the day-ahead market. However, if there is no activity of the storage at the day-ahead market, the batteries are marketed on an hourly basis at the intra-day-market. According to [195] a profit of 3.57 EUR/MWh for vadium redox flow BSS can be assumed per standstill hour for intra-day estimations. Figure 4.13 depicts the revenues of all calculated single and combined business models.

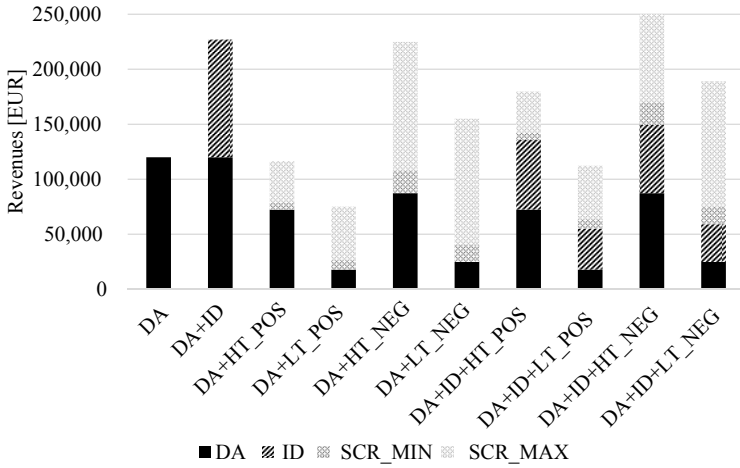

Figure 4.13: Revenues for single and combined revenues at the DA, SCR und ID market in 2013. SCR for two different pre-qualified powers: SCR_MIN ($P_{pq,min}$=0.75 MW), SCR_MAX ($P_{pq,max}$=5 MW).

In the best case (SCR_MAX; $P_{pq,max}$=5 MW), for the combination of marketing on the day-ahead market, offering negative secondary control power and optimal utilisation of downtime on the ID market (DA+ID+HT_NEG), a revenue of about 250 kEUR can be generated. Even if the (estimated) revenues on the ID market are neglected, total revenues of around 225 kEUR are still possible. Compared with the revenues at the DA market, this is an additional revenue of 105 kEUR and shows that a combination of business models can be more profitable. The situation is different if only 0.75 MW SCR can be marketed (SCR_MIN). In this case, it is more profitable to

use the battery system only in the day-ahead market, even more so if the downtime is used to market the battery additionally at the ID market.

Consequently, it is shown that the SCR market for battery systems can be attractive if the market product requirements are changed (either by a reduction of bidding periods or by special conditions for battery systems) or the marketable power is increased by pooling with other market participants.

4.2.3 Preliminary Assessment of Market Based Business Cases for the SPF Prototype

In subsection 4.2.2 and subsection 4.2.3 various large scale BSS market applications are examined under current legal and regulatory conditions. The aim of these chapters is an analysis of which business models or business model combinations could be particularly lucrative for the use of the vanadium redox flow battery of the SPF project. Thus, in subsection 4.2.2 the application of the BSS on the *primary control market* is assessed. In subsection 4.2.3 the combinations of different revenue business cases *participation at the secondary control reserve market*, *arbitrage at the day-ahead-market* and *arbitrage at the intra-day market* are analysed.

A major result of subsection 4.2.2 is that stand-alone BSS are able to participate at the PCR market due to the degrees of freedom which can be used to correct the SOC. With weekly revenues of 3,500 EUR/ MW (average price in 2015), at present experts assume that the commercialization of large batteries in the PCR market can be profitable, as shown in Table 4.2. As shown in subsection 4.2.3 even with a perfect-foresight assumption the revenues for a 5 MW/10 MWh BSS, which participates at the SCR market as well an at the day-ahead and intra-day market, are 250 kEUR at best.

The maximal theoretically possible weekly revenues that can be earned with the four business opportunities described above, are fitted to the BSS of the SPF-project (nominal power of 200 kW and a capacity of 400 kWh) and the results are depicted in Figure 4.14.

It can be concluded that the highest revenues stream of possible business opportunities at the German energy market for the SPF battery is to provide PCR. As in this section only the revenues are analysed and the costs are not considered, the profitability of the PCR business case is analysed further in chapter 5. Since the SPF Protoype is not able to participate at the PCR market, due the market restriction of a minimum pre-qualified power of 1 MW, a pooling of BSS of the same type is considered in chapter 5. The base of the economic assessment is a BSS model which is based on measured values of the BSS applied in the SPF project to provide PCR.

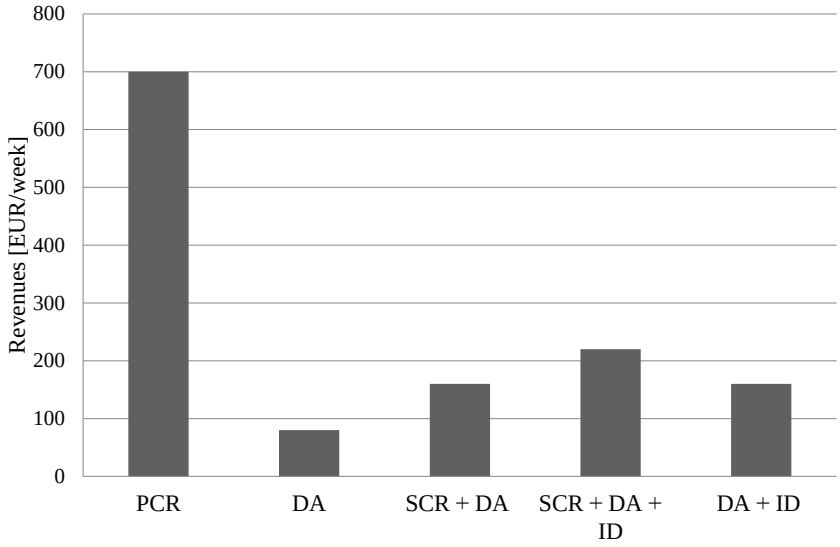

Figure 4.14: Expected weekly yield for the application of the vanadium redox flow battery of the SPF project for different business models. PCR:=primary control reserve, SCR:=secondary control reserve, DA:= day-ahead arbitrage, ID:= intra-day arbitrage.

4.3 Preliminary Assessment of the Self-Consumption Business Case

With the rise of DG the idea of the prosumer (entities that consume and produce), first mentioned in 1980 [196], became more popular. The main motivation to become an electrical prosumer as defined in [197], is that self-consumption of locally generated electricity, as defined in [198], is more profitable than drawing it from alternative supplies. This is the case if the levelised costs of electricity (LCOE) of the DG can compete with the cost to draw electricity from the power grid (electricity retail price). A comprehensive manual to calculate the LCOE for renewable energies was first presented by [199] and has further been discussed by [200] [201] and [202].In order to incorporate the cost of storage, [203] proposed to calculate the levelised cost of stored energy.

A comprehensive overview on grid parity world-wide is given by [204]. It is shown that Europe was the first main market world-wide where grid parity was achieved in 2010. It is quite likely that the market volumes for self-

consumption business cases will grow in the future as the trend of falling LCOE of DG and BSS continues. The LCOE of PV, for example, are assumed to decrease by 30-50 % from 2014 to 2030 [205]. An even more drastic price decline is foretold for BSS, especially for lithium-ion batteries (LIB). The lowest battery cell price for utility scale LIB could decrease by 64 % from 2014 to 2020 [182]. Although normally only addressed as LIB, there are at least four promising types of LIB suitable energy storage applications with different cell chemistries [206] and price reduction potentials till 2020 [182]: lithium manganite (39 %), lithium nickel cobalt aluminum oxide (50 %), lithium-iron phosphate (37 %) and lithium titanate (25 %). A more conservative meta-study conducted by Nykvist et al. indicates that the costs of LIB for battery electric vehicles could fall below 150 USD/kWh by 2025, and therefore decrease by more than 50 % [207]. The lowest battery cell price for utility scale flow batteries is predicted to decrease by 48 % until 2020, making them the second most interesting battery type concerning the price reduction potential [182].

The liberalisation of the energy market since the 1990s has not lead, as theoretically predicted, to a decline of the electricity price for household consumers due to more competition, but to an increase in all 27 member countries of the EU-27, except Finland, between 1998 and 2008 [208]. Since electricity prices are much harder to predict than, for example, the LCOE of PV a large variety of methods have been applied over the past 15 years [209], indicating that the electricity price for households will further rise all over Europe [208]. Keeping in mind the big uncertainty of predicting these prices, the electricity retail price in Germany is likely to increase until 2030, according to a technical report commissioned by the Federal Ministry for Economic Affairs and Energy [210].

In countries with lower LCOE of PV compared to Germany, like Spain for instance, self-consumption systems might have a positive net present value (NPV), but a possible back-toll fee could turns a profitable system to a negative NPV [211]. Therefore, a favourable legislative framework, as it is the case in Germany, is mandatory for this business case. By analysing the Italian market, one can deduce which size is more profitable in a post feed-in market. It can be concluded that small residential PV systems have higher net present values than larger systems, as the economy of scale does not compensate the benefits of smaller systems [212]. Therefore, the trend of installing PV systems in LV grids in Germany is likely to continue. PV systems in southern Germany reached grid parity in 2012 [2]. With only a PV-system to match the demand, the achievable self-consumption rates are limited, and can only be increased by demand side management (DSM) and

BSS come into play. It is shown by [213] that BSS have a higher potential to increase self-consumption than DSM [213]. Consequently, self-consumption increase is mainly realised with residential energy storages (RES), as this business case became profitable in 2013 in Germany [214]. As described before, the benefit in 2013 results from the PV LCOE, which are currently between 9.8 and 14.2 EURct./kWh in Germany [164], and the electricity costs for households, which amount to 28.9 EURct./kWh [166]. It is noteworthy that due to the EEG amendment from 2014 newly installed systems over 10 kW or 10.000 kWh/a are surcharged for own consumption (currently with 6.2 EURct./kWh). Therefore, the theoretically achievable profit margin lies between 8.5 and 19.1 EURct./kWh. This is one of the main reasons why more than 4600 residential storage systems for self- consumption were installed in Germany until June 2015 [215].

In the industry sector the PV generation costs are generally 2 EURct./kWh lower than in household applications because of the larger systems sizes and lie between 7.8 and 14.2 EURct./kWh [164]. The power purchase costs for large customers with a consumption of 100 GWh/a range between 4.1 and 15.6 EURct./kWh. Thus, the theoretical realisable value range (considering the EEG surcharge) is 0 to 5 EURct./kWh.

An resulting interesting research question is, whether it could be economically feasible to pool the prosumer and instead of having a BSS and PV-system in every household share and scale them up. Kastel et al. addressed this question by showing that the pooling of prosumer generators and loads has been beneficial in all calculated scenarios in the UK compared to a single prosumer [216]. This is due to the combination of PV systems, wind turbines and loads. By doing this the self-consumption level could be raised up to 17,5 %, wherefore the economics in case of grid parity improve significantly. However, BSS were not considered in this study. Large scale or pooled BSS that apply a self-consumption maximisation can be addressed as community electricity storage (CES), as defined in [217, 218]. A more detailed definition of CES is given in [219]. Parra et al. [220] conducted a study in which the LCOE of single households in the UK using PV residential storage systems and using a CES instead were compared. It has been shown, that the LCOE could be lowered by 37 % for a 10-household community and 66 % for a 60-household community. In Germany, CES, diverging from the definition in [218] cannot be operated or owned by the DSO using the CES to participate in the energy market because of the unbundling. The CES has to be owned and operated by a citizen cooperative or an external storage operator, for example. In Germany, no similar calculations considering the potential of lowering the LCOE have been conducted, but [221] showed that

by applying CES the losses caused by the grid-compatible storage operation can be lowered by 50 % on average compared to RES. With the existing legal framework the business models for residential storages and CES cannot be directly compared due to the additional burden of extra fees and taxes for CES. Nevertheless, the studies mentioned before seem to indicate that CES have some advantages over residential storages.

Most of the battery systems in Germany used to maximise self-consumption are realised as RES and not as CES, due to the unfavourable actual legal framework described hereafter. Charges and levies for CES mainly depend on the ownership of the electrical grid to which the BSS is connected and on whether the electricity from the storage is consumed in the vicinity of the storage or supplied to a third party. Nonetheless, the exemption from the electricity tax due to the vicinity of generation and load according to the Electricity Taxation Act section 9(1) (german Stromsteuergesetz, StromStG) may not be taken for granted due to the lack of a clear definition of vicinity. In this work the electricity tax is not considered. Despite of their function as temporary storage, CES with a point of common coupling to the public electrical grid as defined by the Federal Court of Justice (BGH), are treated as a final consumer according to the Energy Industry Act (EnWG) and is therefore charged with all levies and charges. As the BSS and the final consumer are treated equally, theoretically several charges and levies are charged twice. Therefore, in section 37(4) and 60(3) of the Renewable Energy Act (EEG 2014) and section 118(6) EnWG, exemptions are made for BSS to avoid the double EEG levy and grid charges. Nevertheless, according to section 5(12) EEG 2014 this applies only if the operator of the PV plant and the BSS is the identical legal entity.

The two bars on the right-hand side of Fig. 4.15 show the expenses for the case where the BSS is connected to the public grid (case 3 and 4); the two columns on the left show the levies and charges for the case, where the electricity is generated, stored and consumed in the vicinity of the storage without the use of the public grid (case 1 and 2). The latter two cases are divided according to whether they apply self-consumption (case 1) or electricity supply from the CES operator to a third party consumer (case 2). If the consumer is the same legal entity as the owner of the PV generator, according to section 61(1) EEG 2014 only a reduced EEG levy of 40 % (=2,5416 ct/kWh) incurs. In all other cases the full EEG levy has to be burdened.

A comprehensive study reviews different possible business cases that can be applied to CES [222]. Furthermore, a guideline concerning the legal framework connected to these business cases is published by the German federal network agency [223]. Although focussing on the EEG 2014, this guideline

is still valid for the EEG that became effective in January 2017.

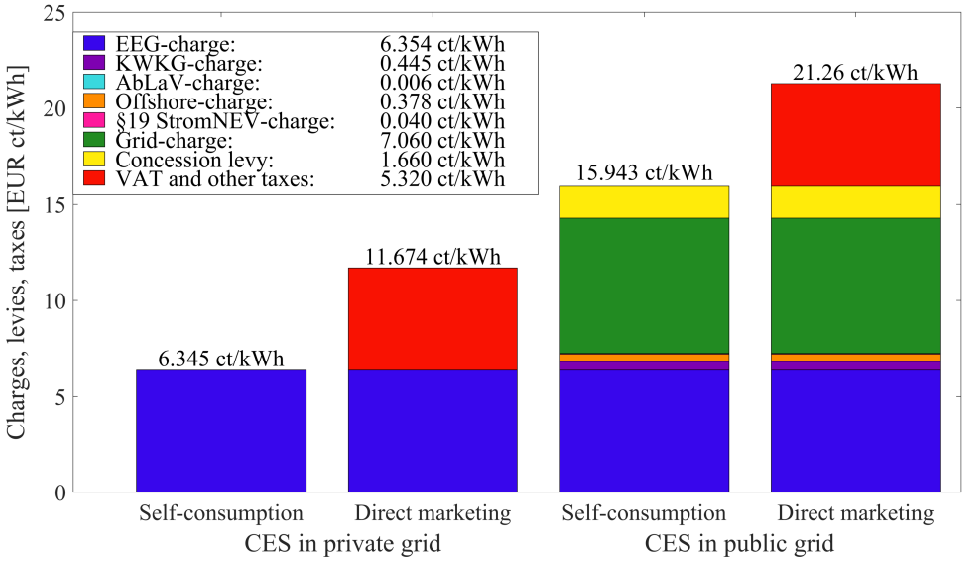

Figure 4.15: Charges, levies and taxes for CES in 2016, based on [222].

In spite of the high tax burden and the unfavourable legal framework mentioned above, several large scale BSS projects to maximise self-consumption and peak shaving in Germany have been realised in the recent years as listed in Table 4.6.

Table 4.6: Overview of recent large scale BSS projects to maximise self-consumption and peak shaving in Germany

Project name	LCOE; NPV ; profit/a	Generator(s)	Battery	Load(s)	RESCR	Operating strategy/ comment	Ref.
MSG EUREF	LCOE=0.52 EUR/kWh	$P_{PV} = 91kW_p$; $P_{wind} = 330kW$	**LIB:** capacity=78 kWh **PbB:** capacity=90 kWh **supercap:** capacity=3 kWh	Total yearly energy demand: approx. 400 MWh/a for office buildings	64%	direct loading/ all values for scenario 03	[224]
Strombank	Positive NPV, in case of no FIT and if no taxes and tariffs apply	$P_{PV} = 64kW_p$ $P_{CHP} = 16.5kW$	**LIB:** $P_{c./disc.} = 100kW$ capacity=100 kWh	14 households 4 industrial facilities	30%-60%	direct loading; forecast based dis-/charging is planned	[225, 226]
IRENE	no profit compared to traditional grid expansion	$P_{PV} = 20MW_p$; $P_{wind} = 23.5MW$ (2022)	**LIB:** $P_{c./disc.} = 70kW$ capacity=162 kWh	$P_{max} = 5.6MW$(2022)	70% (2022)	peak shaving	[14, 20]
Fechheim	N/A	$P_{PV} = 90.5kW_p$	**LIB:** $P_{c./disc.} = 45kW$ capacity=230 kWh	16 households $P_{max} = 30kW$	100%	peak shaving	[227]
Smart Operator	N/A	$P_{PV} = 60kW_p$	**PbB:** $P_{c./disc.} = 30kW$ capacity=150 kWh	110 households	N/A	peak shaving	[228–230]
SmartRegion Pellworm	Profit: 150 kEUR/a (2013)	$P_{PV} = 772kW$; $P_{wind} = 330kW$	**LIB:** $P_{charge} = 560kW$ $P_{disc.} = 1000kW$ capacity=560 kWh **VRFB:** $P_{c./disc.} = 200kW$ capacity=1.6 MWh	20 households $P_{max} = 487kW$	93%	forecast based dis-/charging; using external forecasts	[109], [87]
EEBatt	N/A	$P_{PV} = 300kW_p$	**LIB:** $P_{c./disc.} = 200kW$ capacity=200 kWh	50 households	25%	forecast based dis-/charging; using persistence forecasts	[221, 231, 232]
Smart Grid Solar (Epplas-Hof)	N/A	$P_{PV} = 287kW_p$	**PbB:** $P_{c./disc.} = 72kW$ $P_{disc.} = 72kW$ capacity=330 kWh	16 households	N/A	forecast based dis-/charging	[233, 234]

4.4 Chapter Summary

The German energy storage market was analysed and the two most profitable applications were presented in detail after a literature and market review.

An analysis of 20 potential revenue streams for BSS showed that the primary control reserve market holds the highest revenues for market based applications, whereas the highest cost reduction lies in maximising the self-consumption by using renewable energies, especially for households.

For the market based BSS applications several single and combined business cases were analysed in order to select the most profitable one. The revenues for the primary control reserve application of the SPF prototype was compared with the revenues of the combined business models for arbitrage at the day-ahead market and provision of secondary control reserve. A third combination option which is the participation at the intra-day market was roughly estimated, too. The results show that under current market conditions, even the most promising combined business case (arbitrage at day-ahead and intra-day-market, combined with secondary control reserve) is far from being competitive to the business case primary control reserve. Thus, primary frequency control seems to be the most promising business case for BSS in Germany at the moment. Although the net present value is just becoming positive, there is still a great challenge to make it profitable. Although the degrees of freedom help to achieve this goal, research is still necessary to determine the different benefits of these options, especially for VRFB, since most of the BSS used for primary frequency control are LiB.

As mentioned before, maximisation of the self-consumption is another promising battery application. But, due to additional fees and taxes applying for community electricity storages, this business case is hard to transfer from residential to large scale storages. The additional cost burden for community electricity storage was presented for several scenarios. In spite of existing unfavourable legal framework, it seems especially interesting since in the near future PV systems, which have reached the end of their 20 year period of feeding into the grid with a fixed feed-in tariff, can be used for this applications with an extreme low LCOE. Additionally, several large scale BSS projects in Germany applying those strategies were presented.

In conclusion, it is worth pointing out that large scale BSS are becoming economically feasible in Germany, but the current legal framework has to be adapted to ensure a break through of this technology. Thus, the presented preliminary assessment of the primary frequency control and self-consumption application is extended in chapter 5 and chapter 6 by applying them to the SPF prototype in the pilot region.

Chapter 5

Technical and Economic Assessment of a System Supportive BSS Prototype Providing PCR

As discussed in chapter 2, the best way to increase the number of large batteries in the distribution grid level is by applying an operating strategy that optimally combines a profit-driven and a grid supportive-operation strategy.

The analysis of market-driven applications for large batteries in chapter 4 shows that under the current's legal and regulatory framework the application on the primary control reserve market is by far the most lucrative business model for large scale batteries (see Figure 4.14). This is the main reason why the SmartPowerFlow project focused on this business model (see chapter 3). As mentioned in subsection 4.2.1, another reason is that there are no experiences with vanadium redox flow batteries on the PCR market in Germany. However, the free scalability of the energy-to-power ratio of this storage technology may prove beneficial in the future, especially considering the discussions regarding capacity requirements for batteries providing PCR (see subsection 4.2.1).

In the highly regulated PRC market, the operation strategy is mainly predetermined by the technical restraints and the legal framework in place. Thus, no additional analysis regarding which operating strategy is the best is conducted. However, the novelty of the analysed operation strategy is the grid supportive behaviour of the BSS that is providing PCR. This service has been added to its primary purpose (to provide PCR) by adding a reactive power control strategy.

In this chapter the technical and economic aspects of the grid supportive behaviour of the BSS that is providing PCR are assessed. In section 5.1 some general remarks are given if PCR is provided by a BSS with a special focus on large scale BSS in distribution grids. In section 5.2 a simulation model of the SPF prototype based on measured values is presented. This BSS model is included in the simulation of the operation strategy, which is presented section 5.3. Furthermore, the parameters for a profit maximising operation of the stand-alone BSS are determined by running a parameter variation using the operation strategy model. In section 5.4 the operation strategy is validated along with the BSS model in a field test. Currently, the most common BSS technology to provide PCR (see Table 4.2)) is based on lithium-ion systems. A technical and economic assessment of a pool of VRFB, which provides PCR, is compared to an exemplary lithium-ion system, in section 5.5. A sensitivity analysis, in which the most significant economic parameters are varied, completes the economic assessment. Finally, the chapter is concluded in section 5.6.

5.1 General remarks on providing PCR with BSS

As described in subsection 4.2.1 the active power in- and output of a BSS providing PCR does not depend on the local grid state but on the grid frequency (see Figure 4.1) and is therefore grid compatible, but not grid supportive (BSS behaviours are defined in subsection 2.1.8). Thus, from the DSO's perspective such a grid participant is initially regarded as not grid supportive, as it may contribute to critical grid states. This is discussed in detail in section 7.1. To avoid critical grid states a system supportive behaviour, which combines a grid supportive and a system compatible behaviour, is realised with the SPF battery. This is achieved by connecting the BSS to the LV bus bar of a MV/ LV transformer to ensure that a unfavourable active power flow may not lead to OV issues. The grid supportive behaviour is realised by adding a Q(V)-control to control the voltage to the P(f)-control needed for the provision of PCR (further details in section 3.3).

Thus, the aim of the operating strategy developed in this chapter is to optimally combine the provision of primary control reserve with a reactive power control to increase the hosting capacity for DG (defined in subsection 2.1.5).

The challenge in achieving this goal is that the two applications primary control reserve and voltage control services must be provided with an availability of 100 %. On the one hand, according to current legal requirements, the end user must be provided with electricity within a fixed voltage band at all times (see subsection 2.2.1). On the other hand, a 100 % availability of the component that provides PCR has to be guaranteed and is a requirement to participate in the PCR market (see Table 4.3). However, since battery storages, unlike conventional systems, have a limited capacity, it is important to ensure that the battery charge level is kept at a level, at which the provision of PCR is ensured at all times. Figure 5.1 illustrates this problem: the SOC of the SPF battery decreases almost continuously due to efficiency losses, even if temporarily more negative power (charging) has to be provided as positive power (discharging). With a grid supportive PCR operation mode the BSS would be discharged even further as the inverter draws the energy required for the provision of reactive power from the BSS. A SOC adjustment is therefore mandatory to ensure a 100 % availability of the provision of primary control reserve and voltage control.

As explained in subsection 4.2.1 the optimal SOC for BSS providing PCR is around 50 %, since statistically approximately the same amount of positive and negative balancing power has to be provided over time. However, as the SOC of the BSS providing PCR tends to drop in the long run, the German

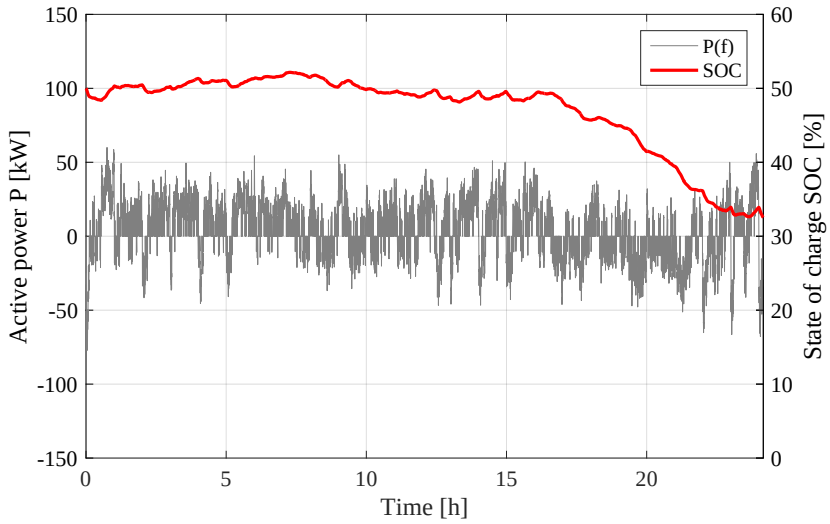

Figure 5.1: PCR-provision with the VRFB-prototype during a field test without SOC adjustment; measured values on day 23/8/2016.

TSOs have defined a total of six *degrees of freedom* for SOC adjustment during battery operation. They are explained in more detail in subsection 4.2.1 and [189].

In this work, the following degrees of freedom have been applied for SOC adjustments:

- **Dead-band**: Possibility to readjust the battery SOC by charging or discharging using the dead-band.
- **Optional overfulfilment**: Option to provide 20 % more balancing power than required.
- **Permissible operating range**: Option to readjust the SOC during 30 seconds in which the requested power has to be fully activated.
- **Schedule transactions**: Optional adjustment of the SOC by purchasing or selling energy at the energy market.

The degree of freedom to adjust the SOC with other technical units is neglected, as it is one of the scopes of this work to show that a stand-alone operation of large scale BSS providing PCR is possible. The option *relocation of the dead-band when grid-time corrections are planned* as this degree of

freedom requires information from the TSO about the target frequency for the upcoming day which was not available in the SPF project.

The first three of the listed degrees of freedom are cost-neutral and can be applied continuously. If the SOC still threatens to reach a critical level, additional charging or discharging is required. These schedule transactions on the intra-day market, result in additional costs. Thus, an optimisation is required to minimise additional costs, while ensuring the availability of the BSS for PCR provision as well as reactive power control (presented in section 5.3).

5.2 Battery System Model Based on Measured Values

As stated in chapter 3 the modelled 200 kW/ 400 kWh VRFB is able to operate in a four quadrant operation mode, with a theoretical apparent power of 630 kVA. The BSS has a pump managing system with four individual pumping circuits, that can be activated according to the needed power in 50 kW steps in order to reduce the self-consumption of the BSS.

According to [235] there are macro [236–238], micro [239] and molecular approaches (e.g. the Molecular Dynamics method [240]) for modelling VRFB. Most of these theoretic battery models, of which some were verified in the laboratory [235–237], aim to improve the battery efficiency or to increase its capacity. In contrast to these models, the aim of the presented BSS model is to analyse the battery operation at the PCR market as realistically as possible over a longer period of time (weeks). The presented BSS model is also used for the economic optimisation of the BSS and to analyse the interaction with the electrical grid and the resulting reactive power need. For market applications, such as in this work, empirical (macro) models, based on measured data to predict the future behaviour without consideration of physicochemical principles, seem to be the most appropriate to employ [235]. Therefore, an empirical approach similar to [241] for LiB based on efficiency characteristics is selected for the VRFB model. In contrast to the VRFB model in [238], the BSS model is verified along with the PCR application in a field test presented in subsection 5.4. Furthermore, the effect of the reactive power provision on the SOC is not considered in [238].

Depending on the application, different time resolutions are used in the BSS models. For PCR one-second time-steps seem appropriate to properly incorporate all DOF. VRFB already in operation have shown an extremely long working life time (up to 270,000 full cycles) and no self-discharge, if

the two electrolytes are stored in different tanks [112]. Nonetheless, the electrolyte in the reaction chamber may cause self-discharge which occurs mainly in idle mode. [242] reports that this effect can be neglected in the process of charging or discharging which happens continuously in both applications. Thus, similarly to the investigation in [243], both effects (calendric and cyclic ageing) are neglected in this work. The inverter and battery are modelled separately in subsection 5.2.1 and subsection 5.2.2.

5.2.1 Inverter Model

The losses occurring during the operation of the inverter can be distinguished into no-load losses and apparent power losses. No-load losses are losses independent of the apparent power and are caused mainly by switching losses of the insulated gate bipolar transistors of the inverter bridge. For the SMA inverter used in the SmartPowerFlow project these losses are 2.3 kW. They were determined by measuring the DC power between battery and inverter at 0 kW active power and 0 kvar reactive power at the AC side. The apparent power losses are composed of the losses due to provision of active and reactive power. For the VRFB-prototype a stable 4-quadrant operation of ±200 kW as well ±400 kvar has been tested and validated in the field, as shown in Figure 5.2.

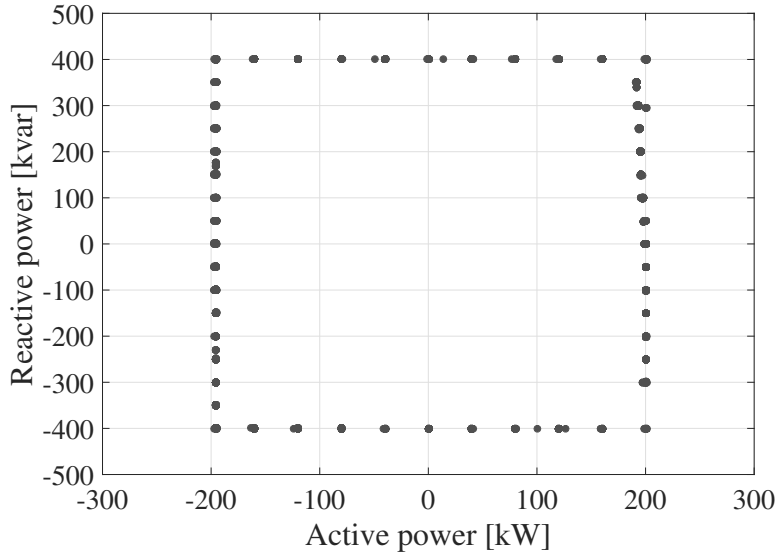

Figure 5.2: 4-quadrant operation mode of the BSS inverter (load perspective).

To determine the active power losses, the active power was altered over the entire operating range of ±200 kW and the apparent power was kept at a constant level of 0 kvar. The resulting active power losses for charging and discharging are depicted in Figure 5.3. The efficiency was determined from the ratio of DC to AC-power for the charging process end vice versa for discharging. At low power ratings of less than 50 kW, the efficiency of the inverter is between 85 % - 95 % and for power ratings greater than 50 kW between 95 % - 98 %.

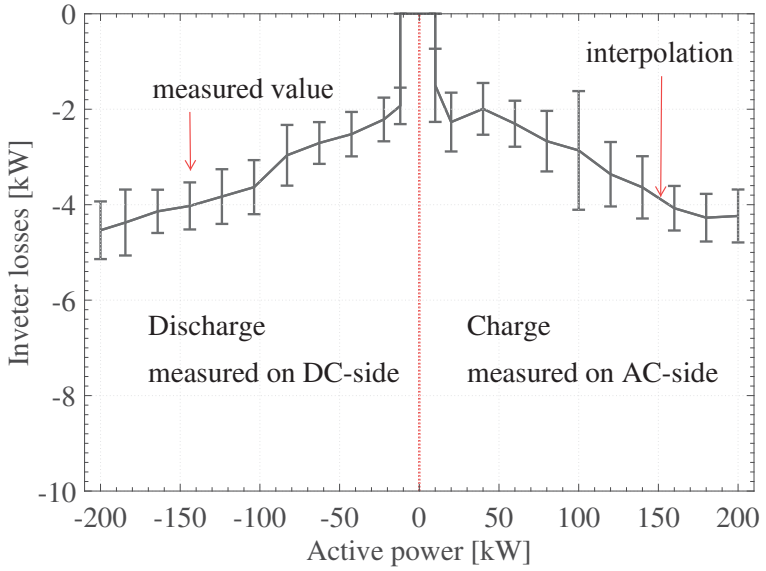

Figure 5.3: Measured active power dependent inverter losses P_{loss} (load perspective).

The methodology to measure the reactive power losses is the same as for the active power losses: the AC-active power is set to 0 kW, whereas the reactive power is varied over the whole operation area of ±400 kvar. The results of this measurement are shown in Fig. 5.4. The measuring point for a reactive power of 0 kvar corresponds to the above-mentioned no-load losses of around 2.3 kW. The losses increase with increasing reactive power and reach a maximum of approximately 9 kW with maximum reactive power.

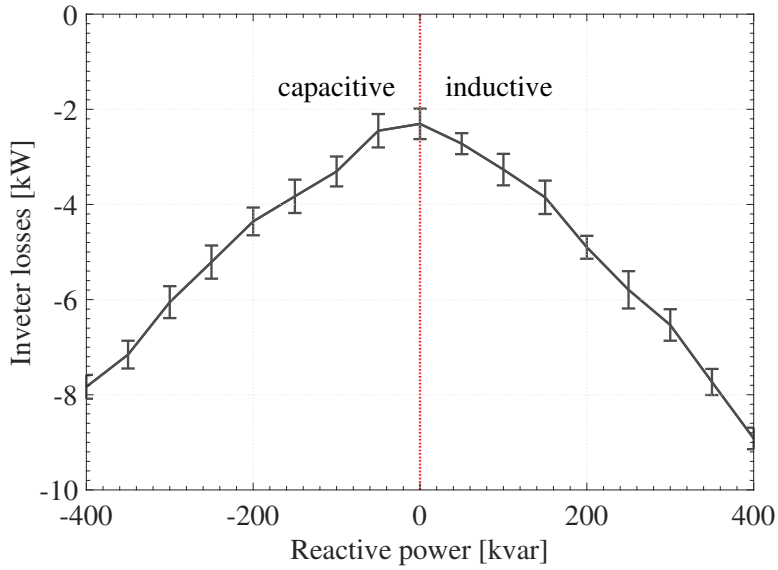

Figure 5.4: Measured inverter losses Q_{loss} at reactive power provision (load perspective).

According to SMA [244] the apparent power losses of the inverter S_{loss} can be approximated by equation (5.5), since the losses are mainly dependent on the absolute value of the apparent current I_s.

$$I_s^2 = I_p^2 + I_q^2 \tag{5.1}$$

$$P = I \cdot V \tag{5.2}$$

$$V := const. \tag{5.3}$$

$$I \propto P \tag{5.4}$$

$$S_{loss} = \sqrt{P_{loss}^2 + Q_{loss}^2} \tag{5.5}$$

where I_p is the absolute value of the active current, I_q is the absolute value of the reactive current, P_{loss} are the active and Q_{loss} the reactive power dependent losses. For data points in between the measurement data, P_{loss} and Q_{loss} are approximated by linear interpolation.

5.2.2 Battery Model

For the modelling of the battery, the charge- and discharge characteristics were measured. The BSS was fully charged and discharged at various power

levels as depicted in Figure 5.5 and Figure 5.6. The discharge was limited to 1 % SOC to avoid a deep discharge. The deviations of charging and discharging powers of the target value can be attributed to various causes such as power drops due to an excessively high electrolyte temperature, the failure of a DC-DC converter inside the battery or incorrect control commands by the battery management system and can be neglected in the model, since these effects can be attributed to the prototype status of the BSS.

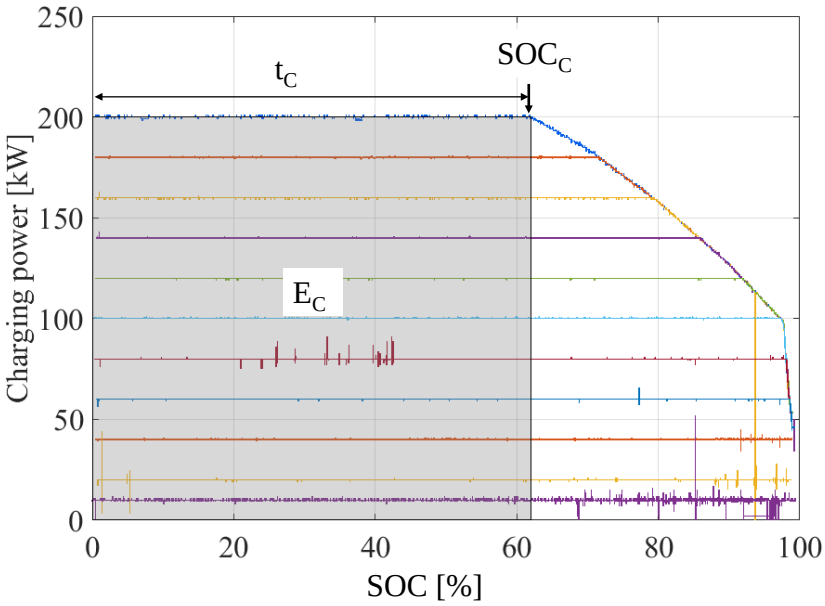

Figure 5.5: Measured battery charging curves.

The charging and discharging curves show that the BSS can only be charged or discharged with a constant power up to a certain SOC. After reaching this power dependant SOC limit, the charging or discharging power drops steadily. For example, a constant charging power of 200 kW can only be maintained during the time period t_C up to a charge level of 62 %. From this point on which is called SOC_C, the charging power drops to 53 kW until the battery is fully charged. The energy supplied to the BSS up to the point SOC_C, is defined as E_C (see Figure 5.5). This also applies to the discharging process. The SOC from which the constant discharge power decreases is referred as SOC_D, the energy taken up to this point is called E_D (see Figure 5.6). To participate in the PCR market, the BSS has to provide the requested power reliably and without interruption. Thus, it can only be

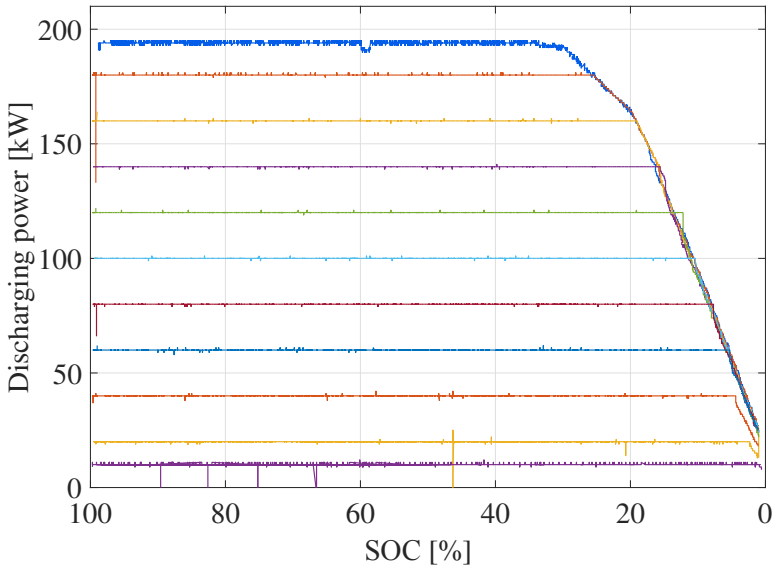

Figure 5.6: Measured battery discharging curves.

operated within the limits SOC_C and SOC_D for a given value of the pre-qualified power. The change of SOC within these limits is calculated in the model as follows:

Charge:

$$\Delta SOC = SOC_C \cdot \frac{\Delta t \cdot P}{E_C}\bigg|_P \tag{5.6}$$

with $SOC_i, SOC_f < SOC_C$

Discharge:

$$\Delta SOC = (100 - SOC_D) \cdot \frac{\Delta t \cdot P}{E_D}\bigg|_P \tag{5.7}$$

with $SOC_i, SOC_f > SOC_D$

where parameters SOC_C and E_C as well as SOC_D and E_D were derived from the characteristic curves. SOC_i is the initial SOC before charging/ discharging and SOC_f the final SOC after charging/ discharging.The values for charging and discharging powers between the measured values are taken from linear interpolation.

The charging and discharging curves were measured in the PCR mode, where all four pumping circuits of the VRFB-prototype are active due to the fast response time that is necessary when providing PCR. The pumps consume 12 kW. This power is taken directly from the grid and purchased at the intra-day market, since this is more cost effective than discharging the BSS. The validation of the 1-second-BSS-model is presented in section 5.4.

The equations used to calculate the amount of energy used for charging and discharging the BSS, as well as its efficiency for a given timespan, are presented in Appendix B.6.

5.3 Methodology: Modelling of a Grid Supportive Application for a Battery Storage System at the Primary Control Reserve Market

The operation strategy is based on a frequency data analysis which ensures a 100 % availability, as required by the TSO during the entire period, in which the primary control reserve and voltage control services are provided.

5.3.1 Input Data and Assumptions

The economic analysis is based on the legal framework of the PCR market. The technical framework concerning the amount of energy that has to be reserved in the future to have access to the PCR market is still uncertain due to different regulations on a national [190] and European level [245] and may result in an E2P-ratio of 2:1 for LiB [246,247]. This is the same E2P-ratio that is applied for the VRFB in this work. The variable E2P-ratio of the VRFB might therefore be an advantage, if the technical requirments change. Nonetheless, from an economic point of view LiB (if possible with a E2P-ratio of 1:1 or even 0.5:1) seems to be preferable [246], due to lower CAPEX. The prices for the energy needed to recharge the battery, the bidding prices, the CAPEX and OPEX of the BSS and all additional data used in this chapter refer to the year 2015, if not stated otherwise.

Revenue Stream and Expenses during Operation

The revenues that can be achieved at the PCR market are determined by the BSS operators' own bidding strategy as well as the structure and costs of the competitors [248]. In this work the bidding strategy is simplified as it is assumed that the BSS can provide PCR for 50 weeks per year (corresponding to

50 bidding periods) [249]. The historical PCR prices fluctuate considerably in the course of one year. The more stable weekly average yearly values of the years 2008-2017 were ranging between 3000 EUR/MW and 4000 EUR/MW (except 2012, 2016 and 2017 [194]). For this work a yearly weekly average of 3500 EUR/MW (which is slightly lower than the value of 2015) is assumed during the entire lifetime of the BSS [194]. Nonetheless, this value might be too high, since in the last two years the average bidding prices dropped drastically and might remain on that low value or drop even further [250]. Therefore, a sensitivity analysis is presented in subsection 5.5.2 in which the influence of the bidding price on the maximal CAPEX to achieve a profitable business case is analysed. This work, as well as most of the related studies [243, 247, 249], assumes a constant yearly revenue stream over the BSS lifetime.

Expenses during PCR provision arise from the necessity to keep the battery charge level between certain limits, to ensure that the demanded power can be supplied at any time, as discussed in subsection 5.2.2. The energy that is needed to correct the charge level is traded at the intra-day market. The medium-term development of the intra-day market is hard to predict. Therefore, the annual average price for the 15-minute product of 33.09 EUR/MWh is used here. [251]. Additionally, a handling fee of 2 EUR/MWh has to be added [252]. As stated in section 5.2, the auxiliary energy to run the pumping system generates further expenses and is traded at the intra-day market as well as the energy needed to maintain the SOC in a target interval. For further simplification it is assumed that the energy can always be traded and that the annual average intra-day price for a 15-minute product is constant. Based on [246] a value-added tax of 19 % on costs and revenues as well as an electricity tax on the traded energy of 20.50 EUR/MWh is taken into account. Since the tax and duty charge for electricity storage is currently in dispute, the energy tax has to be paid in all cases [253]. Finally, the costs for the metering point operation have to be taken into account and are set to 509 EUR/year [254].

Frequency data

To determine the correction limits of the SOC, further explained in subsection 5.3.2, worst case scenarios are analysed. For this, particularly over- and under-frequent months from frequency data, provided by the Swissgrid AG, are used. The data is depicted in grey and blue in Figure 5.7.

Swissgrid AG, the Swiss transmission grid operator, as a result of a comprehensive frequency data analysis, identified a representative heavy and a

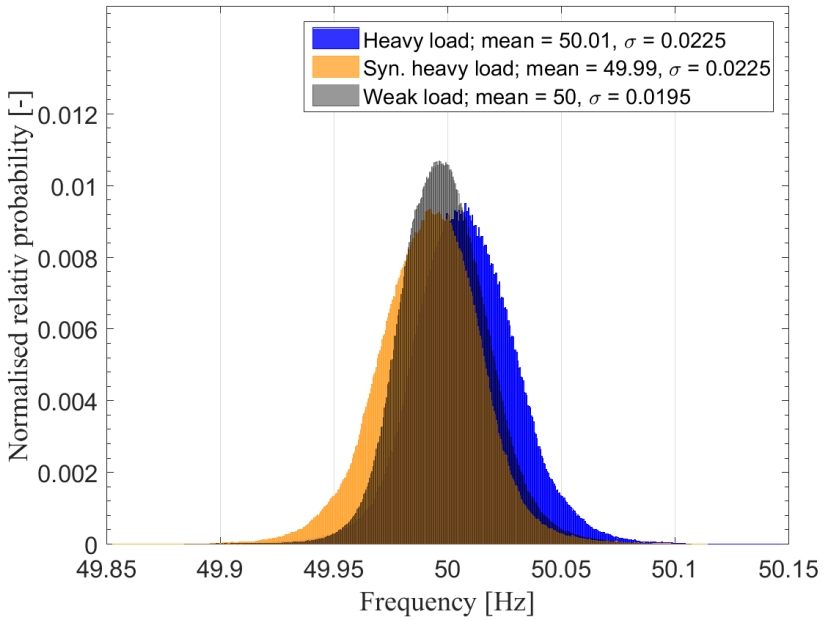

Figure 5.7: Frequency distribution of the used grid frequency data.

weak load month. The data shows an average over-frequency behaviour during the heavy load month, resulting in higher battery charging powers than in average months. The heavy load month shows a stronger frequency fluctuation than the weak-load periods, due to greater load gradients. Therefore, an extreme under-frequent monthly time-series was synthesised by mirroring the heavy-load time-series on the 50 Hz axis and depicted in orange in Figure 5.7. The derived set of two heavy-load monthly time series can be considered the worst-case scenarios from SOC control point of view.

The economic analysis is based on the frequency data of the weak-load month given that this month's frequency time series is approximately normal distributed, as is true for long term frequency time series [249, 255]. Therefore, the charged and discharged PCR power of the BSS is balanced on average [256,257]. Furthermore, the economic analysis was verified using frequency data from year 2013. It shows, very similar results and is therefore not further discussed.

Battery Storage System Parameters

The minimum offered power at the German PCR market is 1 MW. Since the considered VRFB-prototype has a maximum power of 200 kW, a pooling of the battery is analysed. Pooling entails additional costs for additional infrastructure. Those additional costs are neglected in this study due to missing literature concerning this issue. However, pooling increases CAPEX and OPEX of the 1-MW pooling unit, because the largest BSS unit needs to be redundant (n-1 criterion) [190].

Economic Assumptions

The CAPEX and the OPEX, and other economic parameters for the PCR business case (see section 5.5) and for the self-consumption business case (see chapter 6) are presented hereafter.

Capital expenditures

The formula to calculate the investment costs I_0 (:=CAPEX) for a given power P_{max} and a given capacity E_{max} is given by [133]:

$$I_0 = c_P \cdot P_{max} + c_E \cdot E_{max} + C_{per} \tag{5.8}$$

where c_P are the specific cost of the power electronics, c_E are the specific cost of the components needed for the capacity and C_{per} are the costs for the system periphery (e.g. site costs). C may not be able to be scaled with the system design and is very project specific [249]. For VRFB, which are hardly established in the market, currently a large range of cost factors exist and the costs are therefore difficult to generalise [258–260].

Equation 5.8 is applied to adapt the costs found in the literature for commercial BSS to the same configuration as in the SPF project for VRFB in Table 5.1 and for LiB in Table 5.2.

Table 5.1: Minimal, average and maximal specific investment costs for a VRF BSS with 200 kW/ 400 kWh, based on [133] [258] [261] [138].

	Commercial product			**Prototype**
	min.	av.	max.	SPF
Cost $[\frac{EUR}{kWh}]$	565	908	1464	2422

Table 5.2: Minimal, average and maximal specific investment costs for a Li BSS with 200 kW/ 400 kWh, based on [138] [261] [249] [246].

	Commercial product		
	min.	av.	max.
Cost $[\frac{EUR}{kWh}]$	375	711	983

It can be seen that the cost range for both technologies is very high, but for LiB the cost range is not as large and the CAPEX are generally lower [260]. Furthermore, cost reduction potentials are currently mostly discussed for lithium-ion batteries, since the amount of available data for cost learning curves is much broader [207].

Additional Economic Parameters

For the OPEX a value of 2 % of the minimal I_0 is assumed, which includes the replacement costs of components during the life time [137]. The internal rate of return is set to 4 % [249] and the lifetime for the BSS to 15 years [137,249].

5.3.2 Modelling of the Operation Strategy

All parameters that have to be determined for this operating strategy are schematically depicted in Fig. 5.8. The optimisation of the battery optimisation is mainly a maximisation of the PCR revenues and a minimisation of expenses for trading correction energy at the intra-day market. In order to achieve this, the available charging/discharging power has to be allocated between the power that is pre-qualified at the PCR market and the power that is used to adjust the charging level of the battery. Furthermore, the SOC limits at which intra-day trades are triggered have to be determined.

The pre-qualified power P_{pq} determines the theoretical revenues and the usable capacity of the BSS. As described in subsection 2.2.2 the power of the BSS is only constant within a certain power dependant SOC range. The lower and upper limit of this interval is defined as availability limit $SOC_{av,min}$ and $SOC_{av,max}$. Outside these availability limits the BSS does not reach its full power, thus limiting the usable capacity to the capacity interval within these limits.

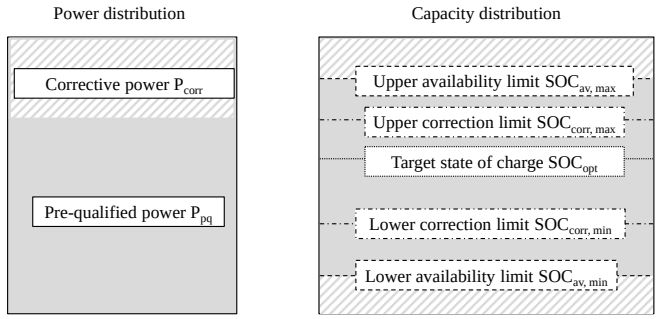

Figure 5.8: Schematic of the variable operation strategy parameters for the PCR-model.

As stated before, the maximum available power of the BSS must be divided between the power to correct the SOC and the power offered at the PCR market. The 30-min period until the transaction is effective is critical. In view of the depicted efficiency losses of the storage system and the asymmetrical position of the availability limits, the upper and lower correction limits are to be determined individually. In order to determine the correction limits, the assumption is made that the availability limits should not be exceeded even in a particularly over- or under-frequent month, even if the SOC is already at the corresponding correction limit at the beginning of the month. The heavy load month was used to determine the upper availability and correction limit and the synthesized under-frequent month was used for the lower limits (grid frequency times-series are depicted in Fig. 5.7).

To ensure that the SOC stays within the availability limits, energy is traded at the intra-day market. This transaction increases or decreases the active power with a delay of 30 minutes for the delivery period of 15 minutes [122] by the contracted value, and is defined as the DOF *schedule transactions*. Besides this cost-generating DOF there are additional DOF that can be used to keep the SOC close to the target SOC at no extra costs: *dead-band,optional over-fulfilment* and *permissible operating range*. These DOF are integrated into the simulation model as well (Fig. 5.9).

The P(f)-characteristic, as defined in [262], is the basis of provision of PCR and the active power control of the BSS. As described in detail in [263], the DOF can be used to regulate the SOC by deviation of the required PCR power P_{PCP}, resulting in a new $P_{PCP,new}$. The DOF *schedule transactions* is triggered when the SOC surpasses a threshold defined as correction limits SOC_{corr}. Therefore, the SOC interval between $SOC_{corr,max}$ and $SOC_{corr,min}$

is narrower than the interval between the availability limits, since it has to be secured that the SOC does not surpass the availability limits during the 30 min delay (Figure 5.8). For the three DOF which are free of charge the actual SOC of the time-step and the set target value SOC_{opt} (in this study set to 60 % due to the low BSS efficiency), as well as the absolute value the of frequency f and the direction of the actual frequency deviation Δf are essential inputs. All DOF can be used separately or combined.

The *dead-band* can be applied for $50\,\mathrm{Hz} \pm 0.01\,\mathrm{Hz}$ and $P_{PCP,new}$ is calculated as follows:

$$P_{PCP,new} = \frac{\Delta f}{0.2\,Hz} \cdot P_{pq} \quad (5.9)$$

If the DOF *optional overfulfilment* is used, the P_{PCP} according to the P(f)-characteristic is exceeded by 20 %.

$$P_{PCP,new} = 1.2 \cdot P_{PCP}. \quad (5.10)$$

When making use of the *permissible operating range* the power gradient ∂P_{PCP} is restricted to the permitted ramp (30 seconds until full activation), instead of using the fast reaction time of BSS.

$$\max\left(|\partial P_{PCP}|\right) = \frac{P_{pq}}{30} \quad (5.11)$$

This DOF is stopped in case of a change of sign between two time-steps (e.g. change from charge to discharge)

The final $P_{PCP,new}$ value calculated after applying all three DOF free of charge is limited to P_{pq}.

$$|P_{PCP}| \leq P_{pq} \quad (5.12)$$

Finally, the DOF *schedule transactions* is activated if the

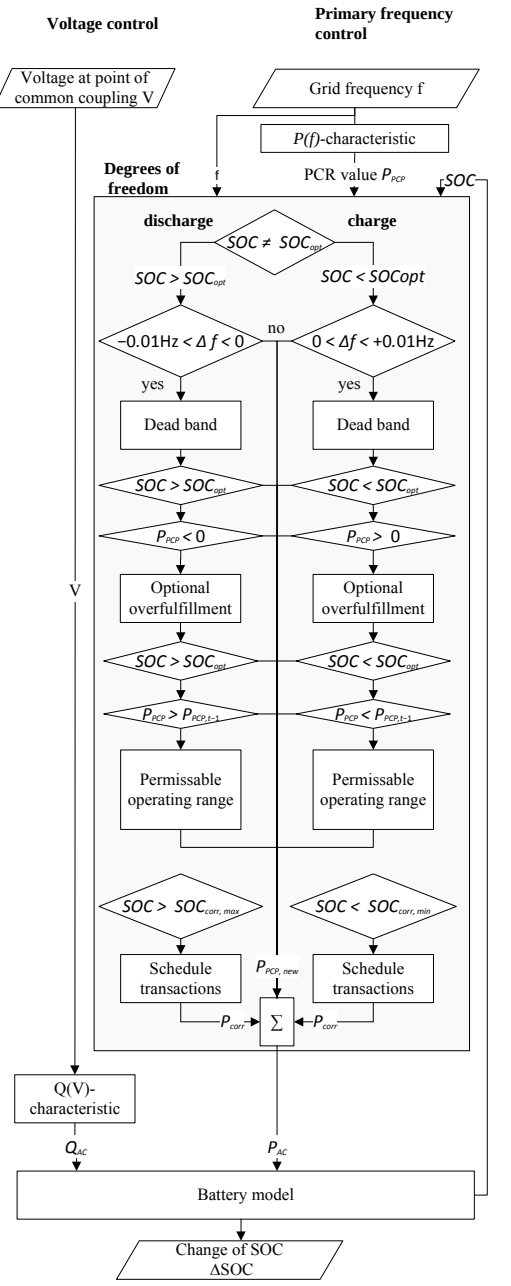

Figure 5.9: Operating strategy model of grid supportive BSS providing PCR.

availability of the BSS is endangered. The voltage time series that is needed as input data for the reactive power control is taken from measurements from the year 2013 at the point of common coupling of the BSS. Two worst case months were identified, each with a particularly high or low reactive power consumption corresponding to the annual average.

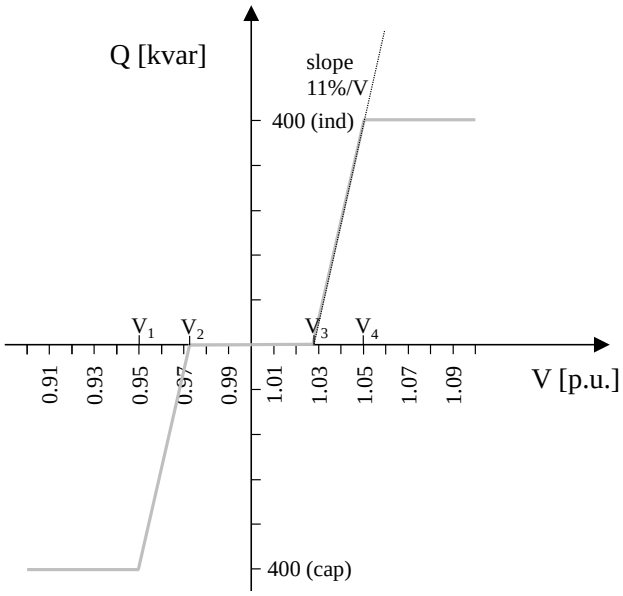

Figure 5.10: Q(V)-characteristic used for the reactive power control.

To define the points of the Q(V)-characteristic, shown in Fig. 5.10, the maximum voltage limits according to DIN EN 50160 of ±0.1 p.u. are taken as a basis [41]. Furthermore, a measurement uncertainty of ±0.01 p.u. is taken into account [26]. Since a maximum voltage drop of 0.04 p.u. can be assumed [18], V_4 is set to 1.05 p.u. (1.1 p.u. - 0.01 p.u. - 0.04 p.u.). In order to keep the Q(V)-control stable a slope of the 11%/V (phase-to-ground-voltage) is proposed by [45] which results in the value of 1.027 p.u for V_3. Since the Q(V)-characteristic is assumed symmetrical to the origin [45], V_2 and V_1 result. A PT1-element is assumed with an amplification factor K=1 and a time delay of T=5 seconds [45].

In order to maximise the net present value with this operation strategy, the maximum P_{pq} that can be provided with the given BSS has to be determined. At the same time the availability of the BSS to provide PCR and reactive power control has to be assured at all time. For this reason P_{pq} was varied in 5 kW steps and tested for the worst case scenarios described before.

5.3.3 Results of the Parameter Determination for a Profit Maximizing Operation

For the PCR operation strategy the worst-case time series for frequency and voltage at the PCC were used for an iterative simulation, by changing the pre-qualified power. Thus, the upper and lower correction limit as well as the corrective energy can be calculated. From an economic point of view, the combination of pre-qualified power, upper and lower correction limits is optimal, when the PCR revenue are maximised and at the same time the costs of the correction energy are minimised.

Table 5.3 lists the parameters, which are calculated with a brute force optimisation/ parameter variation, as described in subsection 5.3.2, for the scenario with the maximum difference between PCR-revenue and corrective energy costs. For a pre-qualified power higher than $P_{pq} = 175\,\text{kW}$ the availability of the BSS to provide PCR and reactive power control can not be ensured.

Table 5.3: Optimal parameters for the PCR operation strategy.

Parameter	**Value**
Pre-qualified power	175 kW
Corrective power	25 kW
Target value	60 % SOC
Upper corrective limit	65 % SOC
Lower corrective limit	47 % SOC
Upper availability limit	72 % SOC
Lower availability limit	22 % SOC

The results in Table 5.3 show that both the availability and the correction limits are arranged asymmetrically around the SOC of 50 %. Due to the efficiency losses during charging and discharging of the battery, the target value and the correction limits are just below or above the SOC of 50 %. Furthermore, it can be seen that due to the battery losses, the distance between the upper correction and upper availability limit is substantially less than the distance between the lower correction and lower availability limit.

5.4 Field Test Validation of the Prototype Applying a Grid Supportive Primary Control Reserve

The behaviour of the VRFB prototype, providing a grid supportive PCR, as well as the identified parameters for the operating strategy were tested and validated through various measurements in the field.

The results and evaluation of the pre-qualification test (see subsection 5.4.1), as well as the field tests for the use of individual degrees of freedom (see subsection 5.4.2) and the identified operating strategy (see subsection 5.4.3) are presented below.

5.4.1 Pre-qualification Test for Primary Control Reserve

According to the pre-qualification criteria for BSS for the PCR market, described in subsection 4.2.1, the usable capacity of the storage system is determined using the variant 1 of the *Doppelhöckertests* according to [190] (see Appendix B.4). The usable capacity for the SPF prototype has been determined using a pre-qualified power of 175 kW in the field. The result of this test for the provision of negative PCR (charging the BSS) is depicted in Figure 5.11.

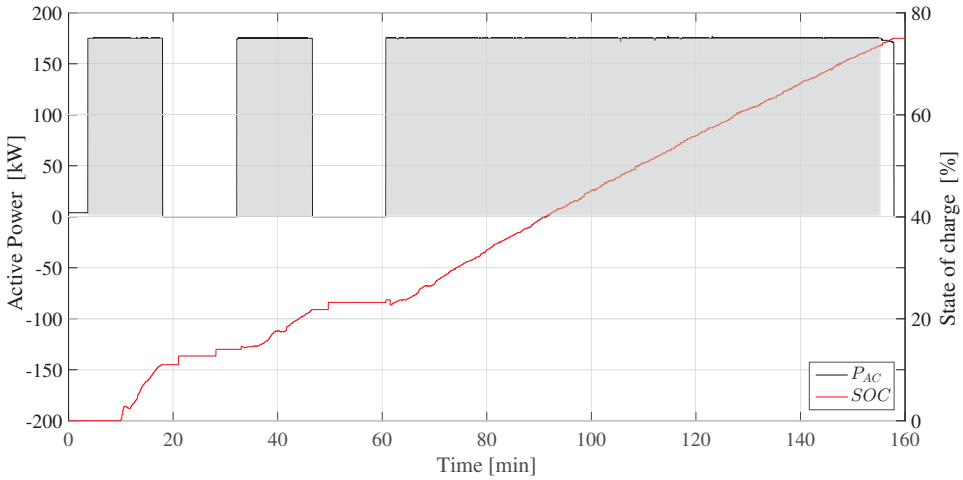

Figure 5.11: Pre-qualification test of the BSS with the calculated pre-qualified power of 175 kW. The grey area represents the usable capacity of the BSS for the provision of negative PCR, determined with the test.

The black line of Figure 5.11 shows the active power of the BSS and the red line the SOC of the BSS. The SOC is 0 % at the beginning of the test. According to the pre-qualification test criteria the system provides twice the full pre-qualified power during 15 minutes with a break of 15 min in between. After another 15 minutes break the pre-qualified power of 175 kW is provided again until the power is reduced automatically by the BSS, as the upper availabilty limit of 72 % is reached (see also Table 5.3).

The resulting usable capacity E_{use} for providing negative PCR is depicted by the grey area in Figure 5.11 and is 368.25 kWh. Thus, it is shown that the 15 and 30-min criterion described in subsection 4.2.1 can be fulfilled. The tests for providing positive PCR are also passed, since the discharging efficiency is slightly better as for charging and is therefore not depicted.

Besides measuring the usable capacity it is shown, that the control system of the prototype is able to fulfil the requirements with a precise and fast response of the BSS.

5.4.2 Testing the Implementation of the Degrees of Freedom in the Field

In this section the field test implementation of the degrees of freedom *dead-band*, *optional overfulfilment*, *permissible operating range* and *schedule transactions* presented in subsection 4.2.1 are shown and discussed.

Figure 5.12(a) and Figure 5.12(b) show the measured values of the BSS operation with the implemented DOF *dead-band*. In Figure 5.12(a) the behaviour of the BSS is depicted for the case that its SOC is below the SOC target value and in Figure 5.12(b) it is vice versa. For both cases the dead-band interval of 50 Hz±0.01 Hz is marked in red. The black line represents the power that has to be provided according to the P(f)-characteristic in % of the pre-qualified power and the measured data are depicted as grey dots. These dots are aligned with the requested power. In Figure 5.12(a) the dead-band is used by the BSS to reduce its power provision between 49.99 Hz to 50 Hz and thus not to discharge the battery any further in this range. At the same time the dead-band interval from 50 Hz to 50.01 Hz is used to charge the battery within the permitted range which is given by the linear P(f)-characteristic. In the right Figure 5.12(b) it is vice versa, as the SOC is higher than the target SOC value and the dead band is used to discharge the battery as much as possible.

The spread of the measured data around the set-point can be explained by the relatively slow one-second measuring intervals, compared to the reaction speed of the battery system which occurs in milliseconds. Thus, the measured

values are delayed. In case of jumps from one set-point to the next, depending on the exact measuring moment, a inaccurate value may be recorded. The measured values are therefore scattered around the set-points. The closer the values are to the nominal frequency the larger are the deviations, since these frequencies occur more often and more jumps occur around the nominal frequency.

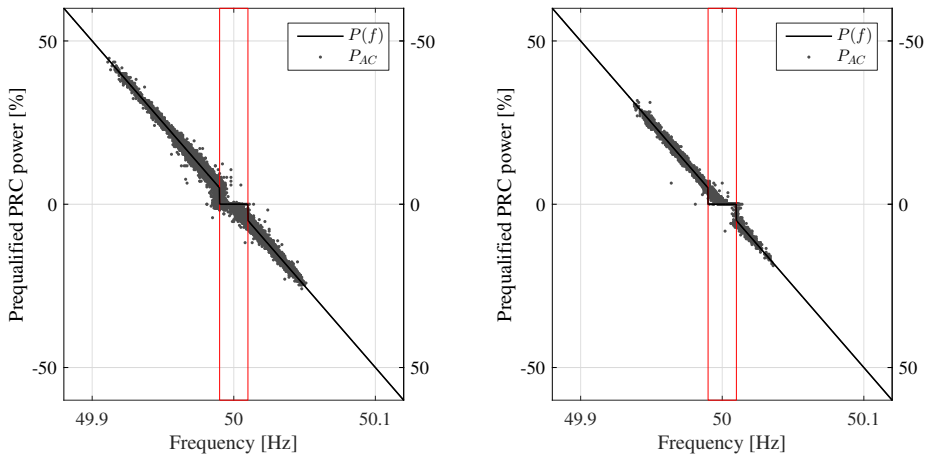

Figure 5.12: Implementation of the DOF *dead band*: (a) shows the data for a SOC of the BSS below the SOC target value and (b) shows the behaviour of the BSS if its SOC is higher than the target value.

Similar to the DOF *dead-band* discussed before, the measured data for the DOF *optional overfulfilment* are depicted in Figure 5.13(a) and Figure 5.13(b). In these graphs the set points for *optional over-fulfilment* are marked as a dotted line, additionally to the P(f)-characteristic. In Figure 5.13(a) it is shown that, in case of a SOC below the SOC target value for frequencies higher than the nominal 50 Hz (and the dead-band), the DOF *optional over-fulfilment* is applied by the BSS to recharge (marked in red). For frequencies below the nominal value the normal P(f)-characteristic is applied. In case of a SOC higher than the SOC target value the behaviour of the BSS is vice versa, as shown in Figure 5.13(b).

For the DOF *permissible operating range* a similar figure is not suitable, due to the mentioned delay in the measurement and its implementation in

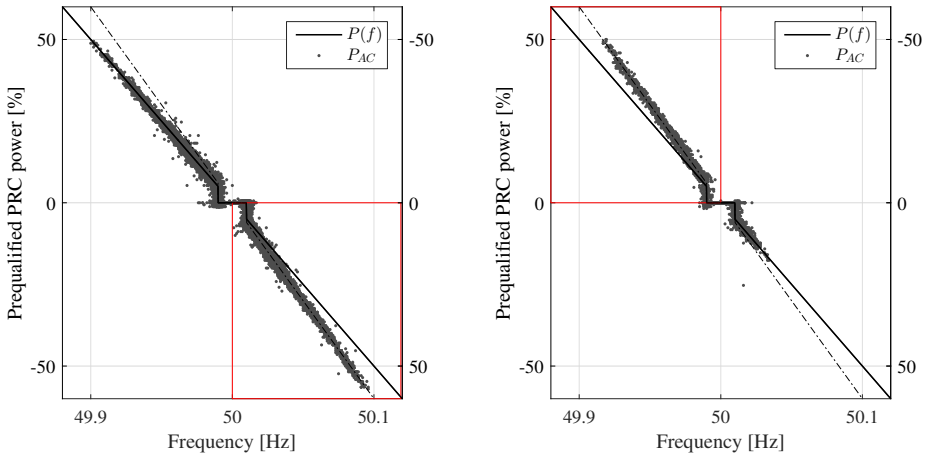

Figure 5.13: Implementation of the DOF *optional over-fulfilment*: (a) shows the data for a SOC of the BSS below the SOC target value and (b) shows the behaviour of the BSS if its SOC is higher than the target value.

the BSS, and is therefore not depicted.

The BSS parameters of Table 5.3 are applied to a simulation of the operation strategy (shown schematically in Fig. 5.9) and are used to illustrate the behaviour of the BSS for these parameters. For this purpose, the required PCR power, the active power and the SOC of the BSS are depicted in separate graphs in Figure 5.14 for a time period of six hours.

In Figure 5.14(a) the course of the provided frequency dependant power $P(f)$ according to the P(f)-characteristic is shown. In the time steps during which the $P(f)$ is zero the frequency is within the dead-band. The dotted line show the adjusted power P_{PCP} that is provided by the BSS according to its SOC, if the DOF are used which are free of charge (see also Figure 5.14). Within the period marked in red, first there is no difference between $P(f)$ and P_{PCP}, since positive control power is demanded but the SOC is below the SOC target value SOC_{opt}. Shortly after this period, the grid frequency is within the dead-band and $P(f)$ is zero. However, since the frequency is higher than the nominal value the DOF *dead-band* is used to recharge the BSS and P_{PCP} becomes negative. Furthermore, the BSS applies the DOF *optional over-fulfilment* and thus the P_{PCP} values (dotted line) become more

negative than the $P(f)$ values.

In Figure 5.14(b) the total active power P_{AC} that is provided by the BSS and P_{PCP} (same P_{PCP} of Figure 5.14(a)) are depicted. In this graph the signs of the power are switched, since the power values are depicted in the more common load perspective which is also used for the load flow calculation. Due to the DOF *schedule transactions* the values of P_{PCP} are shifted to more positive values in order to recharge the BSS. The energy purchased in the scheduled transactions are marked as grey surfaces E_{corr}. In all other time steps the P_{AC} is identical with P_{PCP}. A delay of 30 minutes in between the moment which the energy is purchased to the moment in which it is delivered can be seen some minutes before 3.00 o'clock. At this time step the SOC is below the lower correction limit and the energy is purchased. 30 minutes later the contract is fulfilled and the energy is delivered and the SOC starts to rise again.

The corresponding SOC, the upper and lower SOC correction limits and the target SOC SOC_{opt} value are depicted in Figure 5.14(c). It can be seen that the SOC stays at the lower limit and does not reach SOC_{opt}. However, the SOC does not decrease too much within the depicted time period, such that the pre-qualified power can be provided in every time step.

A more detailed analysis of the battery behaviour and the evaluation of the individual DOF, which are free of charge, as well as the provision of reactive power will be shown and discussed in the following section.

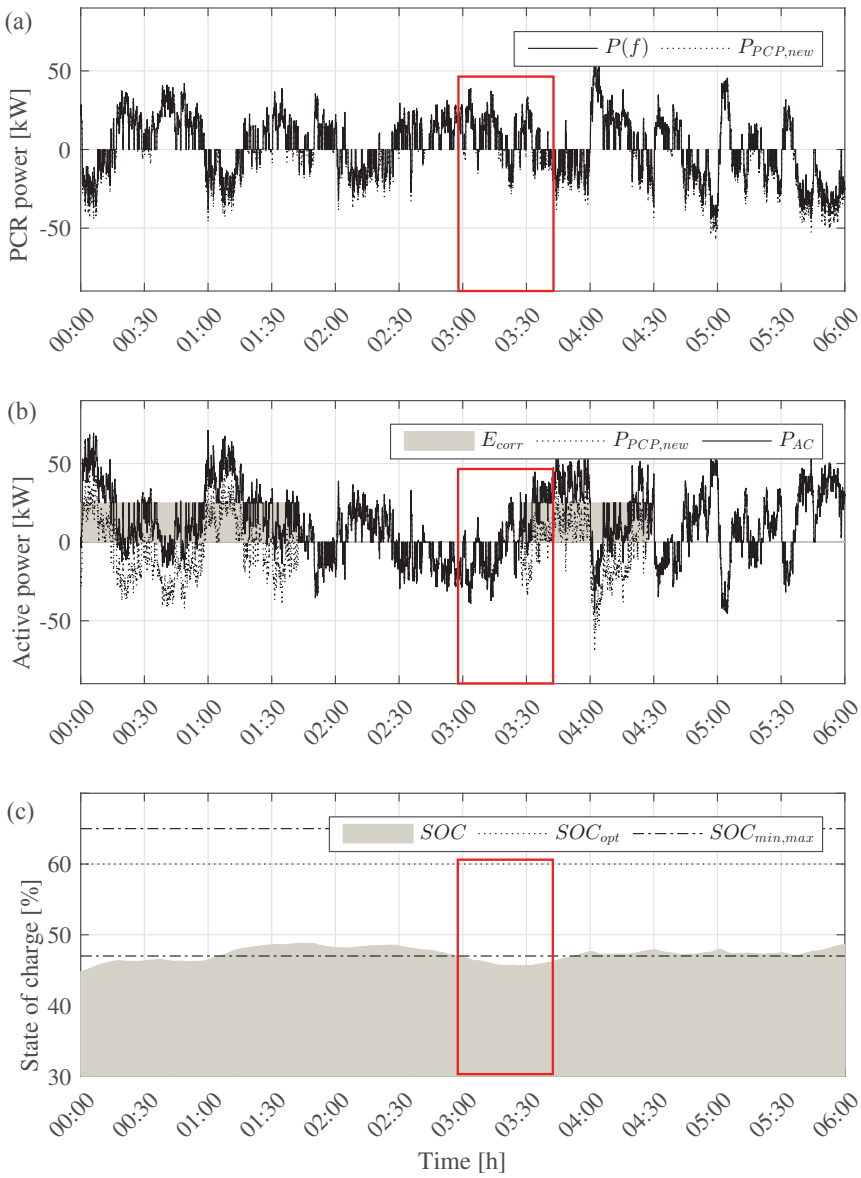

Figure 5.14: Illustration of the parametrised operating strategy with implemented degrees of freedoms. (a) Demanded PCR power with and without application of the DOF free of charge. (b) Active power of the SPF-prototype with and without the application of the DOF. (c) SOC and SOC limits. The interval marked in red depicts the timespan from activation of a scheduled transaction until its fulfilment (45 minutes).

5.4.3 Validation of the Battery Model and the Operation Strategy in the Field

A multi-week field test with the determined parameters demonstrates the performance of the grid-supportive PCR operation strategy, depicted in Figure 5.15. During the whole time, reactive power according to the Q(V)-characteristic is provided (red curveFigure 5.15(a)). As can be seen in Figure 5.15(a), the maximum requested frequency dependant PCR-power P(f) is only 20 kW, or 8.5 % of the pre-qualified power during this period (grey curve).

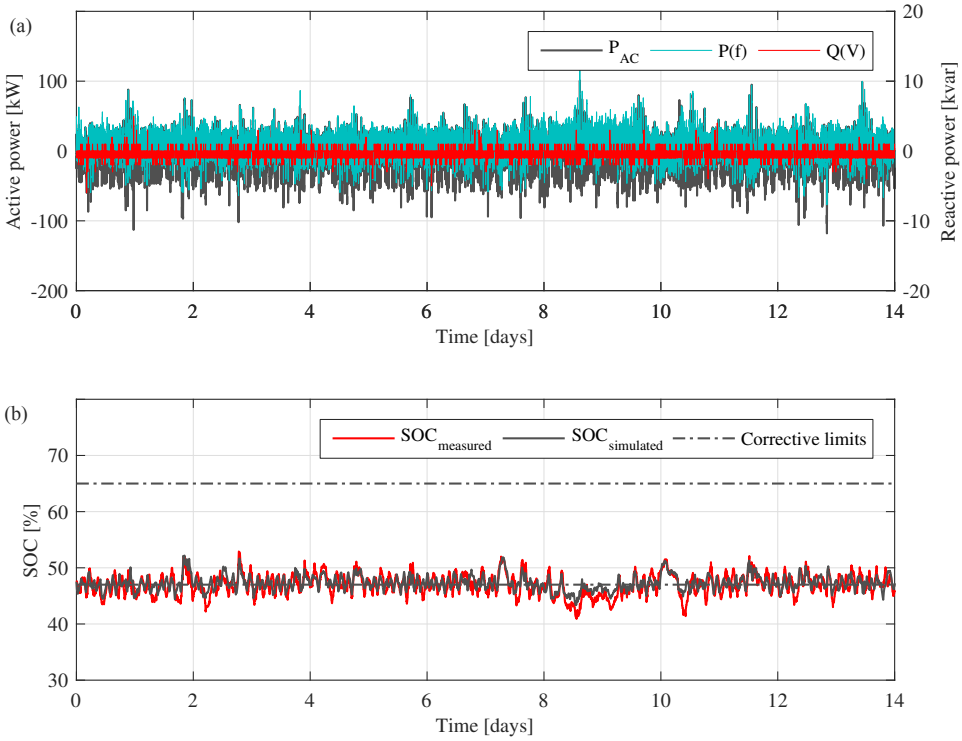

Figure 5.15: Excerpt from the field test of the grid-supportive PCR operating strategy, 03.-17.08.16. (a) Provided active P_{AC} and reactive power Q(V) of the BSS and frequency dependant PCR-power P(f) (generator perspective). (b) Measured and simulated SOC and correction limits.

However, this could be expected, due to the stochastic distribution of the

frequency fluctuations (see Figure 4.9). In Figure 5.15(a) P_{AC} is shown, too. P_{AC} is is the active power, measured at the PCC of the BSS. It can be seen that during the field test the DOF are exclusively applied to charge the battery.

This unsymmetrical application of the DOF (they are mainly used to recharge the BSS) is also reflected in the SOC (Figure 5.15(b). Due to the low system efficiency, the used battery capacity interval is narrow and oscillates around the lower correction limit. Thus, the target value of 60 % is never reached.

For the validation of the battery system model for the PCR provision (section 5.2), the battery parameters were measured during the two weeks mentioned above in the grid-supportive PCR operating mode providing active and reactive power. Ex-post, the SOC curve was simulated by using the calculated active and reactive power as input parameters according to the measured frequency and voltage at the PCC, as depicted in Figure 5.9. For the entire measurement period, a very good match between simulation and measurement was achieved as shown in Fig. 5.15(b), with a relative error of 2.5 % (Least Squares Method). However, the simulated SOC is usually slightly ahead of the measured SOC. This is due to the inertia of the SOC measurement, which is not represented in the model. In this BSS prototype, the SOC is measured via the open circuit voltage of a stack to which no load is connected. Since the electrolyte of the stacks connected to the load has to be mixed with the electrolyte in the tanks before it is pumped into the idle stack, the changed SOC is measured with a certain delay. This delay was quantified to vary between 0-19 minutes.

The evaluation of the field measurements shows that the overall system efficiency, especially at low power, is not very high: The BSS efficiency over the period depicted is 30 %. When the pumping power is taken into account, it is even lower at approximately 23 %. This is considerably lower then for LiB of a similar size, since 72 % round-trip efficiency is reported in [264] for the same application. These low values can mainly be attributed to a low efficiency of the power electronics if they operate at less than 10 % of their nominal power (similar to [264]).

5.5 Technical and Economic Assessment of a Grid Supportive Vanadium Redox Flow Prototype for Primary Control Reserve

In this section firstly, the applied degrees of freedom and the grid supportive behaviour of the BSS are assessed from a technical and economic point of view. Then, the business model of providing a grid supportive PCR with a VRFB is evaluated and compared with a LiB battery providing the same service.

The basis of the economic analysis is a life cycle cost analysis, as described in detail in [21]. With this method, all cash flows before and after any selected reference time are assigned a present value. For this purpose, all expenses and revenues that occur during the life cycle are accumulated or discounted to the reference date with a specified interest factor. The net present value is the sum of all the discounted future cash flows. The NPV is the decisive value to evaluate whether an investment is profitable or not.

The system design of the BSS is given, hence the CAPEX are fixed. Furthermore, disposal costs are neglected, since at the end of the life cycle the electrolyte of a VRFB can still be used and earn revenues [203].

5.5.1 Technical Assesment

The technical assessment is an evaluation of the DOF and the grid supportive behaviour of the VRFB providing PCR. It is not possible to provide PCR with the analysed BSS without the application of the DOF *schedule transactions*. Therefore, an operating mode for the discussed grid-supportive operation strategy, which uses this DOF, is only used as a reference scenario in order to evaluate the efficiency of the other optional and cost neutral DOF, as well as the costs incurred by the reactive power provision. As depicted in Fig. 5.16, the comparison of the individual DOF shows that they differ significantly in their contribution to reduce corrective energy that has to be traded at the intra-day market with the DOF *schedule transactions*. When all cost neutral DOF are employed, the corrective energy can be reduced by approximately 20 %.

However, the economic effects of the DOF are low, as the net revenues only increases by 0.9 %, 1.1 %, and 0.08 % for the DOF dead-band, optional over-fulfilment and permissible operating range, respectively. If all optional DOF are used, the delta net revenues sum up to 2.1 % or a monthly extra revenue of 45.89 EUR. Although, in one third of the simulated time-steps

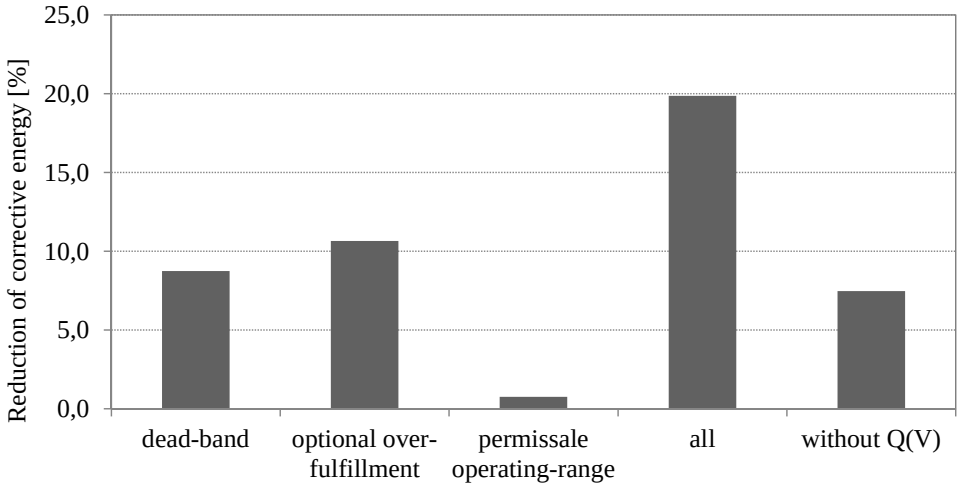

Figure 5.16: Reduction potential of the DOF and energy demand of the voltage control.

the battery has to be charged via intra-day transactions and although over 40 % of the total energy is due to corrective energy, the total costs of the corrective energy (with all DOF) amount only to 7 % of the revenues.

For this same reason, the impact of the provision of reactive power is minimal. This results from a simulation with all DOF, but without a reactive power supply (right column in Fig. 5.16). For the analysed PCR prototype, the monthly expenditures increase by only 14 EUR for additional correction energy needed to provide this service. It can be concluded that the resulting additional cost burden for a grid supportive behaviour of a BSS system providing PCR is very small.

5.5.2 Economic Assessment

The resulting cash-flows and net present values (NPV) for the PCR business case is presented in this section. As described before (section 5.3.1), realistic frequency, grid and economic parameters are used for the analysis of the PCR business case. In Table 5.1 the different CAPEX and in Table 5.3 the operation parameters of the VRFB that have been used for the economic analysis are listed.

Cash-flows

In Figure 5.17 the annual cash flows without discount for the PCR business case for one VRFB prototype and a LiB are depicted. To participate in the PCR market, a minimum of $1 MW_{pq}$ pre-qualified power must be offered. Furthermore, the (n-1)-criteria has to be fulfilled. This means that for the examined prototype a pool of seven BSS with an offered power of 175 kW per BSS has to be in service. The displayed cash flow corresponds to a pool of the seven BSS. The comparison of the revenues and costs shows that, despite the low efficiency of the VRFB system, the annual PCR revenues are more than twice as much as the considered expenditures.

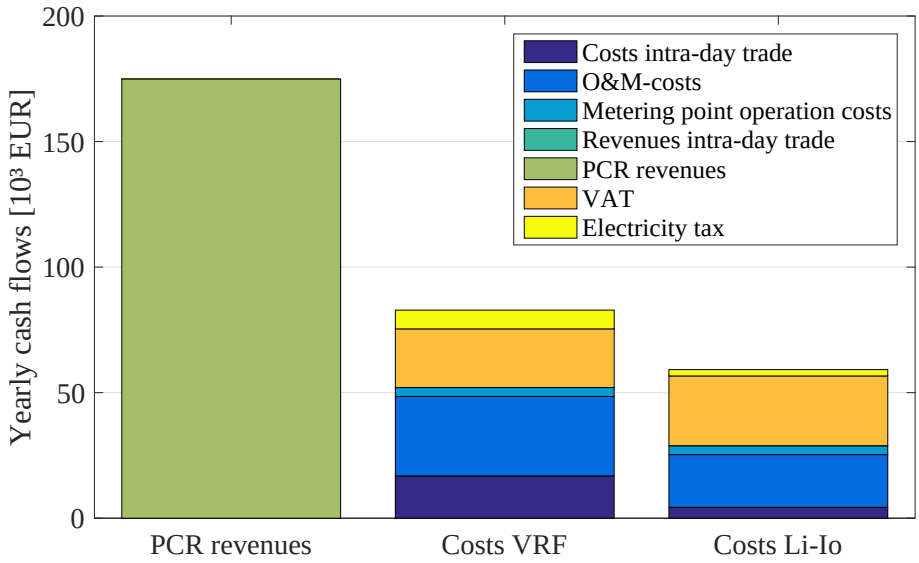

Figure 5.17: Yearly cash flows of a 1 MW-pool of the analysed system design for VRF and Li-Io.

For the LiB, the costs for the intra-day trade are adapted according to [246] and the costs for the reactive power provision is calculated proportionally (see Appendix B.8). The costs for the provision of reactive power for the grid supportive behaviour of the BSS are included in the intra-day trading costs (around 7 % of the ID trading costs). For both technologies the additional costs for the reactive power provision are less than 1 % of the revenues.

Net present value

The calculation and comparison of the net present values, as depicted in Fig. 5.18, shows that the business case is currently only profitable for the LiB, which is sized with the same energy to power ratio (2:1) as the SPF prototype and when assuming a best case CAPEX. For both battery technologies the investment costs listed in Table 5.3 are considered. If the CAPEX of the SPF prototype are considered, the business case for this prototype is far from profitable, hence this case is not displayed in the graph. The negative NPV for the VRFB is mainly due to the high investment costs, as the net cash flow is positive as shown in Figure 5.17.

The result for the PCR-case matches with current investigations in which LiB-systems can be operated profitable at the PCR market under optimistic assumptions [247, 249], however for VRFB the investment costs have yet to fall [147]. The investment costs of VRFB technology would have to decline by 30 % compared to the minimal CAPEX and by 60 % compared to the realistic (average) CAPEX in order to achieve a positive net present value.

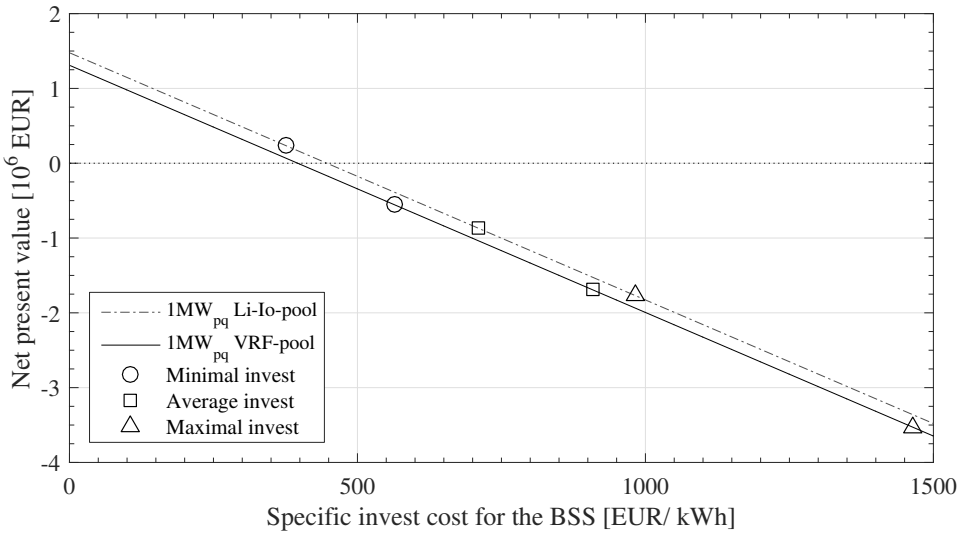

Figure 5.18: Net present value of the PCR application for LIB and VRFB.

Sensitivity Analysis of the Most Significant Economic Parameters

The influence of the PCR market price and the specific investment costs on the profitability of the grid supportive PCR application is depicted in Fig.

5.19. The marginal price at the PCR market represents, in this case, the average weekly bidding price at which a NPV of zero can be achieved. In the graph all price-investment-combinations that are on the dotted lines reach a NPV of zero. Furthermore, the economic results of the VRFB and the LiB presented in this work are compared with the results of the economic analysis for LiB discussed in [247]. In [247] similar assumptions are made as in the analysis in this work: lifetime 14 years (this work: 15 years), OPEX 2 % of CAPEX (same as in this work), discount rate 5% (this works: 4 %), same E2P ratio, CAPEX and market data for same year. For the BSS that is presented in this work the average CAPEX is shown (triangular marker), and for the LiB of [247] two E2P ratios with their respective CAPEX are depicted in Fig. 5.19. In order to evaluate the profitability the yearly weekly average power price for the last three years is also depicted. The comparison of both technologies shows that the investment costs of the VRFB has to fall at least by 27 % to be competitive with the LiB presented in this work. If the assumptions of [247] are considered for a LiB with the same system size (E2P-ratio of 2:1) the CAPEX have to fall even further by at least 45 %. Compared to [247] the application of the LiB presented in this work is less profitable, due to the more conservative cost calculation (see Appendix B.8) and additional cost assumptions, e.g. the additional purchased energy at the ID market due to the grid supportive behaviour of the BSS. However, if longer lifespans are considered, as for example 26 years in [250], the analysed VRFB is close to break even (30 years for a positive NPV) if all other assumptions of the year 2015 are kept constant.

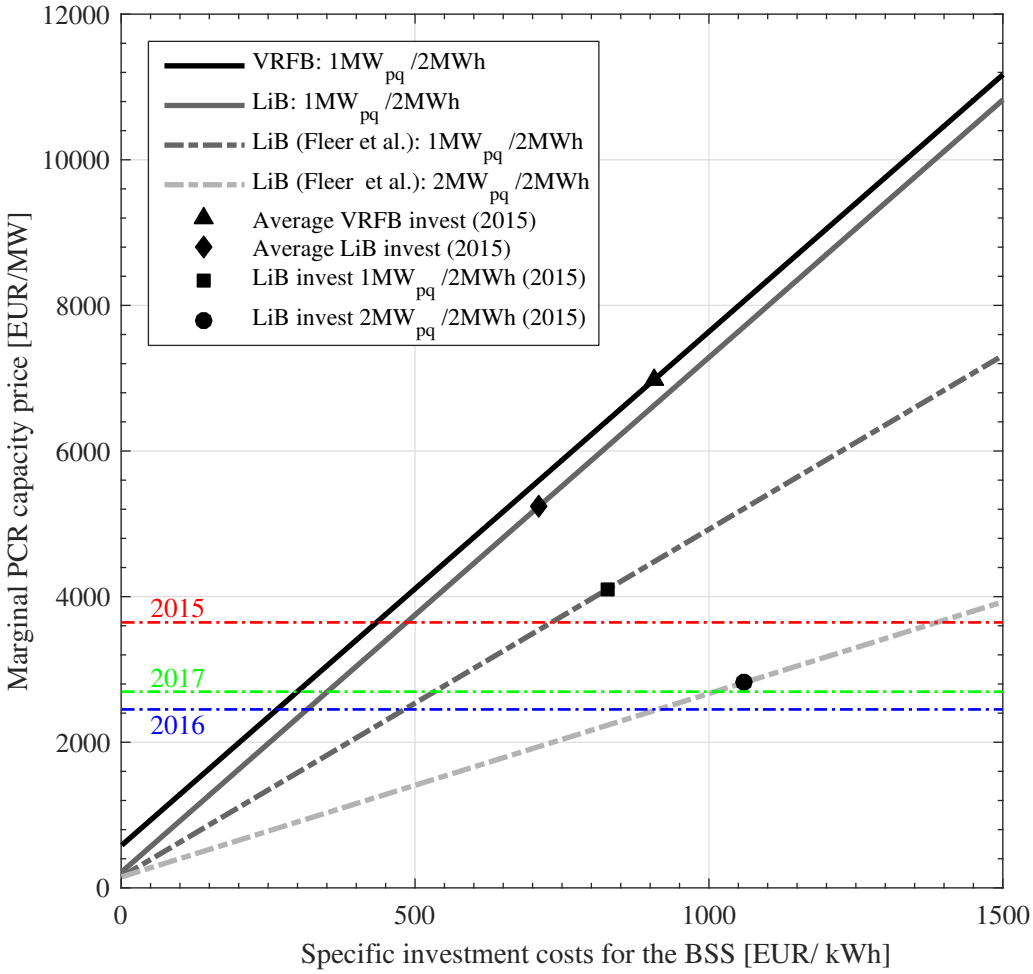

Figure 5.19: Marginal PCR capacity price as a function of the specific investment of the BES. All price-investment combinations of the black and grey lines reach a net present value of zero. The red, blue and green line represent the yearly weekly average power price for 1 MW_{pq} for the last three years. The data for the VRFB are LiB are own calculations, while the data for the LiB are taken from [247].

5.6 Chapter Summary

It is shown that the examined VRF-battery could be parametrised by modelling the operating strategy and the BSS. After this parametrisation the

BSS was able to provide a grid supportive PCR. Furthermore, the economic relevance of the low efficiency of the VRFB at low powers is small, since the energy costs to recharge the BSS account for only a small proportion of the PCR revenue. For this reason, the economic impact of the free degrees of freedom is also very low and costs for the provision of reactive power does not represent any significant additional costs. Unfortunately, under the current legal framework, this grid supportive behaviour is not remunerated. Thus, private-sector battery operators have no incentive to provide this service at the moment.

For a profitable PCR business case the investment costs and the possible PCR revenue are the determining factors. While LiB can achieve positive net present values due to lower efficiency losses and lower CAPEX, investment costs for VRFB are still 30 % and 60 % and therefore too high to break even.

The analysis highlights the current investment uncertainty for battery projects as well as their potential impact on the market if the investment costs continue to decrease. For the investment decision the system, the system design requirements and the legal framework which are currently changed at EU level, are decisive.

Chapter 6

Technical and Economic Assessment of Grid Supportive BSS Providing Self-Consumption

The first application of community storages in Mesopotamia date back to 8,500 BC [265]. In this early age they were used to store wheat that had been harvested by individuals of a community, since it was more effective to store wheat in community storages than in smaller units [265]. These storages even lead to the first accounting systems and as a consequence to the development of a first writing system in order to record how much grain was stored by who [266]. The same idea is applied at present by community electricity storages to electrical energy. As the self-consumption business case has the highest cost reduction potential it is one of the most common applications for storages in Germany, especially for households (see section 4.1). If and how this applications can be adapted to large scale BSS is subject of this chapter.

The legal framework and the possible revenue streams, for different use cases is presented in section 4.3. Since self-consumption is not a market driven application with standardised products, but a cost reduction application, the technical restrictions on the BSS and the operation strategy are much less demanding. Thus, there are plenty of different operation strategies for this application and the most suitable for the purpose of this thesis is identified fist. In order to do that, different large scale storages projects for self-consumption maximisation, which are realised in Germany and their operation strategy are reviewed and categorised in section 6.1. In the next

step, in section 6.2, the two most promising operation strategies are analysed in detail for a whole year for different load profiles, to investigate their robustness. These self-consumption strategies were designed for residential storages and were chosen, because of a more extensive literature for RES, which in turn exists, because it is the most common application in Germany at present. Nonetheless, the results and the operation strategy can be transferred easily to large scale BSS. This adoption is conducted in section 6.3, in which the most promising self-consumption strategy is adapted to VRFB prototype in the pilot region. In contrast to the analysis of the PCR application of chapter 5, this application is only analysed theoretically and not applied in a field test. Nonetheless, the battery is modelled using measured data and adapted to the requirements of the self-consumption maximisation operation strategy, as described in section 2.4. In section 6.4 the results of the technical and economic assessment of the grid supportive VREB in its application as a Community Electricity Storage are discussed. Finally, the chapter is concluded in section 6.5

6.1 Review of different self-consumption strategies for large scale BSS

Although theoretically the larger community electricity storages have a great cost reduction potential compared to residential electricity storages, as shown in section 4.3, the legal framework is more favourable for RES than for CES, resulting in additional burden of extra fees and taxes for CES. Their respective operation strategies however, can be transferred and classified into the following four categories [34,37]: direct loading (a), schedule mode (b), peak shaving (c) and based on a forecast (d). A more detailed description and quantitative comparison of the control strategies for residential systems is presented and analysed in section 6.2. Although being very similar, the control strategies for CES are different, since the incentive programme introduced by the German government only supports storage systems for grid connected PV systems up to 30 kW [37]. As a consequence, CES do not have to limit the rated power of the DG P_{rDG}. For the following graphs it is assumed that the CES is connected to the LV and the yearly energy consumption is equal to the energy production of the DG in the LV grid. It is assumed that all DG are PV systems. As suggested in [267] the ratio between capacity and the rated power of the PV system is 1:1. The implementation of the different operating strategies of the German CES projects listed in Table 4.6 are sorted in four categories (a)-(d):

(a) Direct loading
The generated energy is directly stored in the BSS if the residual power P_{res} of load and generation is positive. This simple strategy maximises the self- consumption rate,as it ensures that the BSS is loaded as soon as possible. Drawback of this strategy are the steep gradients depicted in Figure 6.1 and that, depending on the battery capacity, an excessive feed-in to the grid might occur during peak irradiation around noon, if there is no PV power limitation on the power of the PV systems.

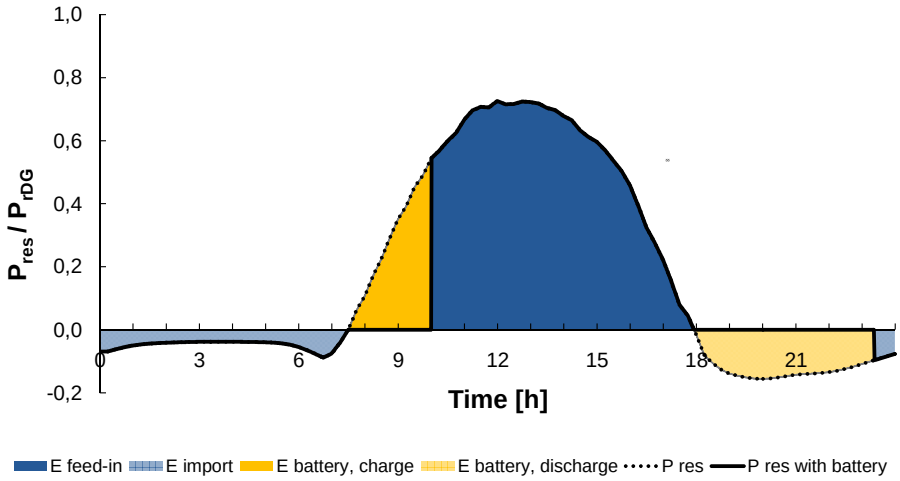

Figure 6.1: Ratio of residual power P_{res} to rated power of the DG P_{rDG} for an exemplary day, for the operating strategy direct loading (generator perspective).

A grid compatible operating strategy using direct loading to ensure a maximal renewable energy self-consumption rate (RESCR) is used by [224] and [225]. In [224] the BSS is placed in the LV side of a micro grid with DG, which is connected to the public grid via one MV/ LV transformer. The charging and discharging of the battery is calculated in 1-hour steps, from measured and synthesised time series. The main differences, compared to [224] are that in the CES project of [225] the generation and load of every participating prosumer is measured every 5-7 seconds and that the BSS is not necessarily placed at the same location as the DG and consumers. The idea of this project is that every participant may use a part of the battery that is virtually partitioned to increase the individual self-consumption ratio.

(b) Schedule based strategy
In this strategy, the time to charge the battery will be shifted to a typical time with high radiation. The schedule mode with constant charging power is depicted in Figure 6.2 showing a more favourable behaviour from a grid perspective because feed-in peaks as in the direct loading strategy are prevented.

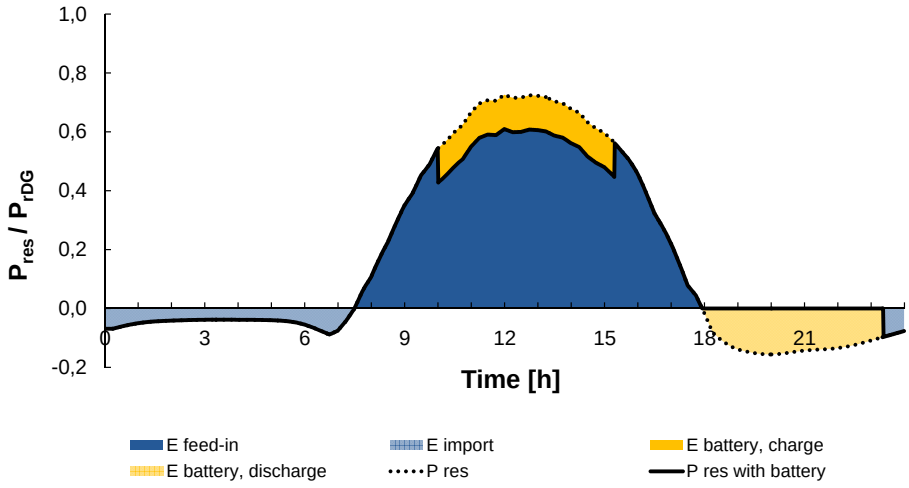

Figure 6.2: Ratio of residual power P_{res} to rated power of the DG P_{rDG} for an exemplary day, for the operating strategy schedule mode (generator perspective).

Nevertheless, the self-consumption rate might be reduced, as for days with lower radiation the BSS might not be fully loaded. Several strategies have been proposed for this purpose. The main differences between [268, 269] and [270] are that [268] and [269] propose a starting point around noon and charge the battery with full power whereas others, while [270] suggest a constant charging power over a larger period. To the author's knowledge, there is currently no CES project in Germany using this strategy.

(c) Peak-shaving (load levelling)
The main objective of the peak shaving strategy (Figure 6.3) is to avoid OV and OL issues by limiting the power at the PCC and using the remaining residual power to charge the battery [267,271,272].

The limitation of power at the PCC should be based on the voltage at the PCC, the power range of the battery, and the PV penetration of

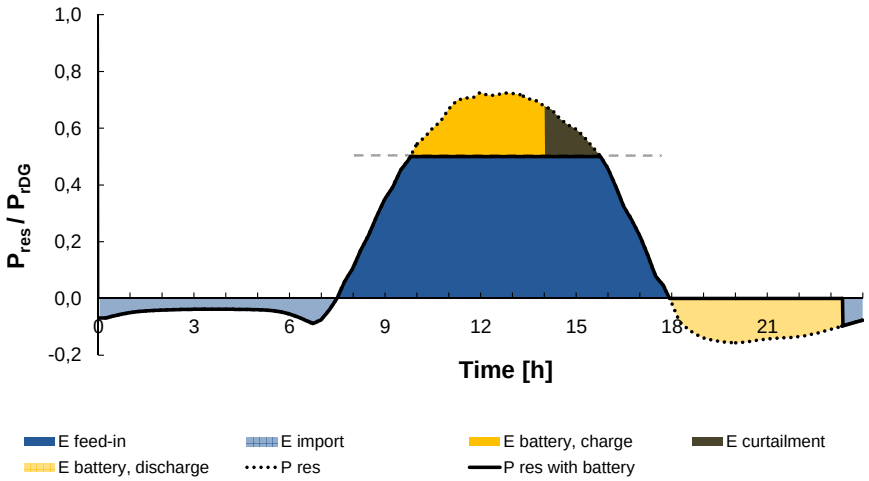

Figure 6.3: Ratio of residual power P_{res} to rated power of the DG P_{rDG} for an exemplary day, for the operating strategy peak-shaving (generator perspective).

the grid [271]. The main objective of this strategy is to not surpass a certain level of P_{res}/P_{rDG} at the PCC of the BSS. There are mainly three possibilities to achieve this aim:

(i) The battery is sized for the worst case, e.g. the day with the highest irradiation and no load, as in [20].

(ii) The power of the DG is curtailed in case of a full battery, as depicted in Figure 6.3 and described in [272].

(iii) Instead of curtailing the DG an additional load is used to reduce the residual load by using, for example, power-to-head [273].

This grid supportive operating strategy is applied to large scale BSS by [14], [20], [227] and [228]. The focus of the IRENE project [20] lies on grid expansion relief. Therefore, one or several BSS are dimensioned and placed strategically in the LV to mitigate the total feeder RPF to 70 % of the cumulated P_{rDG} of the respective feeder in which the BSS are installed. Additionally to this active power control, a reactive power control is implemented. The calculation of the set-points of P and Q are calculated externally and not by the BSS itself. [20]
Similar to the aforementioned project the BSS in Fechheim [227] limits

the power to 40 % of the cumulated P_{rDG} of feeder in which the BSS is allocated with an active power control and uses a reactive power control to reduce the voltage in the case of a fully loaded storage [227].
The aim of the SmartOperator project [228] is to minimise voltage deviations and line utilisation. The BSS is dimensioned to enable a peak shaving of 50 % of the installed PV power in a certain area for a period of 5 hours [228] based on initial studies by [274]. A learning algorithm is used to calculate the forecast of generation and load as well as future grid states, based on real time data of voltage and current [230]. This forecast is used to calculate the active and reactive power flows of the BSS to ensure peak shaving of the PV systems and that the voltage values of the grid nodes stay within given thresholds.
The advantage of peak shaving is that critical voltages might be avoided by limiting the feed-in power. The voltage can be further reduced by absorbing reactive power. In terms of self-consumption maximisation, cloudy or foggy days with reduced radiation may be problematic and can result in reduced self-consumption, as the BSS is not fully charged. On the other hand, during high irradiance days, the power curtailment is high, as can be seen in Figure 6.3 for case (ii). However for case (i) and (iii), the additional investment costs have to be considered critically. This applies in particular for case (i) in a distribution grid with many wind generators, as in this case the energy to power ratio of the BSS needs to be higher as for distribution grids with high shares of PV systems [274]. To avoid these losses or additional investment, an optimisation of the power flow based on a forecast is proposed in the following strategy.

(d) Forecast based strategy
This strategy uses load and weather forecast data to adjust the charging power and feed-in power to achieve a fully charged battery at the end of the day and/or avoid OV and OL (Figure 6.4).

A control loop throughout the day corrects the deviation from the forecast data. This strategy reaches the highest self-consumption rate after the direct loading strategy while still being grid supportive. This is due to the lower curtailment losses compared to other strategies, as shown in [198] and in section 6.2. The main distinctions of this strategy are the forecast techniques. Principally, the previously published studies can be divided into four classes :

(i) Studies using a perfect forecast [267, 275].

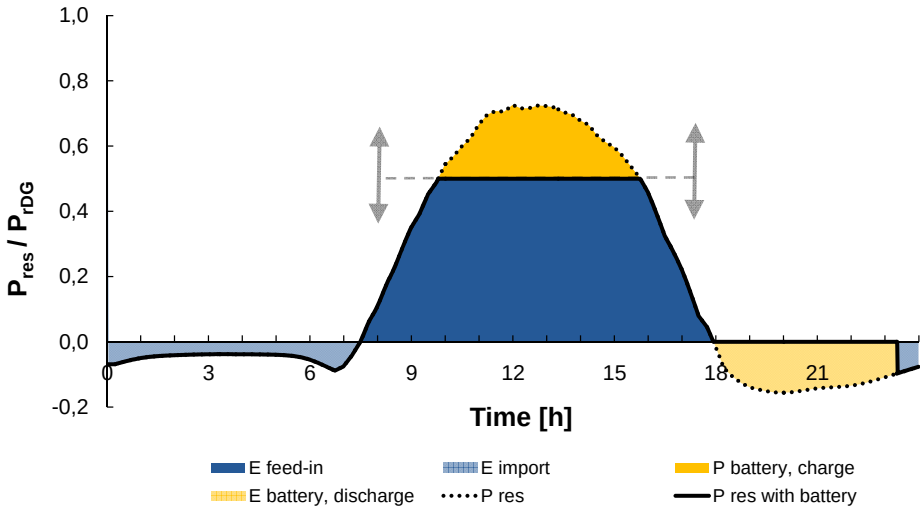

Figure 6.4: Ratio of residual power P_{res} to rated power of the DG P_{rDG} for an exemplary day, for the forecast based operating strategy (generator perspective)

(ii) Studies using synthetic forecasts (modified measured time series) [232,276,277].

(iii) Studies based on external weather-based forecast from meteorological services [273,278–280]

(iv) Studies that base their forecast on a persistence method based on values measured by the PV-system [198,276,281]

Obviously, no prediction errors apply to a perfect forecast. The only distinction is the time resolution, which in the case of [267] is 1 minute and in the case of [275] is 15 minutes.
One proposition for modelling synthetic forecast, which has been presented by [277] and also used by [232], uses the Spherical Harmonic Discrete Ordinate Method [282]. In this model measured data is used to generate the global solar irradiation at ground level for the next days. By forecasting the weather data a minute-based PV power is calculated taking into account the orientation and angle of the power plant. An error analysis of the model has shown that the average error (rRMSE) of the weather forecast for the next day for a given site is 32.5 %. This is very close to the accuracy of approximately 30 % of current numerical weather prediction models for Central Europe [283]. The value increases

for a longer forecast horizon. Instead of a physical model, [276] uses a noise sequence to fabricate a forecast based upon the hourly average of the measured data. This results in an hourly forecast for the next day with a rRMSE of 30 %.

Several studies use external weather forecasts and calculate the AC power profile of the PV system according to predicted irradiance instead of synthesising the forecast data. A simple forecast method in which the historical data of the solar irradiance and the predicted weather conditions (sunny, cloudy, rainy) are used to calculate the PV profile in 1 hour steps is presented by [278]. Also on an hourly basis, [279] predicts the PV power output for different region sizes in Germany based on forecasts for up to three days ahead that are provided by the European Centre for Medium-Range Weather Forecasts (ECMWF). For a single site and day ahead forecast the rRMSE is 36 % could be quantified. Since the rRMSE decreases as the examined area rises, for the whole of Germany the rRMSE is 13 %. Another study uses the irradiance forecast based on the Weather Research and Forecasting (WRF) model [284] and evaluates the deviation of the measured irradiance values of a pyranometer (5-8 %) and the PV power output (3-5 %) on a 15 minute base for a PV plant in Italy [280]. Historical forecast data of irradiance and temperature in 1-hour steps from Meteotest [285] has been used by [273] to calculate the PV output power and it is shown that the RESCR decreases by 15 % if forecast errors are taken into account instead of assuming a perfect forecast.

The persistence forecasting method is based on extrapolating the current or recent PV power plant output taking into account the changing of the sun angle. Since the persistence is based on a stochastic learning technique from a historical pattern, the accuracy highly depends on the forecast horizon due to the change of cloudiness [286]. The forecast method is suitable for minute based forecasts for a given location. For simulation purposes, an autonomy forecasting using a learning algorithm is more preferable compared to the one that depends on the global weather data. The differences between the different persistence forecasts arise in the algorithms used to predict the load and PV output and the values that are used to correct the intra-day deviation from the forecasted values. [276] uses a synthesised forecast data with a noise and a learning algorithm based on historical data to adapt the charging algorithm to the PV output and load within the day. Also [232] uses a synthesised PV forecast; concerning the load an easier method is proposed by predicting it based on the load profile of the past five days. In

this method, the day is divided into three periods: midnight to sunrise, sunrise to sunset and sunset to midnight. Using the arithmetic means of the past five days, the load profiles of each period determine the load for the next two days.
Fully autonomous persistence, which is not dependent on an external or synthesised forecast, is presented in [198] and [281]. In [198] a method is used that assumes a load profile for the predicted weekday, identical to the load profile of the weekday from the previous week, and predicts the PV for the next day based on the day before. To correct prediction errors within the day a proportional plus integral controller (PI-controller) adjusts the feed-in limit by constantly comparing the difference between target and actual SOC. The load prediction in [281] is the same as beforementioned. The study also shows that the forecast of the PV output has a stronger impact on the curtailment losses and self-sufficiency rate than the load forecast compared to a perfect load forecast. Therefore, an elaborated method for the PV persistence forecast is applied, which is presented in detail in subsection 6.3.5. The main difference to [198] and [232] is that the optimisation for the day is conducted only once and the correction due to forecast errors is done by comparing the forecasted SOC with the measured SOC. Thus, inaccuracies may occur as the SOC cannot be measured directly, but is a calculated value from the battery management system. The forecast and operation strategy presented in [198] and [281] lead to similar curtailment losses, but, in difference to [198], the self-sufficiency is higher with the adaptive forecast approach of [281]. The strategy of [281] is evaluated for RES in section 6.2 and applied to CES in subsection 6.3.5.

It is shown, that the adaptive forecast shows advantages over a persistence forecast with a fixed horizon. As the control algorithm based, on autonomous persistence forecasts reaches similar curtailment losses as the one based on external forecasts [281], these forecasts seem to be preferable as they need no additional hardware and are independent of the additional cost of external forecasts or meteorological services. Nowadays, up to one third of the installed residential PV storage systems in Germany are capable of applying a forecast based charging algorithm [34,215].

A forecast based operating strategy is applied to large scale BSS by [87,109,221,232,234].
In the project SmartRegion Pellworm [87,109] different business models

have been tested and affect the operating strategy. The scenario which maximises the RESCR is called "Sustainable Regional Load Supply". The active power flow of the BSS is an output of an optimisation to maximise the profit for the different business models [109] and is combined with an OPF simulation to incorporate grid restrictions to calculate the reactive power flow [87]. The forecast is carried out using a perfect foresight based on measured time-series for load and generation and historic market data. This central approach ensures a grid supportive behaviour of the BSS.

The EEbat project [232] combines the aim to relieve the grid and maximise self-consumption. The grid relief is achieved, by applying the peak shaving strategy using active power control and curtailing the RPF to 50 % of the cumulated PV installed in the LV grid. A persistence forecast for load and generation is used to adjust the charging power and ensure a maximum self-consumption [232]. Furthermore, the differences between using standard load profiles (SLP) [120] and realistic load profiles as inputs for the operation strategy are quantified. For this calculation the RESCR and the financial benefit of a CES allocated in a LV grid consisting of 50 households with PV generation and loads are compared. It is shown, that SLP are sufficiently accurate to be used as input for this operation strategy. Reactive power control is not considered in this study.

A different charging strategy than in the previous paragraph is implemented in the Smart Grid Solar project [234]. To predict the PV generation, a short term weather prediction based on sky-images instead of measured electrical values is implemented. The charging algorithm is simplistic, since the battery is charged with a constant charging power in case the residual power exceeds a given limit. Another control strategy, developed in the same project, is based on the measured voltage at the PCC, which is kept within a given range by charging or discharging the battery [234].

In the next section, the two most promising self-consumption strategies for RES are assessed and compared with the state-of-the-art algorithm by applying specific key performance indicators.

6.2 Techno-economic comparison of the two most promising self-consumption strategies

Since 2013 the increase of self-consumption with RES seems a viable business model for small PV systems in Germany [214]. Nonetheless, the main reasons to invest in RES until 2015 have been soft factors. such as hedging increasing electricity costs and contributing to the German "Energiewende" [37]. For this reason the German government introduced an incentive program, which is also scientifically monitored by [37]. The feed-in limit for the first period of the incentive program was 60 % of its rated PV power and it will decrease to 50 % for the second period, wherefore the 50 % limit is used in this thesis. The aim of this feed-in limit is to reduce OV and OL induced by RES. In order to minimise curtailment losses resulting from feed-in limitations different charging methods for RES are being developed.

This section builds upon a previous study of the same author [287], in which the two most promising strategies out of six control strategies for residential PV storage systems (RES) were identified by a qualitative approach. In this section, three different control strategies for PV storage systems will be presented and analysed in detail. The first one is the state-of-the-art algorithm *direct loading*, explained in section 6.1, and is used as reference for the comparison of two promising storage control strategies analysed in [287]. The second strategy uses a time interval to charge the storage system and thus belongs to the category *schedule based strategy*. The third operation strategy is one of the most promising algorithms of the *forecast based strategy* category and applies a persistence forecast method. To quantify the performance of the algorithms and make them comparable, the performance indicators curtailment loss ratio (CLR), self-consumption ratio (SCR) and self-supply ratio (SSR), as defined in subsection 6.2.1, are used. In subsection 6.2.2, the methodology describing the PV and load profiles, the component models and the implemented operation strategies of the RES are presented. The results of the techno-economic comparison of a schedule based and a forecast based RES are presented and discussed in subsection 6.2.3. The improvement based on the reference control strategy is quantified for both strategies using the performance criteria mentioned before along with a financial assessment in order to determine the most profitable strategy from a PV system owner's point of view. To evaluate the robustness of the results a sensitivity analysis is conducted by using several (extreme) load profiles.

6.2.1 Performance indicators

In order to minimise curtailment losses resulting from feed-in limitations different charging methods for RES have been developed. Besides reducing the CLR, the objective of these control strategies is to increase the SCR and SSR:

(a) Self-consumption ratio (SCR)

The SCR is given by

$$SCR = \frac{E_{\mathrm{PV\_c}}}{E_{\mathrm{PV}}} \tag{6.1}$$

where $E_{\mathrm{PV\_c}}$ [kWh] is the self-consumed PV production [kWh] and E_{PV} the PV production. As stated previously, an increase of the price of electricity and a decrease of the feed-in tariff creates the incentive to use PV energy production for the own consumption.

(b) Self-supply ratio (SSR)

The SSR is given by

$$SSR = \frac{E_{\mathrm{PV\_c}}}{E_{\mathrm{load}}} \tag{6.2}$$

where $E_{\mathrm{PV\_c}}$ [kWh] is the consumed PV production and E_{load} [kWh] the load demand. A high self-supply rate indicates that the PV-storage-systems can fulfil its own load demand.

(c) Curtailment loss ratio (CLR)

The CLR is given by

$$CLR = \frac{E_{\text{curtailment losses}}}{E_{\mathrm{PV}}} \tag{6.3}$$

where $E_{\text{curtailment losses}}$ [kWh] is the total curtailment loss and E_{PV} [kWh] the PV production.

6.2.2 Methodology

In order to evaluate the control strategies performance, one year is simulated in one-minute steps with measured PV data and five different load profiles. This calculation is conducted for three different control strategies for RES. The aim of these strategies is to minimise the energy losses due to the feed-in limitation. The simulation model and the input parameters and operation strategies are presented in this section.

Simulation Model

For the evaluation of the three strategies, different MATLAB simulation programs have been developed. The general schematic of the simulation model is shown in Figure 6.5.

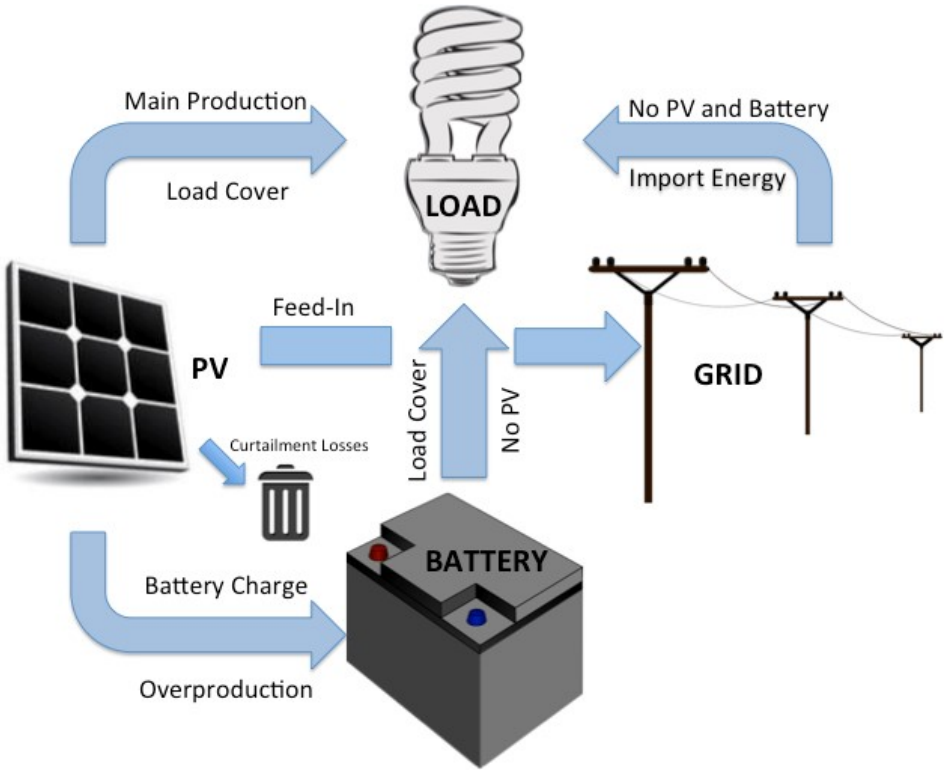

Figure 6.5: Schematic of the RES model and the calculated values.

Load cover

First, the PV power P_{PV} is used first to cover the load requirements in all available periods. In case the available P_{PV} cannot cover the requirement of load demand P_{load}, the system will use the energy stored in the battery P_{bat} to cover the load demand. If the energy in the battery is not sufficient and is fully discharged, the remaining load demand will be covered by importing power from the grid P_{import}.

PV power utilisation

If the P_{PV} is higher than P_{load}, then the residual PV power P_{res} is used to charge the battery (depending on the control specific features). The battery is never charged by drawing power from the grid. If the battery can not be charged any further, the surplus of P_{res} is fed directly into the grid $P_{feed\text{-}in}$. In order to feed P_{res} into the grid, the amount of power has to be less than the curtailment threshold of 50 % of the rated PV power $P_{PV,r}$. If P_{res} is above the curtailment threshold, $P_{feed\text{-}in}$ is limited to this threshold of 50 % of $P_{PV,r}$ and the remaining power will be wasted P_{cur}.

The simulation is conducted for one year in one-minute steps. The result values $P_{feed\text{-}in}$, P_{import}, SOC and P_{cur} are obtained for every simulation step. With these values, the final behaviour of each strategy is evaluated. Equation (6.4) [kW] to equation (6.7) are then used to obtain the values of the performance indicators previously mentioned (see subsection 6.2.1):

$$E_{PV} = \sum_{t_{start}}^{t_{end}} P_{PV} \cdot t \tag{6.4}$$

where t_{start} is the first times-step t_{start}, t_{end} the last time step of the simulation, P_{PV} the PV power and t the time-step in minutes.

$$E_{PV\_c} = \sum_{t_{start}}^{t_{end}} (P_{load} - P_{import}) \cdot t \tag{6.5}$$

where P_{load} is the load demand and P_{import} is the imported power from the electrical grid.

$$E_{load} = \sum_{t_{start}}^{t_{end}} P_{load} \cdot t \tag{6.6}$$

$$E_{curtailment\,losses} = \sum_{t_{start}}^{t_{end}} P_{cur} \cdot t \tag{6.7}$$

Input Data and Battery Model

PV Profile

The input data used for the PV time series is based on measured one-minute steps and presented in subsection 3.4.1.

Load Profiles

For this section, five different load profiles are used in order to analyse different energy usage behaviours that might apply in households. The used profiles are a German standard household profile H0 (SLP) [120] and four extreme measured household behaviours [121]: day active profile (DA), night active profile (NA), heat pump profile (HP), and air conditioning profile (AC) (depicted in Appendix B.9). These extreme household profiles were selected from a pool of 74 German household profiles for being the most extreme ones. The 15-minute mean value of all 74 profiles is nearly identical with the SLP, thus the SLP is taken as a reference [121]. The reason for choosing different load profile behaviours is to determine, if with some specific consumption behaviours, a difference in the benefits of one strategy compared to another exists. The aim is to choose the most profitable strategy, so it can be used on further analysis of the LV grid. The characterization of the load profiles was performed taking into account an annual load demand of 5 MWh. The samples for the SLP used for this analysis were taken in 15-minute steps and then linearly interpolated to generate one-minute step values. The four extreme load profiles (DA, NA, HP and AC) were measured in 1-second steps and aggregated in 1-minute steps. In Figure 6.6 the SLP load and the PV generation profile for an exemplary day are depicted.

Battery Model

For the analysis of this section, a lithium-ion battery system for the RES with a watt-hour efficiency of 95 % and a constant bidirectional battery inverter efficiency of 94 % is assumed. This gives a round-trip efficiency of 84 % for the battery and the inverter, according to [15]. The nominal battery capacity is set to 5 kWh. For an economically optimal performance of the storage system, the SOC of the battery is fixed from 20 % until 90 % of its nominal capacity.

Operation Strategies

The behaviour of the three operation strategies self-consumption (state-of-the-art) [287], schedule mode with constant charging power [276] and the adaptive persistence forecast [281] for an exemplary day with a volatile PV

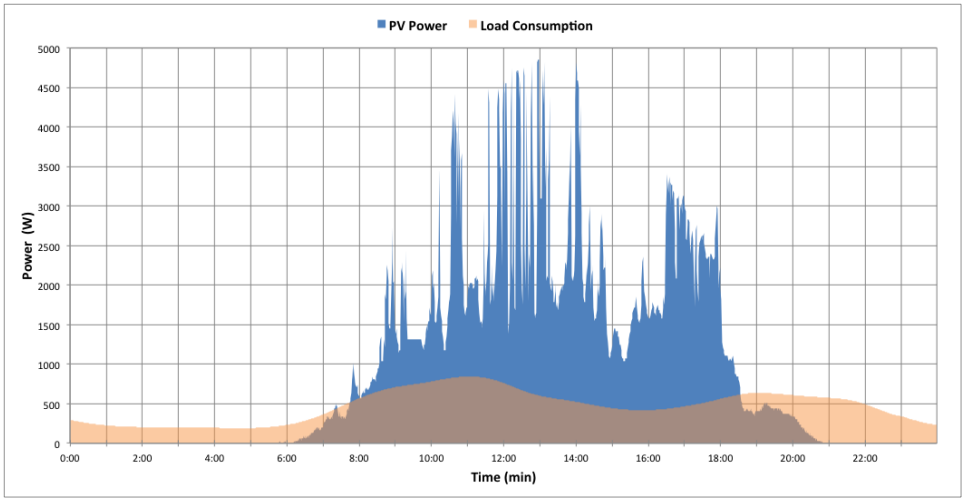

Figure 6.6: Load and PV power generation profiles for a exemplary day (6nd of July).

generation (Figure 6.6) is presented hereafter. For all strategies a feed-in limit of 50 % of $P_{PV,n}$ applies.

Self-Consumption (state-of-the-art)

With this strategy, the main objective is to have the battery charged as soon as possible, in order to use this energy later for own demand in periods with lack of PV power. This means that as soon as there is surplus of power available after load coverage, this power is used directly to charge the battery. When the battery is fully charged, the remaining power will go to the grid within the curtailment established limit. This strategy is the simplest one and is the most wide spread control applied in current PV storage systems. In Figure 6.7, the behaviour of this strategy is depicted for one exemplary day. This strategy ensures that the battery will be charged as a priority in order to increase the self-consumption ratio at maximum. This left the period of the day with the highest irradiance with only the possibility to feed the residual power into the grid, because the battery is already fully charged. This means that with high irradiance, the power may surpass the feed-in limit, and the curtailment losses will be high as well.

Schedule Mode with Constant Charging Power (SMCCP)

In this strategy, the power to charge the battery is calculated for every time step in order to provide a smooth charging for a scheduled period of

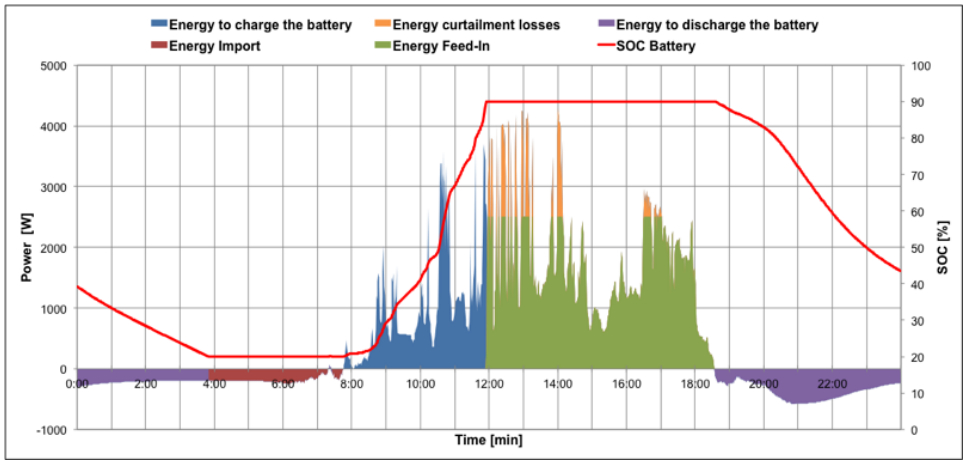

Figure 6.7: Self-consumption strategy. Power flow and battery SOC behaviour.

time (in this case from 9am to 3pm) [276]. This period of time is used to charge the battery, because it is the interval with the maximum probability of available power during the day. Therefore, it is the period with highest probability to exceed the curtailment limit.

The power to charge the battery P_{charge} is given by:

$$P_{charge} = \frac{Q_{bat}}{t_{ch,start} - t_{ch,end}} \tag{6.8}$$

where Q_{bat} is the capacity of the battery available before it reaches full charge and $t_{ch,start}$-$t_{ch,end}$ is the remaining time available to charge the battery between the scheduled period of charge. With this type of control strategy, the system utilisation is improved in order to reduce the curtailment losses and increase as well the profitability of the investment. In Figure 6.8 the behaviour of the SMCCP strategy on an exemplary day is shown. On days with low irradiance, this strategy may not fully charge the battery, because of the internal control algorithm that will look for a specific amount of P_{charge} in every period of time $t_{ch,start}$-$t_{ch,end}$. This means that if the P_{charge} power calculated with equation (6.8) is not available ($P_{res} < P_{charge}$) in certain time steps, the control algorithm will use the residual power P_{res} in this period to charge the battery. This will lead to a remaining higher Q_{bat} in the next charging period and a lower remaining charging time $t_{ch,start}$-$t_{ch,end}$. Thus, if P_{res} remains the same or decreases in the next interval of time, the battery will never be able to be fully charged. In the other hand, on a high

irradiance day, it can be observed that the schedule mode works perfectly well in respect to the aim to reducing the curtailment losses P_{cur} to a minimum. In order to use P_{res} as much as possible to charge the battery, the control algorithm checks if the available P_{res} on every period is enough to cover P_{charge}, which is calculated with equation (6.8).

If $P_{res} > P_{charge}$, then the remaining residual power $P_{res,rem}$ will be compared with the curtailment limit and if necessary limited. Some curtailment losses in the time after the charging period may occur on high irradiance days. This kind of schedule control will help to provide a smooth battery charging and reduce the curtailment losses if forecast data is not available.

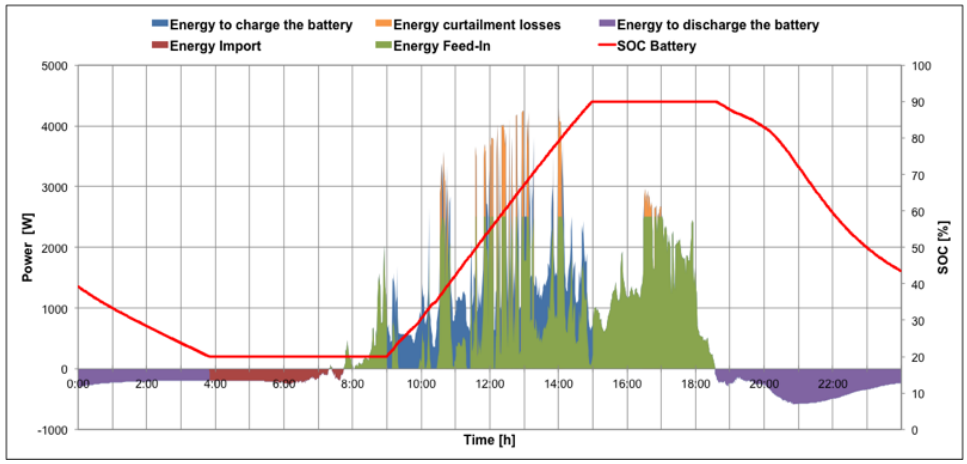

Figure 6.8: Schedule mode with constant charging power strategy. Power flow and battery SOC behaviour.

Adaptive Persistence Forecast (APF)

This type of control strategy requires forecast information. Using this information for a more efficient charging algorithm, the amount of curtailment losses can be reduced and the SCR and SSR can be improved. It should be noted that the forecast accuracy plays a key role with this kind of strategies. As discussed in section 6.2, some strategies rely on external meteorological forecast systems, which in most cases increase the cost, as these services have to be paid and an additional communication infrastructure is necessary. A cost-free alternative is the use of an autonomous forecast like a persistence forecast. This type of forecast method assumes that the weather will remain constant in the near future and predicts the generation and load by using a comparison of measured data from the recent past. By forecasting the PV generation and load consumption, it is possible to improve the perfor-

mance of this control strategy. The persistence forecast method used in this work is explained in section 6.2 and in more detail in [281]. A peculiarity of this strategy is that the PV power and load is determined by a mid-term forecast and the system is performing an adaptive adjustment of P_{charge} for the battery every 15-minute step. This means that if the forecast is not as accurate as expected, the system will adapt and adjust its behaviour. In Figure 6.9, the behaviour of the APF for the exemplary day (see Figure 6.6) is depicted. It can be seen that the battery is charged during most of the radiation period, avoiding a high quantity of curtailment losses P_{cur}.

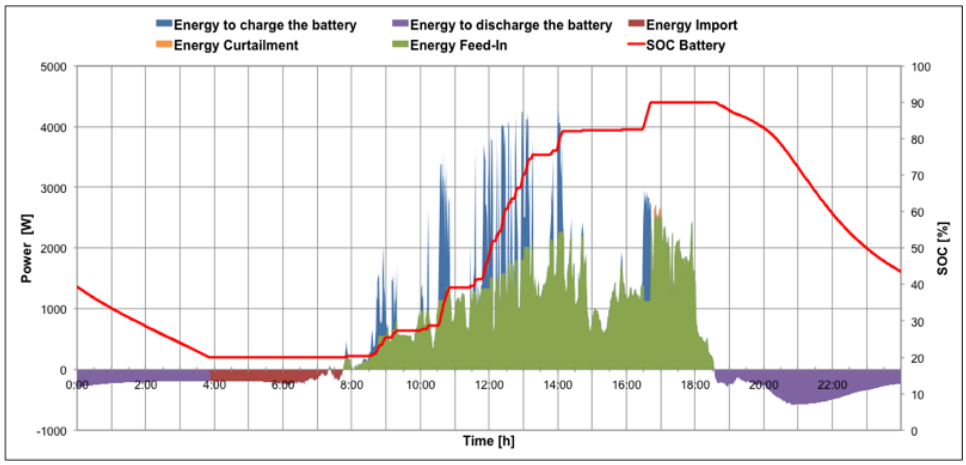

Figure 6.9: Adaptive persistence forecast strategy. Power flow and battery SOC behaviour.

A technical and economic comparison and evaluation of the three strategies presented above is discussed in the next section.

6.2.3 Results and Discussion

Hereafter, the results of the MATLAB simulations of the three control strategies for one-year on minute steps are presented. Furthermore, the performance indicators for each strategy, load variations and the economical evaluation are shown and discussed.

Power Flow at the Point of Common Coupling for the Different Control Strategies for RES

In Figure 6.10, the feed-in power at the point of common coupling for each of the control strategies is depicted. The transparent horizontal plane shows the level of 50 % of the feed-in limit. In Figure 6.10(a), the curtailment losses due to the lack of battery storage are highest. In Figure 6.10(b) the SC strategy is depicted. It can be observed, that on morning periods there is no power flowing to the grid, this means that the power is being stored, but just after full charge the power will start to flow again to the grid and the curtailment losses will start to increase. The SMCCP strategy is depicted in Figure 6.10(c), the power will flow during the whole PV generation period and the curtailment is effectively reduced due to the restriction of the charging period. Finally, Figure 6.10(d) shows the APF strategy.

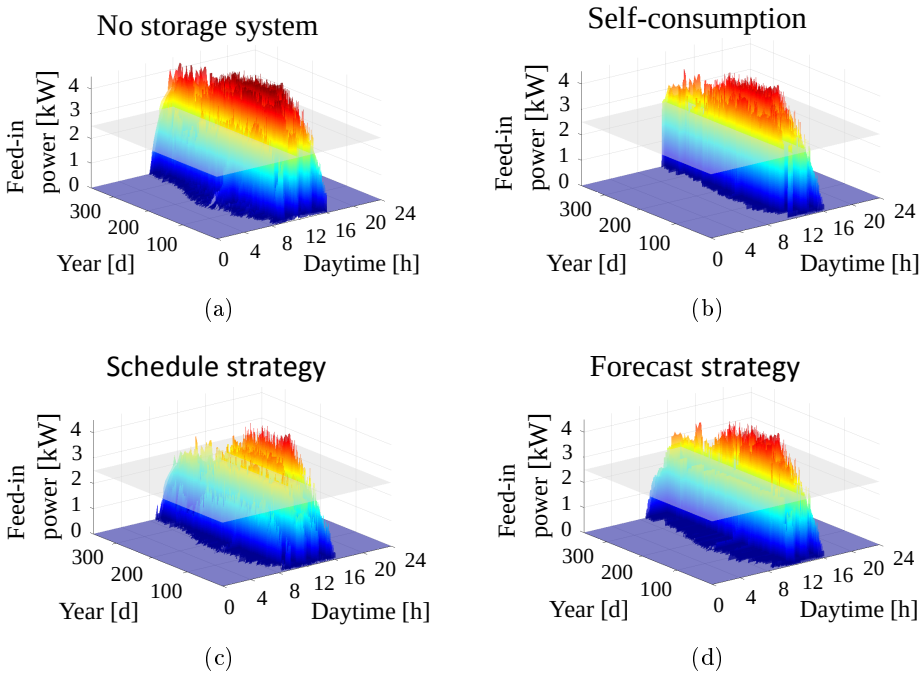

Figure 6.10: Power flow at the PCC of the RES control strategies for an exemplary day: (a) no storage system, (b) state-of-the-art maximal self-consumption strategy, (c) schedule mode with constant charging power, (d) adaptive persistence forecast.

As in Figure 6.10(c) the power is fed-in during the generation period and the intelligent persistence forecast control, shown in Figure 6.10(d), helps to minimize the losses even further than with SMCCP. The technical assessment based on the performance indicators for each of the control strategies is presented in the following subsection.

Technical Analysis Based on Performance Indicators

Self-Consumption Ratio (SCR)

In Figure 6.11, the results for the three strategies and the five different load profiles are shown. It can be observed that the SC strategy maximizes the use of PV in order to have the battery charged as soon as possible. The APF is always less than 1 % below SC strategy, which means that the adaptive algorithm is almost achieving the maximum possible SCR.

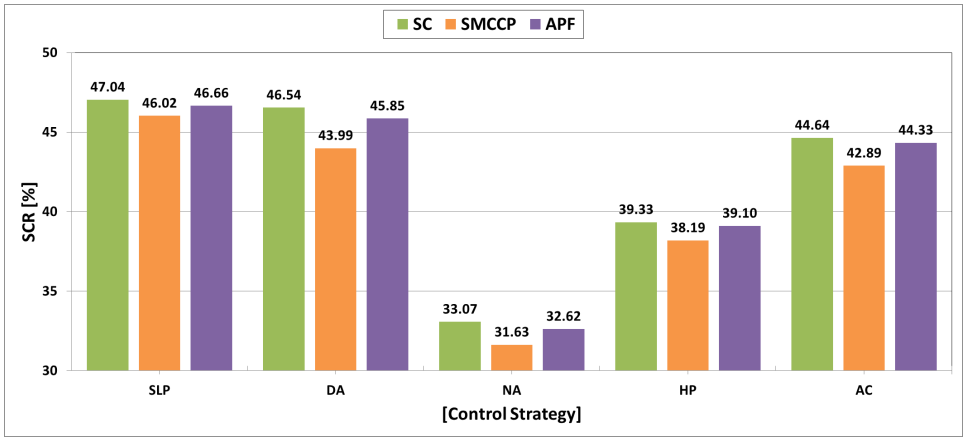

Figure 6.11: Comparison of the self-consumption ratio SCR of the control strategies SC, SMCCP and APF using five different load profiles each.

Self-Supply Ratio (SSR)

Figure 6.12 shows that the SC strategy has the highest values within all the different load profiles. The APF is the second best strategy.

Curtailment Loss Ratio (CLR)

The CLR is shown in Figure 6.13. For the CLR control, the losses are higher, because the battery is fully charged too fast during high irradiance periods. With the APF strategy the losses are reduced by about 50 %. This means that the forecast is quite accurate and the adaptive method is working

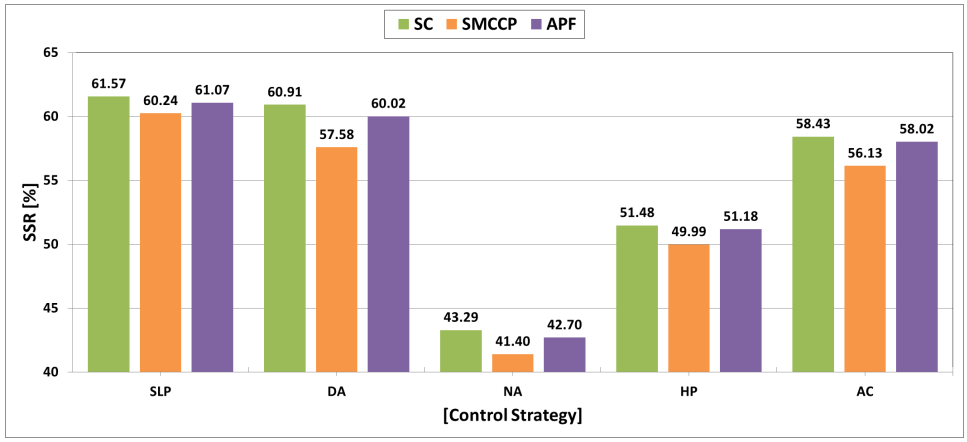

Figure 6.12: Comparison of the self-supply ratio SSR of the control strategies SC, SMCCP and APF using five different load profiles each.

well. However, the main drawback of this strategy is that when the day ahead is not at all similar to the previous day, then the losses will increase and the adaptive part will sometimes not react as fast as required. The ideal adaptive speed is also evaluated in [267]. With the SMCCP control, the losses are reduced by more than 5 % with all the load profiles. This difference shows that the implementation of a SMCCP control strategy might help to reduce energy losses even further.

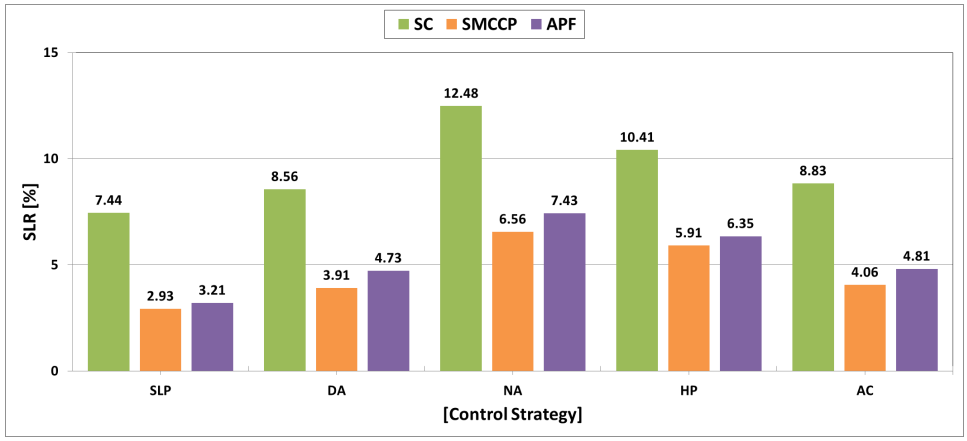

Figure 6.13: Share of losses ratio. Three control strategies using five different load profiles were evaluated.

In this subsection, it is shown that the APF and SMCCP control strategies have a greater impact on the CLR of the PV storage system compared to the SC strategy. Nevertheless, the impact on the SCR and SSR is not very high. This means that the control strategy used on the RES will lead to an improvement for the household owners in terms of quantity of energy feed-in to the grid without compromising a good management of the storage system and at the same time respecting the curtailment limit.

Economic Analysis

In this subsection the economic assessment, which analyses the impact on the implementation of SMCCP or APF control strategies versus a system that only has a SC strategy implemented, is presented. As shown before, the implementation of a different control strategy than SC will cause a decrease in the SCR, SSR, and the CLR. This evaluation will determine the economic improvement that will affect the profit for the system owner. For the economic analysis a feed-in tariff (FIT) of 0.1231 EUR [288] and an electricity price of 0.2881 EUR [289] are assumed. The economic evaluation is highly sensitive on specific prices at the time of the evaluation. In order to determine the annual profit (AP) for the SMCCP and APF strategy compared to the SC strategy, equation (6.9) is used, according to [281]:

$$\Delta AP = (\Delta SLR \cdot E_{PV} + \frac{\Delta SSR}{\eta_{bat}} \cdot E_{load}) \cdot ft - \Delta SSR \cdot E_{load} \cdot ep \qquad (6.9)$$

Where ΔSLR is the change of SLP versus SC strategy, E_{PV} is the total energy generated, ft the feed-in tariff, ΔSSR the change of SSR versus SC strategy, η_{bat} is the round trip efficiency of the battery system, E_{load} the total load demand and ep the electricity price.

6.2.4 Conclusion of the Analysis for Operation Strategies to Maximise Self-Consumption

As self-consumption with PV storage systems becomes more attractive every day as a profitable business case, it is important to examine different operation strategies. They should be grid-supportive, in this case by applying a curtailment limit of 50 % of the installed nominal PV power, and at the same time be profitable for the battery owner. Two autonomously operating control strategies, which fulfil these two aims by relying entirely on locally measured values were investigated and compared with the state-of-the-art

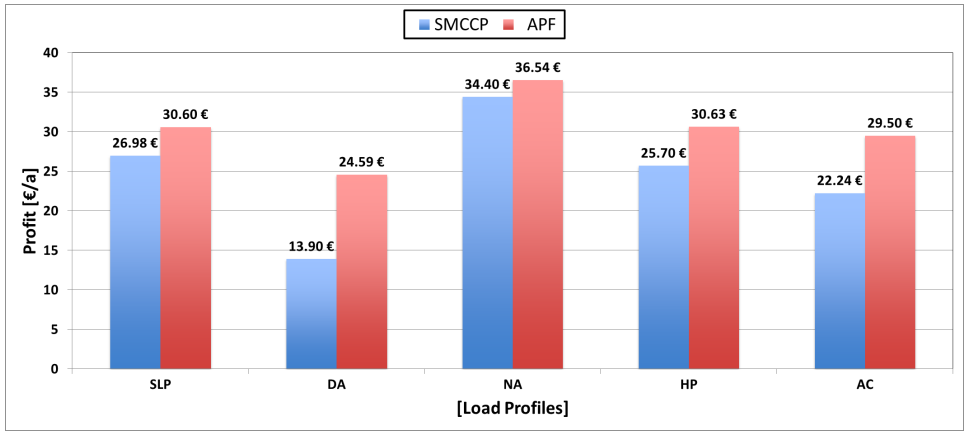

Figure 6.14: Annual profit evaluation for the control strategies SMCCP and APF, using five different load profiles for each.

strategy. By conducting a sensitivity analysis in which different extreme load profiles are used, it is shown that the adaptive persistence forecast control strategy is the one with the best technical and economic performance, taking into account the system utilisation and the owner's economic benefits. For all five load profiles, the APF shows higher values than the SMCCP. Since the annual profit of the APF is highest for all five load profiles, it is used in this work for the RES as well as for the CES applying self-consumption.

6.3 Methodology: Modelling the Battery Storage System as a Community Electricity Storage

All data used in this chapter refer to the year 2015, if not stated otherwise. A simplified VRFB-model that can be applied for CES, used to maximise self-consumption is presented in the following section.

6.3.1 Simplified Battery System Model Based on Measured Values

The more accurate BSS model presented in section 5.2, is simplified in this section for the simulation of a CES in order to reduce computing time. Instead of calculating the losses of the inverter and the battery separately as in the detailed model, in this model the losses are calculated in one step and the losses due to reactive power provision are neglected. Furthermore, a

difference in efficiencies for charging and discharging with the same power is neglected, too. The main difference to the more sophisticated model of section 5.2 is that in this simplified version the capacity of the BSS is not power dependant and the BSS can be charged with a constant power until reaching SOC of 100 %. As shown in [290], the BSS model for the self-consumption operation strategy should be simulated at least in one minute time-steps to avoid the neglect of short-term feed-in peaks. Thus, the time resolution of one minute is assumed to be sufficiently accurate for a BSS model applied as a CES.

For every time step, the BSS can be charged or discharged with different efficiencies due to a varying part load behaviour. This is taken into account by dividing the round-trip efficiency depicted in Fig. 6.15 into two separate efficiencies as shown in equation (6.10) and equation (6.11). Hereby, it is possible to calculate the SOC in every time step, required by the CES operation mode, but also to predict the SOC. This prediction is mandatory in order to minimise curtailment losses by the adaptive persistence forecast algorithm applied in the CES operation mode.

Contrary to the PCR application, the auxiliary power for the pump management is now taken from the battery. This is due to the fact that in this business model energy from PV systems is used for the battery operation. Also contrary to the PCR application only the necessary amount of pumps is used for charging or discharging as the ramp time of the pumps does not have a negative effect on this business case. In the simplified BSS model reactive power provision can not be modelled, and is calculated ex post. The energy needed for the provision of reactive power in the CES operation mode is covered by transactions with the energy market. To obtain a formula for an exponential fit function with two terms, the non-linear least square method was applied. The efficiency curve, the equation of the fit function with 95 % confidence bounds as well as the evaluation of the goodness of the fit are depicted in Fig. 6.15.

As the charging power P_{AC_C} or discharging power P_{AC_D} might be different, according to [291] the SOC of the BSS at the time step t SOC_t, can be calculated using an AC-power dependent round trip efficiency $\eta_{AC}(P_{AC})$.

$$\text{Charge: } SOC_t = SOC_{(t-1)} + \frac{P_{AC_C} \cdot \sqrt{\eta_{AC}(P_{AC_C})} \cdot \Delta t}{C_{nom}} \tag{6.10}$$

$$\text{Discharge: } SOC_t = SOC_{(t-1)} - \frac{\frac{P_{AC_D}}{\sqrt{\eta_{AC}(P_{AC_D})}} \cdot \Delta t}{C_{nom}} \tag{6.11}$$

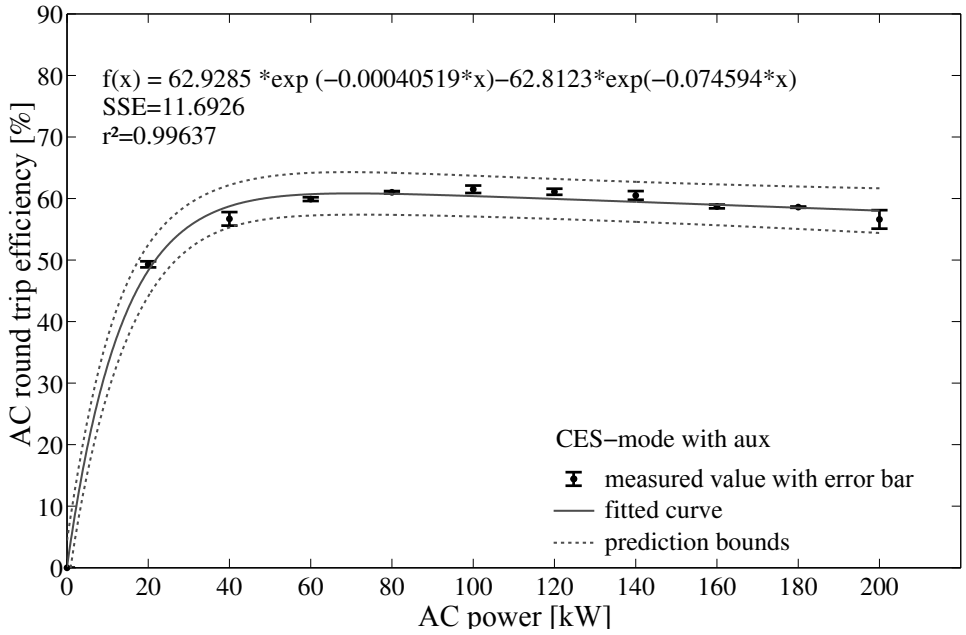

Figure 6.15: Measured round trip efficiency curve and fitted BSS model.

where SOC is the state of charge of the BSS, t the actual time-step, Δt the simulation step size (1 minute) and C_{nom} is the nominal BSS capacity (400 kWh). This 1-minute-model is used to simulate the grid supportive CES presented in subsection 6.3.5.

6.3.2 Lithium-ion Battery Model for CES

The model for the LiB used for the CES application is implemented in the simulation of the operation strategy the same way as the simplified VRFB model presented in subsection 6.3.1. The LiB model itself is the same as for the residential PV systems described in subsection 6.2.2 (BSS round-trip efficiency 84 %, lower SOC limit 20 %, upper SOC limit 90 %). The main difference between the VRFB and LiB is that in the LiB model the round-trip efficiency has only one constant value. The system sizes of a single VRFB and LiB are the same (200kW/ 400kWh).

6.3.3 Economic Assumptions

The economic parameters of the LiB are presented in subsection 5.3.1 and are applied to the PCR and the CES application (CAPEX LiB see Table 5.2,

yearly OPEX 2 % of CAPEX, interest rate 4 %).

The revenues in this business case are caused by a cost reduction strategy that takes advantage of the difference between feed-in tariff and purchase price for electric energy. The parameters FIT (0.1231 EUR/kWh) and ep (0.2881 EUR/kWh) are assumed to be the same as for the residential storage systems presented in subsection 6.2.3. As these parameters depend on the PV system size and the considered year, inter alia, their influence is discussed in the sensitivity analysis of the economic assessment in subsection 6.4.2.

The legal framework for different use cases and their corresponding charges, levies and taxes for CES are shown and discussed in Fig. 4.15. The theoretic best case and the two most promising scenarios which can be realised under the current legal framework are analysed in this assessment and listed hereafter:

(1) Theoretic best case (Th. best)
This case is the theoretical possible best case, which means that there is no FIT and no charges or levies incur. This scenario is highly unlikely at present, yet could become reality in a post-FIT era after 2020 [292].

(2) Self-consumption best case (SC best)
In the case of a geographical proximity in which the consumers and the owners of the PV generator are not the same legal entity but use an own private grid, the self-consumption case applies. Therefore, only the full EEG levy incurs (see column 1 in Fig. 4.15).

(3) Direct marketing best case (DM best)
If the storage operator and grid operator peruse a direct marketing model and sell energy to third party consumer within the own private grid, the EEG levy, the VAT, the business tax and the corporation tax incur. The charges and levies that apply in this case are depicted in column 2 in Fig. 4.15.

6.3.4 Sizing of the Community Electricity Storages

Analogue to the optimal economical sizing of residential storage systems for 1 kWh of storage capacity of the CES, a PV system size of 1 kWp and an annual load demand of 1 MWh is selected for every system [267]. In order to simulate a realistic environment the CES are implemented for the status quo of the grid of the model region presented in section 3.4. As the BSS is connected to the LV-side of the MV/LV-transformer (see section 3.3), if possible all the loads and PV-systems of the same LV-level were gathered for one CES. This leads to a non-optimal sizing of the loads and PV-systems, but increases the hosting capacity of the LV systems and is therefore grid supportive, as the CES are also used for peak shaving as described in the following section. As the installed PV power is 2.0 MW, only the geographically closest loads with a total annual consumption of 2.3 GWh were combined to 5 separate CES systems with the SPF prototype of 400 kWh storage capacity to comply with the sizing rule described before. The sizing of the 5 CES is listed in Table 6.1

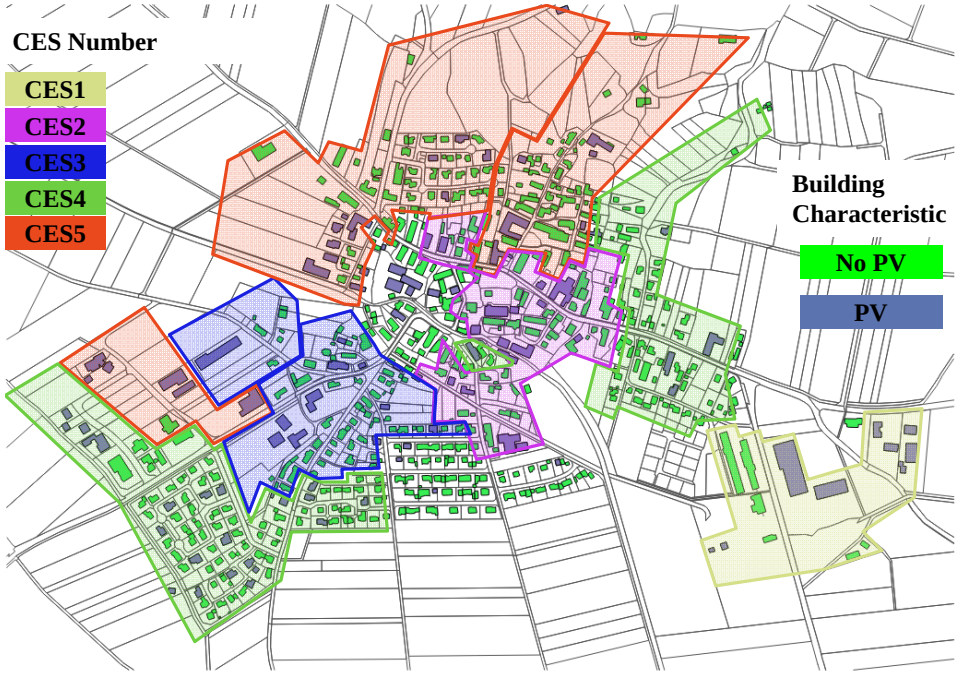

Figure 6.16: Load and generator assignment of the 5 CES in the town of the SPF project.

6.3.5 Modelling of the Operation Strategy

In order to assure a grid supportive behaviour of residential PV-storage systems the German government coupled the incentives for these storages with the condition on limiting the feed-in to 50 % of the maximal PV power. Although these incentives are only granted for residential PV-storage systems, the 50 % limit is used in this study to assure a better comparison with other studies. Preliminary studies indicate that the adaptive persistence forecast control strategy is most profitable from the storage owner's point of view [293,294]. This strategy secures the best results with regards to the performance indicators, which are defined in subsection 6.2.1: CLR, SCR and SSR.

The methodology of the adaptive persistence forecast control strategy was adapted from the strategy initially designed for residential PV storage systems by [15,281] and also applied in section 6.2. The APF strategy aims on minimising the daily feed-in energy and thus maximising the self-sufficiency and the profit. This is achieved by limiting the feed-in power dynamically, always taking the maximum feed-in boundary into account. The dynamic feed-in limit is ideally set each day based on the forecasts such that the battery is completely charged with the energy that exceeds the dynamic limit [15].

For the load prediction [281] uses a method that assumes a load profile for the predicted weekday identical to the load profile of the weekday from the previous week. As the PV output has a stronger impact on curtailment losses and self-sufficiency rate than the load forecast, an elaborated method for the PV persistence forecast, which is based on a moving prediction horizon as well as a on a long term and short term prediction relying on locally measured data of the PV system, is used [281]. First a bell-shaped profile based on the last ten days is calculated. To achieve a higher accuracy a moving horizon is introduced that combines the PV data from the last 4.5 hours with the bell-shaped profile. For the intra-day correction the feed-in limit is adapted dynamically every 15 minutes by running an optimisation with 15 minutes of forecast resolution and 15 hours of optimisation horizon, if the measured values (residual load and battery charge power) differ from the predicted.

For every CES the profiles for the generator and load data is gathered and the prediction is performed only for the accumulated profiles. The resulting charging or discharging power is calculated for every minute time-step. The usable battery capacity is set between 1 % and 99 % of its nominal capacity of 400 kWh. For the simulation of the SOC, the simplified 1-minute battery model as described in subsection 6.3.1 is used to reduce computing

time. Nonetheless, a yearly simulation of the 5 CES including a load-flow calculation of the whole model area takes 31 hours, although the year was partitioned in 16 periods and calculated in parallel on a server with 8 cores with 2.9 GHz and 32 GB RAM. For each period the SOC of the 5 CES were set at 1 % for the first time-step.

As with this simplified battery model only the active power is taken into account, it is assumed that the reactive power to provide the reactive power control based on the Q(V)-characteristic is the same as if the BSS provides PCR and reactive power control. The BSS is connected in both cases to the LV busbar of the MV/LV transformer. These assumptions seem reasonable, as the active power of the two different operation strategies has very little influence on the voltage due the low R/X-ratio on this PCC and therefore it can be neglected.

6.4 Technical and Economic Assessment of a Grid Supportive Vanadium Redox Flow Prototype applied as Community Electricity Storage

6.4.1 Technical Assessment

In this section, the technical results from the simulation of the SPF prototype applied as a CES with the simplified battery model (see subsection 6.3.1) are discussed. In Fig. 6.17(a) the power flows of CES generating the highest profit (CES 1) for the week of highest irradiation of the year are depicted. Fig. 6.17(b) shows the corresponding SOC curve.

It can be seen that from Monday till Wednesday the low solar irradiation is not sufficient to load the CES completely, whereas on the other days the CES is charged to its charging limit of a SOC of 99 %. At night, the storage is capable of supplying the load, and only on Tuesday morning energy is drawn from the grid (cyan). Furthermore, the performance of the forecast-based operating strategy can be shown, as it prevents high feed-in peaks at noon by smoothing the charging process over the day time. Due to the grid feed-in limit of 50 % the PV-power is curtailed (black) on Thursday and on the weekend, as the full capacity is reached before the evening.

In comparison with to the PCR application, the yearly simulation shows that this application reaches relativity high round trip efficiencies of 53 %. If the auxiliary power for the pumps would be drawn from the grid the round trip efficiencies is 60 %. This is on the lower end of the efficiency range that is expected, considering [264] reported 60 % and [15] 84 % for LiB for CES.

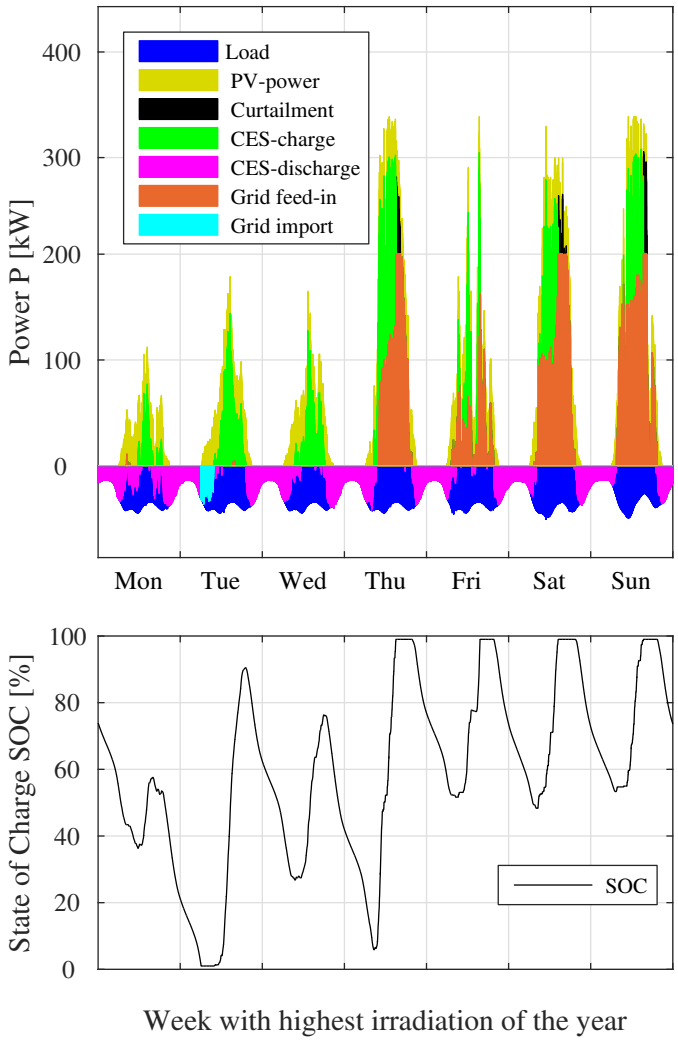

Figure 6.17: Power flows and dis-/charging of CES 1 for the exemplary week with the highest irradiation of the year.

Evaluation of the Operation Strategy based on Performance Indicators

The performance indicators (defined in subsection 6.2.1) self-consumption ratio and self-supply ratio for all 5 CES are listed in Table 6.1. The indicators were calculated with (index PV) and without storage (index CES) in order to evaluate the influence of the CES. It can be seen clearly that the BSS increases the SCR and the SSR. The first row of the table shows the ratio

of the PV systems connected to the CES P_{PV} in kW_p and yearly energy consumption of the load E_{load} in MWh, respectively.

Table 6.1: Sizing and performance indicators of the CES.

	CES 1	CES 2	CES 3	CES 4	CES 5
P_{PV}:E_{load}	1.2:1	1.1:1.1	0.9:0.9	0.9:1.1	1:1.6
SCR_{PV}[%]	33	41	34	37	55
SCR_{CES} [%]	59	52	54	69	60
SSR_{PV} [%]	45	44	45	43	43
SSR_{CES} [%]	68	63	67	63	54

The influence of the dimensioning of the load and PV on the performance indicators, can be shown by the example of CES 5: In this case there is significantly more load connected to this CES than to the other storages, leading to the smallest increase of the self-consumption rate from 55 % without CES (SCR_{PV}), to 60 % with CES (SCR_{CES}). Vice versa the small load to PV ratio of CES1 results in the highest self-supply ratio with CES (SSR_{CES}) of 68 %. The curtailment loss ratio for all CES lies under the negligible level of less than 1 % and can be attributed as the forecast precision as almost no curtailment losses occur compared to a perfect forecast [15, 198]. This is a factor 3 to 7 smaller then the curtailment losses of the same operation strategy applied to a residential PV-storage system (compare with subsection 6.2.3). The negligible curtailment losses and the big reduction potential of CES matches with the results in [221], where RES are compared with CES.

Analysis of the Grid Supportive Behaviour

In the simplified battery model the influence of the reactive power provision on the SOC is not included. But as in the case of CES 1 the PCC is the same for the PCR and the self-consumption operation strategy the same voltage time-series applies and the same energy to recharge the BSS as in the PCR-case can be assumed. For a better comparison between the two BSS-applications this energy is traded in the CES case on the intra-day market as well and causes costs of 14 EUR per month for the provision of reactive power for CES 1.

6.4.2 Economic Assessment

The resulting cash-flows and net present values for the CES business cases is presented in this section. Similar to the economic assessment of PCR

business case in subsection 5.2.2, the CES application is applied to the model region for the VRFB prototype. For the CES cases the economic calculation is based on a load flow calculation of the model grid for one year. Although, the cash-flow and the NPV is calculated for all 5 CES, only the results of the most profitable CES 1 are shown and discussed. The NPV of CES 1 is 6 % higher as for the least profitable CES 5 for the theoretic best case.

Cash-flows

In Fig. 6.18 the annual cash flows, without discount for the CES business cases, for the most profitable VRFB unit and a LiB unit are depicted.

In the self-consumption maximisation business case with the CES the revenues represent savings for the avoided electricity costs by self-consumption of the energy from the PV system. They amount to 25 100 EUR per year for the VRFB and to 26 500 EUR per year for the LiB. To show the range of possible economic results, three best case levies and charges scenarios (introduced in section 4.3) are calculated, as shown in Fig. 4.15. In analogy to the avoided electricity costs, the lost feed-in tariff is not a matter of incurred expenditures, but rather a loss of revenue as a result of self-consumption compared to lost feed-in enumerated with the FIT.

The EEG charge and the VAT (including commercial and corporation tax for CES), on the other hand, are actually incurred for the self-consumed electricity from the CES. As it can been seen in the range of costs of the CES cash flows for the three scenarios, the influence of the levies and

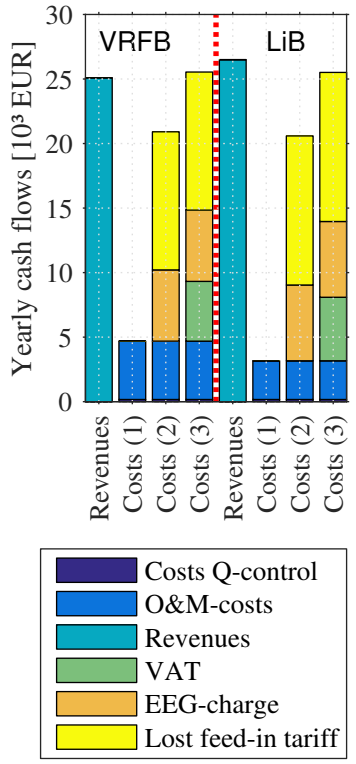

Figure 6.18: Cash-flows of a grid supportive CES application (for CES 1) and different battery technologies (VRFB and LiB) in the three cases: (1) theoretic best case, (2) self-consumption, (3) direct marketing.

charges is the most decisive parameter for the profitability of the CES business cases. This leads to the conclusion that although the revenues for the VRFB are 4.5 times higher then the costs in theory (costs (1)), only in the self-consumption best case (costs (2)) there might be a profitable business case, whereas in the direct marketing case (costs (3)) no profit is earned. This result could be even worse as the OPEX are based on the smallest investment costs and could be almost by a factor 5 higher, if the CAPEX of the prototype were considered instead (for the VRFB).

The costs for the provision of reactive power (dark blue) for the grid supportive behaviour of the BSS are due to the intra-day trading costs to replace the energy needed to provide this service (analogue to the PCR case). As depicted in the graph the additional costs of the reactive power provision are less than 1 % of the revenues. Moreover, the 50 % limit for the CES can be neglected, as the resulting curtailed energy is also less than 1 % of the revenue. It can be seen that with the assumption of a 84 % round trip efficiency the LiB reaches higher incomes and lower costs, but due to the higher usable capacity of the VRFB the results are similar. The effect on the NPV of this more favourable economic results of the LiB are shown in the next section.

Net present values

The calculation and comparison of the net present values, as depicted in Fig. 6.19, shows that none of the two technologies is currently profitable: neither the VRF nor the LiB reach positive NPV. For both BSS the technology dependant investment costs ranges listed in Table 5.1 (VRFB) and Table 5.2 (LiB) are considered. Assuming the CAPEX of the SPF prototype, the business cases are far from profitable, hence this case is not displayed in the graph.

The negative NPV are mainly due to the high investment costs, as in both business cases the net cash flow can be positive as shown in Fig. 6.18. As depicted in Fig. 6.19, the higher round trip efficiency of the LiB compared to the VRFB does not have such a big impact on the NPV as the advantage of VRFB to have a higher usable capacity makes up for the lower higher round trip efficiency. Although maximising self-consumption can be a profitable business case theoretically as shown with the Th.best scenario (assuming minimal investment costs), this case would only apply in a post-FIT scenario without any charges and levies. In a realistic scenario under the current legal framework (SC best), in which the CES is used for self-consumption, the CAPEX of the VRFB and LiB would have to fall at least by 77 % and 73 %, respectively to earn profits. The direct marketing (DM best) is not profitable

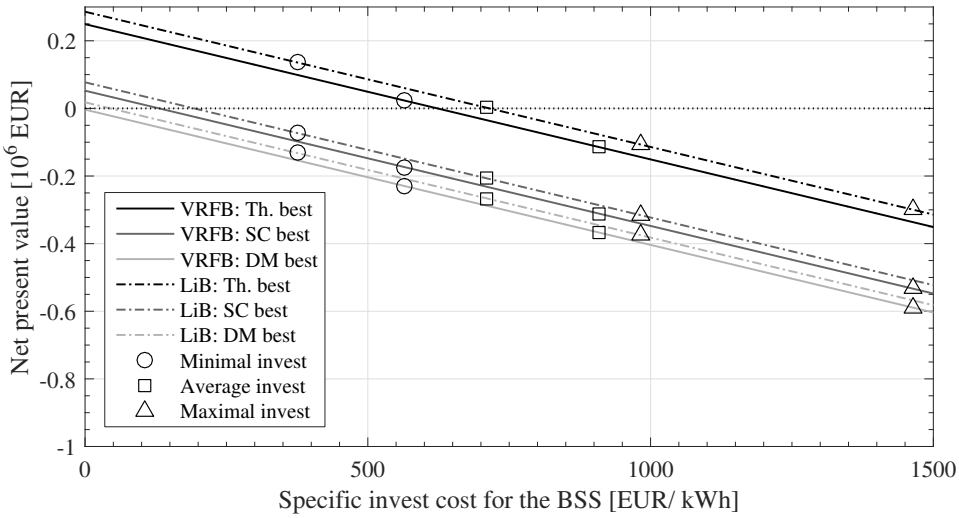

Figure 6.19: Net present value of the CES application for VRFB and LiB for the most profitable single CES unit of the model region (CES 1).

with the analysed parameters for the VRFB, as the charges and levies are too high to achieve an positive NPV, even if the BSS has no investment cost. The same applies to LiB for DM best case as the specific cost of a single BSS unit would have to be 38 EUR/kWh which seems impossible at the moment.

This results are confirmed by several studies: It is shown that under the current legal framework it is not possible to reach a positive NPV for CES with LiB [221, 222, 295]. Nonetheless, CES might become an alternative to residential home storage systems in a post-FIT era (after the year 2020) if the legal framework is adapted [295]. Due to the unfavourable legal framework for CES, a direct subsidy is currently discussed in Germany [296].

Sensitivity Analysis of the Most Significant Economic Parameters

In Fig. 6.20 the economic sensitivity analysis of the CES application with a variation of the parameters FIT and electricity price is depicted. The colours indicate the specific BSS investment cost to reach a NPV of zero. To reach a NPV of zero with the assumption of this paper (year 2015) and for a realistic best case (CES (2): SC best) the specific BSS investment cost would have to be 131 EUR/kWh (marked with a cross on the black 131 EUR/kWh iso line). Thus, the CES is not attractive at present and the FIT would have

to drop below 2 EURct/kWh and the electricity price over 35 EURct/kWh (assumptions: minimal CAPEX and E2P-ratio of 2:1).

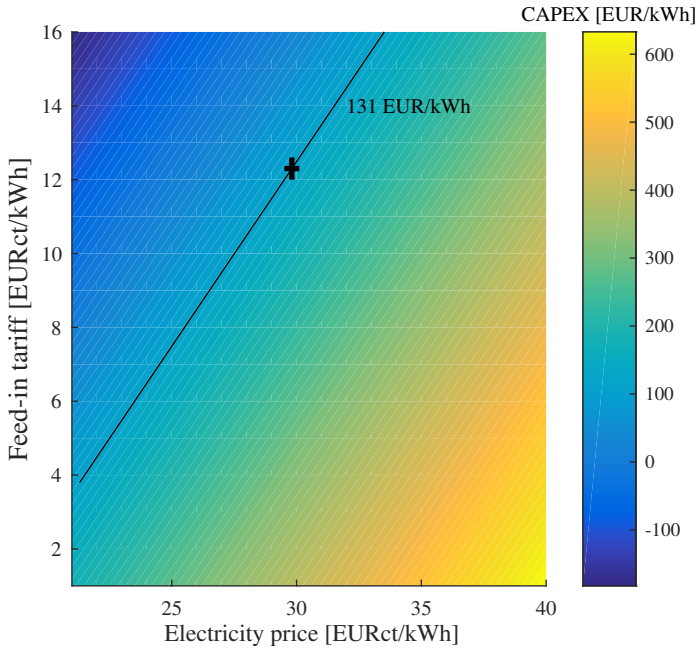

Figure 6.20: CAPEX of the battery system to reach a net present value of zero (SC best: self-consumption best case) for a varying feed-in tariff and electricity price. The marked point represents the assumptions of SC best and the black iso-line an investment cost of 131 EUR/kWh of the battery storage system.

But this may shift in a post FIT period (starting with year 2020) were the CAPEX of VRFB are supposed to have fallen by 48 % compared to the prices of 2014 [182] and the feed-in tariff may drop to a market price of 2-4 EURct/kWh. A drop of 50 % of the assumed CAPEX of the VRFB used in this work (listed in Table 5.1) would result in a specific investment cost range of 283 to 732 EUR/kWh (green to yellow area). A potential rise of the electricity price favours this business case even further. This is especially true if the legal framework is clarified and favours this kind of application by omitting all or most taxes and additional cost burdens as the EEG levy for instance.

6.5 Chapter Summary

In this chapter the operation strategy maximisation of self-consumption for residential and large scale batteries is analysed from a technical and economic point of view. The focus lies on large scale VRFB providing this application. For this purpose a battery model for a VRFB based on measurement data is presented. To identify the most lucrative operation strategy a review of existing operation strategies for residential battery systems is conducted and the most promising is adapted to several CES implemented in a model region. Finally, the technical and economic results of this operation strategy is compared with LiB providing the same service. The main findings of chapter are:

After a review of different self-consumption strategies, the two most promising operation strategies for residential storage systems, which maximise self-consumption and apply peak shaving, are compared with the state-of-the-art self-consumption strategy. The two strategies are: a schedule mode with constant charging power and a strategy based on an adaptive persistence forecast. The APF shows the highest profits for all five analysed load profiles. Thus, it is adapted for the large scale vanadium redox flow battery storage system.

Based on the same data as the detailed vanadium redox flow system model, a simplified model for 1-minute time-step calculations of the SOC, is presented and implemented in the operation strategy for the maximisation of self-consumption. This BSS model is embedded in a load flow calculation of the region in which a VRFB prototype is implemented, in order to asses the economic profitability of a CES.

A clear methodology for the operation strategy of a grid supportive VRFB which maximises the self-consumption is presented. To ensure the grid supportive behaviour, an autonomous reactive power control based on a Q(V)-characteristic and a peak shaving is implemented.

For the maximisation of self-consumption an autonomous adaptive forecast based operation strategy is implemented. The aim of this strategy is to minimise the daily feed-in energy and thus maximise the profit, while at the same time providing a peak shaving of 50 % of the maximal PV power connected to the CES. The evaluation of this strategy via the performance indicators curtailment loss ratio, self-consumption ratio and self-supply ratio, shows that the SCR can be risen by 26 % and the SSR by 23 % compared to PV-systems with no storage. This could relief the higher voltage levels considerably, as the power is generated and consumed locally. Another result is, that this operation strategy operates close to the theoretic maximum, as

the curtailment losses are smaller than 1 %. This is factor 3 to 7 smaller then the curtailment losses of the same operation strategy applied to a residential PV-storage system.

Furthermore, it is shown that the reactive power provision and, therefore, the grid supportive behaviour does not lead to any significant additional costs for neither of the operation strategies (less than 1 % of the costs).

As for the profitability of the self-consumption business case the investment costs, the price of the FIT and above all the incurring charges and levies are the most decisive factors. It is shown that this business case could already be profitable in theory, but due to the legal framework in place, the CAPEX of the VRFB have to fall by 77 % in the best case to reach break even. If a direct marketing business case for self-consumption is pursued no profit can be earned as the incurring charges and levies lead to a negative cash-flow.

The CES application is slightly more profitable if LiB are used instead of VRFB, but no positive NPV can be reached under the current conditions either.

In conclusion, it is worth pointing out that in spite of lower curtailment losses compared to residential PV storage systems and advantages of the economy of scale, it is not clear whether community electricity storages applying self-consumption maximisation will become feasible in the near future due to the current unfavourable legal framework.

The most important result of this chapter is that there is almost no negative impact if the BSS is operated in a grid supportive behaviour by providing reactive power control and peak shaving additionally to its primary purpose. This result is similar to economic finding of a grid supportive VRFB providing primary control reserve, discussed in chapter 5.

Chapter 7

Impact of Large Scale Batteries and other Flexibility Options on Distribution Grid Planning

The main focus of this chapter is the analysis of the impact of the operating strategies, derived from the business cases of self-consumption maximisation and primary control reserve discussed in chapter 5 and chapter 6, on distribution grid planning.

In section 7.1 the traditional approach to implement large BSS in distribution grid planning is presented and the main drawbacks of this approach are shown. For this purpose the already realised large scale BSS PCR and CES projects in Germany (Table 4.2 and Table 4.6) are classified and their impact on traditional grid planning is discussed. To overcome disadvantages of traditional grid planning, an alternative approach (referred to as expert system, as defined in section 2.4) is presented and splitted in two parts: section 7.2 and section 7.3. In section 7.2 the methodology for a techno-economic assessment of flexibility options as a alternative to grid expansion is presented. The flexibility options are: grid supportive self-consumption maximisation with residential and large scale BSS, system supportive primary control reserve with large scale BSS and two reactive power control strategies with PV systems ($\cos\varphi$(P)-control and Q(V)-control). The results of the alternative approach are presented and discussed in section 7.3 and concluded in section 7.4.

7.1 Traditional Approach

How BSS can be implemented in traditional grid planning, as presented in subsection 2.3, is subject to ongoing research. However, [297] shows that DSO only consider active power flows for BSS, which seems a viable proposition as the active power flows are responsible for the revenue streams and a reactive power control is not yet mandatory. Therefore, in the fist part of this section only the active power flows are evaluated using the worst case approach of traditional grid planning and the resulting diversity factors for BSS are listed in Table 7.1. For the assessment of the active power flow German large scale BSS projects that apply PCR (see Table 4.2) and self-consumption (see Table 4.6) are analysed. Secondly, the effect of reactive power control on the planning is discussed briefly as it can be considered independent of the business case, given that the power electronics are able to provide a four quadrants operation. In the last part, deficiencies of the traditional planning methodology are presented and possible steps to alternative planning approaches, are discussed.

- Grid compatible self-consumption
  In the worst case the battery is fully loaded for the RPF scenario and fully discharged in the HLF-case. The resulting diversity factors for implementing BSS in the grid planning are listed in Table 7.1 and result in a neutral behaviour of the BSS. The *direct loading operation strategy* and *schedule operation strategy* are used in the projects Strombank and MSG EUREF (see Table 4.6) andcan be mentioned as an example.

- Grid supportive self-consumption
  For the HLF the same as for grid compatible BSS applies, as the battery might be also fully discharged, too. The difference to the grid compatible BSS arises for the RPF. In this case the battery is used to mitigate the reverse power flow caused by DG with peak shaving. The peak shaving threshold can be either fixed or adaptive as in the case of forecast based charging and discharging. For the projects listed in Table 4.6 that use a forecast based operation mode a peak shaving functionality is implemented. Nevertheless, the rated power of the BSS might be higher than the power used to mitigate the power at the PCC, which is the case in the EEBatt project where the energy to power ratio of the BSS is 1:1. In the case of the latter, the diversity factor is the quotient of the power used for peak shaving purposes and the rated charging power of the BSS. For example, for the project SmartOperator (pure peak shaving) the diversity factor is 1, but it is

< 1 in the EEBatt project (forecast based SC). This operating strategy can solve OV (cable) and OL issues (cable and secondary transformer) if the BSS is installed in the same LV feeder as the DG causing them. The thermal load of the primary transformer is reduced in any case independently of the allocation of loads, DG and BSS, as the peak of the RPF is mitigated in any case, if a diversity factor of > 0 for the BSS is reached.

- System compatible primary control reserve
  It can be deduced from Fig. 4.9, that a BSS providing PFC might discharge or charge with its full rated power at any moment. Depending on the system architecture, some BSS have the capability to be overloaded, as reported in [178] for VRF (100 % over-loading), in [172] for LIB (30 % over-loading for 15 min), and in [298] (25 %) also for LIB. In the worst-case scenario, the normal operation together with the application of the degrees of freedom as described in subsection 4.2.1, can lead to a diversity factor > 1 (referred to as (1+x) in Table 7.1). Depending on the allocation of the BSS it might reduce the hosting capacity of DG of the affected grid as this operation strategy tightens the OV and OL issues. All projects listed in Table 4.2, except the SmartPowerFlow project, where the BSS behaves in a system supportive way, fall into this category.

- System supportive primary control reserve
  The diversity factor for this operating strategy is the same as for the grid compatible behaviour, as the active power flows are the same. The difference here is that a reactive power control is used to solve over-voltage issues.

Table 7.1: Diversity factors for BSS applied for self-consumption (SC) and primary contol reserve (PCR)

	HLF	RPF
grid compatible SC	0	0
grid supportive SC	0	$(0\text{-}1)_{charge}$
system comp./ supp. PCR	$(1+x)_{charge}$	$(1+x)_{disch.}$

In the traditional distribution grid planning reactive power control is usually not considered and only a fixed $cos\varphi$ can be taken into account as only

one time-step for the two worst case scenarios is calculated. In a grid/ system compatible behaviour $cos\varphi$ may be set to 0, while in a grid/ system supportive behaviour it may be set to the maximum favourable value from grid perspective. Nevertheless, this issue has not been analysed systematically yet and may lead to wrong results, if the method of the traditional planning is applied. For an accurate simulation of a reactive power control, a load flow analysis based on time series has to be applied.

It can be concluded that the traditional planning method of passive distribution systems for large scale BSS will lead to over-capacities and uncertainties concerning the reactive power flows. Therefore, CIGRE promotes the shift to active distribution systems as defined in CIGRE WG C6.11 [299], which will incorporate DG and BSS in a more active way than the fit-and-forget approach which is currently used and will allow to apply new/alternative planning approaches more efficiently. This transition is described in detail by [64]. As discussed in section 2.4, BSS, as well as DG and the distribution grids need to be modelled to calculate time-series, in order to simulate the interdependency of the grid participants. Depending on the application and technology different time-steps need to be realised in these models [64].

As for the reactive power control current studies focus on two main directions: a central approach using an AC OPF, such as [87], or an autonomous voltage control, as for example a Q(V) control [26]. It seems as if autonomous voltage control strategies are the more favoured solution at the moment as the technical standard for connecting BSS and DG in MV and LV are aiming in this direction [45]. Thus, the autonomous reactive power control strategies have been favoured in this work.

The challenges of future investigations lie in modelling BSS to calculate active and reactive power time series for different applications in order to apply them for new planning approaches in active distribution systems. This has been realised in this work for BSS applying system supportive primary control reserve (chapter 5) and for a grid supportive community electricity storage (chapter 6). The impact of implementing this large scale BSS (along with other flexibility options) into distribution grids, is analysed in detail in the next two sections by applying new/alternative planing approaches.

7.2 Alternative Approach: Methodology for a Techno-Economic Assessment of Alternatives to Grid Expansion

In this section, a methodology (expert system) is presented to compare the traditional approach of grid reinforcement technically and economically with flexibility options. Five flexibility options are applied with the following methodology:

- All PV systems in the pilot region apply a cosφ(P)-control.
- All PV systems in the pilot region apply a Q(V)-control.
- All PV systems in the pilot region are connected to a RES to maximise self-consumption.
- If technically possible, in every LV-grid a large scale BSS is implemented which provides PCR and Q(V)-control.
- If technically possible, in every LV-grid a large scale BSS is implemented which provides self-consumption maximisation as a CES and Q(V)-control.

In the next subsection, the different flexibility options are explained in detail and their implementation in the model is presented.

7.2.1 Technical Comparison of the Flexibility Options

For the technical comparison, the decisive criterion to arise the shares of renewable energy systems in distribution grids is the increase in hosting capacity (defined in section 2.1). The maximum hosting capacity is reached when limits for OV at a grid node or OL of equipment are reached. For this work, the voltage related hosting capacity is limited by the permissible voltage band of $\pm 10\,\%$ of the nominal voltage [41] for every time-step to have an additional buffer for measurement accuracy. This is stricter than the current specification for voltage magnitude variations in the DIN EN 50160, where it is stated that for a period of one week the value should not surpass $\pm 10\,\%$ of the mean RMS for 95 % of the time during intervals of 10 minutes. The maximal threshold for OL is set to 100 % of the rated apparent power S_r for cables and transformers.

In order to determine the increase of the hosting capacity, the total hosting capacity of the pilot region is determined in the event that no flexibility options are applied (reference scenario). Then, the same value is calculated using the various flexibility options. The increase in hosting capacity is the difference between the two values.

Since the pilot region in the status quo has no OL or OV issues, PV systems are installed successively in the village following the expansion path described in section 3.5. After the integration of each additional PV system, a load flow calculation with MATPOWER [300] is conducted for the worst case scenario of a given year. For the RES and cosφ(P) option, 4 consecutive minutes (worst minute $-2/+1$ minutes) are calculated. The strategies using a Q(V)-control (PCR, CES and Q(V)) are calculated in seconds and for a longer time period of 60 consecutive seconds (worst second $-29/+30$ seconds) in order to check the stability of the control.

In every time-step it is checked whether OL or OV limits are violated in one of the 12 LV-grids. If this is the case, the maximum hosting capacity is reached and the expansion of additional PV systems in this LV-grid is stopped, while being continued in the remaining LV grids. With other words: all possible PV systems according to the expansion pathway are integrated in every LV-grid until the hosting capacity or the PV expansion potential of every LV grid is reached. The total hosting capacity of the pilot region results from the individual values of the respective LV grids.

7.2.2 Economic Comparison of the Flexibility Options

The economic analysis is based on the PV expansion pathway until 2025 (see also subsection 3.5). The future PV systems are integrated into the electrical grid model according to their predicted year of construction. If, as a result, OV or OL occurs in the load flow calculation, automatic (traditional) grid expansion measures are applied based on [18] as described in section 2.3. If OL or OV is not solved by these measures the solution of [78] is taken into account, which implies adding a NAYY 240 mm^2 line from the MV/LV transformer directly to the PCC where the problem appears, to solve the remaining issues. In this way, the total technical PV potential of 4.6 MW$_p$ for the year 2025 from Fig. 3.13 can be reached in all cases. This is different to the methodology for the technical comparison in which for every flexibility option a different amount of PV-systems are integrated until the maximal hosting capacity is reached.

The costs of the scenarios are calculated using the net present value method for the period 2013-2050. All costs are discounted for the reference year using a discount rate of 4 %. The installation costs applied in the calculation are listed in Table 7.2. A lifetime of 40 years is assumed for cables and 45 years for transformers respectively. In the year 2050 the residual values of the grid equipment are taken into account.

The operating costs consist of the grid loss costs and the costs of the reac-

tive power supply of the large BSS, as it is assumed that the DSO reimburses the cost for the reactive power supply to the BSS operator. It is assumed that the grid status achieved in 2025 will remain unchanged until 2050. In this way it is possible to compare the cost of the various flexibility options with the pure grid expansion for the period 2013-2050, as these options may increase or decrease the operating costs. For the grid losses, 64.40 EUR/MWh are agreed with the DSO of the pilot region. The cost for the additional energy required to provide reactive power control is set to 55.59 EUR/MWh for the large scale BSS. The cost for the purchased energy is composed of the sum of EUR 33.09 EUR/MWh for procurement on the intraday market, 20.50 EUR/MWh for electricity tax and 2 EUR/MWh additional costs for the trading participation. In the case of the cosφ(P) and Q(V)-control of PV systems, costs for lost profits are considered when the inverter has to reduce the active power due to the reactive power control (see subsection 7.2.3). These costs are set to 12.31 EUR/MWh, which represents the missed feed-in tariff [301]. Investment costs of BSS or PV systems are not considered, as within this study it is assumed that the cost burden is taken by a third party investor pursuing a business model.

Table 7.2: Assumed operating expenditures for the automated grid expansion, based on [18] and [78]. Cable costs include earthworks.

Equipment	Sizing	Costs
NAYY	150 mm^2	60 kEuro/km
NAYY	240 mm^2	65.5 kEuro/km
NA2XS2Y	185 mm^2	80 kEuro/km
Oil-immersed transformer	630 kVA	10 kEuro

7.2.3 Flexibility options

In this subsection the different flexibility options used in this chapter are presented and summarised in Table 7.3. The purpose of all control methods is to prevent OL and OV.

Table 7.3: Control strategies and control devices of the five flexibility options employed in this work.

Flexibility option	Control device	P-control (business case)	Q-control
cosφ(P)	PV system	maximum feed-in; using feed-in tariff	cosφ(P)-characteristic [47] (Fig. 7.1)
Q(V)	PV system	maximum feed-in; using feed-in tariff	Q(V)-characteristic PV [45] (Fig. 7.2)
RES	PV/RES system	self-consumption; adaptive persistence forecast [281, 302]	-
PCR+Q(V)	large BSS	P(f)-characteristic [303]	Q(V)-characteristic BSS (Fig. 5.10)
CES+Q(V)	large BSS	like RES; with cumulated profiles	Q(V)-characterisic BSS (Fig. 5.10)

cosφ(P)-control

The cosφ(P)-control is the state of the art for the reactive power control by PV systems connected to LV grids and is described in detail in [47]. For most of the installed PV systems in Germany the rated apparent inverter power is smaller than the rated PV-module power. In such cases, it may happen that an undersized inverter cannot supply the requested active and reactive power in accordance with [47]. If this is the case, the requested reactive power has priority. As a result the active power is reduced and the revenues of the PV plant owner are reduced accordingly.

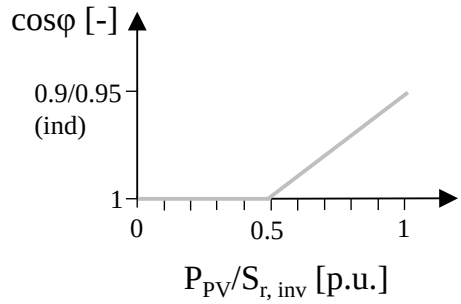

Figure 7.1: cosφ(P)-control chacteristics, according to [47].

As shown in Fig. 7.1 the reactive power is dependant on the ratio of the actual PV power P_{PV} and the rated inverter apparent power $S_{r,\,inv}$. When the active PV power exceeds 50 % of the rated inverter apparent power, the power factor cosφ is reduced.

The minimum power factor depends on the rated apparent power of the PV inverter (see Table 7.4).

Table 7.4: Power factor depending on the rated PV system inverter power $S_{r,\,inv}$.

$S_{r,\,inv} \leq$13.8 kVA	$S_{r,\,inv} >$13.8 kVA
cosφ(P)=0.95	cosφ(P)=0.90

As PV systems in Germany reach their maximal power only a few hours a year, the rated inverter power is often sized smaller than the rated PV system power. Thus, in the analysed region the rated inverter power is set to 85 % of the rated module power.

Q(V)-control

In the case of the Q(V)-control, the reactive power is adjusted as a function of the voltage at the PCC of the PV system or BSS. Therefore, reactive power is only supplied when it is really needed. In this work, the Q(V)-control is applied to inverters of PV systems without RES and large scale BSS, with two different characteristics: Q(V)-characteristic PV and Q(V)-characteristic BSS.

The characteristics of the Q(V)-curve for PV inverters installed in Germany are not yet regulated but are discussed in a variety of studies [45, 78, 304]. As previous investigations have shown, the stability of this control strategy depends to a large extent on the set control parameters [304, 305]. In this assessment, the stable configuration of [45] is implemented (see Fig. 7.2). As in the cosφ(P)-case, the PV system owners may lose part of their income if the PV inverter is not sized accordingly.

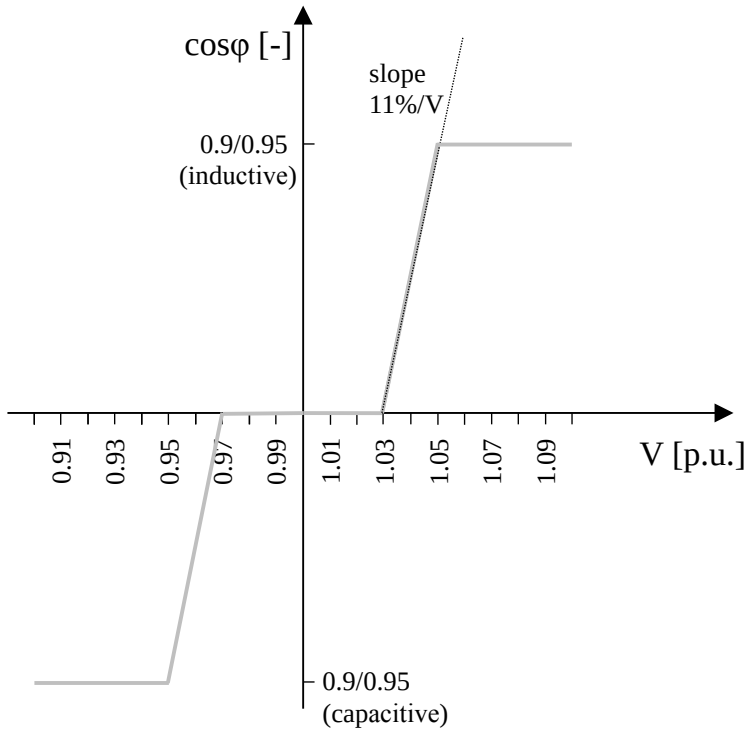

Figure 7.2: Q(V)-characteristic used for the reactive power control for PV systems, according to [45].

If the voltage at the PCC is lower than 0.97 p.u. or higher than 1.03 p.u., the supplied or absorbed reactive power increases linearly until a maximum reactive power value Q_{max} is reached, which is calculated with the power factor cosφ=0.9 or cosφ=0.95 dependant on the rated apparent power of the inverter analogue to the cosφ(P)-control (see Table 7.4). The linear slope is 11 % Q_{max}/V (phase-to-ground-voltage).

The Q(V)-characteristic for large scale BSS is depicted in (Fig. 5.10) and based on [18,26,41,45]. It has been implemented in the VRFB prototype.

For both Q(V)-controls a PT1-element is assumed with an amplification factor K=1 and a time delay of T=5 seconds [45].

Residential Storage Systems

Another type of flexibility option to reduce OL and OV is the implementation of RES with feed-in limitation. Since 2013, the increase of the self-

consumption with RES can be a viable business model for small PV plants in Germany [214]. To push this storage application the German government launched an incentive program for RES, which is also scientifically monitored [37]. One of the main requirements to take part in this incentive program is to limit the feed-in power of the corresponding PV system to 50 %. This feed-in limit is also employed in this study. The adaptive persistence forecast control strategy, presented in section 6.2, may be the most profitable from the storage owner's point of view. This strategy secures the best results with regards to the performance indicators (defined in section 6.2): curtailment loss ratio ratio (CLR), self-consumption ratio (SCR) and self-supply ratio (SSR). For all RES analysed in this work a lithium-ion battery system with a watt-hour system-round-trip efficiency of 84 % and an usable battery capacity between 20% and 90% of its nominal capacity C is assumed [302].

As introduced before and applied in chapter 6, [37, 302] present a sizing rule for an economical sizing of RES: C should be 1 kWh for a nominal PV power P_{PV_p} of 1 kWp and an annual load consumption LC of 1 MWh. To size the RES, lowercase symbols c, p_{PV_p} and lc are introduced to eliminate the units:

$$c = \frac{C[kWh]}{1\,kWh};\ p_{PV} = \frac{P_{PV_p}[kW_p]}{1\,kW_p};\ lc = \frac{LC[MWh]}{1\,MWh} \tag{7.1}$$

The sizing rule of [37,302] can now be written as follows:

$$c : p_{PV} : lc = 1 : 1 : 1 \tag{7.2}$$

However in most cases, the actual sizing deviates from this economical best case, as $p_{PV} \neq lc$ for most of the PV systems in the pilot village the storage capacity is sized to match the lower value. This is shown in equation (7.3) where c depends on p_{PV_p} and lc. C is limited to 30 kWh, according to [37].

$$c = p_{PV},\ if\ p_{PV} \leq lc \quad and \quad c = lc,\ if\ lc \leq p_{PV} \tag{7.3}$$

Pooled Large Scale BSS for Primary Control Reserve

In this subsection the focus lies on large scale BSS providing a system supportive PCR. In the SPF-project the BSS is connected to the LV busbar of a MV/LV-transformer, where it provides PCR according to a P(f)-function and reactive power according to a Q(V)-function. The applied system supportive PCR operation strategy and simulation model is presented and validated along with the applied the Q(V)-control characteristics in chapter 5.

Within the village described in section 3.4, large BSS are connected to the twelve LV grids within this test region. However, the BSS in the SmartPowerFlow project has a rated power of 200 kW and can lead to OL in some MV/LV-transformers. Therefore, the BSS are sized so that the hosting capacity of the pilot region is not reduced compared to the reference scenario, in which no flexibility options are applied. The apparent power reserve of every MV/LV-transformer, when the maximal number of PV systems in the reference scenario are installed, is used as sizing criterion for the BSS. The BSS are sized in 50 kW steps for every LV grid according to the apparent power reserve mentioned above.

The BSS allocated and sized in this way are integrated into the grid model and the hosting capacity assuming a worst case scenario can be calculated. The most critical grid state arises when maximum reverse power flow caused by the PV systems and maximum grid feed in by the BSS providing PCR occurs at the same time. The maximum PV power output is determined by a simulation over the period of one year with the data set and model as described in section 3.4. The maximum PCR value is determined using a worst case data set from the Swiss grid operator Swissgrid. The data is described in detail in subsection 5.3.1.

Community Electricity Storages

The VRFB-prototype battery model of the SPF-project is also used to simulate a CES operation mode. This mode has not been implemented in a field test, but is based on field test data (voltage at the PCC, charge and discharge characteristics of the BSS). As for the PCR option, the BSS is connected to the LV-busbar of the MV/LV transformer and the same reactive power control applies. Instead of providing PCR the active power of the BSS is used in this case to maximise self-consumption with the same operation strategy as the RES. Although the incentives of [37] are only granted for RES (30 kWh limit), the 50 % limit is used also for CES to assure a better comparison. A simplified 1-min battery model of the SPF-prototype for the CES application, the operation strategy, all simulation assumptions and a the technical and economic assessment of this BSS application is presented and analysed in detail in chapter 6. For every CES, the profiles of the generators and loads are summed. The calculation of the dynamic feed-in limit is performed only for the accumulated profiles. The operation strategy applies these accumulated profiles. The resulting charging or discharging power is calculated for every 1-min time-step. Thus, the load flow calculation for this application is also conducted in 1-min time-steps.

It is assumed that the sizing rule of RES (see equation 7.2) applies to CES, too. Since the BSS is connected to the LV-side of the MV/LV-transformer, all the loads and PV systems of the same LV-grid were assigned to one CES if possible, otherwise the loads of nearby LV grids were assigned. This leads to a non-optimal sizing of the loads and PV systems, but increases the hosting capacity of the LV grids by preventing OL of the MV/LV-transformers. To avoid OL due to the reactive power flow induced by the Q(V)-control, the CES are installed at LV-grids with MV/LV-transformers with at least 250 kVA rated apparent power.

7.3 Alternative Approach: Results and Discussion

Firstly, the resulting sizing, allocation and performance of the three storage options are presented and discussed. Secondly, the impact on the grid of the various flexibility options are compared under technical and economic criteria.

7.3.1 Sizing, Allocation and Performance of the Storage Options

Residential Storage Systems

When the sizing rule presented in equation 7.2 is applied to the reference scenario only 31 % of the RES of the pilot region lie within the economical favourable range of p_{PV}:lc of 0.5:2. As curtailment losses depend on the sizing of the RES and the c:p_{PV}:lc-ratio varies greatly, the impact of the sizing on performance indicators is severe, as listed in Table 7.5.

The performance indicators were calculated by simulating a given year in 1-minute steps. It can be seen that the bigger the difference ratio between lc and the PV size the poorer the performance of the storage system. In the first case in the table, almost all of the load can be covered by the PV system but the curtailment losses are high. In the second case, the PV power is consumed completely and no losses occur but the total load cover is modest. In the third case the performance indicators show typical values of an economically optimised system, as presented in subsection 6.2.3. The average household curtailment loss in the pilot village amounts to 6.5 %. The average RES size is 5.1 kWh and 92 % of the RES are below 10 kWh. However, as large PV systems with a non-optimal p_{PV}:lc-ratio curtail large amounts of energy, the total losses for the village rises to 9.3 %.

Table 7.5: Performance indicators for different RES system sizings.

c:p_{PV}:lc-ratio	SCR	SSR	CLR
1:100:1	1%	87%	11%
1:1:100	100%	13%	0%
1:1:1	51%	73%	3%

Grid Supportive Pooled Battery Storage System for PCR

The sizing and allocation of the BSS providing PCR results from applying the methodology described in subsection 7.2.3. As for the VRFB-prototype the ratio of rated reactive power to rated active power (Q2P) and the ratio of rated capacity to rated active power (E2P) is kept 2:1 for all BSS within the pool. Thus, in Table 7.6, only the installed rated power $P_{bat,r}$ and the maximum prequalifiable power $P_{bat,\ pq}$ of each BSS for every low voltage grid are listed. In T2, T7, T8 and T9 no BSS are installed, as this would reduce the hosting capacity compared to the reference scenario. The cumulative rated BSS-power is 1.2 MW with a maximal pre-qualified power of 1.05 MW which is enough to participate at the PCR-market (compare market restrictions Table 4.3).

Table 7.6: Installed rated power $P_{bat,r}$ of each BSS for every LV grid.

LV-grid	T1	T3	T4	T5	T6	T10	T11	T12
$P_{bat,r}$ [kW]	400	100	50	100	100	100	300	50
$P_{bat,pq}$ [kW]	350	87.5	43.75	87.5	87.5	87.5	262.5	43.75

Grid Supportive Community Electricity Storages

In the status quo there are 2.1 MW of PV power installed in the pilot village. As the sizing rule of equation 7.2 has been applied, only the geographically closest loads with a cumulated LC of 2.3 GWh, were combined to 5 separate CES systems with a C of 400 kWh, as depicted in Figure 6.16. To comply with the sizing rule, by installing more and more PV systems, more CES can be installed, too. For every 400 kW of additional cumulated PV power a new CES is added. In total eight CES are installed in the pilot village until 2025.

Performance Indicators and Allocation

The performance indicators SCR and SSR and the allocation for all eight CES are listed in Table 7.7. The indicators were calculated with (index PV) and without storage (index CES) in order to evaluate the influence of the CES. It can be seen that the BSS increases the SCR and the SSR. The first row of the table shows the ratio of the PV systems connected to the CES P_{PV} in kW_p and the cumulated LC in MWh, respectively.

Table 7.7: Allocation, sizing and calculated performance indicators of the CES for the year 2025.

	CES 1	CES 2	CES 3	CES 4	CES 5	CES 6	CES 7	CES 8
LV-grid	T1	T6	T9	T10	T11	T4	T7	T12
p_{PV}:lc	1.2:1	1.1:1.1	0.9:0.9	0.9:1.1	1:1.6	1:1.4	1.1:1.3	0.7:0.6
SCR_{PV}[%]	33	41	34	37	55	43	46	30
SCR_{CES} [%]	51	59	52	54	69	60	63	47
SSR_{PV} [%]	45	44	45	43	43	41	41	51
SSR_{CES} [%]	67	62	68	63	54	56	56	79

The influence of the dimensioning of the load and PV can be shown by the example of CES 5. In this case, there is significantly more load connected to this CES than to the other storages, leading to the smallest increase of the self-consumption rate from 55 % without CES (SCR_{PV}), to 60 % with CES (SCR_{CES}). The oversized CES 8 on the other hand, results in the highest self-supply ratio with CES SSR_{CES} of 79 %. The curtailment loss ratio for all CES lies under the negligible level of less than 1 %. This is a factor 3 to 7 smaller then the curtailment losses of the same operation strategy applied to one optimal sized residential PV-storage system, if compared with [293] and Table 7.7 and a factor 9 smaller for the whole village. The negligible curtailment losses and the reduction potential of CES matches with the results of [221], who compared RES with CES for LiB .

7.3.2 Technical Assessment

To compare the flexibility options technically, the relative and absolute increase of additionally installed PV systems (Fig. 7.3) as well as the additional maximum hosting capacity (Fig. 7.4) is calculated for every flexibility option.

For this purpose, the status quo of the grid is expanded with PV systems according to section 3.5 until in every single LV grid the maximal amount of PV systems are integrated. The sum of the status quo of PV systems (2.1 MW) and additional PV installations (1.1 MW) represents the hosting

capacity of 3.3 MW for PV systems in the village without flexibility and is used as a reference scenario.

As shown in Fig. 7.3 for all flexibility options, additional PV systems can be integrated compared to the reference scenario. For the scenario with large scale BSS providing PCR, the additional PV system power is increased by 21 % (1.4 MW), with cosφ(P) by 52 % (1.7 MW) and by 53 % (1.7 MW) with Q(V), by 78 % for CES (2.0 MW) and by 129 % for RES (2.6 MW). The relative values are the ratio to the additional PV system of the reference scenario (1.1 MW) and the additional PV system power of the corresponding flexibility option. In the different LV grids, the additionally installed PV power varies greatly depending on the grid topology. For the grids T1, T5, T11 and T12, the full PV potential can be connected to the grids for all scenarios, because the hosting capacity is not reached in any of these grids.

In the case of the two reactive power control scenarios cosφ(P) and Q(V), more PV systems can be connected to the grids T2, T3, T6, T7, T9 and T10, as in the scenario without flexibility in which OV limits the hosting capacity. The reactive power control flexibility options can solve the OV issues such that further PV systems can be connected until the OL threshold is reached.

In contrast to the two previous flexibility options, the RES option limits the feed-in power. As a result, OL and OV occurs at higher penetration rates and thus more PV systems can be connected to the grids T2, T3, T6, T7 and T9 compared to all other options. For the grids T2, T3 and T6 OV is the limiting factor, as in the reference scenario, whereas for T7 the 250 kVA MV/LV-transformer is limiting the hosting capacity due to OL when a installed PV system power of 503 kVA is reached in this LV grid. In T9 the whole technical PV-potential can be hosted.

The main difference from the scenario in which large scale BSS provide system supportive PCR to the other flexibility options, is that in this case the BSS represent additional generators connected to the grid. This is due to worst case assumptions applied in traditional grid planning in which the PV systems and the BSS act as generators providing their maximum power. Nevertheless, additional PV systems can be installed in the grids T2, T6, T7, T9 and T10.

The option with the second highest increase of PV systems is the CES option, even if in T2, T3, T5 and T8 there are no CES installed. This can be seen for T2 and T3, in which other options such as reactive power control options perform better, even if in T2 the voltage is reduced by CES in other LV-grids and therefore still outperforms the reference scenario.

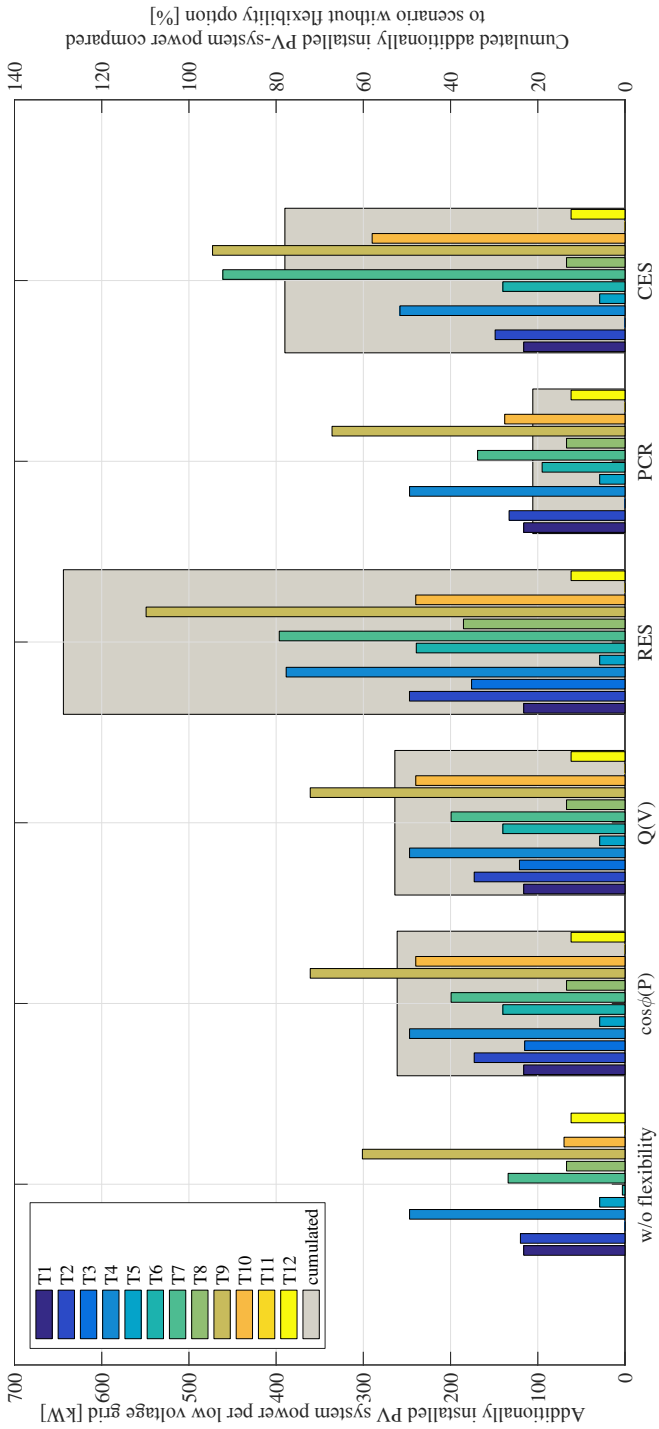

Figure 7.3: Relative and absolute increase of additionally installed PV system power for the whole pilot village and every LV grid seperatly.

The increase of the (additional maximal) hosting capacity for the whole village of the flexibility options with respect to the reference scenario is shown in Fig. 7.4.

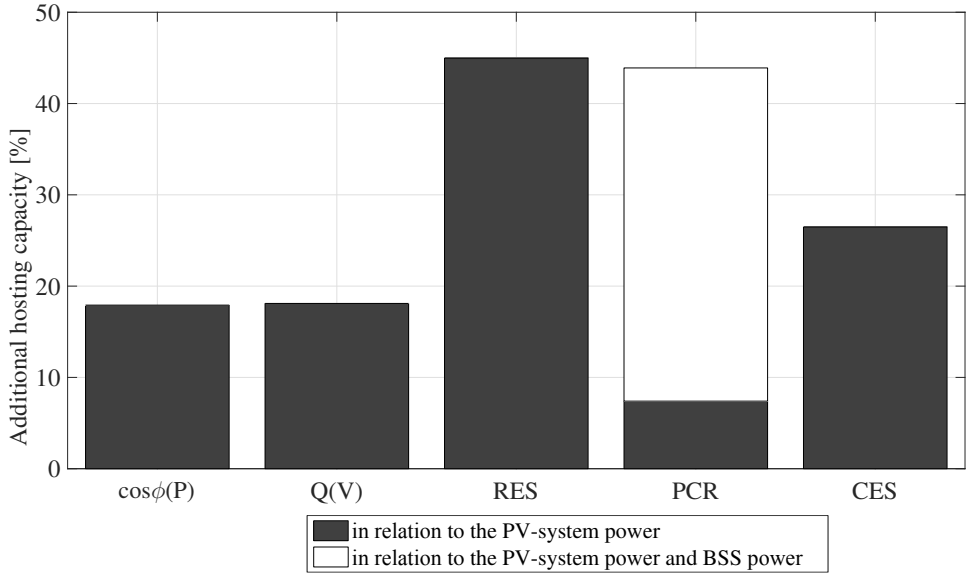

Figure 7.4: Relative increase of maximum hosting capacity of the PV-system power with 3.3 MW (reference scenario) for the whole the village.

Unlike in Fig. 7.3, in Fig. 7.4 the shown values are the relative increase of the hosting capacity. These relative values are the ratio of the hosting capacity of the reference scenario (3.3 MW) to the hosting capacity of the corresponding flexibility option. The hosting capacity depicted can be increased for all flexibility options: the hosting capacity can be increased with cosφ(P) and Q(V) by 18 %, by 27 % for CES and by 45 % for RES, by 7 % for BSS proving PCR. If the hosting capacity is not limited to the maximum amount of PV systems that can be connected to grid, but also in cooperates BSS systems that act as a generator, the increase of hosting capacity is much higher for the PCR option (44 %). In the RES and CES scenarios the nominal power of the RES/CES cannot be considered as additional generators connected to the system, since these systems only have a time shifting purpose. Since these systems are designed to increase self-consumption they do not feed into the grid at all (RES) or at least not at the same time as the PV systems (CES).

The implementation of the flexibility options cosφ(P) and Q(V) lead to a

similar increase in the hosting capacity, which is also confirmed by the results of [45]. Whether the Q (V)-control results in higher reactive power flows as the cosφ(P)-control to reach the same hosting capacity depends on several factors, such as the set voltage on the MV busbar (here 1.03 p.u.) of the HV/MV-substation, the set-points of the Q(V)-characteristic and the grid topology. The increase in hosting capacity of the cosφ(P)- and of the Q(V)-option are close to the reported value of 20 %-40 % for rural grids calculated by [45].

In conclusion, all flexibility options are able to increase the hosting capacity compared to a scenario without flexibility option in the pilot region. The economic aspect of the options is analysed in the next section.

7.3.3 Economic Assessment

In this section the economic aspects of traditional grid expansion versus the application of flexibility options are presented. As described in section 3.5 a PV-expansion pathway, based on the aims of the Bavarian government and the resultant grid reinforcement, is considered until 2025 for the economic assessment. The distribution grid of the pilot region is described in section 3.4. Although the entire distribution grid (MV and LV) is considered for the automated grid expansion, the grid reinforcement only takes place in LV. This is due to the PV expansion methodology causing new PV systems only to be connected to LV, as they are relativity small roof top installations.

The net present value method is applied to compare the different flexibility options. For the calculation of the net present value it is assumed that the grid will remain at the status of the year 2025 until 2050. In Fig. 7.5 the costs that have to be borne by the DSO and by the BSS or RES owner are shown.

The costs that concern the DSO are: the grid expansion costs, costs to due grid losses and additional costs due to Q-management. The grid expansion costs are net present values of the grid assets minus the residual values of the assets in the year 2050. The operation expenditures consist of the costs due to grid losses and the costs connected to the reactive power control of the large scale BSS. It is assumed that the large scale BSS operator is reimbursed for the additional costs caused by the Q-management. As shown in Fig. 7.5 all flexibility options result in lower grid reinforcement and lower overall costs compared to the reference scenario without flexibility option. The costs for the grid losses could only be lowered in the RES scenario by 8 kEUR. All other flexibility options result in rising grid losses: 15 kEUR for PCR and CES, 21 kEUR for cosφ(P) and 23 kEUR for Q(V). The higher grid losses are

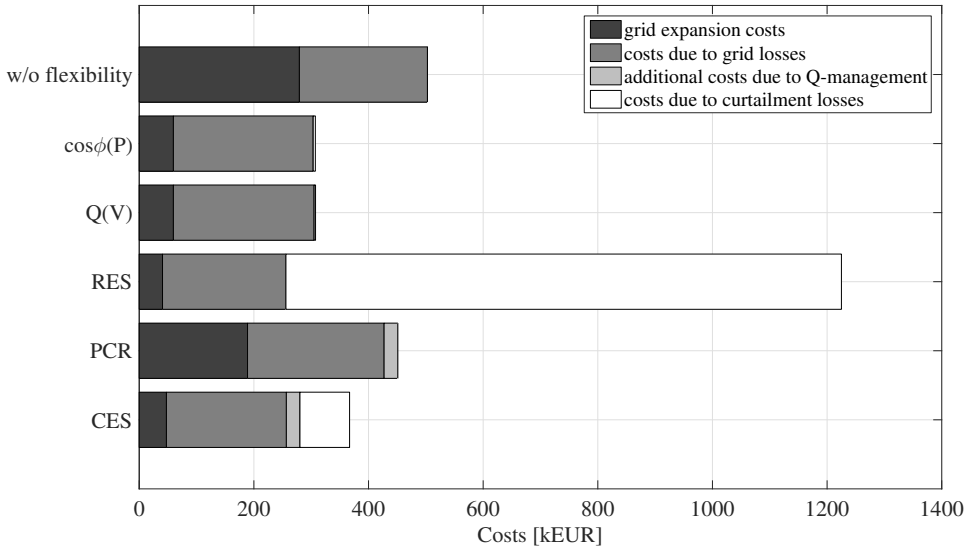

Figure 7.5: Total costs borne by the DSO and by the BSS or RES owner for all scenarios.

caused by the increase in thermal losses induced by the additional reactive power in the grid caused by the reactive power control of these flexibility options. A much higher influence of the flexibility options can be seen in the grid reinforcement costs: The RES-option may save up to 85 %, the CES-option 83 %, the options cosφ(P) and Q(V) 79 % and the PCR-option 32 % of the grid expansion costs until 2025. For the CES and PCR-option, however, additional costs of 24 kEUR arise that have to be reimbursed to the BSS operator for the ancillary service of providing reactive power control.

In a more holistic cost assessment in addition to the costs of the DSO, the curtailment losses by the BSS or RES have to be considered, too. These costs are not reimbursed and are borne by the battery owners. In the cosφ(P) and Q(V)-option these costs apply only in the case when the active power has to be reduced to provide the requested reactive power. Even if these costs are very low for these two options, it can be shown that the Q(V)-control is able to reduce the curtailment losses by 50% from 4 kEUR to 2 kEUR. Furthermore, the RES-option which is the most profitable solution from the DSO's point of view appears to be the least profitable if the curtailment losses are also taken into account. This is due to the 50 % feed-in limit, which with a the non-optimal storage sizing (see subsection 7.3.2) for RES, leads to total costs that exceed the costs of the reference scenario by more

than 100 %. Finally, the CES-option shows a high cost saving potential compared to RES by sharing large scale BSS to maximise self-consumption. This is especially true if non optimal sizing of the RES is applied. For the pilot village the costs due to curtailment losses can be reduced by 91 %, turning the CES-option into the most profitable one, if storage systems are integrated into a existing grid to prevent future grid expansion costs.

Future studies might analyse how the set value of the voltage on the HV/MV busbar influences the reduction of grid expansion costs. As in this this work the on-load tap changer of the HV/MV transformer is not taken into account, future studies might also evaluate the impact of diverse decentralised autonomous reactive power control strategies on the control of the on-load tap changer. They might cause unwanted oscillations, for example.

Another interesting research question would be to analyse the additional cost saving potential if the applied OV and OL criteria would not be as strict as in this work. In this work, as common practice in the DSO distribution grid planning, the OV and OL threshold can not be surpassed in any simulated time-step. But for oil immersed transformers a higher OL limit might be applied, as suggested by [13]. The OV limit could also be applied less strict, as according to DIN-EN 50160 [41], only 95 % of the 10-minute RMS average of the voltage values must not exceed $\pm 10\%$ of V_n. A further restriction is that the interval of $+10\%/-15\%$ of V_n can not be surpassed. Applying the less strict OV and OL criteria described above, would probably affect the maximum hosting capacity as well as the cost saving potential considerably, as for example most of the MV/LV transformer in rural areas in Germany are oil immersed transformers.

7.4 Chapter Summary

In this chapter the traditional approach to implement large scale BSS in distribution grid planning is presented and the disadvantages by this state of the art approach are discussed. In order to overcome this disadvantages an alternative approach is presented. With this new approach five flexibility options are analysed as an alternative to PV induced traditional grid expansion for a specific pilot region. The options are: two reactive power control strategies with PV inverters, one residential and two large scale BSS applications. The flexibility options are assessed from a technological and an economical point of view.

The main finding of the technological evaluation is that for all flexibility options the hosting capacity for PV systems can be increased in the distribu-

tion grid of the pilot region compared to the reference case which represents traditional grid expansion. The most effective flexibility options in descending order are: RES, CES, Q(V), cosφ(P) and PCR. However, if in the case of PCR the additional BSS are considered as generators, PCR becomes the second most effective option. The amount of additional PV systems that can integrated in a LV-grid depends highly on the topology of the grid. It is shown, that the analysed reactive power control options (Q(V) for CES, PCR and PV systems, cosφ(P) for PV systems) can relieve LV-grids with long feeders, OV issues and low capacity utilisation of the MV/ LV transformers, since in these cases the hosting capacity of the grid can be increase until OL occurs in the MV/ LV transformers. In the reference scenario as well as in the RES-option the hosting capacity is limited by mainly by OV. In the RES-case this issue is addressed successfully by limiting the feed-in power by applying a 50 % feed-in limit to the operation strategy. Nonetheless, this feed-in limit causes a 9.3 % of CL due to non optimal sizing of the individual RES-systems. This high amount of CL may put the CES-options as a viable alternative considering that with this option the CL can be reduced by 91 % pursuing the same business model. The PCR-option represents a special case: In spite of adding additional generator capacity to the grid (from the DSO's perspective) the hosting capacity is increased due to the grid supportive behaviour of the Q(V)-control.

The economic assessment shows that from a DSO's point of view all flexibility options are preferable alternatives to traditional grid expansion for the analysed pilot region and PV-expansion pathway. From all scenarios the RES-option shows the highest cost saving potential. The cost saving ranking order is the same as the technical ranking, which is based on the capability of the flexibility option to increase the hosting capacity and therefore reduce grid expansion costs. It is shown that the reduction of the grid expansion costs has the most impact on the DSOs' costs as all flexibility options lead to similar grid operation costs. However, the ranking order is changed considerably if the costs resulting from CL are integrated in a more holistic cost assessment. These CL lead to additional costs which could surpass the avoided grid expansion costs for RES-option. However, the CES-option however is able to reduce the CL substantially and is therefore still more economical than traditional grid expansion, which turns it into a viable alternative to the RES-option.

In conclusion, all analysed flexibility options are capable of reducing the grid expansion costs compared to a scenario with only traditional grid expansion. Furthermore, it shown that market driven storage applications like PCR may be grid supportive, if the BSS is sized and allocated properly and

combined with a reactive power control strategy.

Finally, DSO are therefore encouraged to consider the integration of additional PV and battery storage systems not as a problem which triggers grid expansion, but as part of the solution for reducing future grid expansion costs. This is due to the great cost reduction potential, when a grid/system supportive BSS is integrated in a distribution grid, compared to traditional grid expansion.

Chapter 8

Conclusion

In this chapter the context of the thesis is covered, the motivation and research objectives are described and the general conclusions of the work are drawn. Furthermore, the added value of the presented research is highlighted and possible future work is presented.

Context of the Thesis and Motivation

Electrical energy systems are changing all over the world, as conventional power plants are being replaced by renewable energy systems as part of the energy transition. The survey area of this thesis is limited to Germany, which has a leading role in promoting the energy transition. This limitation is necessary, due to the national character of technical regulations and the legal framework. Nevertheless, most of the results can be transferred to other nations in the EU and beyond. Renewable energy systems are mainly connected to the distribution network in a decentralised manner, due to their smaller system size. This may cause inefficient grid operation and increased grid expansion measures that have to be borne by the general public. Therefore, alternatives are investigated and evaluated. The project SmartPowerFlow was initialised and funded, to analyse these alternatives to traditional grid expansion and is an essential part of this work.

Main Research Objective

The main research objective of the thesis is to quantify the reduction potential of grid expansion measures, caused by a growing share of renewable

energy systems, when battery storage systems are applied. However, the sole re-financing of large scale battery storage systems on distribution grid level is difficult, even if the battery prices are falling rapidly. There are two reasons for this: Firstly, it is unclear from a legal and regulatory point of view how battery storage system operators may be remunerated for the avoided grid expansion. Secondly, the prices of grid equipment in distribution grids is several times lower than in transmission grids and thus it is very difficult for large scale battery storage systems to compete with traditional grid expansion in these low voltage levels. Therefore, the focus of this work lies on the analysis of promising combinations of a profitable and grid supportive operation strategies for large scale battery systems in general, and for a specific Vanadium Redox Flow Battery prototype in particular.

Thesis Contribution

The thesis covers a literature review, simulation-based assessments and verification of the simulated results in a field test. By reviewing the literature about the integration of large scale battery systems in distribution grid planning in chapter 2, the gaps in research are identified and the contributions of this thesis are derived. The main contributions address these research gaps and are listed hereafter:

Thesis Contribution 1
The most profitable market based business case and the business case with the highest cost reduction potential are identified for the German energy sector: primary control reserve and maximising the self-consumption of generated PV energy (chapter 4). Two simulation models, which are created for these two applications for a large scale Vanadium Redox Flow Battery prototype are based on based on measured values, are described in chapter 5 and chapter 6. Both applications are combined with an autonomous reactive power control. As a result, high quality time-series are created and applied to distribution grid planning.

Thesis Contribution 2
In chapter 5 and chapter 6 techno-economic assessments of both grid supportive business cases applied to a Vanadium Redox Flow Battery prototype implemented in a specific pilot region, which is presented in chapter 3, are conducted. As a result, the possible profits and the additional cost burden of the grid supportive behaviour for the two business cases are quantified.

Thesis Contribution 3
The high quality time-series for both grid supportive business cases are applied to an alternative distribution grid methodology called expert system. As a result, future grid expansion costs are quantified for a given DG expansion pathway of a pilot region, in chapter 7. The costs are compared with the costs caused by the implementation of large scale battery systems (applying the two identified grid supportive business cases) and other more common alternatives to traditional grid expansion.

Main Highlights and Conclusions

The general conclusions and main highlights of the work are presented here, as extensive conclusions on each discussed topic can be found in the summary of each chapter.

- The pilot grid for the allocation of the vanadium redox flow battery systems prototype was selected by a search algorithm which maximises the impact on future grid expansion costs, as presented in chapter 3. A primary criterion in the search algorithm is to find a grid connection point at which the grid is not stressed any further but, if possible, released as much as possible. The algorithm finds locations, at which grid supportive and at the same time market-driven applications of the battery are possible to combine.

- In chapter 5, the simulation model of the grid supportive primary control operation mode is validated in a the field test. This simulation model is later used for a technical and economic assessment of the application in a pilot region. However, it turned out that from a technical point of view the battery system is not optimally suited for this application. The reason for this is that in the primary control reserve mode in about 90 % of the time only 20 % of the offered power is needed. In this requested power range, the battery prototype showed a very low performance (e.g. 15 % efficiency at 5 % of the rated power). However, from an economic point of view, the low system efficiency is negligible as correction energy costs traded at the energy market accounted for only a small proportion of the revenues. For the same reason, the positive economic impact of the degrees of freedom free that are free of charge is low, too. Likewise, the extra cost burden for the provision

of reactive power caused by the grid supportive behaviour can be neglected as it represents only 0.5 % of extra costs. Overall, investment costs and revenues from the primary control reserve market are the deciding factors for the profitability of this business case. While Li-Ion batteries can achieve positive net present values due to lower investment costs under today's conditions, the average investment cost of vanadium redox flow batteries for a profitable operation are still 60 % too high. However, since this is a new technology, a high cost-saving potential can be expected. The economic analysis showed the current investment uncertainty for battery projects, but also their potential for a strong impact on the market if lower investment costs can be realised in the future. To ensure investment security, it seems mandatory to harmonise the regulatory framework at the EU and national levels.

- The second most promising revenue opportunity is analysed in chapter 6 for the pilot region: the application of large scale battery system as a community electricity storage in order to maximise the self-consumption of a community. For the profitability of the grid supportive self-consumption business case, the investment costs, the price of the feed-in tariff and above all the incurring charges and levies are identified as the most decisive factors. It is shown that this business case could already be profitable in theory, but due to the legal framework in place, the investment costs of the vanadium redox flow battery system would have to fall by 77 % in the best case to reach break even. If a direct marketing business case for self-consumption is pursued no profit can be earned as the incurring charges and levies lead to a negative cash-flow, at present. Furthermore, it is shown that the reactive power provision and therefore the grid supportive behaviour does not lead to any significant additional costs for this operation strategy (less than 1 % of the costs). Finally, the economic results of this operation strategy are compared with lithium-ion batteries providing the same service. It follows, that the community electricity storage application is slightly more profitable if lithium-ion batteries are used instead of vanadium redox flow batteries. But no positive net present value can be reached under the current conditions either. Finally, it is worth pointing out that in spite of lower curtailment losses compared to residential PV storage systems and advantages of the economy of scale, it is not clear whether community electricity storages applying self-consumption maximisation will become feasible in the near future due to the current unfavourable legal framework.

- In chapter 7 the traditional approach to implement large scale battery systems in distribution grid planning is presented and the disadvantages by this state of the art approach are discussed and alternatives are presented. The disadvantages of traditional distribution grid planning are: Only active power flows are taken into account and reactive power control is usually not considered, or only a fixed $cos\varphi$ can be taken into account as only one time-step for the two worst case scenarios is calculated. Furthermore, as there are no experiences with large scale batteries in distribution grids, the diversity factors used to adapt the active power of the battery systems might be very extreme to cover all possible grid states of the worst case assumptions. It can be concluded that the traditional planning method will lead to over-capacities and uncertainties concerning the reactive power flows.

- In order to overcome these disadvantages of traditional grid planning with large scale battery systems, an alternative approach is presented in chapter 7, which is based on detailed simulation models of the battery systems. The simulation models of chapter 5 and chapter 6 provide detailed time series of all relevant variables for the distribution grid planning and include the individual behaviours of the grid users. The time series represent a more realistic loading situation than with the worst case assumption of the traditional distribution grid planning. These two large scale battery systems flexibility options are assessed along with a cosφ(P)-control and Q(V)-control for PV systems and residential storage systems. It is shown that these five flexibility options increase the hosting capacity for PV systems, compared to a scenario without, by up to 45 % for the pilot region. Furthermore, the results of the economic assessment indicates that the analysed flexibility options might be a viable alternative to traditional grid expansion as all of them show a cost reduction potential.

In summary, the present work provides a set of tools for an assessment of an implementation of grid supportive and of market-driven and other profit orientated applications of large scale batteries at the distribution grid level. Finally, the main conclusion of the thesis is, that grid supportive and profit orientated battery applications are not contradictory. Thus, DSO are encouraged to consider the integration of additional PV and battery storage systems not as a problem which triggers grid expansion but as part of the solution for reducing future grid expansion costs. This is due to the great cost reduction potential if a grid/system supportive behaviour is applied which largely exceeds the extra costs.

Future work

It can be concluded from this thesis, that large scale battery systems may contribute to reduce future grid expansion costs if they become feasible. As this work is limited to a predetermined Vanadium Redox Flow Battery prototype implemented in a specific pilot region, several proposals regarding further work result:

- Further studies could determine to what extent the battery systems power and capacity can be sized optimally for a grid supportive primary control reserve and community electricity storage.
- Another research question would be whether, from a technical and economic point of view, it makes more sense to transfer the proposed methodology of a profit orientated and grid supportive battery application to other battery technologies as well as to battery systems connected to other voltage levels.
- The characteristics of the Q(V)-curve could be optimised to reduce grid losses and still increase the hosting capacity for DG. Further issues are the stability of the operation strategy and the interaction with the automatic tap changer of the transformer in the HV/MV substation.
- Future studies could examine if the economics of large battery projects could be increased by combining several market driven business models with the same battery. A promising combined application, could be a community storage system which at the same time provides primary control reserve.
- The assessment of the flexibility options is limited to a specific pilot region in Bavaria and a specific deterministic PV expansion pathway. Further research projects could therefore analyse whether the results of this work can be generalised by considering other distribution grids and PV expansion pathways through a probabilistic approach.
- Finally, in this thesis, the flexibility options to increase the hosting capacity for renewable energy systems are examined and evaluated separately. However, as it is shown that each measure has its advantages and disadvantages, future studies should highlight how the different flexibility options can be combined best.

Bibliography

[1] Federal Ministry for Economic Affairs and Energy (BMWi), "Renewable Energy Sources in Figures," Tech. Rep., 2017. 1

[2] E. Karakaya, A. Hidalgo, and C. Nuur, "Motivators for adoption of photovoltaic systems at grid parity: A case study from Southern Germany," *Renew. Sustain. Energy Rev.*, vol. 43, pp. 1090–1098, 2015. 1, 88

[3] Federal Ministry of Economic Affairs and Energy (BMWi) and Federal Ministry for the Environment, Nature Conservation Building and Nuclear Safety (BMU), "Energiekonzept für eine umweltschonende, zuverlässige und bezahlbare Energieversorgung," p. 32, 2010. 1

[4] A. Keane and M. O'Malley, "Optimal Allocation of Embedded Generation on Distribution Networks," *IEEE Trans. Power Syst.*, vol. 20, no. 3, pp. 1640–1646, aug 2005. 1

[5] T. Ackermann, G. Andersson, and L. Söder, "Distributed generation: a definition," *Electr. Power Syst. Res.*, vol. 57, no. 3, pp. 195–204, apr 2001. 1, 10

[6] C. Gonzalez, R. Ramirez, R. Villafafila, A. Sumper, O. Boix, and M. Chindris, "Assess the impact of photovoltaic generation systems on low-voltage network: software analysis tool development," in *2007 9th Int. Conf. Electr. Power Qual. Util.* IEEE, oct 2007, pp. 1–6. 1

[7] S. Nykamp, A. Molderink, J. L. Hurink, and G. J. Smit, "Statistics for PV, wind and biomass generators and their impact on distribution grid planning," *Energy*, vol. 45, no. 1, pp. 924–932, sep 2012. 1, 19

[8] A. von Oehsen, Y.-M. Saint-Drenan, T. Stetz, and M. Braun, "Vorstudie zur Integration großer Anteile Photovoltaik in die elektrische Energieversorgung - Ergänzte Fassung vom 29.05.2012,"

Frauenhofer IWES, Studie im Auftrag des BSW - Bundesverband Solarwirtschaft e.V., Kassel, Tech. Rep. November 2011, 2012. 1

[9] A. Mohring and J. Michaelis, "Techno-ökonomische Bewertung von Stromspeichern im Niederspannungsnetz," Fraunhofer ISI, Karlsruhe, Tech. Rep., 2013. 2

[10] C. Breyer, B. Müller, C. Möller, E. Gaudchau, L. Schneider, M. Resch, K. Gajkowski, and G. Pleßmann, "Vergleich und Optimierung von (de-) zentral orientierten Ausbaupfaden zu einer Stromversorgung aus EE in Deutschland," Reiner Lemoine Institut gGmbH, Berlin, Tech. Rep., 2013. 2

[11] T. Stetz, M. Kraiczy, K. Diwold, M. Braun, B. Bletterie, C. Mayr, R. Bründlinger, B. Noone, A. Bruce, and I. Macgill, "High Penetration PV in Local Distribution Grids Outcomes of the IEA PVPS Task 14 Subtask 2," Tech. Rep. July, 2014. 2

[12] T. Stetz, M. Rekinger, and I. Theologitis, "Transition from Uni-Directional to Bi-Directional Distribution Grids," Tech. Rep., 2014. 2

[13] G. Kerber, "Aufnahmefähigkeit von Niederspannungsverteilnetzen für die Einspeisung aus Photovoltaikkleinanlagen," PhD Thesis, TU München, 2011. 2, 25, 189

[14] B. Meyer, H. Mueller, R. Koeberle, M. Fiedeldey, C. Hoffman, and J. Bamberger, "Impact of large share of renewable generation on investment costs at the example of aw distribution network," in *22nd Int. Conf. Exhib. Electr. Distrib. (CIRED 2013)*, no. 1241. Institution of Engineering and Technology, 2013. 2, 31, 92, 135

[15] J. Weniger, J. Bergner, and V. Quaschning, "Integration of PV power and load forecasts into the operation of residential PV battery systems," in *4th Sol. Integr. Work.*, 2014, pp. 383–390. 2, 145, 159, 160, 162

[16] Association of German Grid Operators (VDN), "TransmissionCode 2007 - Netz- und Systemregeln der deutschen Übertragungsnetzbetreiber," p. 90, 2007. 2, 15, 68, 69, 74, 81

[17] Federal Network Agency (BNetzA), "Monitoringbericht 2014," Bundesnetzagentur, Berlin, Tech. Rep., 2014. 2, 67

[18] German Energy Agency (dena), "dena-Verteilnetzstudie. Ausbau- und Innovationsbedarf der Stromverteilnetze in Deutschland bis 2030." Berlin, 2012. 2, 13, 15, 17, 18, 19, 20, 23, 24, 25, 40, 43, 50, 67, 113, 174, 175, 178

[19] S. Nykamp, V. Bakker, A. Molderink, J. L. Hurink, and G. J. Smit, "Break-even analysis for the storage of PV in power distribution grids," *Int. J. Energy Res.*, vol. 38, no. 9, pp. 1112–1128, jul 2014. 3

[20] A. Armstorfer, H. Müller, H. Biechl, B. Alt, R. Sollacher, D. Most, A. Szabo, R. Köberle, and M. Fiedeldey, "Operation of battery storage systems in smart grids," in *Int. ETG-Kongress 2013*, 2013, pp. 1–8. 3, 92, 135

[21] J. Bühler, "Instandhaltungs- und Erneuerungsoptimierung von städtischen Mittelspannungsnetzen," PhD thesis, Technische Universität Darmstadt, 2013. 3, 4, 123

[22] J. Riewe and M. Sauer, "Einsatz- und Rechtsrahmen für moderne Batteriegroßspeicher – Eigenständiger Speichermarkt oder Modell der Netzbetriebsintegration?" *Ew. - Zeitschrift des Instituts für Energie- und Wettbewerbsr. der Kommunalen Wirtschaft e.V.*, vol. 2/2014, pp. 77–129, 2014. 4

[23] H. Schwintowski, "Konfiguration und rechtliche Rahmenbedingungen für den modernen Batteriespeichermarkt," *Ew. - Zeitschrift des Instituts für Energie- und Wettbewerbsr. der Kommunalen Wirtschaft e.V.*, vol. 2/2015, pp. 81–98, 2015. 4

[24] Reiner Lemoine Institut, Technology Solar, LEW-Verteilnetz, and Younicos, "SmartPowerFlow," http://forschung-energiespeicher.info/ (accessed 2018-07-30). 5

[25] K. Heuck, K.-D. Dettmann, and D. Schulz, *Elektrische Energieversorgung*, 8th ed. Wiesbaden: Vieweg+Teubner, 2010. 10

[26] T. Stetz, "Autonomous Voltage Control Strategies in Distribution Grids with Photovoltaic Systems: Technical and Economic Assessment." PhD thesis, University of Kassel, 2014. 11, 16, 113, 172, 178

[27] C. Schwaegerl, M. H. J. Bollen, K. Karoui, and A. Yagmur, "Voltage control in distribution systems as a limitation of the hosting capacity for distributed energy resources," in *CIRED 2005 18th Int. Conf. Exhib. Electr. Distrib.* Turin: IET, 2005, pp. 6–9. 11, 16

[28] S. Papathanassiou, N. Hatziargyriou, P. Anagnostopoulos, and L. Aleixo, "Capacity of Distribution Feeders for Hosting DER," CIGRE Work. Gr. C6.24, Tech. Rep., 2014. 11, 16

[29] L. F. Ochoa, C. J. Dent, and G. P. Harrison, "Distribution Network Capacity Assessment: Variable DG and Active Networks," *IEEE Trans. Power Syst.*, vol. 25, no. 1, pp. 87–95, 2010. 11

[30] T. Kornrumpf, M. Zdrallek, M. Roch, D. Salomon, P. Pyro, and I. Hobus, "Flexibility options for medium-voltage grid planning," *CIRED - Open Access Proc. J.*, vol. 2017, no. 1, pp. 2287–2291, oct 2017. 11

[31] H. Ibrahim, A. Ilinca, and J. Perron, "Energy storage systems - Characteristics and comparisons," *Renew. Sustain. Energy Rev.*, vol. 12, no. 5, pp. 1221–1250, jun 2008. 12

[32] A. Poullikkas, "A comparative overview of large-scale battery systems for electricity storage," *Renew. Sustain. Energy Rev.*, vol. 27, pp. 778–788, 2013. 12

[33] G. L. Soloveichik, "Battery Technologies for Large-Scale Stationary Energy Storage," *Annu. Rev. Chem. Biomol. Eng.*, vol. 2, no. 1, pp. 503–527, jul 2011. 12

[34] M. Sterner, F. Eckert, M. Thema, and F. Bauer, "Der positive Beitrag dezentraler Batteriespeicher für die stabile Stromversorgung," FNES, OTH Regensburg, Tech. Rep., 2015. 13, 63, 132, 139

[35] Forum Network Technology / Network Operation in the VDE (FNN), "Connecting and operating storage units in low voltage networks," Tech. Rep. June, 2013. 13, 14

[36] TÜV Süd, "Grid compabitility certified by TÜV SÜD," 2015. 13

[37] K.-P. Kairies, D. Magnor, and D. U. Sauer, "Scientific Measuring and Evaluation Program for Photovoltaic Battery Systems(WMEP PV-Speicher)," *Energy Procedia*, vol. 73, pp. 200–207, jun 2015. 13, 132, 141, 179, 180

[38] Federal Ministry of Justice and Consumer Protection, "Law on electricity and gas supply (Energiewirtschaftsgesetz-EnWG)," 2015. 15, 68, 73

[39] Association for Electrical; Electronic & Information Technology (VDE), "Power transformers - Part 2: Temperature rise for liquid-immersed transformers (IEC 60076-2:2011); German version EN 60076-2:2011," 2012. 15

[40] VDE, "Power cables - Part 603: Distribution cables of rated voltage 0,6/1 kV; German version HD 603 S1:1994/A3:2007, parts 0, 1, 3-G and 5-G," 2010. 15

[41] German Institute for Standardisation (DIN), "Voltage characteristics of electricity supplied by public distribution networks; German version EN 50160: 2010 + Cor.: 2010," 2011. 15, 37, 68, 113, 173, 178, 189

[42] G. Kerber and R. Witzmann, "Loading Capacity of Standard Oil Transformers on Photovoltaic Load Profiles," in *10th World Renew. Energy Congr. Exhib.*, 2008, pp. 1198–1203. 15

[43] M. Labed, M. Brand, and H. Rose, "A Cost-Effective Approach for The Grid Integration of Distributed Renewable Resources," *Int. J. Emerg. Technol. Adv. Eng.*, vol. 4, no. 3, pp. 249–252, 2014. 15

[44] T. Ackerman, M. Koch, H. Rothfuchs, N. Martens, and T. Brown, "Verteilnetzstudie Rheinland-Pfalz," Tech. Rep., 2014. 15, 23, 24, 25

[45] B. Engel, S. Laudahn, O. Marggraf, and A. Schnettler, "Vergleich von technischer Wirksamkeit sowie Wirtschaftlichkeit zeitnah verfügbarer Verfahren zur Sicherung der statischen Spannungshaltung in Niederspannungsnetzen mit starker dezentraler Einspeisung," TU Braunschweig, RWTH Aachen, TU München, FGH, Tech. Rep., 2014. 15, 23, 24, 25, 113, 172, 176, 177, 178, 187

[46] German Association of the Energy and Water Industry (BDEW), "Technische Richtlinie Erzeugungsanlagen am Mittelspannungsnetz," 2008. 16

[47] Association for Electrical; Electronic & Information Technology (VDE), "VDE-AR-N 4105 Erzeugungsanlagen am Niederspannungsnetz – Technische Mindestanforderungen für Anschluss und Parallelbetrieb von Erzeugungsanlagen am Niederspannungsnetz," p. 80, 2011. 16, 176

[48] ENTSO-E, "Requirements for Grid Connection Applicable to all Generators," 2013. 16

[49] European Committee for Electrotechnical Standardization (CENELEC), "Requirements for generating plants to be connected in parallel with distribution networks - Part 1: Connection to a LV distribution network above 16 A," 2015. 16

[50] CENELEC, "Requirements for generating plants to be connected in parallel with distribution networks - Part 2: Connection to a MV distribution network," p. 5, 2015. 16

[51] Forum Network Technology / Network Operation in the VDE (FNN), "Anschluss und Betrieb von Speichern am Niederspannungsnetz," 2014. 16

[52] Deutsche Energie-Agentur GmbH (dena), "dena-Studie Systemdienstleistungen 2030. Sicherheit und Zuverlässigkeit einer Stromversorgung mit hohem Anteil erneuerbarer Energien ." Berlin, Tech. Rep., 2014. 16, 70, 73

[53] Agora Energiewende, "Stromverteilnetze für die Energiewende," Berlin, Tech. Rep., 2014. 16

[54] EURELECTRIC, "Ancillary Services Unbundling Electricity Products – an Emerging Market," p. 84, 2004. 16

[55] M. Braun, "Provision of Ancillary Services by Distributed Generators. PhD thesis." PhD Thesis, Kassel University, 2008. 17

[56] "Federal Network Agency (BNetzA)," http://www.bundesnetzagentur.de, accessed 2017-09-30. 17

[57] J. Schlabbach and K.-H. Rofalski, *Power System Engineering*. Weinheim, Germany: Wiley-VCH Verlag GmbH & Co. KGaA, jun 2008. 17

[58] Hermann Nagel. Hrsg. Rolf R. Cichowski, *Systematische Netzplanung*, 2nd ed. Berlin : VDE-Verl.; Frankfurt, M. : VWEW-Energieverl., 2008. 17, 18, 20

[59] H . Lee Willis, *Power Distribution Planning Reference Book*, 2nd ed. CRC Press, 2004. 17, 18

[60] T. Gonen, *Electric Power Distribution Engineering*, 3rd ed. CRC Press, 2014. 17, 18

[61] Lakervi and Holmes, *Electricity Distribution Network Design*, 2nd ed. Institution of Engineering and Technology, jan 2003. 17

[62] L. Jendernalik, C. Mensmann, and H. Wohlfarth, "Target planning of electrical distribution grids as a fundamental module for a successful asset management," in *IET Conf. Publ.* IET, 2009, pp. 381–381. 17

[63] L. Bochanky, *Planung öffentlicher Elektroenergieverteilungsnetze: Gestaltung, Bemessung, Betriebsweise, Netzrückwirkungen*, 1st ed. Dt. Verl. d. Grundstoffindustrie, 1985. 17

[64] F. Pilo, S. Jupe, F. Silvestro, K. E. Bakari, and C. Abbey, "Planning and Optimization Methods for Active Distribution Systems," CIGRE, Tech. Rep. August, 2014. 17, 18, 19, 20, 172

[65] ETG-Task Force Aktive EnergieNetze, "Aktive Energienetze im Kontext der Energiewende: Anforderungen an künftige Übertragungs- und Verteilungsnetze unter Berücksichtigung von Marktmechanismen," Energietechnische Gesellschaft im VDE (ETG) (ed.), Tech. Rep., 2013. 17, 20

[66] W. Kaufmann, *Planung öffentlicher Elektrizitätsverteilungs-Systeme.* VDE-Verlag, 1995. 18

[67] Deutsche Gesellschaft für Sonnenenergie e.V., "EEG Anlagenregister," http://www.energymap.info, accessed: 2015-05-20. 18, 37

[68] S. Nykamp, "Integrating Renewables in Distribution Grids: Storage, regulation and the interaction of different stakeholders in future grids," PhD thesis, University of Twente, 2013. 19, 20, 51

[69] G. Wirth, "Modellierung der Netzeinflüsse von Photovoltaikanlagen unter Verwendung meteorologischer Parameter," PhD thesis, Carl von Ossietzky Universität Oldenburg, 2014. 19, 20, 39, 51

[70] R. Pardatscher, R. Witzmann, G. Wirth, G. Becker, M. Garhamer, and J. Brandtl, "Research on the impact of photovoltaic power generation in low and medium voltage grids," in *Int. ETG-Kongress 2011*, Würzburg, 2011. 19, 20

[71] M. Resch, J. Bühler, H. Huyskens, and A. Sumper, "Optimale Positionierung von Großbatterien in Verteilnetzen," in *30. Symp. Photovoltaische Solarenergie.* OTTI e.V., 2015, p. 37. 19, 20, 37

[72] J. Büchner, O. Flörcken, S. Dierkes, L. Verheggen, and M. Uslar, "Moderne Verteilernetze für Deutschland," BMWi, Tech. Rep. 44, 2014. 20

[73] Agora Energiewende, "Stromspeicher in der Energiewende," Agora Energiewende, Berlin, Tech. Rep., 2014. 20

[74] V. Liebenau, J. Schwippe, S. Kuch, and C. Rehtanz, "Network extension planning considering the uncertainty of feed-in from renewable energies," *2013 IEEE Grenoble Conf.*, 2013. 20

[75] T. Schmidtner, "Probabilistische Methoden in der Netzplanung "Niederspannung"," in *VDE-Kongress 2012 - Intelligente Energieversorgung der Zukunft.* VDE-Verlag, 2012. 20

[76] V. Neimane, "On development planning of electricity distribution networks," Phd thesis, KTH, 2001. 20, 30

[77] J. Kays, "Agent-based Simulation Environment for Improving the Planning of Distribution Grids," PhD thesis, Technischen Universität Dortmund, 2014. 20

[78] T. Stetz, K. Diwold, M. Kraiczy, D. Geibel, S. Schmidt, and M. Braun, "Techno-economic assessment of voltage control strategies in low voltage grids," *IEEE Trans. Smart Grid*, vol. 5, no. 4, pp. 2125–2132, 2014. 23, 25, 174, 175, 177

[79] B. Idlbi, K. Diwold, T. Stetz, H. Wang, and M. Braun, "Cost-benefit analysis of central and local voltage control provided by distributed generators in MV networks," in *2013 IEEE Grenoble Conf.* IEEE, jun 2013. 23, 24, 28, 30, 31

[80] B. Idlbi, A. Scheidler, T. Stetz, and M. Braun, "Preemptive network reinforcement at LV level considering uncertainty in prediction of PV penetration scenarios," in *2015 IEEE Eindhoven PowerTech.* IEEE, jun 2015. 23, 24, 25

[81] A. Keane, L. F. Ochoa, C. L. T. Borges, G. W. Ault, A. D. Alarcon-Rodriguez, R. a. F. Currie, F. Pilo, C. Dent, and G. P. Harrison, "State-of-the-Art Techniques and Challenges Ahead for Distributed Generation Planning and Optimization," *IEEE Trans. Power Syst.*, vol. 28, no. 2, pp. 1493–1502, may 2013. 26

[82] S. Ganguly, N. C. Sahoo, and D. Das, "Recent advances on power distribution system planning: A state-of-the-art survey," *Energy Syst.*, vol. 4, no. 2, pp. 165–193, 2013. 26, 27, 29, 30

[83] P. S. Georgilakis and N. D. Hatziargyriou, "A review of power distribution planning in the modern power systems era: Models, methods and future research," *Electr. Power Syst. Res.*, vol. 121, pp. 89–100, apr 2015. 26

[84] A. Rezaee Jordehi, "Optimisation of electric distribution systems: A review," *Renew. Sustain. Energy Rev.*, vol. 51, pp. 1088–1100, 2015. 26

[85] A. Alarcon-Rodriguez, G. Ault, and S. Galloway, "Multi-objective planning of distributed energy resources: A review of the state-of-the-art," *Renew. Sustain. Energy Rev.*, vol. 14, no. 5, pp. 1353–1366, 2010. 26

[86] R. Viral and D. Khatod, "Optimal planning of distributed generation systems in distribution system: A review," *Renew. Sustain. Energy Rev.*, vol. 16, no. 7, pp. 5146–5165, 2012. 26

[87] S. Koopmann, M. Scheufen, and A. Schnettler, "Integration of stationary and transportable storage systems into multi-stage expansion planning of active distribution grids," in *IEEE PES ISGT Eur. 2013.* IEEE, oct 2013. 27, 28, 30, 31, 92, 139, 140, 172

[88] S. Wong, K. Bhattacharya, and J. Fuller, "Electric power distribution system design and planning in a deregulated environment," *IET Gener. Transm. Distrib.*, vol. 3, no. 12, p. 1061, 2009. 27, 30, 31

[89] W. El-Khattam, Y. Hegazy, and M. Salama, "An Integrated Distributed Generation Optimization Model for Distribution System Planning," *IEEE Trans. Power Syst.*, vol. 20, no. 2, pp. 1158–1165, may 2005. 27, 28, 30, 31

[90] K. Zou, A. P. Agalgaonkar, K. M. Muttaqi, and S. Perera, "Distribution system planning with incorporating DG reactive capability and system uncertainties," *IEEE Trans. Sustain. Energy*, vol. 3, no. 1, pp. 112–123, 2012. 27, 28, 30, 31

[91] S. Haffner, L. Pereira, L. Pereira, and L. Barreto, "Multistage Model for Distribution Expansion Planning with Distributed Generation - Part II: Numerical Results," *IEEE Trans. Power Deliv.*, vol. 23, no. 2, pp. 924–929, apr 2008. 28, 30, 31

[92] S. Haffner, L. L. Pereira, L. L. Pereira, and L. Barreto, "Multistage Model for Distribution Expansion Planning With Distributed Generation -Part I: Problem Formulation," *IEEE Trans. Power Deliv.*, vol. 23, no. 2, pp. 915–923, apr 2008. 28, 30, 31

[93] E. Naderi, H. Seifi, and M. S. Sepasian, "A Dynamic Approach for Distribution System Planning Considering Distributed Generation," *IEEE Trans. Power Deliv.*, vol. 27, no. 3, pp. 1313–1322, jul 2012. 28, 30, 31

[94] C. L. T. Borges and V. F. Martins, "Multistage expansion planning for active distribution networks under demand and Distributed Generation uncertainties," *Int. J. Electr. Power Energy Syst.*, vol. 36, no. 1, pp. 107–116, 2012. 28, 30, 31

[95] A. Bagheri, H. Monsef, and H. Lesani, "Integrated distribution network expansion planning incorporating distributed generation considering uncertainties, reliability, and operational conditions," *Int. J. Electr. Power Energy Syst.*, vol. 73, pp. 56–70, dec 2015. 28, 30, 31

[96] H. Falaghi, C. Singh, M.-R. Haghifam, and M. Ramezani, "DG integrated multistage distribution system expansion planning," *Int. J. Electr. Power Energy Syst.*, vol. 33, no. 8, pp. 1489–1497, 2011. 28, 30, 31

[97] V. F. Martins and C. L. T. Borges, "Active Distribution Network Integrated Planning Incorporating Distributed Generation and Load Response Uncertainties," *IEEE Trans. Power Syst.*, vol. 26, no. 4, pp. 2164–2172, nov 2011. 28, 30, 31

[98] M. Sedghi, M. Aliakbar-Golkar, and M.-R. Haghifam, "Distribution network expansion considering distributed generation and storage units using modified PSO algorithm," *Int. J. Electr. Power Energy Syst.*, vol. 52, no. 0, pp. 221–230, nov 2013. 28, 30, 31

[99] H. Chen, Z. Wang, H. Yan, H. Zou, and B. Luo, "Integrated Planning of Distribution Systems with Distributed Generation and Demand Side Response," *Energy Procedia*, vol. 75, no. 51322702, pp. 981–986, aug 2015. 28, 30, 31

[100] H. Saboori, R. Hemmati, and V. Abbasi, "Multistage distribution network expansion planning considering the emerging energy storage sys-

tems," *Energy Convers. Manag.*, vol. 105, pp. 938–945, 2015. 28, 30, 31

[101] E. Kaempf and M. Braun, "Expert Systems as Support to Strategic Network Planning," Fraunhofer IWES Kassel, Tech. Rep., 2015. 29, 30, 31

[102] S. Khator and L. Leung, "Power distribution planning: a review of models and issues," in *IEEE Trans. Power Syst.*, vol. 12, no. 3, 1997, pp. 1151–1159. 29

[103] T. Gorien, "Distribution-system planning using mixed-integer programming," vol. 128, no. 2, pp. 70–79, 1981. 29

[104] S. Abapour, K. Zare, and B. Mohammadi-ivatloo, "Dynamic planning of distributed generation units in active distribution network," vol. 9, pp. 1455–1463, 2015. 29, 30, 31

[105] J. Partanen, "A modified dynamic programming algorithm for sizing, locating and timing of feeder reinforcements," *IEEE Trans. Power Deliv.*, vol. 5, no. 1, pp. 277–283, 1990. 30

[106] A. Barin, L. F. Pozzatti, L. N. Canha, R. Q. Machado, A. R. Abaide, and G. Arend, "Multi-objective analysis of impacts of distributed generation placement on the operational characteristics of networks for distribution system planning," *Int. J. Electr. Power Energy Syst.*, vol. 32, no. 10, pp. 1157–1164, 2010. 30, 31

[107] V. Vahidinasab, "Optimal distributed energy resources planning in a competitive electricity market: Multiobjective optimization and probabilistic design," *Renew. Energy*, vol. 66, pp. 354–363, jun 2014. 30, 31

[108] K. Engels and H.-J. Haubrich, "Probabilistic evaluation of voltage stability in MV networks," in *2000 Power Eng. Soc. Summer Meet. (Cat. No.00CH37134)*, vol. 4. IEEE, 2000, pp. 2075–2080. 30, 31

[109] S. Koopmann, S. Nicolai, and A. Schnettler, "Multifunctional operation of a virtual power plant in an active distribution grid: Modelling approaches and first field test experiences from the SmartRegion Pellworm project," in *IEEE PES Innov. Smart Grid Technol. Eur.* IEEE, oct 2014. 31, 32, 92, 139, 140

[110] P. Hallberg, J. Rios-Alba, P. Birkner, F. Hankan, and A. Kroll, "Decentralised Storage: Impact on Future Distribution Grids," Union of the Electricity Industry (EURELECTRIC), Tech. Rep. june, 2012. 31, 32

[111] A. Z. Weber, M. M. Mench, J. P. Meyers, P. N. Ross, J. T. Gostick, and Q. Liu, "Redox flow batteries: a review," *J. Appl. Electrochem.*, vol. 41, no. 10, pp. 1137–1164, sep 2011. 36

[112] P. Alotto, M. Guarnieri, and F. Moro, "Redox flow batteries for the storage of renewable energy: A review," *Renew. Sustain. Energy Rev.*, vol. 29, pp. 325–335, jan 2014. 36, 100

[113] F. Díaz-González, A. Sumper, O. Gomis-Bellmunt, and R. Villafáfila-Robles, "A review of energy storage technologies for wind power applications," *Renew. Sustain. Energy Rev.*, vol. 16, no. 4, pp. 2154–2171, may 2012. 36

[114] S. Eckroad, "Vanadium Redox-Flow Batteries," EPRI, EPRI. Palo Alto, Tech. Rep. 3, 2007. 36

[115] C. Ponce de León, A. Frías-Ferrer, J. González-García, D. A. Szánto, and F. C. Walsh, "Redox flow cells for energy conversion," *J. Power Sources*, vol. 160, no. 1, pp. 716–732, sep 2006. 36

[116] G. Fuchs, B. Lunz, M. Leuthold, and D. U. Sauer, "Technology Overview on Electricity Storage," Institute for Power Electronics and Electrical Drives (ISEA), RWTH Aachen University, Aachen, Tech. Rep., 2012. 36

[117] German Energy Agency (dena), "DENA Grid Study II: Integration of Renewable Energy Sources in the German Power Supply Systems from 2015-2020 with an Outlook to 2025," Berlin, Tech. Rep., 2010. 37

[118] J. Scheffler, "Bestimmung der maximal zulässigen Netzanschlussleistung photovoltaischer Energiewandlungsanlagen in Wohnsiedlungsgebieten," PhD thesis, TU Dresden, 2002. 39

[119] V. Quaschning, "Systemtechnik einer klimaverträglichen Elektrizitätsversorgung in Deutschland für das 21. Jahrhundert," habilitation thesis, TU Berlin, 2000. 39

[120] C. Fünfgeld and R. Tiedemann, "Anwendung der Repräsentativen VDEW-Lastprofile step by step," *VDEW Mater.*, vol. M-05/2000, 2000. 50, 140, 145, xix, xx

[121] T. Tjaden, B. Joseph, and V. Quaschning, "Repräsentative elektrische Lastprofile für Wohngebäude in Deutschland auf 1-sekündiger Datenbasis," 2015. 50, 145, xxi, xxii

[122] European Power Exchange (EPEX). (2016) Produkte: Intraday Auktion. https://www.epexspot.com/de/produkte/intradayauction/deutschland, accessed 2016-09-30. 51, 110, xix

[123] A. Gonzalez Quintairos, J. Bühler, B. Kleinschmitt, and M. Resch, "Analysis of Potential Distribution and Size of Photovoltaic Systems on Rural Rooftops," *GI_ Forum*, vol. 1, pp. 220–224, 2015. 53, 54

[124] Bayerisches Staatsministerium für Wirtschaft und Medien, Energie und Technologie, "Energieatlas Bayern," https://www.energieatlas.bayern.de/, accessed 2018-07-30. 54

[125] R. W. Andrews, J. S. Stein, C. Hansen, and D. Riley, "Introduction to the open source PV LIB for python Photovoltaic system modelling package," in *Photovolt. Spec. Conf. (PVSC), 2014 IEEE 40th*, 2014, pp. 170–174. 55

[126] Helmholtz-Zentrum Geesthacht, "coastDat2," http://www.coastdat.de/, accessed 2018-07-30. 55

[127] Bayerisches Staatsministerium für Wirtschaft und Medien, Energie und Technologie, "Bayerisches Energieprogramm: für eine sichere, bezahlbare und umweltverträgliche Energieversorgung," Tech. Rep., 2016. 56

[128] G. Corey and J. Eyer, "Energy Storage for the Electricity Grid : Benefits and Market Potential Assessment Guide A Study for the DOE Energy Storage Systems Program," Sandia National Laboratories, New Mexico, Tech. Rep. February, 2010. 62

[129] P. T. Moseley and J. Garche, *Electrochemical Eenrgy Storage for Renewable Sources and Grid Balancing*, 2015. 62, 64, 65, 74, 80

[130] B. Battke, "Multi-purpose technologies, lock-in and efficiency - Policy implications from the case of stationary electricity storage," PhD thesis, ETH Zürich, 2014. 62

[131] H.-P. Beck, B. Engel, L. Hofmann, R. Menges, T. Turek, and H. Weyer, "Eignung von Speichertechnologien zum Erhalt der Systemsicherheit," Energie-Forschungszentrum Niedersachsen, Gosslar, Tech. Rep., 2013. 62, 63

[132] G. Fuchs, B. Lunz, M. Leuthold, and D. Sauer, "Technology Overview on Electricity Storage," Tech. Rep. June, 2012. 62, 64

[133] F. Genoese, "Modellgestützte Bedarfs- und Wirtschaftlichkeitsanalyse von Energiespeichern zur Integration erneuerbarer Energien in Deutschland," PhD Thesis, Karlsruhe, 2013. 62, 108

[134] H. Ibrahim, R. Beguenane, and A. Merabet, "Technical and financial benefits of electrical energy storage," in *Electr. Power Energy Conf. EPEC 2012*, 2012, pp. 86–91. 62

[135] Consentec GmbH, "Description of load-frequency control concept and market for control reserves," Tech. Rep., 2014. 62

[136] R. Sioshansi, P. Denholm, and T. Jenkin, "Market and Policy Barriers to Deployment of Energy Storage," *Econ. Energy Environ. Policy*, vol. 1, no. 2, pp. 47–64, 2012. 62

[137] M. Sterner and I. Stadler, *Energiespeicher - Bedarf, Technologien, Integration.* Berlin, Heidelberg: Springer Berlin Heidelberg, 2014. 63, 70, 109

[138] A. A. Akhil, G. Huff, A. B. Currier, B. C. Kaun, D. M. Rastler, S. B. Chen, D. T. Bradshaw, and W. D. Gauntlett, "Electricity storage handbook," Tech. Rep. July, 2013. 63, 108, 109

[139] S. Spiecker, P. Vogel, and C. Weber, "Ökonomische Bewertung von Netzengpässen und Netzinvestitionen," *uwf*, vol. 17, pp. 321–331, 2009. 63

[140] Frontier Economics and Consentec GmbH, "Relevance of established national bidding areas for European power market integration - an approach to welfare oriented evaluation," Tech. Rep. October, 2011. 63, 64

[141] L. Hirth and I. Ziegenhagen, "Balancing power and variable renewables: Three links," *Renew. Sustain. Energy Rev.*, vol. 50, pp. 1035–1051, oct 2015. 64, 73

[142] C. K. Narula, R. Martinez, O. Onar, M. R. Starke, and G. Andrews, "Economic Analysis of Deploying Used Batteries in Power Systems," Oak ridge national laboratory, Tech. Rep., 2011. 64

[143] Zentralverband Elektrotechnik und Elektronikindustrie e. V. (ZVEI), "Energieeinsparung durch Blindleistungskompensation," Tech. Rep., 2012. 64, 67

[144] B. Battke, T. S. Schmidt, D. Grosspietsch, and V. H. Hoffmann, "A review and probabilistic model of lifecycle costs of stationary batteries in multiple applications," *Renew. Sustain. Energy Rev.*, vol. 25, pp. 240–250, 2013. 65

[145] S. Aschenbrenner, "Untersuchung verschiedener Geschäftsmodelle für den Einsatz eines Batteriespeichers im Niederspannungsnetz - Theoretische Betrachtungen und Bestimmung von Kenngrößen," Masterthesis, Hochschule Regensburg, 2013. 65

[146] M. Klausen, "Market Opportunities and Regulartory Framework Conditions for Stationary Battery Storage Systems in Germany," *Energy Procedia*, vol. 135, pp. 272–282, oct 2017. 65

[147] A. Malhotra, B. Battke, M. Beuse, A. Stephan, and T. Schmidt, "Use cases for stationary battery technologies: A review of the literature and existing projects," *Renew. Sustain. Energy Rev.*, vol. 56, pp. 705–721, apr 2016. 66, 126

[148] Deparment of Energy (DOE), "Global Energy Storage Database," http://www.energystorageexchange.org, accessed 2018-07-30. 66, 72

[149] EPEX-SPOT, "EPEX-SPOT-Data for 2013," 2014, http://www.epexspot.com, accessed 2015-09-30. 67, 82

[150] Regeleistung.net, "Ausschreibungsübersicht 2013," 2013, https://www.regelleistung.net, accessed 2016-09-30. 67

[151] Amprion, "Netznutzungsvertrag 2013," 2013, http://www.amprion.net, accessed 2017-09-30. 67

[152] 50 Hertz, "Preisblatt 2014," 2014, http://www.50hertz.com, accessed 2016-05-25. 67

[153] Tennet, "Netznutzungsvertrag 2012," 2012, http://www.tennet.eu/, accessed 2016-09-30. 67

[154] H. Rubel and C. Pieper, "Revisiting Energy Storage," Boston Consulting Group, Frankfurt, Tech. Rep., 2011. 67

[155] D. Böttger and T. Bruckner, "Marktszenarien für eine erfolgreiche und nachhaltige Energiewende 11." in *Energieversorgungssysteme der Zukunft*, Leipzig, 2014, p. 38. 67

[156] USV System, "Different UPS-systems," 2015, http://www.online-usv.de/de/produkte/intro.php, accessed 2015-05-20. 67

[157] E.ON, "E.ON Grundversorgung Strom (Doppeltarif)," 2014, https://www.eon.de accessed 2014-09-30. 67

[158] EnBW, "Intelligente Stromzähler," 2014, http://www.enbw.com/, accessed 2014-09-30. 67

[159] RWE, "RWE EDL21 Meter Strom," 2014, http://www.rwe.de/, accessed 2014-09-29. 67

[160] Vattenfall, "Easy Spar Aktiv," 2014, http://www.vattenfall.de/, accessed 2014-09-30. 67

[161] Amprion, "Entgelte," 2014, http://www.amprion.net/, accessed 2017-09-30. 67

[162] Tennet, "Netzentgelte," 2014, http://www.tennet.eu/, accessed 2014-09-30. 67

[163] TransnetBW, "Entgelte Netznutzung," 2014, https://www.transnetbw.de/, accessed 2016-03-31. 67

[164] C. Kost, J. N. Mayer, J. Thomsen, N. Hartmann, C. Senkpiel, S. Philipps, S. Nold, S. Lude, and T. Schlegl, "Studie Stromgestehungskosten Erneuerbare Energien," Fraunhofer-Institut für solare Energiesysteme ISE, Tech. Rep. November, 2013. 67, 89

[165] German Association of the Energy and Water Industry (BDEW), "Strompreisanalyse," Berlin, Tech. Rep., 2014. 67

[166] BDEW, "Industriestrompreise," Berlin, Tech. Rep. April, 2014. 67, 89

[167] S. Roon, M. Sutter, F. Samweber, and K. Wachunger, "Netzausbau in Deutschland," Konrad-Adenauer-Striftung e.V., Tech. Rep., 2014. 67

[168] U. Leprich, "Netze, Speicher, Lastmanagement," in *BUND-Tagung "Welches Stromnetz braucht die Energiewende?"*, Stuttgart, 2014. 67

[169] European Network of Transmission System Operators (ENTSO-E, "Appendix 1 - Load-Frequency Control and Performance," Tech. Rep., 2009. 68, 77

[170] UCTE, "Operation Handbook," UCTE, Tech. Rep., 2004. 68

[171] F. Díaz-González, M. Hau, A. Sumper, and O. Gomis-Bellmunt, "Participation of wind power plants in system frequency control: Review of grid code requirements and control methods," *Renew. Sustain. Energy Rev.*, vol. 34, pp. 551–564, 2014. 68

[172] M. Koller, T. Borsche, A. Ulbig, and G. Andersson, "Review of grid applications with the Zurich 1MW battery energy storage system," *Electr. Power Syst. Res.*, vol. 120, pp. 128–135, 2015. 70, 74, 171

[173] C. Pape, N. Gerhardt, P. Härtel, A. Scholz, R. Schwinn, T. Drees, A. Maaz, J. Sprey, C. Breuer, and A. Moser, "Roadmap Speicher: Speicherbedarf für Erneuerbare Energien - Speicheralternativen - Speicheranreiz - Überwindung rechtlicher Hemmnisse (Kurzzusammenfassung)," IWES, IAEW, Stiftung Umweltenergierecht, Tech. Rep., 2014. 70, 73

[174] T. Thien, H. Axelsen, M. Merten, H. Axelsen, S. Zurmùhlen, and M. Leuthold, "Planning of Grid-Scale Battery Energy Storage Systems: Lessons Learned from a 5 MW Hybrid Battery Storage Project in Germany," in *Battcon - Int. Station. Batter. Conf. 2015*, 2015, p. 10. 70, 74

[175] T. Aundrup, H.-P. Beck, A. Becker, and A. Berthold, "Batteriespeicher in der Nieder- und Mittelspannungsebene - Anwendungen und Wirtschaftlichkeit sowie Auswirkungen auf die elektrischen Netze," Energietechnischen Gesellschaft im VDE (ETG), Tech. Rep., 2015. 70, 74

[176] J. Bühler, M. Resch, J. Wiemann, and J. Twele, "Lebenszyklusanalyse von Großbatterien am deutschen Regelenergiemarkt," in *9. Int. Energiewirtschaftstagung*, 2015, p. 44. 70

[177] A. Gitis, T. Thien, M. Leuthold, P. Dirk, and U. Sauer, "Optimization of Battery Energy Storage Systems for Primary Control Reserve," in

8th Int. Renew. Energy Storage Conf. Exhib. (IRES 2013) 2013, 2013, p. 8. 70

[178] T. Sasaki, T. Kadoya, and K. Enomoto, "Study on Load Frequency Control Using Redox Flow Batteries," *IEEE Trans. Power Syst.*, vol. 19, no. 1, pp. 660–667, 2004. 70, 71, 171

[179] "Größter kommerzieller Batteriespeicher Europas in Schwerin am Netz," sep 2014, http://www.zeit.de/news/2014-09/16, accessed 2014-09-16. 72

[180] D. U. Sauer, B. Lunz, and D. Magnor, "Marktanreizprogramm für dezentrale Speicher insbesondere für PV-Strom," Tech. Rep., 2013. 73

[181] H. Kondziella, K. Brod, T. Bruckner, S. Olbert, and F. Mes, "Stromspeicher für die "Energiewende" - eine akteursbasierte Analyse der zusätzlichen Speicherkosten," *Zeitschrift für Energiewirtschaft*, vol. 37, pp. 249–260, 2013. 73

[182] International Renewable Energy Agency (IRENA), "Battery Storage for Renewables : Market Status and Technology Outlook," IRENA, Tech. Rep. January, 2015. 73, 88, 166

[183] W. Gawlik, "Speicher für die Energiewende," *e i Elektrotechnik und Informationstechnik*, vol. 130, no. 8, pp. 250–250, dec 2013. 73

[184] J. Auer, J. Keil, and A. Stobbe, "Moderne Stromspeicher," DB Research, Frankfurt am Main, Tech. Rep., 2012. 73

[185] A. Moser, M. Zdrallek, H. Krause, and F. Graf, "Nutzen von Smart-Grid-Konzepten unter Berücksichtigung der Power-to-Gas-Technologie," DVGW Deutscher Verein des Gas- und Wasserfaches e.V., Tech. Rep., 2014. 73

[186] German TSO, "Anforderungen an die Speicherkapazität bei Batterien für die Primärregelleistung," p. 9, 2015. 73

[187] VDN, "Transmission Code 2003 - Unterlagen zur Präqualifikation für die Erbringung von Primärregelleistung für die ÜNB," Tech. Rep., 2003. 74

[188] M. Otte, J. Patt, and J. Lück, "Beschluss BK6-10-097," Bundesnetzagentur, Tech. Rep., 2011. 74

[189] German TSO, "Eckpunkte und Freiheitsgrade bei Erbringung von Primärregelleistung - Leitfaden für Anbieter von Primärregelleistung," p. 9, 2014. 74, 75, 78, 98

[190] Deutsche Übertragungsnetzbetreiber, "Anforderungen an die Speicherkapazität bei Batterien für die Primärregelleistung," 50hertz, Amprion, Tennet, TransnetBW, Tech. Rep., 2015. 78, 79, 105, 108, 115, ix

[191] ENTSO-E, "Implementation Guideline - Requirements for Grid Connection Applicable to all Generators," 2013. 78

[192] European Commission, "Draft regulation establishing a guideline on electricity transmission system operation - Provision final version," 2016. 79

[193] M. Klausen, M. Resch, and J. Bühler, "Analysis of potential single and combined business models for stationary battery storage systems," in *10th Int. Renew. Energy Storage Conf. Exhib. (IRES 2016)*, 2016, p. 10. 80, 81

[194] Deutsche Übertragungsnetzbetreiber (ÜNB), "regelleistung.net," https://www.regelleistung.net, accessed 2016-09-30. 82, 106

[195] C. Sterzing, "Wirtschaftlichkeitsanalyse großer stationäer Batteriespeicher im Load-Levelling-Betrieb," 2014. 85

[196] A. Toffler, *The Third Wave*, 1980. 87

[197] S. Grijalva and M. U. Tariq, "Prosumer-based smart grid architecture enables a flat, sustainable electricity industry," in *ISGT 2011*. IEEE, jan 2011, pp. 1–6. 87

[198] J. Moshövel, K.-P. Kairies, D. Magnor, M. Leuthold, M. Bost, S. Gährs, E. Szczechowicz, M. Cramer, and D. U. Sauer, "Analysis of the maximal possible grid relief from PV-peak-power impacts by using storage systems for increased self-consumption," *Appl. Energy*, vol. 137, pp. 567–575, 2015. 87, 136, 137, 139, 162

[199] W. Short and D. J. Packey, "A Manual for the Economic Evaluation of Energy Efficiency and Renewable Energy Technologies," Tech. Rep. March, 1995. 87

[200] F. Ueckerdt, L. Hirth, G. Luderer, and O. Edenhofer, "System LCOE: What are the costs of variable renewables?" *Energy*, vol. 63, pp. 61–75, dec 2013. 87

[201] J. Ondraczek, N. Komendantova, and A. Patt, "WACC the dog: The effect of financing costs on the levelized cost of solar PV power," *Renew. Energy*, vol. 75, pp. 888–898, mar 2015. 87

[202] K. Branker, M. Pathak, and J. Pearce, "A review of solar photovoltaic levelized cost of electricity," *Renew. Sustain. Energy Rev.*, vol. 15, no. 9, pp. 4470–4482, dec 2011. 87

[203] I. Pawel, "The Cost of Storage – How to Calculate the Levelized Cost of Stored Energy (LCOE) and Applications to Renewable Energy Generation," *Energy Procedia*, vol. 46, pp. 68–77, 2014. 87, 123

[204] C. Breyer and A. Gerlach, "Global overview on grid-parity," *Prog. Photovoltaics Res. Appl.*, vol. 21, no. 1, pp. 121–136, jan 2013. 87

[205] Eero Vartiainen, G. Masson, and C. Breyer, "PV LCOE in Europe 2014-30," European PV Technology Platform Steering Commitee, Tech. Rep. July, 2015. 88

[206] T. Horiba, "Lithium-Ion Battery Systems," *Proc. IEEE*, vol. 102, no. 6, pp. 939–950, jun 2014. 88

[207] B. Nykvist and M. Nilsson, "Rapidly falling costs of battery packs for electric vehicles," *Nat. Clim. Chang.*, vol. 5, no. 4, pp. 329–332, mar 2015. 88, 109

[208] B. Moreno, A. J. López, and M. T. García-Álvarez, "The electricity prices in the European Union. The role of renewable energies and regulatory electric market reforms," *Energy*, vol. 48, no. 1, pp. 307–313, dec 2012. 88

[209] R. Weron, "Electricity price forecasting: A review of the state-of-the-art with a look into the future," *Int. J. Forecast.*, vol. 30, no. 4, pp. 1030–1081, oct 2014. 88

[210] Ewi, Gws, and Prognos, "Entwicklung der Energiemärkte - Energiereferenzprognose," Ewi, Gws, Prognos, Basel/Köln/Osnabrück, Tech. Rep., 2014. 88

[211] D. L. Talavera, J. De La Casa, E. Muñoz-Cerón, and G. Almonacid, "Grid parity and self-consumption with photovoltaic systems under the present regulatory framework in Spain: The case of the University of Jaén Campus," *Renew. Sustain. Energy Rev.*, vol. 33, pp. 752–771, 2014. 88

[212] D. Chiaroni, V. Chiesa, L. Colasanti, F. Cucchiella, and F. Frattini, "Evaluating solar energy profitability: A focus on the role of self-consumption," *Energy Convers. Manag.*, vol. 88, pp. 317–331, 2014. 88

[213] R. Luthander, J. Widén, D. Nilsson, and J. Palm, "Photovoltaic self-consumption in buildings : A review," *Appl. Energy*, vol. 142, pp. 80–94, 2015. 89

[214] J. Hoppmann, J. Volland, T. S. Schmidt, and V. H. Hoffmann, "The economic viability of battery storage for residential solar photovoltaic systems - A review and a simulation model," *Renew. Sustain. Energy Rev.*, vol. 39, pp. 1101–1118, 2014. 89, 141, 179

[215] K.-P. Kairies, D. Haberschusz, D. Magnor, M. Leuthold, and D. U. Sauer, "Wissenschaftliches Mess- und Evaluierungsprogramm Solarstromspeicher - Jahresbericht 2015," Institut für Stromrichtertechnik und Elektrische Antriebe RWTH Aachen, Tech. Rep., 2015. 89, 139

[216] P. Kästel and B. Gilroy-Scott, "Economics of pooling small local electricity prosumers -LCOE & self-consumption," *Renew. Sustain. Energy Rev.*, vol. 51, pp. 718–729, nov 2015. 89

[217] R. Arghandeh, J. Woyak, A. Onen, J. Jung, and R. P. Broadwater, "Economic Optimal Operation of Community Energy Storage Systems in Competitive Energy Markets," *Appl. Energy*, vol. 135, pp. 1–17, 2014. 89

[218] A. Nourai, R. Sastry, and T. Walker, "A vision & strategy for deployment of energy storage in electric utilities," in *IEEE PES Gen. Meet.* IEEE, jul 2010. 89

[219] E. Gaudchau, M. Resch, and A. Zeh, "Quartierspeicher: Definition, rechtlicher Rahmen und Perspektiven," *Ökologisches Wirtschaften - Fachzeitschrift*, vol. 31, no. 2, may 2016. 89

[220] D. Parra, M. Gillott, S. A. Norman, and G. S. Walker, "Optimum community energy storage system for PV energy time-shift," *Appl. Energy*, vol. 137, pp. 576–587, jan 2015. 89

[221] A. Zeh, M. Rau, and R. Witzmann, "Comparison of decentralised and centralised grid-compatible battery storage systems in distribution grids with high PV penetration," in *Prog. Photovoltaics Res. Appl.*, dec 2014, p. 11. 89, 92, 139, 162, 165, 183

[222] V. Jülch, J. Thomsen, N. Hatmann, T. Junne, U. Lea, and M. Arnold, "Betreibermodelle für Stromspeicher," Fraunhofer ISE, IER Stuttgart, Compare Consulting, Tech. Rep. August, 2016. 90, 91, 165

[223] Federal Network Agency (BNetzA), "Leitfaden zur Eigenversorgung," Tech. Rep., 2016. 90

[224] F. Moehrke, F. Grueger, H. Triebke, O. Arnhold, and J. Myrzik, "Model-based quantification of a microgrid via key performance indicators," in *9th Int. Renew. Energy Storage Conf. (IRES 2015)*, no. March, 2015. 92, 133

[225] Y. Lachmann, O. Prahl, M. Knösel, J. Mühlbach, N. Nau, J. Papenheim, M. Kubach, M. Schellenberger, E. Sebastian, P. Schmidt, and E. Heller, "Strombank - Abschlussbericht," Tech. Rep., 2017. 92, 133

[226] R. Thomann, "Innovatives Betreibermodell für Quartierspeicher," in *Kongress Energie- und Energiespeichertechnologien*, no. November, Stuttgart, 2014, p. 17. 92

[227] M. Siller, "Stromspeicher zur Netzstabilisierung," in *Bayer. Energiekongress*, 2013, p. 25. 92, 135, 136

[228] A. Schnettler, J. Nilges, A. Stolte, S. Nykamp, T. Smolka, C. Matrose, and S. Willing, "Improving quality of supply and usage of assets in distribution grids by introducing a smart operator," in *22nd Int. Conf. Exhib. Electr. Distrib. (CIRED 2013)*, no. 0718, 2013, pp. 0718–0718. 92, 135, 136

[229] "Lechwerke Verteilnetze," http://www.lew-verteilnetz.de/, accessed 2018-07-30. 92

[230] P. Goergens, F. Potratz, C. Matrose, S. Schumann, A. Schnettler, S. Willing, and T. Smolka, "An online learning algorithm approach

for low voltage grid management," in *22nd Int. Conf. Exhib. Electr. Distrib. (CIRED 2013)*, vol. 5, 2013, pp. 0702–0702. 92, 136

[231] A. Jossen, H. Gasteiger, and M. Müller, "EEBatt - Dezentrale Stationäre Batteriespeicher zur effizienten Nutzung Erneuerbarer Energien und Unterstützung der Netzstabilität - Zwischenbericht 2015," Tech. Rep., 2015. 92

[232] A. Zeh and R. Witzmann, "Operational Strategies for Battery Storage Systems in Low-voltage Distribution Grids to Limit the Feed-in Power of Roof-mounted Solar Power Systems," *Energy Procedia*, vol. 46, pp. 114–123, 2014. 92, 137, 138, 139, 140

[233] I. Meyer, "Quartiersspeicher von IBC SOLAR als Baustein für die Energiewende in Bayern - press release," 2015, http://www.ibc-solar.de/uploads/media/150505-Epplas-IBC-ZAE.pdf, accessed 2017-09-30. 92

[234] P. Luchscheider, "Smart Grid Solar: A Bavarian Smart Energy Project," in *31st EU PVSEC*. Bayerisches Zentrum für angewandte Energieforschung, 2015. 92, 139, 140

[235] Q. Zheng, X. Li, Y. Cheng, G. Ning, F. Xing, and H. Zhang, "Development and perspective in vanadium flow battery modeling," *Appl. Energy*, vol. 132, pp. 254–266, 2014. 99

[236] A. Tang, J. Bao, and M. Skyllas-Kazacos, "Studies on pressure losses and flow rate optimization in vanadium redox flow battery," *J. Power Sources*, vol. 248, pp. 154–162, feb 2014. 99

[237] S. König, M. R. Suriyah, and T. Leibfried, "Innovative model-based flow rate optimization for vanadium redox flow batteries," *J. Power Sources*, vol. 333, pp. 134–144, 2016. 99

[238] B. Turker, S. Arroyo Klein, E.-M. Hammer, B. Lenz, and L. Komsiyska, "Modeling a vanadium redox flow battery system for large scale applications," *Energy Convers. Manag.*, vol. 66, pp. 26–32, feb 2013. 99

[239] G. Qiu, A. S. Joshi, C. R. Dennison, K. W. Knehr, E. C. Kumbur, and Y. Sun, "3-D pore-scale resolved model for coupled species/charge/fluid transport in a vanadium redox flow battery," *Electrochim. Acta*, vol. 64, pp. 46–64, 2012. 99

[240] D. Frenkel, "Understanding Molecular Simulation," in *Underst. Mol. Simul.* Elsevier, 2002. 99

[241] C. Betzin, H. Wolfschmidt, and M. Luther, "Electrical operation behavior and energy efficiency of battery systems in a virtual storage power plant for primary control reserve," *Int. J. Electr. Power Energy Syst.*, vol. 97, no. February 2017, pp. 138–145, apr 2018. 99

[242] A. Tang, J. Bao, and M. Skyllas-Kazacos, "Thermal modelling of battery configuration and self-discharge reactions in vanadium redox flow battery," *J. Power Sources*, vol. 216, pp. 489–501, 2012. 100

[243] A. Zeh, M. Müller, M. Naumann, H. Hesse, A. Jossen, and R. Witzmann, "Fundamentals of Using Battery Energy Storage Systems to Provide Primary Control Reserves in Germany," *Batteries*, vol. 2, no. 3, p. 29, sep 2016. 100, 106

[244] T. Rösinger, "SMA Solar Technology AG, personal communication (Email), 04 May, 2017," SMA Solar Technology AG. 102

[245] European Network of Transmission System Operators (ENTSO-E), "Guideline on Transmission System Operation (SO GL) - Draft," p. 149, 2016. 105

[246] J. Fleer and P. Stenzel, "Impact analysis of different operation strategies for battery energy storage systems providing primary control reserve," *J. Energy Storage*, 2016. 105, 106, 109, 125, xvii

[247] J. Fleer, S. Zurmühlen, J. Badeda, P. Stenzel, J.-F. Hake, and D. U. Sauer, "Model-based Economic Assessment of Stationary Battery Systems Providing Primary Control Reserve," *Energy Procedia*, vol. 99, pp. 11–24, nov 2016. 105, 106, 126, 127, 128

[248] D. J. Swider, "Handel an Regelenergie- und Spotmärkten - Methoden zur Entscheidungsunterstützung für Netz- und Kraftwerksbetreiber," PhD thesis, Universität Stuttgart, 2006. 105

[249] Aundrup, Thomas and Beck, Hans-Peter and Becker, Andreas and Berthold, Andreas, "Batteriespeicher in der Nieder- und Mittelspannungsebene - Anwendungen und Wirtschaftlichkeit sowie Auswirkungen auf die elektrischen Netze," Energietechnische Gesellschaft im VDE (ETG), Tech. Rep., 2015. 106, 107, 108, 109, 126

[250] J. Fleer, S. Zurmühlen, J. Meyer, J. Badeda, P. Stenzel, J. F. Hake, and D. Uwe Sauer, "Price development and bidding strategies for battery energy storage systems on the primary control reserve market," *Energy Procedia*, vol. 135, pp. 143–157, 2017. 106, 127

[251] Fraunhofer ISE, "Durchschnittliche Preise in Deutschland. Energy Charts," www.energy-charts.de, accessed 2017-09-30. 106

[252] A. Ruhland, "Nachladen: Intraday Ablauf und Kostenschätzungen, , personal communication (email), 01 may, 2017." 106

[253] K. Bourwieg, "Eine regulatorische Einordnung von Stromspeichern im aktuellen Rechtsrahmen," BMWi, Tech. Rep., 2015. 106

[254] LVN, "Entgelte für Messstellenbetrieb, Messung und Abrechnung bei Energieentnahme und -einspeisung mittels Lastgangmessung," Preisblatt 4, 2016. 106

[255] Consentec, "Beschreibung von Regelleistungskonzepten und Regelleistungsmarkt," 50Hertz Transmission GmbH, Studie im Auftrag der deutschen Übertragugsnetzbetreiber, 2014. 107

[256] R. Hollinger, L. M. Diazgranados, F. Braam, T. Erge, G. Bopp, and B. Engel, "Distributed solar battery systems providing primary control reserve," *IET Renew. Power Gener.*, vol. 10, no. 1, pp. 63–70, 2016. 107

[257] P. T. Moseley and J. Garche, *Electrochemical Eenrgy Storage for Renewable Sources and Grid Balancing*, 2015. 107

[258] B. Battke, T. S. Schmidt, D. Grosspietsch, and V. H. Hoffmann, "A review and probabilistic model of lifecycle costs of stationary batteries in multiple applications," *Renew. Sustain. Energy Rev.*, vol. 25, pp. 240–250, sep 2013. 108

[259] Wietschel, *Energietechnologien der Zukunft. Erzeugung, Speicher, Effizienz und Netze*, M. Wietschel, S. Ullrich, P. Markewitz, F. Schulte, and F. Genoese, Eds. Wiesbaden: Springer Fachmedien, 2015. 108

[260] Fraunhofer UMSICHT and Fraunhofer IWES, "Abschlussbericht Metastudie "Energiespeicher" Studie im Auftrag and des Bundesministeriums and für Wirtschaft and und and Energie (BMWi)," 2014. 108, 109

[261] D. U. Sauer, B. Lunz, and D. Magnor, "Marktanreizprogramm für dezentrale Speicher insbesondere für PV-Strom," RWTH Aachen, Tech. Rep., 2013. 108, 109

[262] German TSO, "PRL-Rahmenvertrag," p. 2013. 110

[263] M. Resch, J. Bühler, M. Klausen, and A. Sumper, "Impact of operation strategies of large scale battery systems on distribution grid planning in Germany," *Renew. Sustain. Energy Rev.*, vol. 74, pp. 1042–1063, jul 2017. 110

[264] M. Schimpe, M. Naumann, N. Truong, H. C. Hesse, S. Santhanagopalan, A. Saxon, and A. Jossen, "Energy efficiency evaluation of a stationary lithium-ion battery container storage system via electrothermal modeling and detailed component analysis," *Appl. Energy*, vol. 210, no. June 2017, pp. 211–229, 2018. 122, 160

[265] J. Diamond, *Guns, Germs, and Steel: The Fates of Human Societies.* New York: W.W. Norton & Co, 1997. 131

[266] Y. Varoufakis and B. Hildebrand, *Time for Change.* München: Carl Hanser Verlag GmbH & Co. KG, jul 2015. 131

[267] J. Weniger, T. Tjaden, and V. Quaschning, "Sizing and grid integration of residential PV battery systems," in *8th Int. Renew. Energy Storage Conf. Exhib. (IRES 2013)*, 2013. 132, 134, 136, 137, 152, 158

[268] J. Struth, K.-p. Kairies, M. Leuthold, and A. Aretz, "PV-Benefit: a Critical Review of the Effect of Grid Integrated PV-Storage-Systems," in *Iternational Renew. Energy Storage Conf. (IRES 2013)*, 2013, p. 10. 134

[269] Y. Ueda, K. Kurokawa, K. Kitamura, K. Akanuma, M. Yokota, and H. Sugihara, "Study on the overvoltage problem and battery operation for grid-connected residential PV systems," *22nd Eur. Photovolt. Sol. Energy Conf.*, no. September, pp. 3094–3097, 2007. 134

[270] M. Schneider, P. Boras, H. Schaede, L. Quurck, and S. Rinderknecht, "Effects of Operational Strategies on Performance and Costs of Electric Energy Storage Systems," *Energy Procedia*, vol. 46, no. Ires 2013, pp. 271–280, 2014. 134

[271] F. Marra, G. Yang, C. Traeholt, J. Ostergaard, and E. Larsen, "A Decentralized Storage Strategy for Residential Feeders With Photovoltaics," *IEEE Trans. Smart Grid*, vol. 5, no. 2, pp. 974–981, mar 2014. 134, 135

[272] J. von Appen, T. Stetz, M. Braun, and A. Schmiegel, "Local Voltage Control Strategies for PV Storage Systems in Distribution Grids," *IEEE Trans. Smart Grid*, vol. 5, no. 2, pp. 1002–1009, mar 2014. 134, 135

[273] Y. Riesen, P. Ding, S. Monnier, N. Wyrsch, and C. Balli, "Peak Shaving Capability of Household Grid-Connected PV-System with Local Storage: A Case Study," in *28th Eur. Photovolt. Sol. Energy Conf. Exhib.*, 2013, pp. 3740–3744. 135, 137, 138

[274] S. Nykamp, A. Molderink, J. L. Hurink, and G. J. M. Smit, "Storage operation for peak shaving of distributed PV and wind generation," in *2013 IEEE PES Innov. Smart Grid Technol. Conf.* IEEE, feb 2013. 136

[275] J. Li and M. A. Danzer, "Optimal charge control strategies for stationary photovoltaic battery systems," *J. Power Sources*, vol. 258, pp. 365–373, jul 2014. 136, 137

[276] C. Williams, J. Binder, M. Danzer, F. Sehnke, and M. Felder, "Battery Charge Control Schemes for Increased Grid Compatibility of Decentralized PV Systems," in *28th Eur. Photovolt. Sol. Energy Conf. Exhib.*, 2013, pp. 1–6. 137, 138, 145, 147

[277] M. Lodl, R. Witzmann, and M. Metzger, "Operation strategies of energy storages with forecast methods in low-voltage grids with a high degree of decentralized generation," *2011 IEEE Electr. Power Energy Conf.*, pp. 52–56, 2011. 137

[278] T. Niimura, K. Ozawa, D. Yamashita, K. Yoshimi, and M. Osawa, "Profiling residential PV output based on weekly weather forecast for home energy management system," in *2012 IEEE Power Energy Soc. Gen. Meet.* IEEE, jul 2012. 137, 138

[279] E. Lorenz, J. Hurka, D. Heinemann, and H. G. Beyer, "Irradiance Forecasting for the Power Prediction of Grid-Connected Photovoltaic Systems," *IEEE J. Sel. Top. Appl. Earth Obs. Remote Sens.*, vol. 2, no. 1, pp. 2–10, mar 2009. 137, 138

[280] G. Chicco, V. Cocina, P. Di Leo, and F. Spertino, "Weather forecast-based power predictions and experimental results from photovoltaic systems," in *2014 Int. Symp. Power Electron. Electr. Drives, Autom. Motion*. IEEE, jun 2014, pp. 342–346. 137, 138

[281] J. Bergner, J. Weniger, T. Tjaden, and V. Quaschning, "Feed-in Power Limitation of Grid-Connected PV Battery Systems with Autonomous Forecast-Based Operation Strategies," in *29th Eur. PV Sol. Energy Conf. Exhib.*, Amsterdam, 2014. 137, 139, 145, 149, 153, 159, 176

[282] K. F. Evans, "The spherical harmonics discrete ordinate method for three-dimensional atmospheric radiative transfer," *J. Atmos. Sci.*, vol. 55, no. 3, pp. 429–446, 1998. 137

[283] S. Dierer, J. Remund, R. Cattin, T. Koller, P. Strasser, and BFE, "Einspeiseprognosen für neue erneuerbare Energien," Bundesamt für Energie BFE, Tech. Rep., 2010. 137

[284] "The Weather Research & Forecasting," http://www.wrf-model.org/, accessed 2015-10-01. 138

[285] "Meteotest," http://www.meteotest.ch/, accessed 2015-10-01. 138

[286] S. Pelland, J. Remund, J. Kleissl, T. Oozeki, and K. De Brabandere, "Photovoltaic and solar forecasting: state of the art," International energy agency (IEA), Tech. Rep., 2013. 138

[287] M. Resch, B. Ramadhani, J. Bühler, and A. Sumper, "Comparison of control strategies of residential PV storage systems," in *9th Int. Renew. Energy Storage Conf. (IRES 2015)*, 2015, p. 18. 141, 145

[288] Federal Network Agency (BNetzA), "Bestimmung der Förderssätze für Fotovoltaikanlagen §31 EEG 2014 für die Kalendermonate Oktober 2015, November 2015 und Dezember 2015," Tech. Rep., 2015. 153

[289] German Association of the Energy and Water Industry (BDEW), "Erneuerbare Energien und das EEG: Zahlen, Fakten, Grafiken (2015)," Berlin, Tech. Rep., 2015. 153

[290] J. Weniger, J. Bergner, D. Beier, M. Jakobi, T. Tjaden, and V. Quaschning, "Grid Feed-in Behavior of Distributed Pv Battery Systems," in *31st Eur. PV Sol. Energy Conf. Exhib.*, Hamburg, 2015, pp. 1603–1606. 155

[291] N. Strauch, "Einsatz von Energiespeicher-Technologien in Inselsystemen mit hohem Anteil Erneuerbarer Energien," PhD thesis, TU Darmstadt, 2013. 155

[292] Öko-Institut e.V, "Die Entwicklung der EEG-Kosten bis 2035," Tech. Rep., 2015. 157

[293] O. C. Rascon, M. Resch, J. Bühler, and A. Sumper, "Techno-economic comparison of a schedule-based and a forecast-based control strategy for residential photovoltaic storage systems in Germany," *Electr. Eng.*, vol. 98, no. 4, pp. 375–383, dec 2016. 159, 183

[294] O. C. Rascon, M. Resch, B. Schachler, J. Buhler, and A. Sumper, "Increasing the hosting capacity of distribution grids by implementing residential PV storage systems and reactive power control," in *2016 13th Int. Conf. Eur. Energy Mark.* IEEE, jun 2016, pp. 1–5. 159

[295] Y. Lachmann, O. Prahl, M. Knösel, J. Mühlbach, N. Nau, J. Papenheim, M. Kubach, M. Schellenberger, E. Sebastian, P. Schmidt, and E. Heller, "Strombank - Abschlussbericht," Tech. Rep., 2017. 165

[296] Federal Ministry of Economic Affairs and Energy (BMWi), *Mieterstrom - Rechtliche Einordnung, Organisationsformen, Potenziale und Wirtschaftlichkeit von Mieterstrommodellen (MSM)*, 2017, no. 17.01.2017. 165

[297] T. Schürer, "Elektrische Speicher aus der Sicht eines Verteilnetzbetreibers," in *Fachforum Energiespeicher im Kontext der Energiewende*. Nürnberg: IHK Akademie Mittelfranken, 2015. 170

[298] R. Hollinger, L. M. Diazgranados, and T. Erge, "Trends in the German PCR market: Perspectives for battery systems," in *2015 12th Int. Conf. Eur. Energy Mark.* IEEE, may 2015, pp. 1–5. 171

[299] C. D'Adamo, B. Buchholz, C. Abbey, M. Khattabi, S. Jupe, and F. Pilo, "Development and operation of active distribution networks: Results of CIGRÉ C6.11 Working group," in *CIRED - 21st Int. Conf. Electr. Distrib.*, no. June, 2011. 172

[300] R. Zimmerman, C. Murillo Sanchez, and R. Thomas, "MATPOWER: Steady-State Operations, Planning, and Analysis Tools for Power Systems Research and Education," *Power Syst. IEEE Trans.*, vol. 26, no. 1, pp. 12–19, 2011. 174

[301] Federal Ministry of Justice and Consumer Protection, "Renewable Energy Act (Erneuerbare - Energien - Gesetz - EEG 2014)," p. 74, 2014. 175

[302] J. Weniger, T. Tjaden, and V. Quaschning, "Sizing of residential PV battery systems," *Energy Procedia*, vol. 46, pp. 78–87, 2014. 176, 179

[303] R. Kunert, J. Bühler, B. Schachler, and M. Resch, "Technisch-wirtschaftliche Optimierung der Teilnahme einer Großbatterie am Markt für Primärregelleistung," in *4. Konf. Zukünftige Stromnetze für Erneuerbare Energien*. Berlin: OTTI e.V., 2017, p. 7. 176

[304] C. Elbs, R. Pardatscher, R. Nenning, and R. Witzmann, "Einsatz der Q (U)-Regelung bei der Vorarlberger Energienetze GmbH," Illwerke und Tech. Univ. München, Tech. Rep., 2014. 177

[305] H. Basse, J. Backes, and T. Leibfried, "Dynamic effect of voltage dependent reactive power control of dispersed generation," in *ETG-Kongress*, 2009, p. 6. 177

Appendices

Appendix A

Publications

This chapter presents the publications related to the specific topics of this thesis the author has contributed to.

Peer Reviewed Journal Publications

Published

Resch M, Bühler J, Klausen M, Sumper A. Impact of operation strategies of large scale battery systems on distribution grid planning in Germany. *Renewable and Sustainable Energy Reviews*; 74:1042–63; 2017. doi:10.1016/j.rser.2017.02.075.

Camacho Rascon O, Resch M, Bühler J, Sumper A. Techno-economic comparison of a schedule-based and a forecast-based control strategy for residential photovoltaic storage systems in Germany. *Electrical Engineering*; 98:375; 2016. doi:10.1007/s00202-016-0429-7.

Klausen M, Resch M, Bühler J. Analyis of a Potential Single and Combined Business Model for Stationary Battery Storage Systems. *Energy Procedia*;99:321–31; 2016. doi:10.1016/j.egypro.2016.10.122.

Submitted and Under Revision

Resch M, Buehler J, Schachler B, Kunert R, Meier A, Sumper A. Technical and Economic Comparison of Grid Supportive Vanadium Redox Flow Batteries for Primary Control Reserve and Community Electricity Storage

in Germany. *International Journal of Energy Research* (recommended for publication with minor changes - 2nd revision) 2018.

Resch M, Bühler J, Schachler B, Sumper A. Grid Expansion versus Flexibility Options in German Distribution Grids: Application to a Pilot Grid. *Sustain Energy, Grids and Networks* (submitted) 2018.

Publications in Technical and Scientific Magazines

Gaudchau E, Resch M, Zeh A. Quartierspeicher: Definition, rechtlicher Rahmen und Perspektiven. *Ökologisches Wirtschaften - Fachzeitschrift*; 31:26; 2016. doi:10.14512/OEW310226.

Publications in Proceedings of Scientific Conferences

Kunert R, Bühler J, Schachler B, Resch M. Technisch-wirtschaftliche Optimierung der Teilnahme einer Großbatterie am Markt für Primärregelleistung. In *4. Konf. Zukünftige Stromnetze für Erneuerbare Energien*; Berlin; OTTI e.V.; 2017.

Camacho Rascon O, Resch M, Schachler B, Buhler J, Sumper A. Increasing the hosting capacity of distribution grids by implementing residential PV storage systems and reactive power control. In *13th International Conference on the European Energy Market (EEM)*; Porto; IEEE; 2016. doi:10.1109/EEM.2016.7521338.

Gonzalez Quintairos A, Bühler J, Kleinschmitt B, Resch M. Analysis of Potential Distribution and Size of Photovoltaic Systems on Rural Rooftops. In *GI Forum*; Salzburg; 1:220–4; 2015. doi:10.1553/giscience2015.

Bühler J, Resch M, Wiemann J, Twele J. Lebenszyklusanalyse von Großbatterien am deutschen Regelenergiemarkt. In *9. Int. Energiewirtschaftstagung*; Wien; 2015. doi:10.13140/RG.2.1.4454.6400.

Resch M, Bühler J, Huyskens H, Sumper A. Optimale Positionierung von Großbatterien in Verteilnetzen. In *30. Symp. Photovoltaische Solarenergie*; Bad Staffelstein; OTTI e.V.; 2015. doi:10.13140/RG.2.1.1308.9123.

Resch M, Ramadhani B, Bühler J, Sumper A. Comparison of control strategies of residential PV storage systems. In *9th International Renewable Energy Storage Conference (IRES)*; Düsseldorf; 2015. doi:10.13140/RG.2.1.3668.2084.

Supervised Bachelor, Master Thesis and Internship

Title of master thesis: Entwicklung eines netzdienlichen Eigenverbrauchsmodells mit Quartierspeichern im Verteilnetz
Author: Andreas M. Meier (Technical University Berlin)
Supervisor: Matthias Resch (Reiner Lemoine Institute)
Submission date: February 2017

Title of master thesis: Techno-economic analysis on the effect of different control strategies for residential PV storage systems on a distribution grid
Author: Oscar Camacho Rascon (University Oldenburg)
Supervisor: Matthias Resch (Reiner Lemoine Institute)
Submission date: February 2016

Title of master thesis: Economic and legal analysis of potential business models for grid connected electrical storage devices
Author: Nadja Mira Klausen (University Leipzig)
Supervisor: Matthias Resch (Reiner Lemoine Institute)
Submission date: June 2015

Internship

Topic: Investigation on the Control Strategy of Residential PV Storage Systems
Student: Bagus Fajar Ramadhani (University Oldenburg)
Supervisor: Matthias Resch (Reiner Lemoine Institute)
Date of internship: February to March 2014

Contributions to Bachelor and Master Thesis

Within the Framework of the SmartPowerFlow Project

Title of master thesis: Analysis of potential distribution and size of photovoltaic systems on rural rooftops
Author: Ana González Quintairos (Technical University Berlin)
Supervisor: Dr.-Ing. Jochen Bühler (Reiner Lemoine Institute)

Submission date: January 2015

Title of master thesis: Technisch–wirtschaftliche Analyse eines Eigenverbrauchsmodells mit Quartierspeichern im Verteilnetz
Author: Kathrin Hebler (Technical University Berlin)
Supervisor: Jochen Bühler (Reiner Lemoine Institute)
Submission date: July 2016

Title of master thesis: Technisch-wirtschaftliche Optimierung der Teilnahme einer Großbatterie am Markt für Primärregelleistung
Author: Rita Kunert (Technical University Berlin)
Supervisor: Jochen Bühler (Reiner Lemoine Institute)
Submission date: April 2017

Title of bachelor thesis: Einsatzmöglichkeiten von Großbatterien im Regelenergiemarkt
Student: Johannes Wiemann (University of Applied Sciences HTW Berlin)
Supervisor: Jochen Bühler (Reiner Lemoine Institute)
Submission date: August 2014

Appendix B

Additional Information

B.1 Information on Vanadium Redox Flow Battery Technology

The peculiarity of the vanadium redox flow technology is the possibility for the spatial separation of energy medium and energy converter. Furthermore, the two electrolytes are stored in separate tanks. Therefore, the power and the storage capacity can be sized independently and the tank size determines the energy capacity of the battery. The electrolytes are pumped from the tanks into a charging and discharging unit called stack. The pumping system can be realized as a cascade operation mode, which allows to supply only the needed stacks according to the power demand. This reduces the self-discharge within the stacks considerably. An additional advantage is that, in the event of a damaged membrane, no mutual contamination of the electrolytes can occur. The spatial separation of the electrolytes also has a positive effect on the self-discharge rate, which is vanishingly small. In addition, vanadium can be completely regenerated by external treatment and thus recycled without loss after the end of the life time of the battery storage system. Other positive aspects of this storage technology is the capability for an easy scale-up due to the system design and the immunity to depth discharge. In addition, this technology shows am excellent cycle stability and no memory effect. On the other hand, due to the comparatively low energy and power density, the relatively high maintenance costs of all necessary auxiliary equipment (e.g. pumps), the high commodity price and the poor availability of the element vanadium must be considered disadvantageous.

Leistung und Energie*	CellCube FB 200-400	
Nennladeleistung / Max. AC Ladeleistung / Kontinuierliche **Ladeleistung**	200 kW	
Nennentladeleistung / Max. AC Ausgangsleistung / Kontinuierliche **Entladeleistung**	200 kW	
Kapazität des Energiespeichers	400 kWh (Nutzung leistungsabhängig)	
Batterie- und Systemspannung		
Ausgangsspannungsoption	400 VAC	
Einschaltdauer / Reaktionszeit	**< 60 ms**	
Steuerung		
Kontrolle über externe Schnittstellen	seriell, TCP/IP, Bus Systeme	
Monitoring		
Zustandserfassung über Fernabfrage via E-Mail	Ladezustand (SOC), verfügbare Energie, Lade- / Entladeleistung, u.a.	
Wirkungsgrad		
Lade-/ Entladungszyklus DC	bis zu 70 %	
Multi Stage Betriebsführung reduziert Energieverluste	durch Selbstentladung bei kleinen Lasten	
Entladezeit bei Nennleistung	**DC-Batterieleistung**	**AC-Inverterleistung**
Entladezeit (Autonomie)		
1 Stunde**	220 kW	200 kVa
2 Stunden**	140 kW	130 kVa
3,5 Stunden**	110 kW	100 kVa
5 Stunden**	80 kW	70 kVa
Selbstentladung		
Selbstentladung im Cold Standby**	< 300 W	
Selbstentladung im Tank	vernachlässigbar (< 1 % pro Jahr)	
Größe und Gewicht		
Dimension L x B x H (trockener Zustand)	6.000 x 2.438 x 5.792 mm	
Gewicht (leerer Zustand)	20.000 kg	
Gesamtgewicht (gefüllter Zustand)	60.000 kg	

Figure B.1: Data sheet of the CellCube FB 200-400 DC (only available in German).

B.2 Data sheet of the inverter SCS630 developed in the SmartPowerFlow project

Technical data	Sunny Central Storage 500	Sunny Central Storage 630	Sunny Central Storage 720
DC connection			
Max. DC power (at cos φ =1)	560 kW	713 kW	808 kW
Voltage range	430 V to 850 V	500 V to 850 V	480 V to 850 V
Rated voltage	449 V	529 V	577 V
Max. input current	1400 A	1400 A	1400 A
AC connection			
Rated power (at 25°C) / nominal AC power (at 50°C)	550 kVA / 500 kVA	700 kVA / 630 kVA	792 kVA / 720 kVA
Nominal AC voltage / nominal AC voltage range	270 V / 243 V to 310 V	315 V / 284 V to 362 V	324 V / 292 V to 372 V
AC power frequency / range	50 Hz, 60 Hz / 47 Hz to 63 Hz		
Rated power frequency / rated grid voltage	50 Hz / 270 V	50 Hz / 315 V	50 Hz / 324 V
Max. AC current / max. total harmonic distortion	1411 A / 0.03		
Power factor at rated power / displacement power factor adjustable	1 / 0.0 leading to 0.0 lagging		
Feed-in phases / connection phases	3 / 3		
Efficiency[1]			
Max. efficiency	98.6%	98.7%	98.6%
Protective devices			
DC side disconnection device	Motor-driven load-break switch		
AC side disconnection device	AC circuit breaker		
DC overvoltage protection	Type I surge arrester		
Lightning protection (according to IEC 62305-1)	Lightning Protection Level III		
Stand-alone grid detection active / passive	● /–		
Grid monitoring	●		
Ground fault monitoring / remote-controlled ground fault monitoring	○ / ○		
Insulation monitoring	○		
Surge arrester for auxiliary power supply	●		
Protection class (according to IEC 62103) / overvoltage category (according to IEC 60664-1)	I / III		
General data			
Dimensions (W / H / D)	2562 / 2272 / 956 mm (101 / 89 / 38 inch)		
Weight in kg	1900 kg / 4200 lb		
Operating temperature range	–25°C to 62°C / –13°F to 144°F		
Noise emission[2]	63 db(A)	64 db(A)	64 db(A)
Max. self-consumption (operation)[3] / self-consumption (night)	1900 W / < 100 W	1900 W / < 100 W	1950 W / < 100 W
External auxiliary supply voltage	230 V / 400 V (3 / N / PE)		
Cooling concept	OptiCool		
Degree of protection: electronics / connection area (according to IEC 60529) / according to IEC 60721-3-4	IP54 / IP43 / 4C2, 4S2		
Application in unprotected outdoor environments / indoor	● / ○		
Maximum permissible value for relative humidity (non-condensing)	15% to 95%		
Maximum operating altitude above MSL 2000 m / 3000 m	● / ○		
Fresh air consumption (inverter)	3000 m^3/h		
Features			
DC connection / AC connection	Ring terminal lug / ring terminal lug		
Display	HMI touch display		
Communication / protocols	Ethernet (optical fiber optional), Modbus		
Color enclosure / door / base / roof	RAL 9016 / 9016 / 7004 / 7004		
Guarantee: 5 / 10 / 15 / 20 / 25 years	● / ○ / ○ / ○ / ○		
Configurable grid management functions	Reactive power setpoint, dynamic grid support (e.g. LVRT)		
Certificates and approvals (more available on request)	EN 61000-6-2, EN 61000-6-4, EMC-conformity, CE-conformity, BDEW-MSRL-manufacturer's declaration, Arrêté du 23/04/08		
● Standard features ○ Optional features – Not available			
Type designation	SCS 500	SCS 630	SCS 720

Figure B.2: Data sheet of the inverter SCS630

B.3 Ranking of the Possible Points of Common Coupling of the Battery Storage System

Ranking	Transformer	ΣΔVmax	Vmin	Vmax,1	Vmax,2	Vmax,3	Vmax,4	Vmax,5	Vmax,6	Vmax,7
-	-	[%]	[%]	[%]	[%]	[%]	[%]	[%]	[%]	[%]
1	T1	159	85	107	106	107	110	109	107	108
2	T2	156	85	106	106	107	107	106	112	107
3	T3	146	85	105	105	106	106	107	106	106
4	T4	142	87	106	105	105	104	104	104	104
5	T5	133	88	103	106	108	104	103	104	106
6	T6	132	85	107	107	107	107	107	107	0
7	T7	120	88	103	107	103	111	118	106	0
8	T8	120	88	103	103	107	106	109	105	103
9	T9	118	85	108	109	107	110	109	0	0
10	T10	118	85	105	104	105	104	105	105	0
11	T11	118	85	105	104	106	104	105	104	0
12	T12	113	85	110	106	106	110	106	0	0
13	T13	111	85	106	106	102	102	102	103	
14	T14	108	88	108	108	105	105	105	105	0
15	T15	101	85	105	105	105	105	106	0	0
16	T16	101	85	104	106	104	106	106	0	0
17	T17	95	85	102	106	105	102	105	0	
18	T18	95	85	104	104	103	103	106	0	
19	T19	94	81	105	104	104	105	0		
20	T20	94	85	104	103	104	106	102	0	
21	T21	90	85	107	107	107	109	0	0	0
22	T22	90	86	106	101	106	101	106		
23	T23	90	87	104	105	103	105	108	0	0
24	T24	88	88	105	106	103	105	109	0	0
25	T25	88	85	103	103	102	104	101	0	0
26	T26	86	85	106	106	106	108	0	0	0
27	T27	85	88	104	104	104	104	109	0	0
28	T28	82	86	102	103	102	102	103		
29	T29	82	85	100	100	104	102	101	0	0
30	T30	78	86	103	101	101	102	101		
31	T31	72	85	110	110	107	0	0	0	0

Figure B.3: Ranking of the Possible Points of Common Coupling for the Battery Storage System at the MV/ LV transformers in the Grid Region of Lechwerke Verteilnetze (excerpt)

B.4 Pre-qualification Test for BSS to Participate in the PCR market

To participate in the German primary control market, the technical units (in this thesis a battery storage system) must complete a pre-qualification test. The performance curve required in this context for batteries is a modification of the general pre-qualification test and additionally serves to determine the usable storage capacity. The test procedure is depicted in schematically in Figure B.4

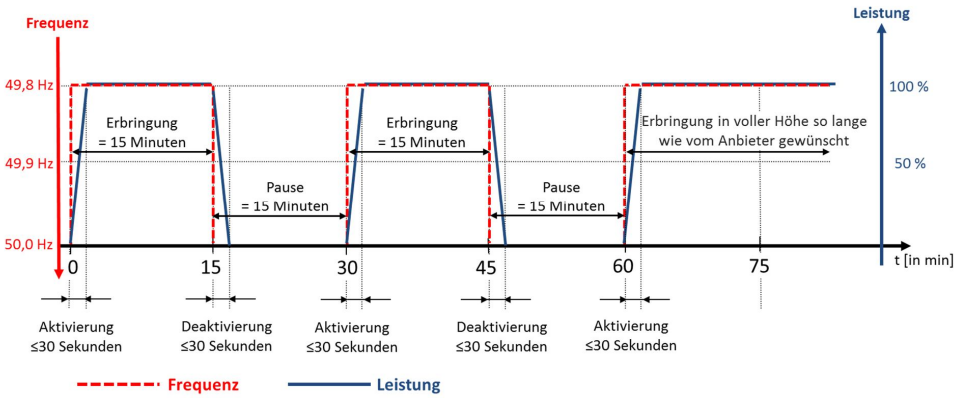

Figure B.4: Schematic of the modified German PCR pre-qualification test [190] (only available in German). Conventional PCR providers only have to complete the first two phases of activation. Standalone storages need to full-fill the third phase. The third phase can be used to determine the usable storage capacity.

B.5 Grid Implementation Plans of the Battery Prototype in the SmartPowerFlow Project

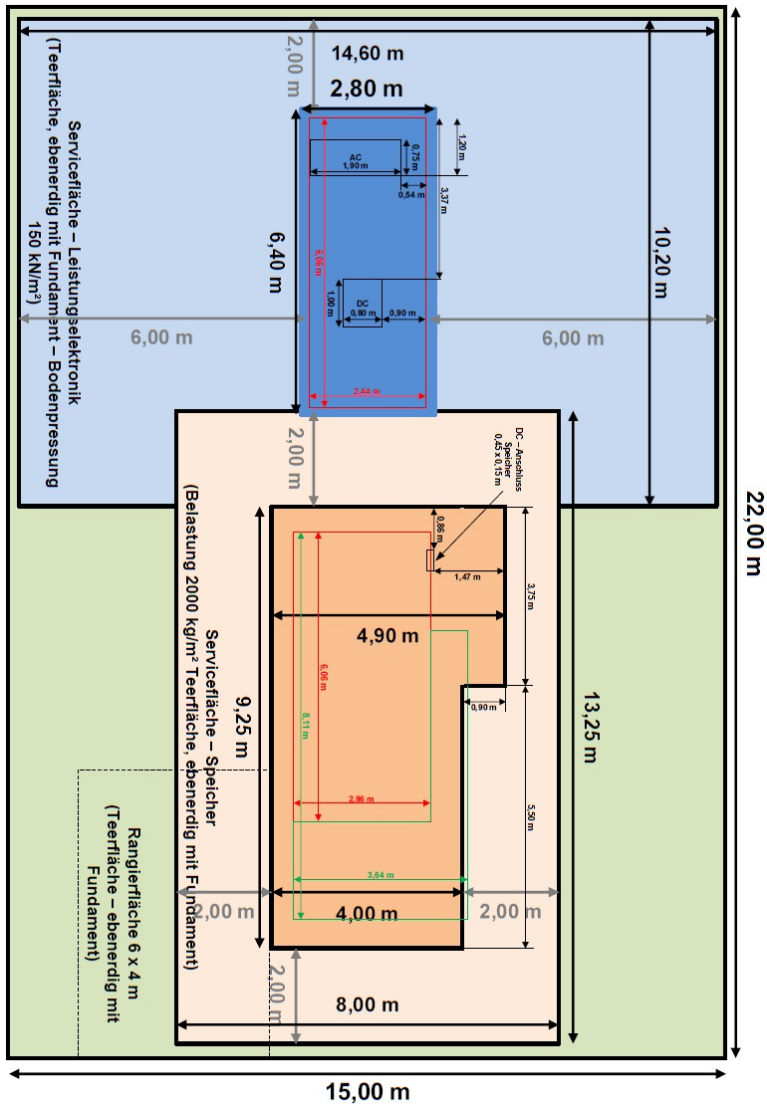

Figure B.5: Foundation plan of the SPF battery storage system (only available in German).

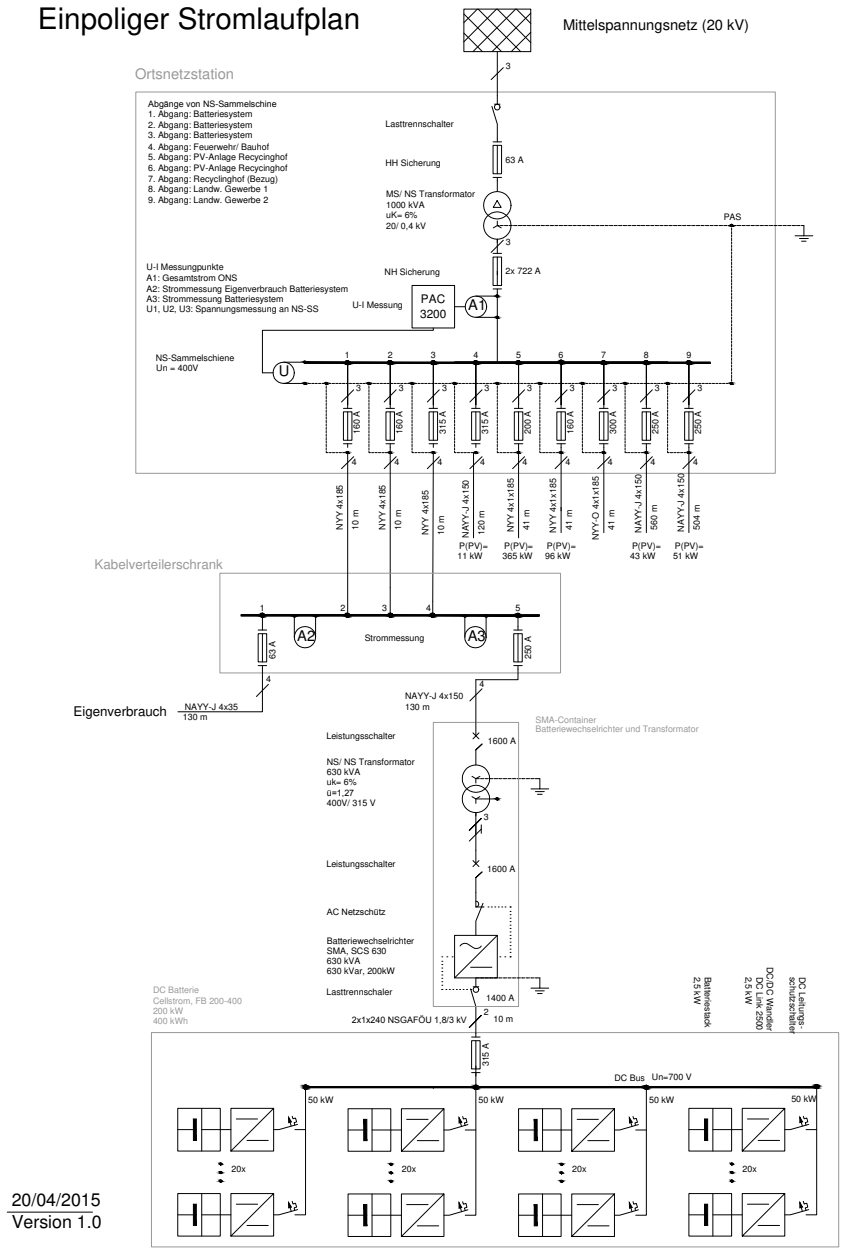

Figure B.6: Single line diagram of the grid connection of the SPF battery storage system (only available in German).

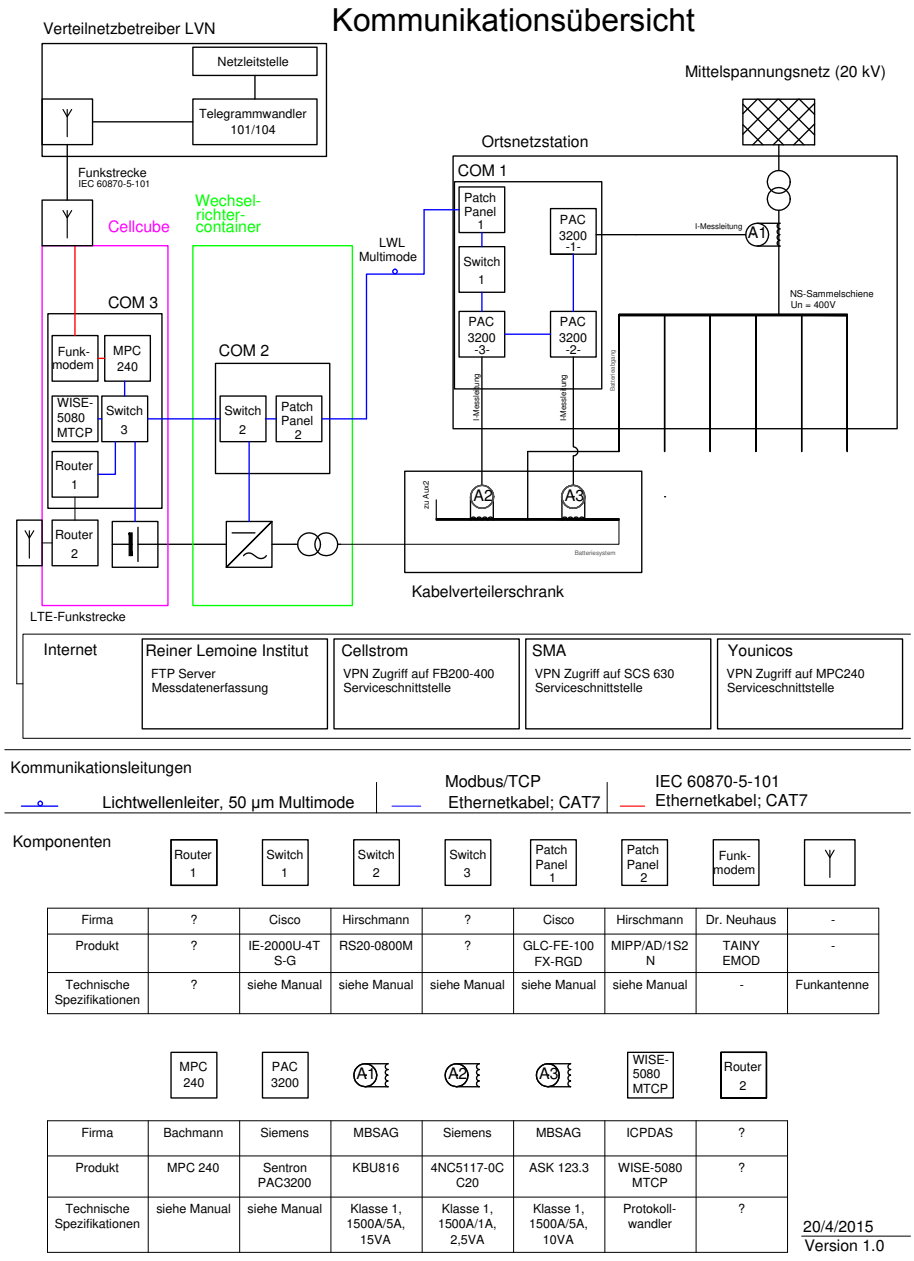

Firma	?	Cisco	Hirschmann	?	Cisco	Hirschmann	Dr. Neuhaus	-
Produkt	?	IE-2000U-4T S-G	RS20-0800M	?	GLC-FE-100 FX-RGD	MIPP/AD/1S2 N	TAINY EMOD	-
Technische Spezifikationen	?	siehe Manual	siehe Manual	siehe Manual	siehe Manual	siehe Manual	-	Funkantenne

Firma	Bachmann	Siemens	MBSAG	Siemens	MBSAG	ICPDAS	?
Produkt	MPC 240	Sentron PAC3200	KBU816	4NC5117-0C C20	ASK 123.3	WISE-5080 MTCP	?
Technische Spezifikationen	siehe Manual	siehe Manual	Klasse 1, 1500A/5A, 15VA	Klasse 1, 1500A/1A, 2,5VA	Klasse 1, 1500A/5A, 10VA	Protokoll-wandler	?

Figure B.7: Communication schematic of the SPF battery storage system (only available in German).

Hilfsstromversorgung

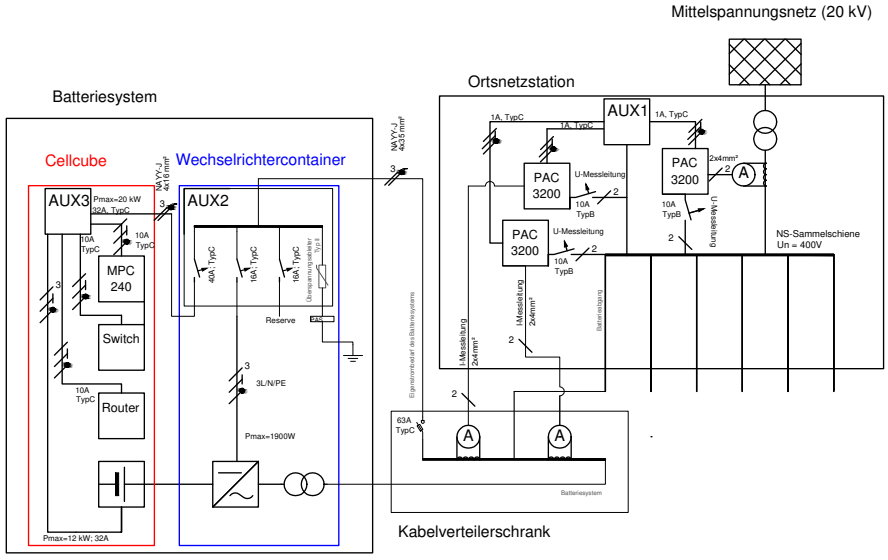

Komponenten

	Router	Switch	MPC 240			PAC 3200
Firma	-	-	Bachmann	Cellstrom	SMA	Siemens
Produkt	-	-	MPC 240	FB 200-400	SCS 630	Sentron PAC3200
Technische Spezifikationen	-	-	siehe Manual	Pn= 200 kW En= 400 kWh	Sn= 630 kVA Imax= 1283A (bei 315 V)	siehe Manual

Kommentare

AUX2 entspricht Stationsunterverteilung STSD im SMA Manual
AUX3 entspricht Stromlaufplan 001976_V01_FN200-400-2 der Firma Cellstrom GmbH

Version 0.3

Figure B.8: Auxiliary power of the SPF battery storage system (only available in German).

B.6 Energy Quantities and Efficiency for the PCR Application

The simulation model returns all values and performances in each time step Δt =1 s. The amount of energy of the primary control power fed-in or taken from the grid without using the degrees of freedom for the time t is calculated as follows (the sign convention: generator perspective):

$$E_{P(f),pos} = \int_t P(f)\ dt \quad \text{if } P(f) < 0 \tag{B.1}$$

$$E_{P(f),neg} = \int_t P(f)\ dt \quad \text{if } P(f) > 0. \tag{B.2}$$

where P(f) is the required power according to the P(f)-characteristic without the application of the DOF.

The amount of energy for the primary control power fed-in or taken from the grid $E_{PCP,pos}$ and $E_{PCP,neg}$ with the application of the degrees of freedom for the time time t is calculated as follows:

$$E_{PCP,pos} = \int_t P_{PCP}\ dt \quad \text{if } P_{PCP} > 0 \tag{B.3}$$

$$E_{PCP,neg} = \int_t P_{PCP}\ dt \quad \text{if } P_{PCP} < 0 \tag{B.4}$$

where P_{PCP} required PCR power with the application of the DOF.

The purchased and sold amount of energy $E_{corr,pos}$ and $E_{corr,neg}$ to correct the state of charge is therefore calculated by:

$$E_{corr,pos} = \int_t P_{corr}\ dt \quad \text{if } P_{corr} > 0 \tag{B.5}$$

$$E_{corr,neg} = \int_t P_{corr}\ dt \quad \text{if } P_{corr} < 0 \tag{B.6}$$

where P_{corr} is the power to correct the state of charge.

The total amount of energy fed-into and taken from the grid $E_{AC,pos}$ and $E_{AC,neg}$ is calculated as follows:

$$E_{AC,pos} = \int_t P_{AC}\ dt \quad \text{für } P_{AC} > 0 \tag{B.7}$$

$$E_{AC,neg} = \int_t P_{AC}\ dt \quad \text{für } P_{AC} < 0. \tag{B.8}$$

where P_{AC} is the total amount of power fed-into and taken from the grid.

Not included in the simulation is the power to run the pumps P_{pump} for the electrolyte pumps. Within the SPF prototype, this energy demand is covered with auxiliary power taken from the grid, but for the profitability analysis it is also calculated to be optionally drawn from the BSS. Thus, the amount of correction energy needed is increased. Furthermore, this additional consumption is relevant for efficiency considerations and is optionally included in the energy balance:

$$E_C = \int_t (P_{AC} - P_{pump})\ dt \quad \text{für } P_{AC} > 0 \tag{B.9}$$

$$E_D = \int_t (P_{AC} + P_{pump})\ dt \quad \text{für } P_{AC} < 0. \tag{B.10}$$

where E_C and E_D is the total energy to charge or discharge the BSS and P_{pump} the power needed to run the pumping system.

Due to the power-dependant battery behaviour, the efficiency is not defined globally, but must be considered separately for different operating modes. Nonetheless, the formula to calculate the AC-power dependant round-trip efficiency η_{AC} is given by:

$$\eta_{AC} = \frac{E_C}{E_D} \tag{B.11}$$

For the operation of the grid supportive PCR operation mode an efficiency can be calculated by comparing two moments with same SOC for a defined period. By considering the power on the AC-side of the BSS, the inverter of the system is automatically included, so that the calculated efficiency is the BSS efficiency of the overall system.

B.7 Simulated State of Charge Profile for the Year 2013

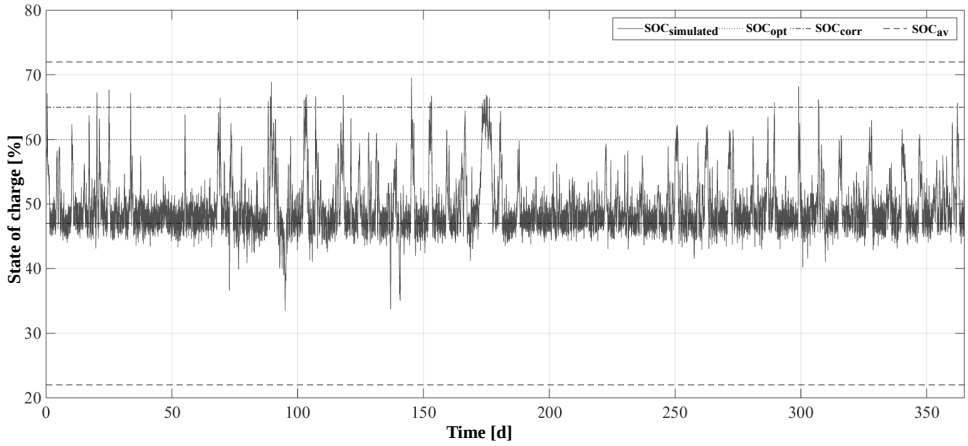

Figure B.9: Simulated state of charge profile for frequency data of the year 2013 (publicly available frequency data by 50Hertz Transmission GmbH). SOC_{av} is the availability limit. Outside this threshold the BSS does not reach its full power. SOC_{opt} is the set state of charge target value and SOC_{corr} is the correction limit. The DOF *schedule transactions* is triggered when the SOC surpasses the correction limits.

B.8 Amount of Correction Energy for the LiB applied for PCR

For an indicative comparison of the PCR operating costs of the two systems considered technologies (VRFB and LiB), the results of [246] are applied. Therefore, the ratio of the positive correction energy and the total energy taken from the grid for a similar battery size and operation strategy are taken from [246]:

$$\frac{E_{corr,pos,\text{Li-Io}}}{E_{AC,pos,\text{LiB}}} = 0.22 \tag{B.12}$$

The same ratio for the VRFB prototype without reactive power provision is:

$$\frac{E_{corr,pos,\text{VRF}}}{E_{AC,pos,\text{VRFB}}} = 0.55 \tag{B.13}$$

The ratio of these two parameters results in a factor from which the (smaller) amount of required correction energy for the application of the reactive power control of the LiB can be approximated:

$$E_{corr,pos,Q(V),\text{LiB}} = \frac{0.22}{0.55} \cdot E_{corr,pos,Q(V),\text{VRFB}} \tag{B.14}$$

The frequency data applied in [246] and in this thesis are for the same year and should thus be (almost) identical. The sold corrective energy is zero in for the VRFB analysed for the given frequency data, which is simliar to the amount of sold corrective energy in [246]. Thus, the sold corrective energy is neglected for both technologies.

B.9 Generation and Load Profiles

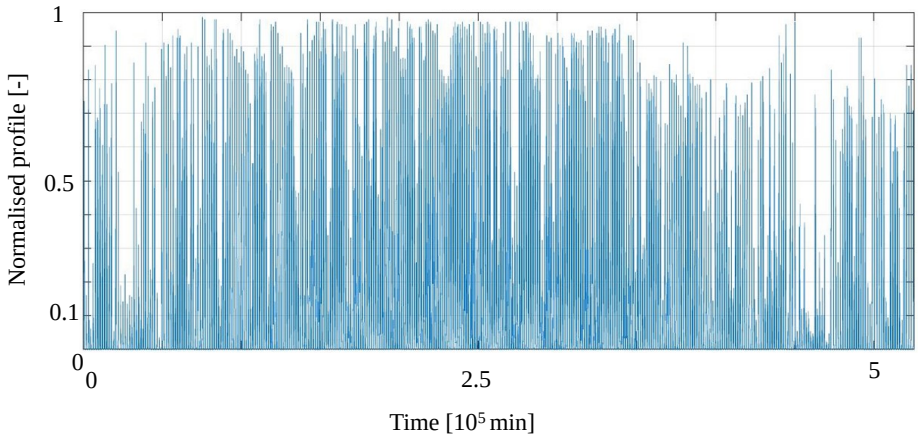

Figure B.10: Normalised PV power generation profile for one year in minutes (measured).

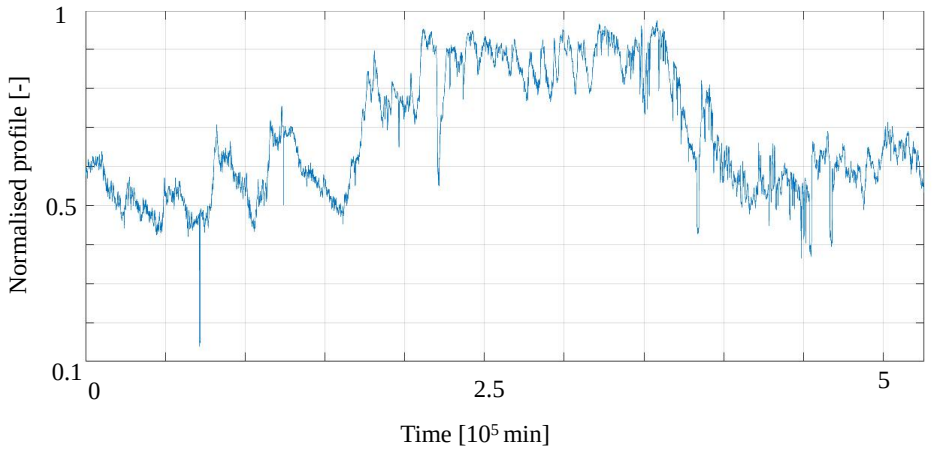

Figure B.11: Normalised hydro power generation profile for one year in minutes, based on [122].

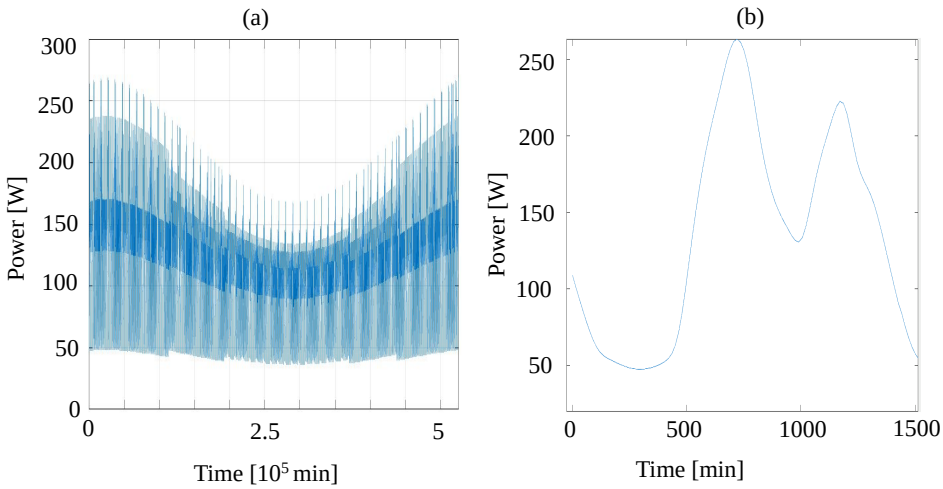

Figure B.12: Standard load profile H0 (SLP) [120]. (a) Whole year. (b) Exemplary Day.

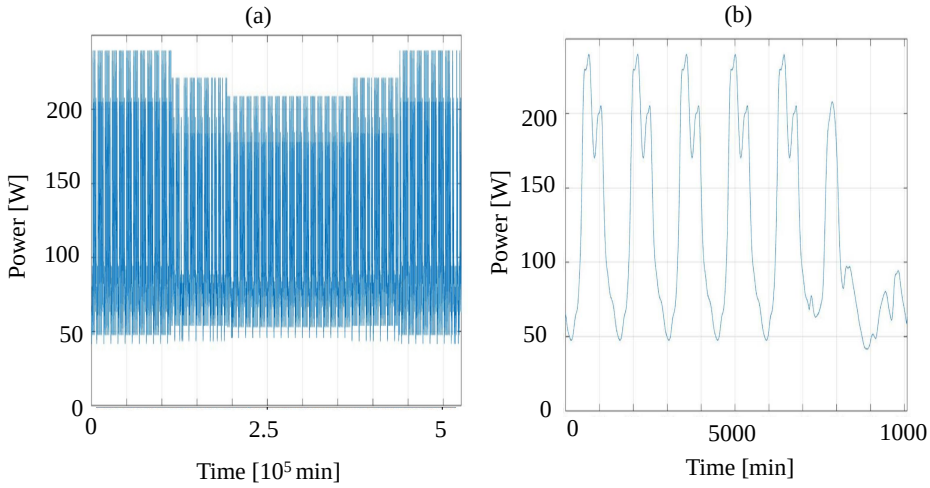

Figure B.13: Commercial load profile (G0) [120]. (a) Whole year. (b) 7 days example.

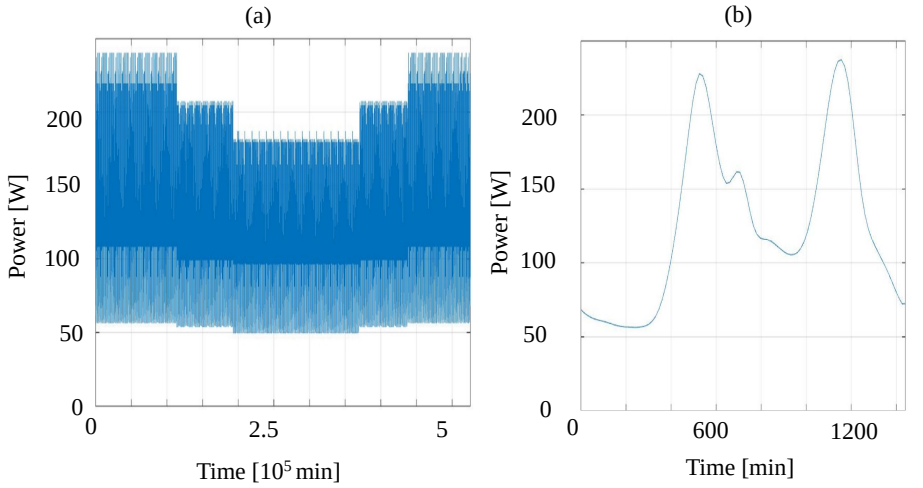

Figure B.14: Agricultural load profile (L0) [120]. (a) Whole year. (b) Exemplary day.

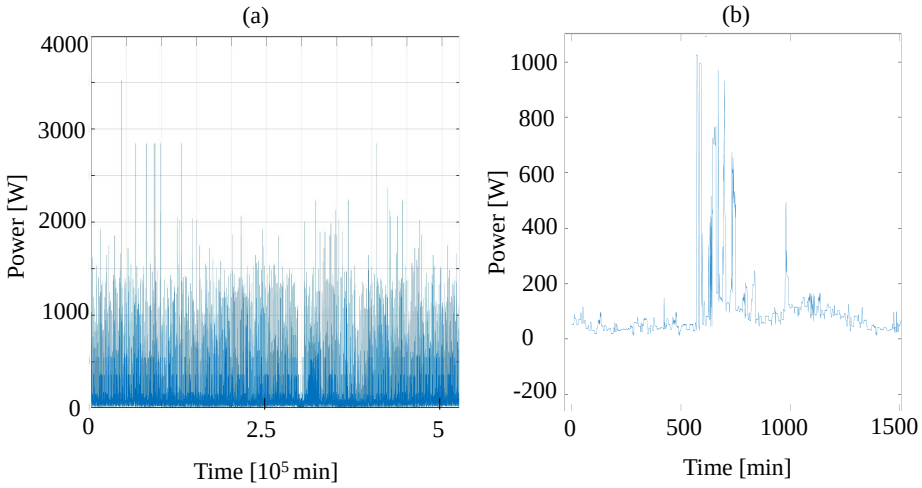

Figure B.15: Day active profile (DA) [121]. (a) Whole year. (b) Exemplary Day.

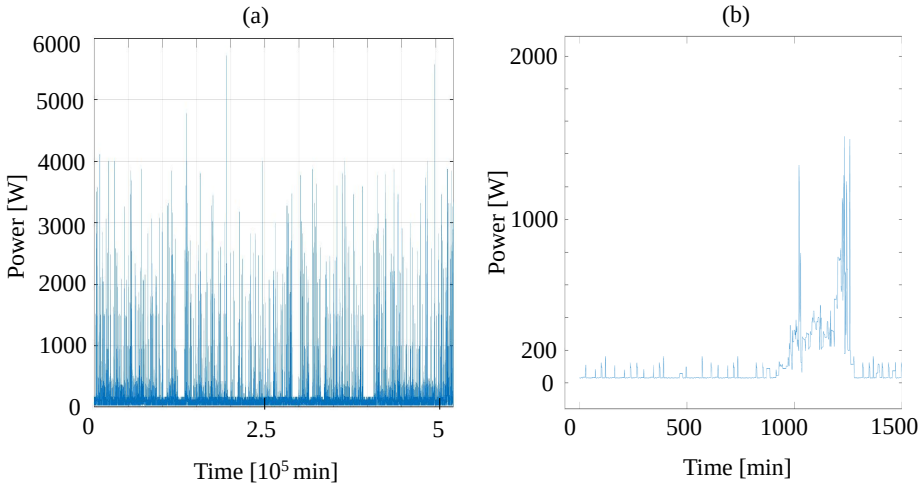

Figure B.16: Night active profile (NA) [121]. (a) Whole year. (b) Exemplary Day.

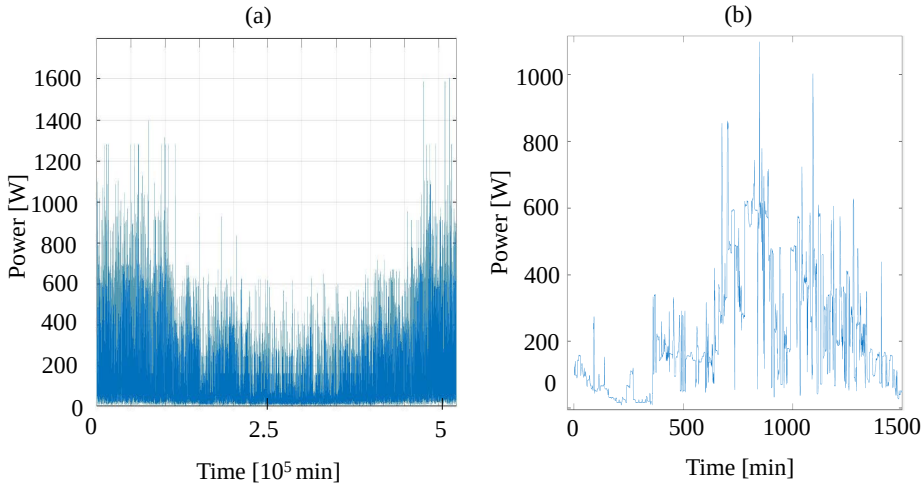

Figure B.17: Heat pump profile (HP) [121]. (a) Whole year. (b) Exemplary Day.

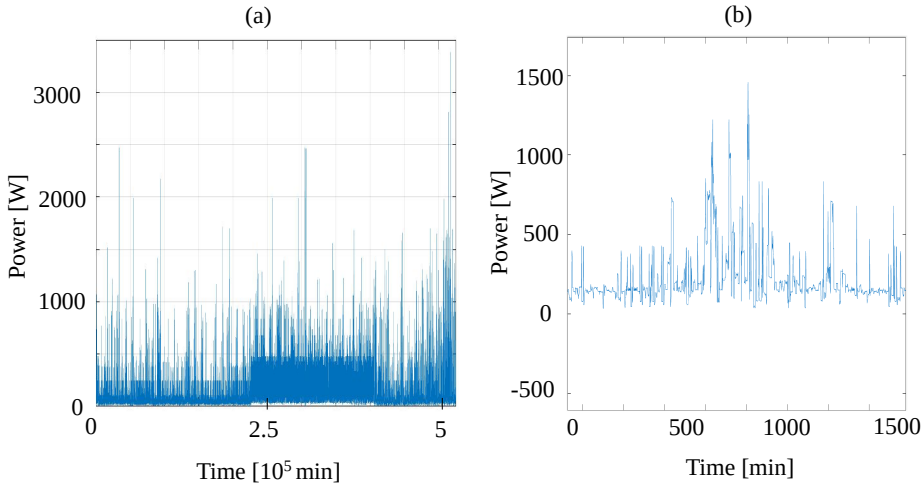

Figure B.18: Air conditioning profile (AC) [121]. (a) Whole year. (b) Exemplary Day.

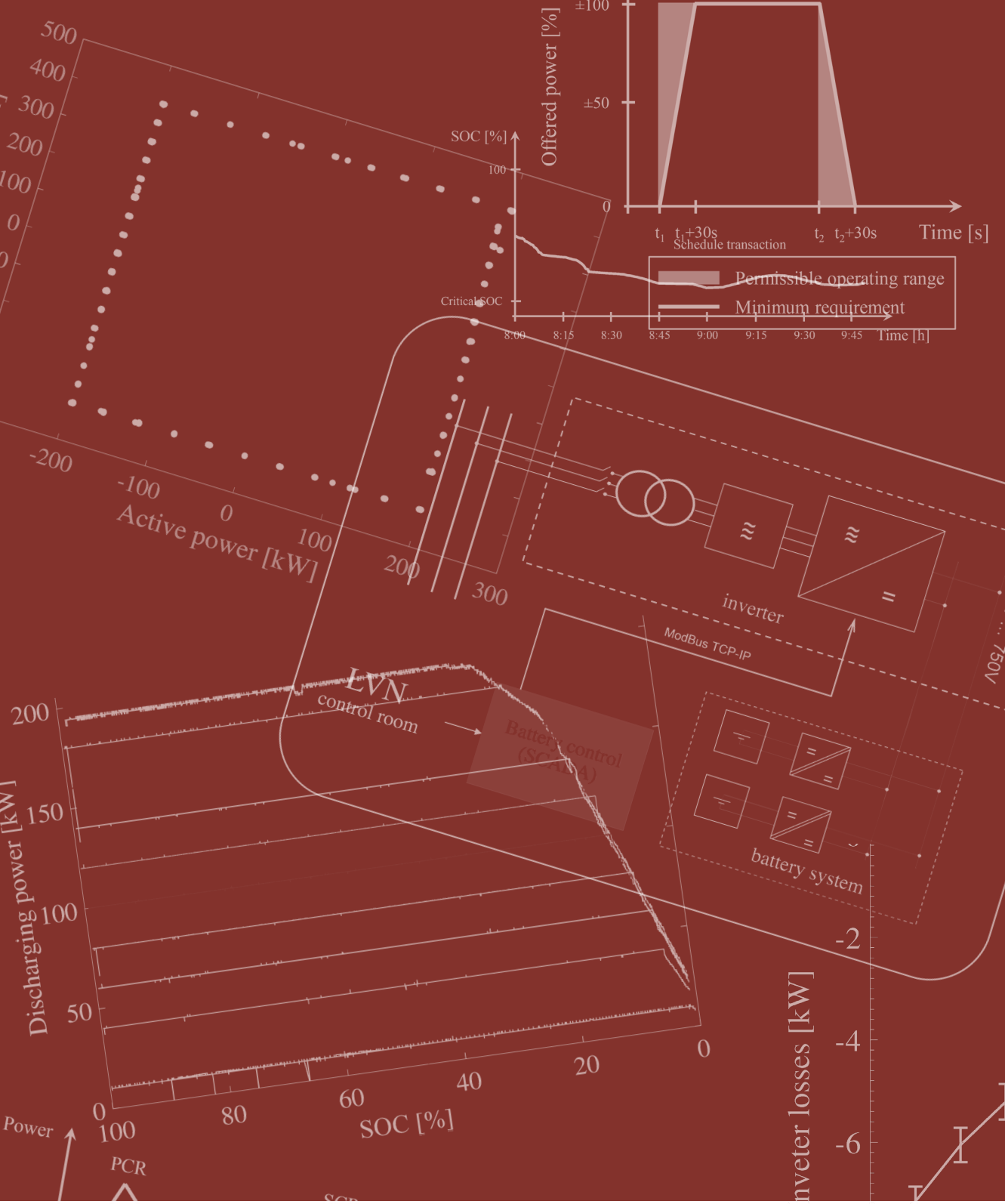

Departament d'Enginyeria Elèctrica
UNIVERSITAT POLITÈCNICA DE CATALUNYA
REINER LEMOINE INSTITUT